UNIVERSITY OF SOUTHAMPTON

FACULTY OF NATURAL AND ENVIRONMENTAL SCIENCES

Biological Sciences

Understanding the Meiotic Competence of Oocytes Derived from Oogonial Stem Cells

by

Larissa Zárate-García

Thesis for the degree of Doctor of Philosophy

June 2017

UNIVERSITY OF SOUTHAMPTON

ABSTRACT

FACULTY OF BIOLOGICAL AND ENVIRONMENTAL SCIENCES

School of Biological Sciences

Thesis for the degree of Doctor of Philosophy

UNDERSTANDING THE MEIOTIC COMPETENCE OF OOCYTES DERIVED FROM OOGONIAL STEM CELLS

By Larissa Zárate-García

This thesis investigates whether Oogonial Stem Cells (OSCs) exist and can be isolated from the adult mouse ovary. It also examines their ability to differentiate into oocyte-like cells *in vitro*. Transmembrane domains in the DEAD-box polypeptide 4 (DDX4) – the germline marker used in this antibody-based isolation – are examined using *in silico* protein modelling. The specificity of this antibody to DDX4 is tested in male and female germline cells. It is shown that the DDX4 antibody may have some specificity for DDX4, but the existence of a surface-bound DDX4 is unlikely. OSC-like cells can be isolated from the ovary using the DDX4 antibody by Fluorescence-Activated Cell Sorting (FACS). However, gene expression analysis and protein immunofluorescence show that these cells do not initially express DDX4 or possess germline identity. Despite this, they acquire some pre-meiotic and oocyte-specific markers in culture, including DDX4. Critically, the cells never express meiosis-specific markers even in the presence of meiotic enhancers BMP4 and retinoic acid. It is unlikely that these ovarian cells are being sorted by means of a cell surface DDX4 expression, because another antibody to a larger DDX4 epitope fails to detect DDX4 in isolated cells. These findings highlight that freshly isolated OSCs are not germ stem cells, and are not being isolated by their DDX4 expression, but instead may reflect an artefact of the antibody used or procedure adopted. Altogether this work offers support to the established dogma that the adult ovary is populated at birth by a fixed number of oocytes, and that adult *de novo* production is a rare or insignificant event.

Table of Contents

List of Figures

List of Tables

Declaration of Authorship

I, Larissa Zarate-Garcia

declare that this thesis and the work presented in it are my own and has been generated by me as the result of my own original research.

Understanding the Meiotic Competence of Oocytes Derived from Oogonial Stem Cells

I confirm that:

1. This work was done wholly or mainly while in candidature for a research degree at this University;
2. Where any part of this thesis has previously been submitted for a degree or any other qualification at this University or any other institution, this has been clearly stated;
3. Where I have consulted the published work of others, this is always clearly attributed;
4. Where I have quoted from the work of others, the source is always given. With the exception of such quotations, this thesis is entirely my own work;
5. I have acknowledged all main sources of help;
6. Where the thesis is based on work done by myself jointly with others, I have made clear exactly what was done by others and what I have contributed myself;
7. Parts of this work have been published as: Zarate-Garcia et al. (2016)

Signed: .....

Date: .....

Acknowledgements

First I would like to thank Prof. Keith Jones for his supervision and encouragement during the time that it took me to develop my PhD, and specially for giving me the opportunity to prove my value and skills.

I would also like to thank the rest of the Jones´ lab. Dr Simon Lane for patiently training me in all aspects of gene expression analysis and oocyte collection and visualisation. Dr Julie Merriman for her utmost advise on reactives, techniques and how to deal with 14 undergraduates during demonstrations. Dr Stephanie Morgan for training me in tissue immunostaining and Western blot, and sharing coffee and comments on the latest papers published and my results.

Also, I would like to thank Dr Neil Smyth for providing me with embryonic mouse fibroblasts, Monika Papayova for giving me a hand with PCRs, and Dr Kathrin Deinhart and Dr Joanne Bailey for their advise on cell culturing and their help during my Western blotting crisis.

Last, but not least, I would like to thank my family and friends for always being there and lightening my days. Specially my mum for being my role model and teaching me that failure is not defeat, and that hard work is the answer. Also thank you very much for filling my suitcases with Spanish food everytime I fly back from home. A quick mention to Ana and Beatriz for their advise on how to survive a thesis writing, Fanny the Gipsy Hill cat for cuddling me at 6am every day, Promega´s fluffy toys, the Beer Rebellion, croissants from SUSU Shop, Thaddeus Arlington´s motivational memes and soundtrack provided by Travis, Ash, Lord of the Lost, Birthday Massacre, Penny Dreadful, Sherlock and Star Trek Into Darkness.

Finally, thank you very much to Diego for listening patiently about DDX4 and cell growth for 4 years and supporting me through good and bad days with all his heart.

Definitions and Abbreviations

aa	Amino Acid
AMH	Anti-Müllerian Hormone
APC	Allophycocyanin
ATP	Adenosine Triphosphate
BMP	Bone Morphogenetic Factor
BMPR	Bone Morphogenetic Factor Receptor
cAMP	Cyclic Adenosine Monophosphate
cDNA	Complementary DNA
cKit	Proto-oncogene Kit Receptor
cGMP	Cyclic Guanosine Monophosphate
CM	Control Medium, not supplemented with growth factors
DAPI	4',6-Diamidino-2-Phenylindole
Dazl	Deleted in Azoospermia-Like
Ddx4	DEAD (Asp-Glu-Ala-Asp) Box Polypeptide 4
$DDX4^{C25}$	Epitope correspondent to residues 700 to the C-terminus of Human DDX4
$DDX4^{351}$	Epitope correspondent to residues 373 to the C-terminus of Human DDX4
DEADc	DEAD (Asp-Glu-Ala-Asp) domain
DMEM	Dulbecco´s Modified Eagle´s Medium
DNA	Deoxyribonucleic Acid
dpp	Days Post Partum
Dppa3	Developmental Pluripotency-Associated Protein 3
E0.0	Embryonic Day
EGF	Embryonic Growth Factor
EpiESC	Epiblast-derived Embryonic Stem Cell

ESC	Embryonic Stem Cell
ExE	Extraembryonic Ectoderm
FACS	Fluorescence-Activated Cell Sorting
FBS	Foetal Bovine Serum
FGF	Foetal Growth Factor
Figα	Folliculogenesis Specific BHLH Transcription Factor
FSH	Follicle-Stimulating Hormone
Gdf9	Growth Differentiation Factor 9
GDNF	Glial-Derived Neutrophilic Factor
GFP	Green Fluorescent Protein
GnRH	Gonadotropin-releasing Hormone
GSC	Germ Stem Cell
GV	Germinal Vesicle
GVBD	Germinal Vesicle Breakdown
H1foo	H1 Histone Family Member O, Oocyte Specific
HELICc	Helicase domain
ICM	Inner Cell Mass
Ifitm3	Interferon-Induced Transmembrane Protein 3
iPSC	Induced Pluripotent Stem Cell
JAK	Janus Kinase
KitL	Stem Cell Factor / Kit Ligand
LIF	Leukemia Inhibitory Factor
Lin28A	Lin-28 Homolog A
LH	Luteinising Hormone
MI	Meiosis I
MII	Meiosis II

MACS	Magnetic-Activated Cell Sorting
MEF	Mitotically-inactive Embryonic Fibroblast
MeioB	Meiosis Specific with OB Domains
MeioC	Meiosis Specific with Coiled-Coil Domain Protein
MPF	Maturation Promoting Factor, CDK1-cyclin B1 kinase
mRNA	Messenger RNA
Nobox	Newborn Ovary Homeobox Protein / NOBOX Oogenesis Homeobox Protein
NSN	Non-Surrounded Nucleolus
OSC	Oogonial Stem Cell
OSCM	OSC Medium, supplemented with growth factors
PGC	Primordial Germ Cell
PI	Propidium Iodide
PMT	Photomultiplier Tube
Pou5f1	POU Class 5 Homeobox 1
Prdm	PR Domain Zinc Finger Protein
RA	Retinoic Acid
RAR	Retinoic Acid Receptor
Rec8	REC8 Meiotic Recombination Protein
RNA	Ribonucleic Acid
Rps29	Ribosomal Protein S29
RXR	Retinoid X Receptor
SN	Surrounded Nucleolus
Sohlh	Spermatogenesis- and Oogenesis-specific Helix-Loop-Helix transcription factor
Stat3	Signal Transducer and Activator of Transcription 3
Stra8	Stimulated by Retinoic Acid 8

Sycp3	Synaptonemal Complex Protein 3
TE	Trophectoderm or Trophoblast
Utf1	Undifferentiated Embryonic Cell Transcription Factor 1
VE	Visceral Endoderm
Ybx2	Y-Box-Binding Protein 2
Zfp296	Zinc Finger Protein 296
Zp3	Zona Pellucida 3

Chapter 1

Introduction

This thesis focuses on the competency of oogonial stem cells derived from the adult mouse ovary to enter meiosis and produce oocytes *in vitro*. Therefore, in this introduction I will provide a review on a number of topics required to understand this project. I will give an insight into the dynamics of the female mammalian germline, and of the genetic and metabolic pathways for germ stem cells and oocytes using the murine developmental timing. I will then explain the importance of the oogonial stem cells in assisted reproduction technologies, methods to obtain them and current knowledge on their differentiation into oocyte-like cells. I will also introduce the controversy around their existence in the adult ovary.

1.1 General Considerations of the Female Mammalian Germline

The follicle defines the functional unit that guarantees fertility in female Metazoans. In the mammalian ovary, it consists of an oocyte at different stages of meiosis protected by a variable number of layers of granulosa cells, in what is called the cumulus-oocyte complex (Fig. 1.1) (Oktem and Urman, 2010). The cell layers within the follicle have the ability to grow, differentiate and mature independently and in response to paracrine and endocrine factors as soon as the female mammal reaches sexual maturation (Dokshin et al., 2013; Edson et al., 2009; McGee and Hsueh, 2000; Oktem and Urman, 2010; Peters, 1969). In preovulatory stages, an outer layer of theca cells, a space filled with follicular fluid called antrum and the zona pellucida that surrounds the fully-grown oocyte complete the functional unit and prepare it for ovulation and fertilisation (Fig. 1.1) (Oktem and Urman, 2010).

The current dogma in reproductive biology is that the mammalian postnatal ovary contains a fixed reserve of follicles that are depleted throughout the fertile life (Zuckerman, 1951). In women, the complete follicle depletion initiates menopause at around 45-50 years old (Zuckerman, 1951), but the reserve of follicles can be compromised earlier in life by other factors (Fig. 1.1): premature ovarian failure, polycystic ovary syndrome, endometriosis, lack of gonadotropic receptors, mutations in the germline, environmental insults – chemotherapy and endocrine disruptors as an example –, lifestyle and advanced

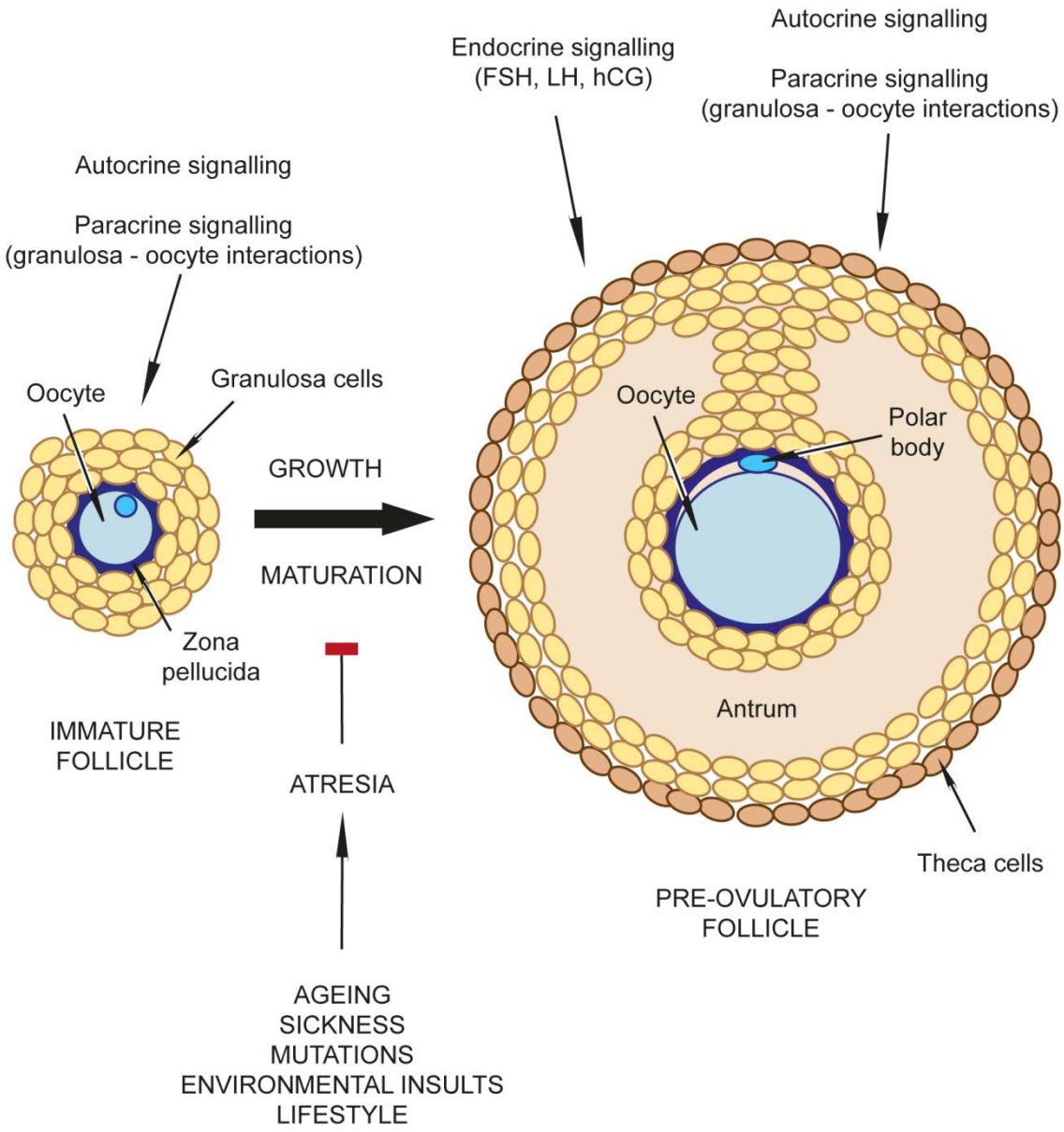

Figure 1.1. Development of the follicle. Diagram showing the development of the cumulus-oocyte complex by inner and outer metabolites, together with the factors that can cause its death by atresia.

maternal age (Comim et al., 2013; Franks et al., 2008; Hamdan et al., 2016; Jones and Lopez, 2013; Meldrum et al., 2016; Morgan et al., 2012; Poulton et al., 2010).

Nowadays, assisted reproduction, cryopreservation of ovarian tissue, *in vitro* maturation of follicles and mitochondrial donation comprise the only possibilities to make the most of this limited reserve of gametes and produce healthy offspring genetically related to the female patient (Barritt et al., 2001; Fulka et al., 2009; Jones and Lopez, 2013; Legro, 2016; Meldrum et al., 2016; Poulton et al., 2010).

1.2 Determination of Primordial Germ Cells in the Mouse Embryo

Primordial germ cells (PGCs) are unipotent precursors of oocytes and sperm (Matsui and Okamura, 2005). In the mouse their precursors differentiate from embryonic day 5.5 (E5.5) in the posterior epiblast (Fig. 1.2; Fig. 1.3) (Chang et al., 2002; Hayashi et al., 2007). This epiblast provides the essential factors and environment for this early determination (Hayashi et al., 2007; Lawson et al., 1999). PGCs first appear in the mouse at E7.5 in the hindgut (Fig. 1.2; Fig 1.4) (Chang et al., 2002; Hayashi et al., 2007).

1.2.1 Role of Bone Morphogenetic Factors

The establishment of PGCs in inferior Metazoans, such as *Caenorhabditis elegans* and *Drosophila*, depends on maternal factors for totipotency stored in the zygote (Strome and Lehmann, 2007). In mammals, this competence relies on the expression of inductive signals produced by the extraembryonic ectoderm (ExE) and visceral endoderm (VE) that surround the posterior epiblast (Fig. 1.3) (Hayashi et al., 2007).

This signalling cascade starts in the embryo mouse at E5.5–E6.0 (Fig. 1.2; Fig. 1.3). Epiblast cells are by then increasing their expression of *Smad1* and *Smad5* (Fig. 1.3B) (Matsui and Okamura, 2005; Okamura et al., 2005). These proteins are receptor-regulated transcription factors that respond to extracellular transforming growth factor beta (TGF-β) superfamily signalling proteins (Kingsley, 1994; Wharton and Derynck, 2009). Here, the TGF-β proteins are the ExE-expressed bone morphogenetic factors BMP4 and BMP8b (Matsui and Okamura, 2005) and the VE-expressed BMP2, which initiate the differentiation of PGC-like cells as homodimers in a dose-dependent manner (Fig. 1.3B) (Lawson et al., 1999).

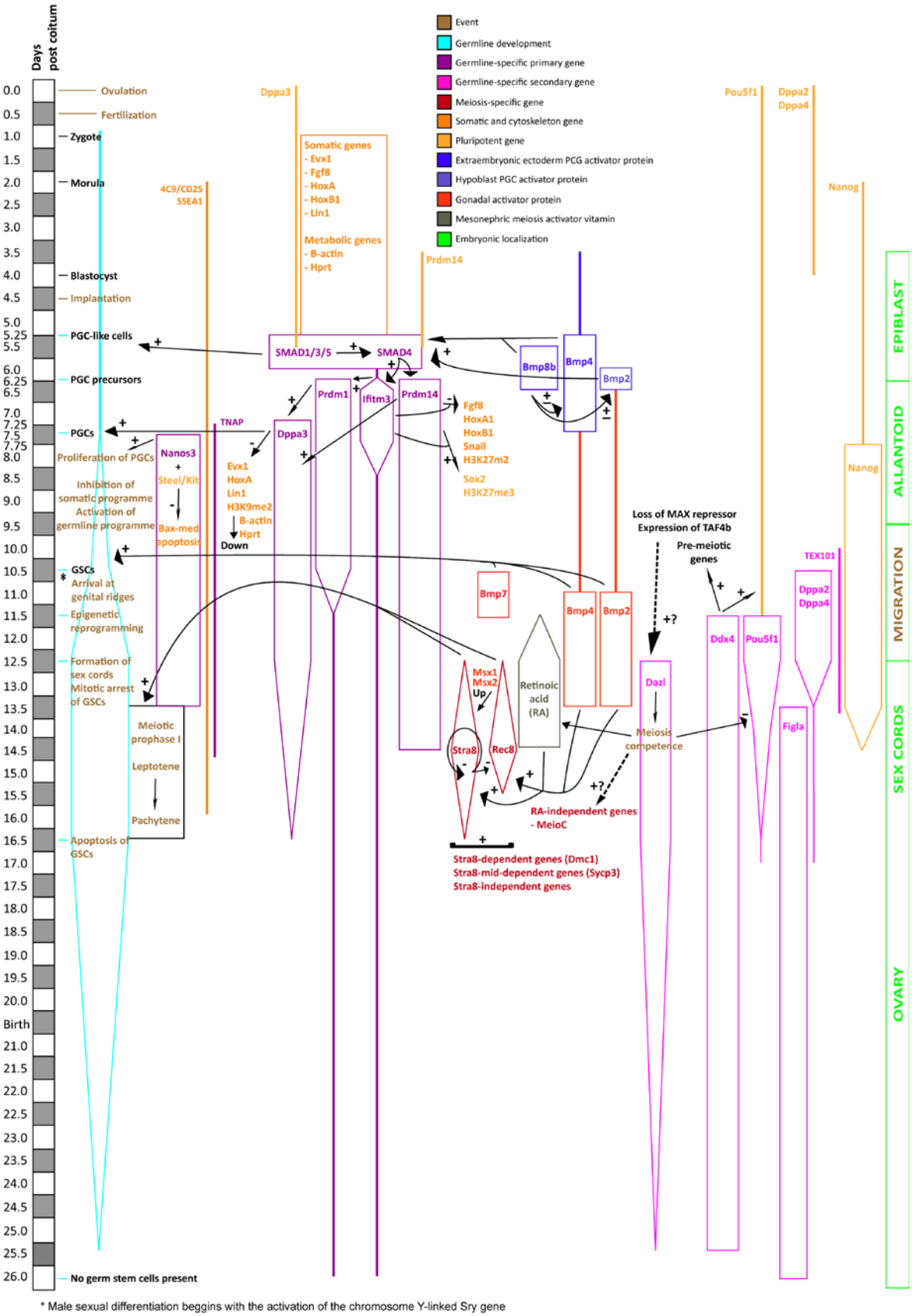

Figure 1.2. Gene expression pathways for the differentiation of the germline in mouse. Diagram showing the timing and functions of the genes involved in the determination of PGCs, GSCs and meiosis in the female mouse.

BMP8b modulates the expression of BMP4 and BMP2 in the ExE (Fig. 1.2; Fig. 1.3B) (Pesce et al., 2002; Ying et al., 2001), whereas BMP2 augments the effect of BMP4 (Ying and Zhao, 2001). Only BMP4 and BMP8b start the signalling cascade in the cell surface of cells in the epiblast (Fig. 1.3) through separate transmembrane BMP heteromeric receptors (Fig. 1.3B) (Ying et al., 2001). These heterodimers are formed by a type I and a type II receptor with intracellular serine/threonine kinases (Shi and Massagué, 2003). BMP type II receptor phosphorylates type I receptor, which in turns phosphorylates SMAD1 and SMAD5 in their C-terminal region (Fig. 1.3B) (Hayashi et al., 2002; Shi and Massagué, 2003). These transcription factors can then join SMAD4 to translocate into the nucleus and activate BMP-target genes (Fig. 1.2; Fig. 1.3B) (Chang and Matzuk, 2001; Chuva de Sousa Lopes et al., 2004b; Dudley et al., 2007; Pesce et al., 2002; Tremblay et al., 2001). The activation of this signalling cascade is dose-dependent, therefore, those cells in the epiblast that receive the highest doses of BMP4 and BMP8b are recruited as PGC precursors (Fig. 1.3A) (Lawson et al., 1999; Ying et al., 2000). These cells are not entirely committed to the germ line (Fig. 1.3A), since they can also differentiate into the extraembryonic pre-allantois, which will form the placenta (Matsui and Okamura, 2005).

Type I ALK2 receptor was believed to be crucial in supporting PGC formation (Chuva de Sousa Lopes et al., 2004a). However, the current hypothesis is that type I receptors BMPR1A and 1B and type II BMPR2 currently bind BMP4 and BMP8b to start the germline determination (Dudley et al., 2007; Ohinata et al., 2009).

Also elusive is the reason for the time window for the determination of PGC-like cells, which is very brief and specific of the posterior epiblast (Pesce et al., 2002; Yoshimizu et al., 2001). Transplantation of cells from other parts of the embryo into this specific region induces their transformation into PGCs, and suggests the requirement for a defined environment (Tam and Zhou, 1996). Mice knocked-out in *Smad1*, *Smad5*, *Bmp4* and *Bmp8b* all lack PGCs or have its population dramatically reduced, indicating an involvement at similar levels in the same physiological process (Chang and Matzuk, 2001; Matsui and Okamura, 2005; Ying et al., 2001). However, epiblast younger than E5.25 remains unaffected by BMP4 (Okamura et al., 2005), whereas epiblast older than E6.0 exposed to BMP4 and BMP8b has the PGC population deployed or dramatically reduced (Matsui and Okamura, 2005; Pesce et al., 2002; Ying et al., 2001). This suggests that the expression of *Smad1* and *Smad5* is ultimately responsible for the determination of the germline (Chang and Matzuk, 2001), but it could also be that the proto-oncogene protein WNT3 confers the epiblast the ability to respond to BMP4 (Ohinata et al., 2009).

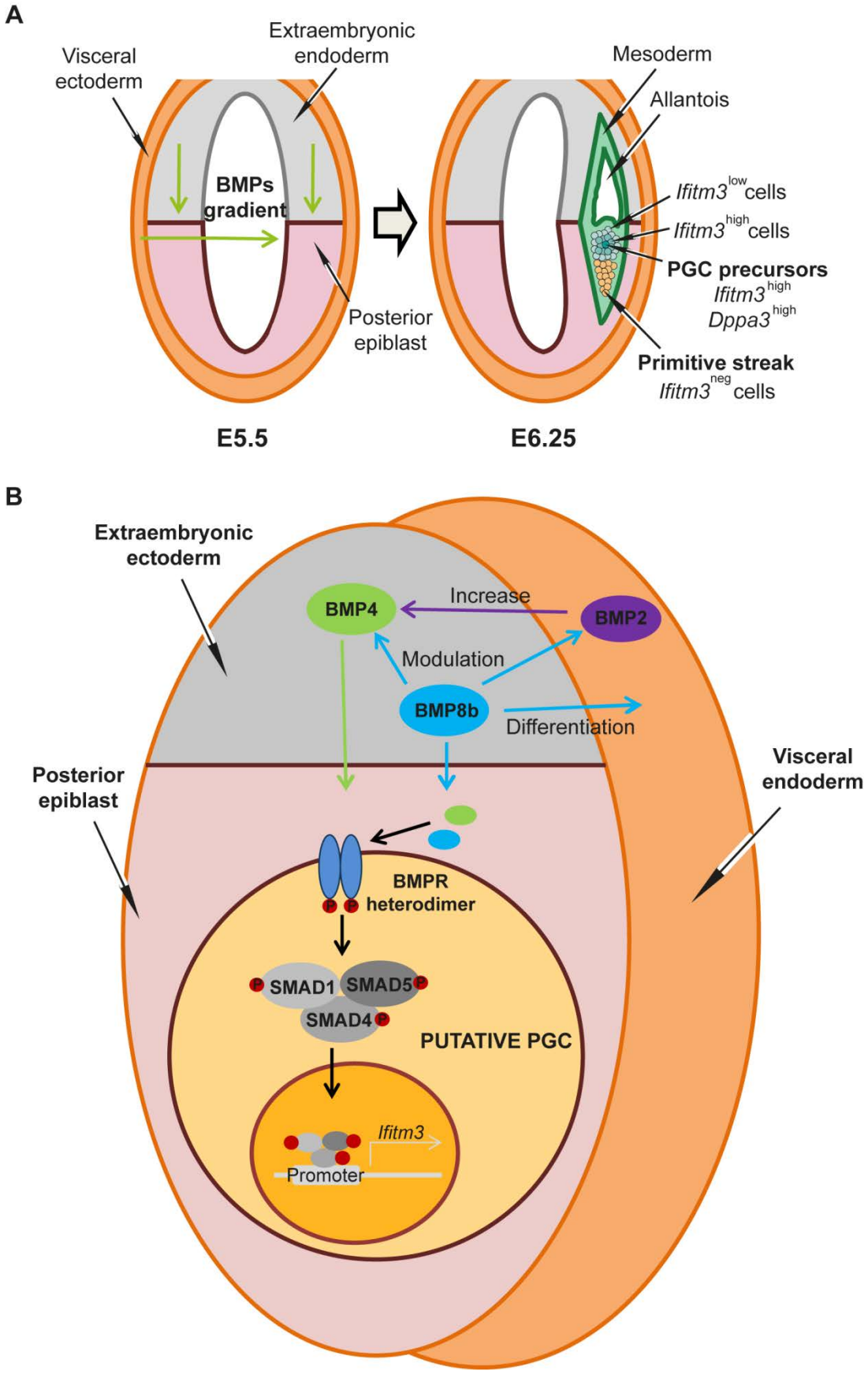

Figure 1.3. Determination of PGCs in the mouse embryo. (A) Site of formation of PGC precursors (in green) at E6.25 after induction by BMPs gradients. **(B)** Signalling pathway for the determination of putative PGCs in the proximal epiblast between E5.5 and E6.25.

Interestingly, BMP4 is maintained from here onwards (Fig. 1.2) possibly to promote the phenotypic maintenance of PGC, induce the founder population growth and control the number of PGCs through apoptosis (Childs et al., 2010b; Pesce et al., 2002; Ross et al., 2014).

1.2.2 Founding Primordial Germ Cells

At E6.25, interferon-induced transmembrane protein 3 gene (*Ifitm3/FRAGILIS*) is the first BMP-target gene to be expressed in those cells in the epiblast that receive the highest doses of BMP4 and BMP8b (Fig. 1.2; Fig. 1.3B) (Lange et al., 2003; Saitou et al., 2002). *Ifitm3*-positive cells congregate via cell-cell interactions in clusters in certain cell niches where PGC will be definitely formed (Matsui and Okamura, 2005; Tanaka et al., 2005). The cytoplasmic IFITM3 protein signal is strong enough in a restricted number of these PGC precursors to record an immediate activation from PR domain zinc finger protein 1 (*Prdm1*/*BLIMP1*) at E6.25 (Fig. 1.2) (Saitou, 2009; Saitou et al., 2002; Tanaka and Matsui, 2002). *Prdm1* is a nuclear pluripotency marker that identifies the first restricted PGCs (Lange et al., 2003; Tanaka et al., 2005) and downregulates the somatic mesodermal programme in them (Fig. 1.2) (Ohinata et al., 2005). Any other *Prdm1*-negative cells in the epiblast enter somatic differentiation (Ohinata et al., 2005).

Similarly at around E6.5 the PR/SET domain 14 gene (*Prdm14*/*PRDM14*) is expressed in PGC precursors (Fig. 1.2) (Yamaji et al., 2008). Mouse embryos knocked-out for *Prdm14* failed to acquire pluripotency and the corresponding epigenetic reprogramming, with cells failing to activate SRY (sex determining region Y)-box 2 (*Sox2*), reduce histones H3K9 dimethyl (H3K9me2) and H3K27 dimethyl (H3K27me2) and upregulate histone H3K27 trimethyl (H3K27me3) (Fig. 1.2) (Yamaji et al., 2008). It is likely that PRDM14 is stabilised in the chromatin at its target genes by oligomerized CBFA2T2, a co-repressor protein that ultimately determines the acquisition of pluripotency in PGCs (Tu et al., 2016).

Activation of developmental pluripotency-associated protein 3 gene (*Dppa3*/*STELLA*) at E7.25 by PRDM1 provides the ultimate master controller of germline fate (Fig. 1.2) (Hayashi et al., 2012b; Saitou et al., 2002; Sato et al., 2002; Xu et al., 2011b). *Dppa3* is a nuclear maternal transcript that represses the homeobox genes Hox responsible for the somatic cellular fate (Fig. 1.2) (Gehring and Hiromi, 1986; Sato et al., 2002), although its presence is dispensable in the germline determination (Bortvin et al., 2004; Saitou et al., 2002). Its absence compromises and even blocks the cleavage of pre-implantation embryos, and produces smaller litters than the expected (Bortvin et al., 2004). At this

embryonic stage, the posterior epiblast has developed into other embryonic layers. One of them is the allantois, where the PGCs allocate near the posterior hindgut (Fig. 1.4A).

The cell adhesion molecule E-cadherin is expressed together with *Ifitm3* in PGC precursors, and its blockage leads to inhibition of PGC differentiation (Okamura et al., 2003). It is possible that E-cadherin initiates an as yet unknown independent pathway, since in somatic cells it activates phosphatidylinositol 3-kinase (PI3K) and mitogen-activated protein kinase (MAPK) (Laprise et al., 2002; Pece et al., 1999). E-cadherin could also mediate interactions between IFITM3 and other cell surface molecules within the same cell or in neighbouring cells (Matsui and Okamura, 2005).

In summary, *Ifitm3*, *Prdm1*, *Prdm14* and *Dppa3* are the key primordial markers that determine the founding mouse PGCs at E7.5, and provide them with pluripotency, epigenetic reprogramming and repression of the mitotic fate (Fig. 1.2: Fig. 1.4A) (Chuva de Sousa Lopes and Roelen, 2008; Hayashi et al., 2012b; Lange et al., 2003; Saitou, 2009; Saitou et al., 2002; Sato et al., 2002; Tanaka and Matsui, 2002; Tanaka et al., 2005; Xu et al., 2011b; Yamaji et al., 2008).

1.2.3 Further Modifications and Migration Towards the Genital Ridges

PGCs present strong tissue non-specific alkaline phosphatase (*TNAP*/*Akp2*/*ALP*) activity (Fig. 1.2: Fig. 1.3A), consistent with an active Golgi complex (MacGregor et al., 1995; Saitou, 2009). Tracking of this enzyme in mouse showed that fewer than 10 PGS exist at E7.5, and that they proliferate to over 100 the following day at the base of the allantois near the hindgut (Fig. 1.4A) (Ginsburg et al., 1990). At the same time that this proliferation takes place, which is mediated by BMP7, BMP4 and BMP2 (Ross et al., 2007), the nuclear homeobox protein NANOG maintains pluripotency and self-renewal (Fig. 1.2) (Yamaguchi et al., 2009). *β-actin* and *Hprt* housekeeper genes expression decrease as well (Fig. 1.2), either because their cell cycle lengthens or their metabolic activity decreases (Saitou et al., 2002).

PGCs prepare for their migration towards the genital ridges at around E7.5, when β-catenin is downregulated. This in turn reduces E-cadherin, which causes the PGCs to lose adhesion and gain motility (Bendel-Stenzel et al., 2000; Di Carlo and De Felici, 2000). Shortly after, the genital ridges start to secrete the chemokine SDF1, which binds to to its specific receptor CXCR4 in PGCs, and attracts them towards the future gonads (Doitsidou et al., 2002; Molyneaux et al., 2003).

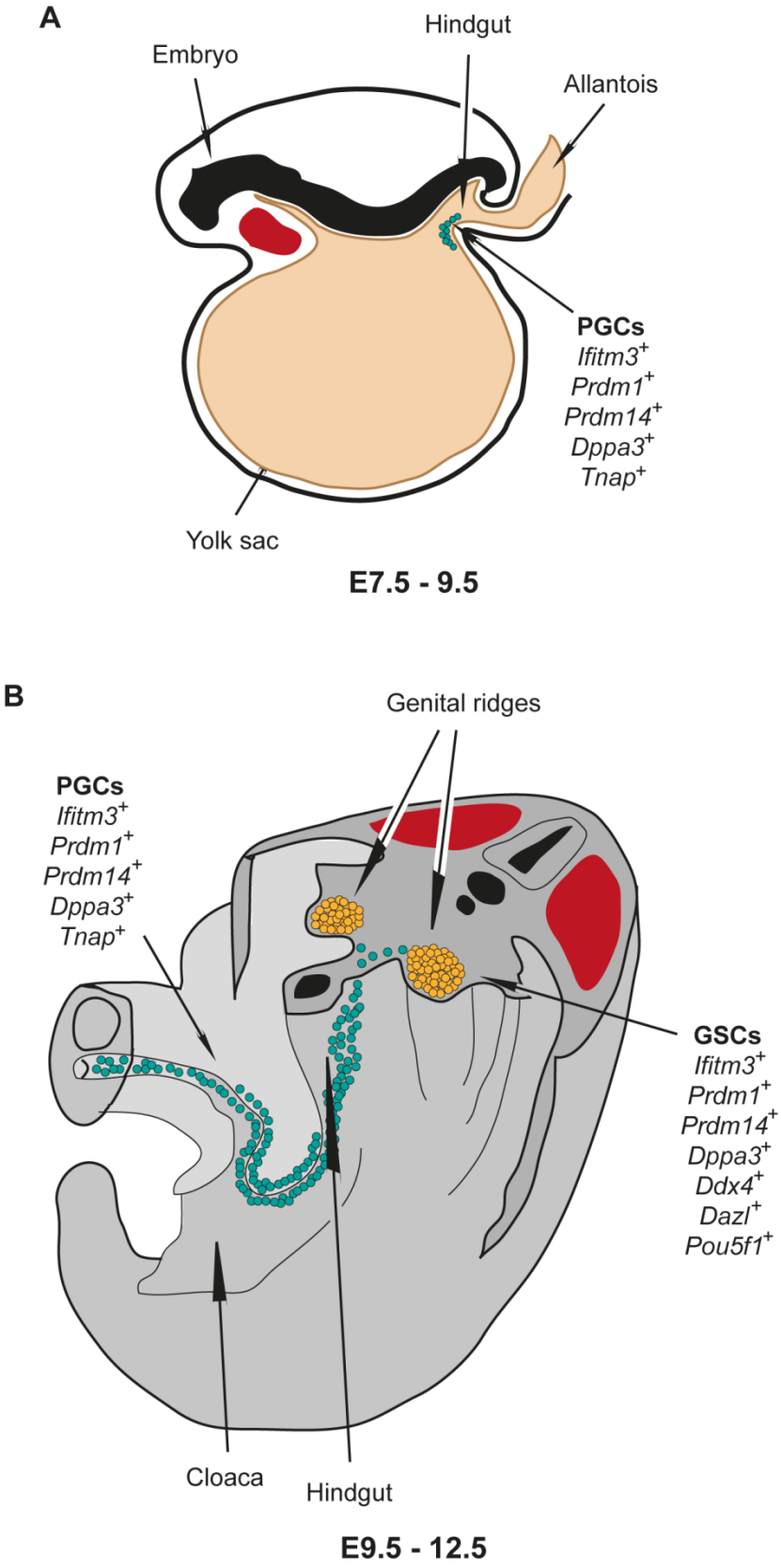

Figure 1.4. Migration of PGCs towards the genital ridges. (A) Site of formation and proliferation of PGCs (in green) at E7.5. **(B)** PGCs (in green) enter the embryo from the hindgut, and migrate though the hindgut until reaching the genital ridges, where they differentiate into germ stem cell cysts (in yellow).

PGCs migrate towards the genital ridges between E9.5 and E12.5 in a ‘travelling niche’ (Fig. 1.4B, in green) along the basal surface of the hindgut created by hindgut-secreted stem cell factor (*Steel*/*KitL*) and its receptor *cKit* in PGCs. Here, the KITL factor controls the proliferation and motility of each PGC individually (Gu et al., 2009; Gu et al., 2011), but also cell survival by inhibiting BAX-dependent apoptosis with the aid of NANOS3 and DND1 (Fig. 1.2) (Cook et al., 2009; Runyan et al., 2006; Suzuki et al., 2008).

The initiation of this migration and the driving into the genital ridges is also attributed to other factors: the extension of processes from the cell surface that physically link PGCs into extensive networks (Gomperts et al., 1994); a low adherence to and a high ability to translocate within a compact extracellular matrix rich in fibronectin, laminin and collagen IV (De Felici et al., 1992; García-Castro et al., 1997); an interaction between the PGC cell surface galactosyltransferase and glycosyl acceptors in the path (Bandyopadhyay et al., 2004); and the regulations of the insulin growth factor IGF/igf2b migration signalling pathway (Sang et al., 2008), and that of the G protein c subunit 1 and Hedgehog Gγ1/Hh attractant pathway (Deshpande et al., 2009). Also involved could be cell surface markers that are internalised once PCGs are safely deposited in the genital ridges as it happens with the protein 4C9/CD25 (Yoshinaga et al., 1991).

The PGCs enter the embryo from the hindgut and establish in the genital ridges (Fig. 1.4B, in yellow) at E11.5 – E12.5 (Chang et al., 2002). It is possible that the network formed by cell surface processes has an important role in the attraction and accumulation of PGCs in the genital ridges, although the processes disappear when the cells acquire non-motile and non-adherent characteristics (Gomperts et al., 1994).

1.3 Determination of Female Germ Stem Cells

1.3.1 Formation of Intercellular Bridges in Germ Cells

Once the PGCs attach to the genital ridges, which will give rise to the sex cords (Fig. 1.2: Fig. 1.4B), they start to differentiate into oogonia, female germ stem cells (GSCs), through an active mitosis (Fig. 1.2; Fig. 1.4B, in yellow) (Pepling and Spradling, 1998; Tam and Snow, 1981). The nucleus decondenses to facilitate access to DNA, and acquires a fibrillar nucleolus and granular aspect, whereas the number of mitochondria increases (Baker and Franchi, 1967).

However, the oogonium does not fully complete cytokinesis, and oogonia end up interconnected by cytoplasmic bridges (Mork et al., 2012a). Through synchronous division they form groups of around 30 multinucleated syncytial clones called cysts (Fig. 1.4, in yellow) (Pepling and Spradling, 1998). Consequently, any signal propagates along the syncytium and provides a simultaneous initiation of meiosis (Lei and Spradling, 2016; Mork et al., 2012a; Oktem and Urman, 2010). Around 25,000 cells form the germline population by E13.5 in the mouse (Tam and Snow, 1981).

Interestingly, here again the BMP family plays an active role. *Bmp7* knockout mice presented reduced mitotic GSCs, therefore at this stage it is involved in the proliferation of oogonia (Fig. 1.2) (Ross et al., 2007). In addition, BMP2 and BMP4 upregulate to promote proliferation of oogonia and to prepare the selected oogonia to transition to oocytes (Fig. 1.2) (Chakraborty and Roy, 2015; Pellegrini et al., 2003).

1.3.2 Activation of Secondary Germline-specific Markers

During this proliferation oogonia produce many germline-specific proteins that modify mRNA in the cytoplasm (Fig. 1.4B). One of them is DEAD (Asp-Glu-Ala-Asp) box polypeptide 4 (*Ddx4*/*Mvh*/*Vasa*) (Fig. 1.2) a cytoplasmic ATP-dependent RNA helicase that provides germ cell proliferation and maintenance possibly through activation of other pre-meiotic genes (Castrillon et al., 2000; Fujiwara et al., 1994; Medrano et al., 2012; Tanaka et al., 2000; Toyooka et al., 2000). Although *Ddx4* knockout female mice are fertile, their male counterparts present germline apoptosis and meiotic blockage that leads to infertility (Tanaka et al., 2000). The reason for this is that DDX4 is involved in the RNA-silencing pathway of spermatogenesis (Bernstein et al., 2001; Kotaja et al., 2006). On the other hand, deleted in azoospermia-like (*Dazl*) (Fig. 1.2) is a RNA-binding protein that performs post-transcriptional modifications in pre- and post-meiotic mRNA (Reynolds et al., 2005) and epigenetic reprogramming of GSCs (Haston et al., 2009). Through studies in knockout mice it has been reported to be indispensable for the meiotic activation in both sexes (Koubova et al., 2014).

Also expressed from here onwards is a POU class 5 homeobox 1 (*Pou5f1*/*OCT4*) isotype with a germline-specific distal enhancer (Fig. 1.2) (Yeom et al., 1996). This is a maternal homeodomain transcription factor involved in the self-renewal and pluripotency of the germline by modulating the expression of pluripotency and differentiation factors (Masui et al., 2007; Niwa et al., 2000; Zuccotti et al., 2009b; Zuccotti et al., 2012). Similar

to PRDM14, POU5F1 also requires CBFA2T2 to gain stabilisation in the chromatin at its target genes (Tu et al., 2016).

Interestingly, some markers are only expressed within this brief window of proliferating oogonia, and until their commitment to oogenesis or apoptosis (Fig. 1.2). Such is the case of developmental pluripotency-associated 2 and 4 (*Dppa2* and *Dppa4*), which contain SAP motifs for the control of RNA transcription and processing (Maldonado-Saldivia et al., 2007), and testis expressed 101 protein (*Tex101*), a cell surface glycoprotein with unknown function in the female GSCs, but essential for sperm motility (Fujihara et al., 2014). It is likely that the three are involved in the maintenance of a pluripotent status in the oogonium, and that their downregulation is essential for the cell to commit to meiosis and initiate oocyte differentiation (Fujihara et al., 2014; Maldonado-Saldivia et al., 2007).

1.4 Meiosis and Folliculogenesis

Oogenesis and spermatogenesis consist on the reductive nuclear division of a diploid germ stem cell to create four haploid daughter cells. In female mammals, meiosis is accompanied by the development of the follicle and requires two periods of arrest (Fig. 1.5) (Bowles and Koopman, 2007). In the first period, the primary oocyte is arrested in diplotene of prophase I until the follicle is selected to grow (Fig. 1.5). In the second arrest, the fully-grown oocyte stays in metaphase II until it is ovulated and fertilised (Fig. 1.5). The two small daughter cells, so-called polar bodies, accompanying each asymmetric meiotic division will undergo atresia (Fig. 1.5) (Bowles and Koopman, 2007).

1.4.1 Role of Retinoic Acid

Meiosis in female mice occurs between E12.5 and E16.5 (Fig. 1.2), but its induction requires the previous expression of *Dazl*. DAZL allows oogonia to respond to all-trans retinoic acid (RA) (Fig. 1.2; Fig. 1.6) (Soh et al., 2015). How this happens is unknown, but it is possibly thanks to a meiotic and oogenic gene network modulated by TAF4b (Grive et al., 2016) and to the loss of expression of the MAX repressor (Fig. 1.2) (Suzuki et al., 2016). Also essential is that WNT4/β-catenin tandem promotes the synthesis of the female differentiation factor follistatin (Mizusaki et al., 2003), which leads to the accumulation of RA by downregulating the retinoic acid metabolizing protein CYP26B1 (Bowles et al., 2006).

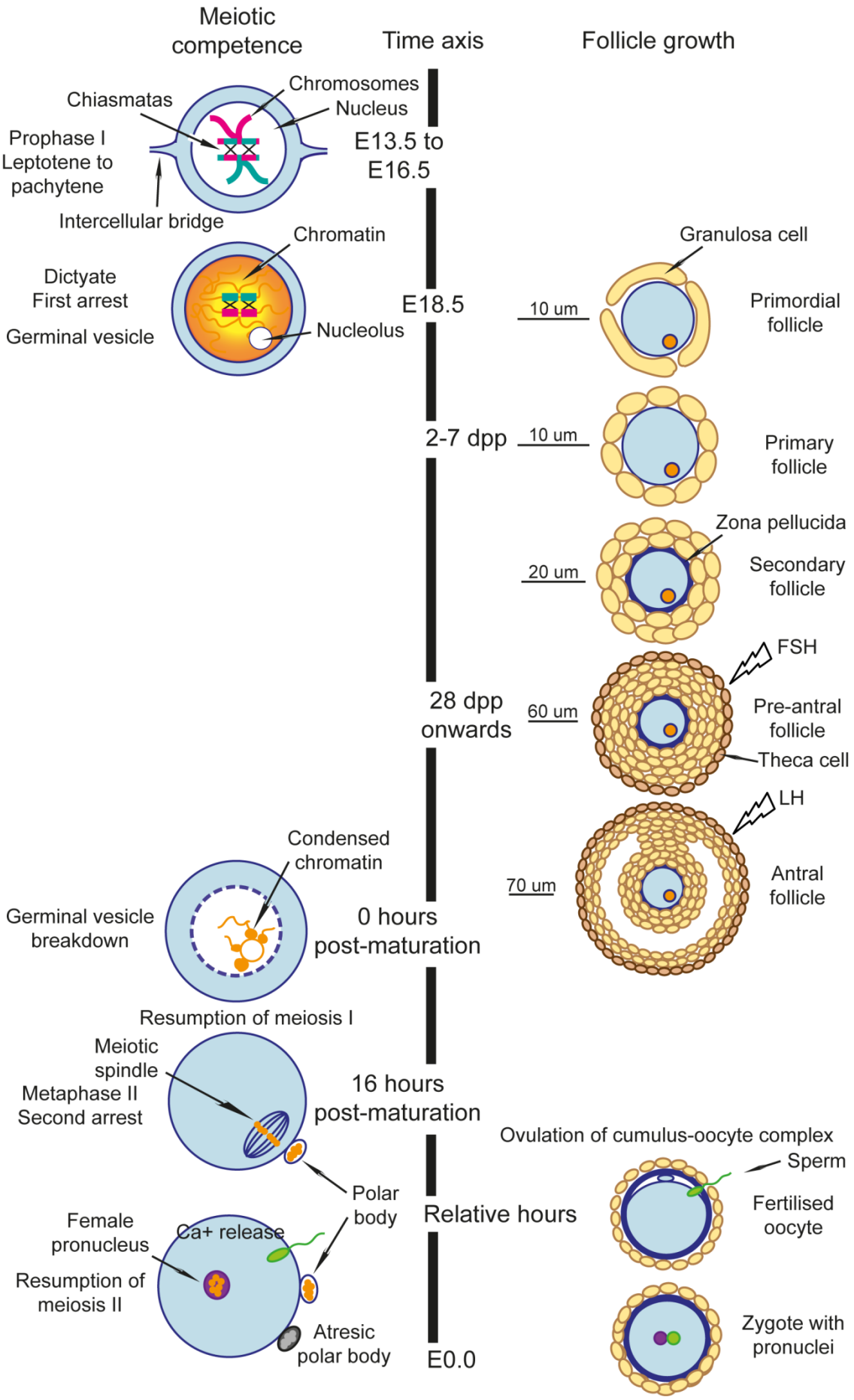

Figure 1.5. Oocyte and follicle development in the female mouse.

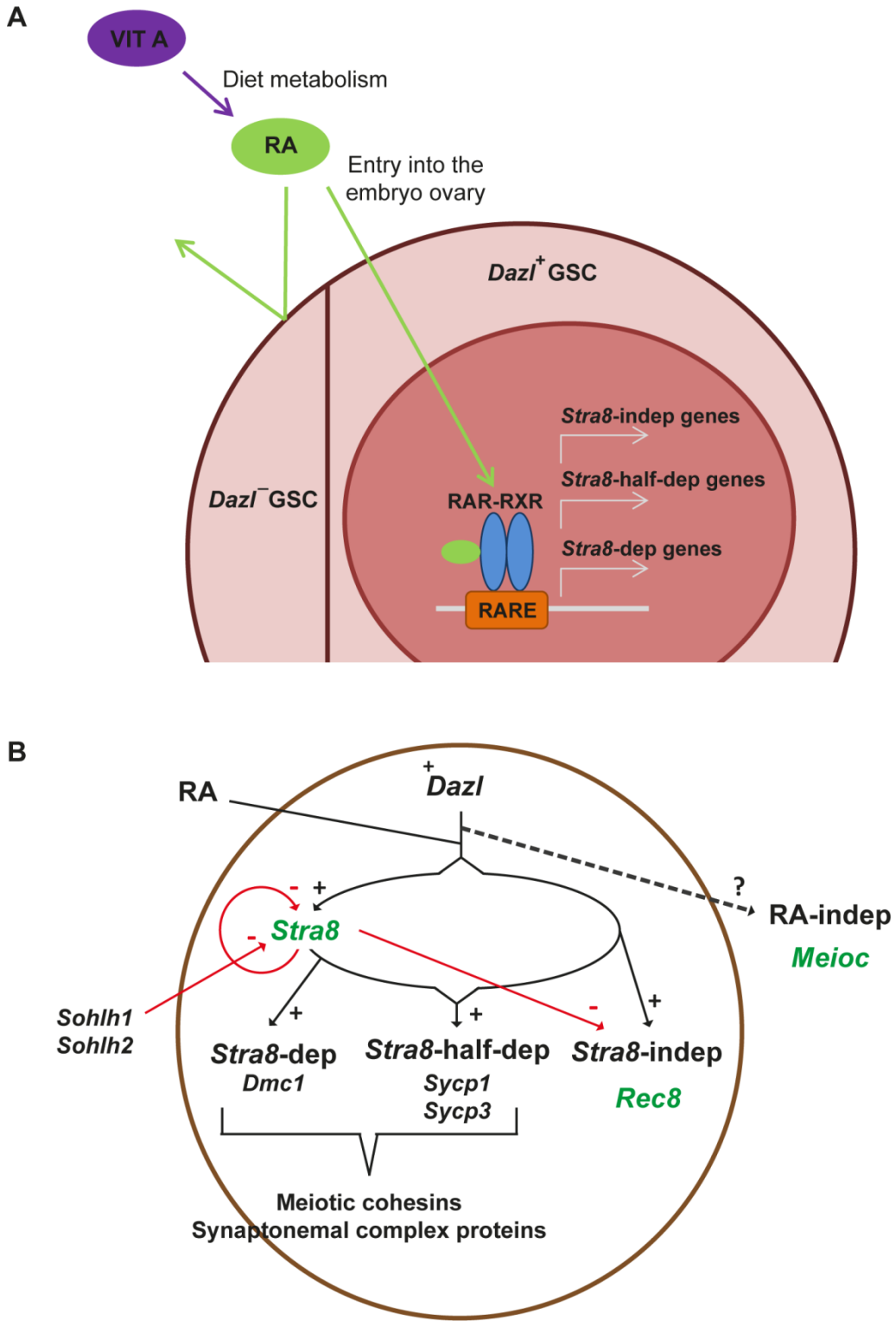

Figure 1.6. Onset of meiosis in mouse embryonic ovary. (A) Diagram showing the effect of retinoic acid in *Dazl*-positive and *Dazl*-negative germ stem cells. **(B)** Diagram showing the multiple pathways required for the onset of meiosis. Adapted from Soh et al., (2015).

RA binds in the nucleus to three all-trans retinoic acid receptor isotypes (RARα, β and γ) (Fig. 1.6A), which in turn heterodimerize with one of the isotypes of retinoid X receptor (RXRα, β and γ) and bind the retinoic acid response element (RARE) (Fig. 1.6A) (Pöpperl and Featherstone, 1993). This complex can open and access the chromatin to activate genes of interest (Fig. 1.6A) (Bastien and Rochette-Egly, 2004).

RAR isotypes have only been studied in the male mouse, with *Rarα* and *γ* having important and redundant roles in GSC proliferation and differentiation (Gely-Pernot et al., 2012; Ikami et al., 2015; Law, 2013; Li et al., 1993; Lufkin et al., 1993). Although both switch on the expression of *stimulated by retinoic acid 8* (*Stra8*) gene, *Rarα* is the only receptor indispensable for the premeiotic differentiation of type A spermatogonia and the progression of spermatogenesis (Chung et al., 2004; Doyle et al., 2007; Gely-Pernot et al., 2012), providing increased germ cell apoptosis and few abnormal spermatozoa that caused infertility in adult knockout male mice (Lufkin et al., 1993). *Rarα* also resolves homozygous double strand breaks during meiosis (Law, 2013). On the other hand, the identity of the RXR remains unknown, but none of the RXRα, β and γ knockout mutant male mice have exhibited sterility due to lack of meiosis (Kastner et al., 1996; Krezel et al., 1996; Sucov et al., 1994). However, it is unknown if the same isotypes take part in the female meiosis, given that its time frame is different from that of the male mouse.

1.4.2 Onset of Meiosis

RA induces three meiotic prophase pathways coordinated by *Stra8* and REC8 meiotic recombination protein (*Rec8*) genes: dependent, partially dependent and independent from *Stra8* pathways (Fig. 1.2; Fig. 1.6). The *Stra8*-independent pathway is the first to activate, and stores meiotic structural proteins required by the chromosomal programme, which is regulated by *Stra8* and activates the last (Soh et al., 2015).

STRA8 leads the DNA replication and meiotic prophase, produces meiotic cohesion of the chromosomes, forms the synaptonemal complex through the synaptonemal complex protein 3 (*Sycp3*), and allows progression of meiosis under the control of the endonuclease SPO11 and the recombinase DMC1 (Fig. 1.6B) (Anderson et al., 2008; Baltus et al., 2006; Bowles and Koopman, 2007). BMP4 stimulates and increases the muscle segment homeobox-like genes *Msx1* and *Msx2* to maintain *Stra8* expression (Fig. 1.2) (for a review see Le Bouffant et al., 2011).

In the later stages of the meiotic prophase, *Stra8* downregulates itself and *Rec8* (Fig. 1.2; Fig. 1.6) to ensure that the chromosomal programme is activated only once in each oogonium, which protects the future oocytes from polyploidy (Soh et al., 2015). *Stra8* could also be downregulated by spermatogenesis and oogenesis specific basic helix-loop-helix SOHLH1 and SOHLH2 (Fig. 1.6) (Desimio et al., 2015). Meiosis-induced oogonia become refractory to further waves of RA (Soh et al., 2015).

Very recently, a meiotic pathway mediated by meiosis specific with coiled-coil domain protein (*MeioC*) that does not require STRA8 signalling or RA has been reported (Fig. 1.2; Fig. 1.6B) (Abby et al., 2016). MEIOC stabilizes meiotic transcripts and prevents their degradation (Abby et al., 2016), but its interaction with STRA8 and REC8 is unknown.

1.4.3 Prophase I, Chromosome Recombination and First Meiotic Arrest

Prophase I of meiosis comprises five stages: leptotene, zygotene, pachytene, diplotene and diakinesis At leptotene, the axial element forms along already duplicated chromosomes, formed by two sister chromatids (Page and Hawley, 2004a). Chromosomes are condensing into recognisable meiotic X-shapes and pair with their homologues (Zickler and Kleckner, 2015a).

During zygotene, paired chromosome homologs align and bind the synaptonemal complex. This is a protein filament structure that runs along the axial elements of the chromosomes (Page and Hawley, 2004b; Schramm et al., 2011). Its formation and function is controlled by SYCP3 (Yuan et al., 2000; Yuan et al., 2002)

At pachytene, the synaptonemal complex is fully formed (Fig. 1.5) (Page and Hawley, 2004b). Importantly, the non-sister chromatids of each homologous pair physically link and form bivalent chromosomes. These bivalents exchange DNA through chiasmata (Fig. 1.5), which allow genetic variation in the offspring (Zickler and Kleckner, 2015b). This meiotic recombination requires the formation and repair of double-strand breaks in the DNA (Zickler and Kleckner, 2015b), which is mediated first by the topoisomerase SPO11 (Keeney and Neale, 2006) and then by the exonuclease MEIOB (Luo et al., 2013; Souquet et al., 2013).

Last, at diplotene the synaptonemal complex degrades and the bivalents partially uncoil to allow for some DNA transcription (Fig. 1.5). It is here, at E20.0 where the first arrest takes place in the oocyte (Fig. 1.5), and is maintained until puberty with the onset of the menstrual cycle (Kerr et al., 2013). Low maturation promoting factor (MPF), a CDK1-

cyclin B1 kinase also involved in the M-phase of mitosis, is responsible for this arrest (Jones, 2004; Jones, 2005). This quiescent stage is also known as dictyate (Fig. 1.5), and is used to accumulate maternally inherited mRNA, perform essential mRNA translation, acquire epigenetic modifications and repair DNA damage (Bernstein et al., 2011; Kageyama et al., 2007; Liu and Aoki, 2002; Ma et al., 2013)..

1.4.4 Formation of Germinal Vesicle Oocytes and Perinatal Apoptosis of Female Germ Stem Cells

Shortly after meiosis activates in a few selected cells its sister germ cells act as 'nurse cells' and send cytoplasmic organelles and components towards the egg precursors. This acquisition of extra components could allow the oocyte to grow up to 70 µm and to maintain a good quality (Grive et al., 2016; Wang et al., 2017). These precursors are by now arrested at dictyate stage and have developed a Balbiani body (Lei and Spradling, 2016; Pepling and Spradling, 1998; Pepling and Spradling, 2001).

The Balbiani body is a perinuclear cloud of mitochondria and endoplasmic reticulum that enclose Golgi elements (Pepling et al., 2007; Wessel, 2012). In the mouse it is present in oocytes still attached to germline cysts and in the primordial follicle (Pepling et al., 2007). It may accumulate RNA transferred from the 'nurse cells' thanks to the presence of Trailer Hitch protein (*Tral*). This RNA may enrich the oocyte with reprogramming and protective factors against transposition (Pepling et al., 2007).

The egg precursors develop into germinal vesicle (GV) oocytes upon removal of intercellular bridges and inactivation of the nucleus (McGee and Hsueh, 2000; Wang et al., 2017). Non-meiotic oogonia undergo apoptosis and die between E20.5 and 5 days *post-partum* (dpp) in the mouse (Pepling and Spradling, 2001), erasing any presence of GSCs from the ovary (Fig. 1.2) (Abir et al., 2002; Baker and Franchi, 1967).

Selection of oogonia for apoptosis is not well understood, but their lack of Balbiani body could be a biomarker of removal (Pepling et al., 2007). Another biomarker could be partitioning-defective protein (*Par6*) (Wen et al., 2009), which is involved in the polarity of cytoplasmic components (Macara, 2004). This nuclear protein is exclusive in mouse oocytes between E17.5 and 3 dpp, and could protect meiotic cells from undergoing apoptosis as their *Par6*-negative 'nurse cells' are destroyed (Wen et al., 2009)..

1.4.5 Primordial Follicle Assembly and Establishment of Follicle Reserve

To guarantee its survival, the oocyte must attract pregranulosa cells to organise into a single layer and define the primordial follicle (Fig. 1.5) (Kerr et al., 2013). Pregranulosa cells are believed to derive from the ovarian surface epithelium, although they are not truly epithelial cells (Mora et al., 2012). The asembly process is not fully understood, but seems to be driven by factors such as TAF4B (Grive et al., 2014) and oocyte-somatic bidirectional pathways that are also implicated in oocyte survival, with some explained below.

Oocyte-derived TGF-β activin A decreases the expression of *KitL* in pregranulosa cells. This supresses oocyte-pregranulosa bidirectional communication, inhibits granulosa differentiation and avoids a premature follicle assembly until oocytes are mature enough (Childs and Anderson, 2009; Coutts et al., 2008). Activin A then regulates the expression of the neurotrophin *Ntf5* in murine pregranulosa cells, possibly to enhance follicle formation, growth and survival (Childs et al., 2010a). Last, the WNT4/β-catenin pathway downregulates activin A and E-cadherin, which causes germinal cyst breakdown and activation of JNK kinase and oestrogen receptors essential in follicle assembly (Coutts et al., 2008; Kipp et al., 2007; Liu et al., 2010; Niu et al., 2016).

Binding of surface protein JAGGED1 in pregranulosa cells with NOTCH2 receptor in oocytes attracts pregranulosa cells and establishes identity and proliferation of granulosa cells (Trombly et al., 2009). NOTCH2 also causes germ cell nest breakdown (Xu and Gridley, 2013) possibly by upregulating the transcription factors *Hes1* and *Hey2* in oocytes and pregranulosa cells (Trombly et al., 2009).

The germ cell-specific factor in the germline alpha (*Figα*) also plays a role in follicle assembly, although the factors that it modulates are still unknown (Soyal et al., 2000). FIGα knockout female mice lose most of their oocytes due to inability to assemble primordial follicles (Bayne et al., 2004; Soyal et al., 2000).

The surviving pool of 8,000 primordial follicles forms the mouse ovarian reserve of potentially fertilisable oocytes at sexual maturation. Interestingly, two classes of primordial follicles exist in the newborn ovary given the sequential expression of forkhead box L2 (*Foxl2*) in their granulosa cell precursors (Mork et al., 2012b). In mice, the first class arises from *Foxl2*-negative cell precursors that migrate from the ovarian epithelium towards the ovarian medulla between E11.5 and E14.5, and assemble before birth (Mork et al., 2012b). This is the first follicular wave to grow and be ovulated, and contribute to fertility up to the

early adulthood (Zheng et al., 2014). The second class of primordial follicles arises from *Foxl2*-negative granulosa cell precursors in the ovarian cortex between E15.5 and 4 dpp, and assemble postnatally (Mork et al., 2012b). Such second wave gradually replaces the exhausting pool of medullar follicles, and becomes the sole source of follicles from early adulthood until the end of the fertile life in mice (Zheng et al., 2014).

Those oocytes unable to assemble into follicles undergo atresia and are lost dramatically (Peters, 1969). Oocyte atresia is not well studied, and may occur due to: failure of meiosis; unrepaired DNA damage; insufficient pregranulosa cells; and failure during restructuration of germline cysts into individual oocytes (Kerr et al., 2013). DNA damage-induced apoptosis is initiated through activation of the oocyte-specific TAp63α, an homologue of the p53 tumour supressor that transcriptionally induces *Puma* and *Noxa*. These in turn activate the proapoptotic *Bax* and *Bak* and inhibit BCL-2 prosurvival factors (Kerr et al., 2012; Suh et al., 2006). Proliferating cell nuclear antigen (PCNA) has also been observed to upregulate *Bax* and *Bak*, as well as other proapoptotic factors such as caspase-3 and TNFα (Xu et al., 2011a).

1.4.6 Primary to Pre-antral Follicle Growth

From 3 dpp onwards, primordial follicles periodically overcome the oocyte-, granulosa- and proximal follicle-derived inhibitory signals that maintain them in a dormant stage (Adhikari and Liu, 2009; Da Silva-Buttkus et al., 2009; Reddy et al., 2010). As a result, they develop independently of gonadotropins and form a pool of primary, secondary and pre-antral follicles (Fig. 1.5) (Oktem and Urman, 2010).

During early folliculogenesis, granulosa-oocyte bidirectional communication continue through gap, adherens and heterophilic junctions (Anderson and Albertini, 1976; Mora et al., 2012). SOHLH1 is essential in the transition from primordial to primary follicle and activates many important transcription factors: *Lhx8*, newborn ovary homeobox protein (*Nobox*), *Figα* and zona pellucida proteins (*Zp1-3*) (Pangas et al., 2006). NOBOX specifies the postnatal oocyte-specific gene expression and allows the GV oocyte to increase in size up to 70 µm (Rajkovic et al., 2004). The zona pellucida is formed under the influence of FIGα as soon as oocyte growth starts (Liang et al., 1997; Wassarman and Josefowicz, 1978). Meanwhile, granulosa cells acquire a cuboidal shape and proliferate to form several layers to transition from primary to secondary follicle (Fig. 1.5) (Fortune et al., 2000; McGee and Hsueh, 2000), after modulation by oocyte-specific growth differentiation

factor-9 (*Gdf9*) (Dong et al., 1996) and BMP15 (Fenwick et al., 2013). The outer is the thecal cell layer.

Interestingly, thecal cells express luteinizing hormone (LH) receptors that allow for a small production of androgens. They in turn activate the production of follicle-stimulating hormone (FSH) receptors in granulosa cells (Eppig et al., 2002; Sen et al., 2014; Young and McNeilly, 2010). Gonadotropins FSH and LH are released at small pulses by the hypothalamic-pituitary-gonadal axis (see Section 1.4.7). FSH is essential in the development of primary to pre-antral follicles (Meduri et al., 2008; Sen et al., 2014). Anti-Müllerian hormone (AMH) synthesised by granulosa cells inhibits FSH to prevent recruitment of large numbers of primary follicles (Durlinger et al., 2002).

Other paracrine and autocrine pathways from oocytes, stroma and somatic cells help in granulosa proliferation, oocyte development and maintenance of the dictyate arrest (Eppig, 1991; Oktem and Urman, 2010; Pincus and Enzmann, 1935). This pool of growing follicles faces further atresia checkpoints, with a much more reduced mouse strain-dependent final population (Johnson et al., 2004; Kerr et al., 2013; Peters, 1969).

1.4.7 Graafian Follicles, Germinal Vesicle Breakdown and Second Meiotic Arrest

At 21 dpp sexual maturation takes place in mice, when the current follicle pool is less than 2,500 (Kerr et al., 2013). From here onwards, the hypothalamic-pituitary-gonadal axis regulates the menstrual cycle. It starts when the anterior hypothalamic neurons release pulses of gonadotrophin-releasing hormone (GnRH). The hormone binds to GnRH receptors in gonadotropic cells, endocrine cells in the anterior pituitary gland. Here, GnRH regulates production and pulse release into the bloodstream of FSH and LH (Kumar and Boehm, 2013).

To prepare for ovulation, the pre-antral follicle matures into Graafian follicle (Fig. 1.5). Increasing quantities of FSH form the preantral cavity, which is filled with follicular fluid, whereas the thecal layer vascularises and increases production of androgens in response to LH. These androgens are transformed intro oestrogen – progesterone and oestradiol – by granulosa cell-based FSH-dependent aromatases (Knight and Glister, 2006; Oktay et al., 1997; Oktem and Urman, 2010; Young and McNeilly, 2010). As more thecal-derived androgens are transformed, higher levels of oestradiol are present in the bloodstream (Young and McNeilly, 2010). This causes a sudden high LH surge and a minor FSH peak from the anterior pituitary gland, that reaches the Graafian follicle and triggers germinal

vesicle breakdown (GVBD) in the oocyte, expansion of cummulus-oocyte complex (COC) and ovulation of COC from the ovary (Fig. 1.5) (Christensen et al., 2012; Mattioli and Barboni, 2000; Sun et al., 2009; Vaccari et al., 2009).

The oocyte resumes meiotic progression through a MAP kinase-dependent closure of gap junctions between granulosa cells and oocytes, which in turn decreases the granulosa-to-oocyte difussion of cyclic guanosine monophosphate (cGMP) (Norris et al., 2008; Shuhaibar et al., 2015; Vaccari et al., 2009). Consequently, a reduction of the cGMP pool in the oocyte allows for cyclic adenosine monophosphate (cAMP) hydrolysis in the cytoplasm. This cAMP decrease inactivates cAMP-dependent protein kinases A, which in turn allows the activity of MPF that leads to the prophase-to-metaphase transition (Bornslaeger and Schultz, 1986; Conti et al., 2012). This transition requires the GV oocyte to undergo GVBD to complete the first meiotic division (Fig. 1.5) (Sun et al., 2009). The GVBD only occurs in oocytes bigger than 60 µm, possibly under a spatially and temporally rise in MPF (Jones, 2004; Jones, 2005). During GVBD the nuclear envelope breaks down, then chromosomes condense and the meiotic spindle forms (Fig. 1.5) (Holt et al., 2013; Sun et al., 2009).

At metaphase I the bivalent chromosomes align at the equatorial plate of the meiotic spindle and the microtubules provide the tension to pull the homologous chromosomes apart at anaphase I, and so segregate them during telophase I (Duro and Marston, 2015a; Jones, 2004). This is an asymmetric cell division leading to the formation of a first polar body, which is small and later degrades. Sister chromatids remaining in the oocyte are bound by cohesins in the region of their centromeres and remain together (Garcia-Cruz et al., 2010). It is this first meiotic division that often leads to mis-segregation of chromosomes and so generates aneuploid embryos (Jones, 2008).

After meiosis I, two diploid daughter cells result: the oocyte and the first polar body, which are enclosed in the same zona pellucida (Fig. 1.5) (Oktem and Urman, 2010). The oocyte rapidly enters meiosis II and is arrested at metaphase II, where chromosomes are aligned in the equatorial plate of a well formed meiotic spindle (Fig. 1.5) (Duro and Marston, 2015b; Madgwick and Jones, 2007). This oocyte is arrested because of high MPF activity (Jones, 2005), and this is maintained by the presence of high levels of the meiosis II-specific protein Emi2 which acts to prevent degradation of the MPF subunit cyclin B1 (Shoji et al., 2006; Wu et al., 2007).

1.4.8 Cumulus Expansion, Ovulation and Resumption of Metaphase II

In Graafian follicles, the oocyte is surrounded by tight layers of cumulus cells (Fig. 1.5). After exposure to LH, oocyte-granulosa gap junctions close and granulosa-based hyaluronan synthase produces hyaluronic acid (Fülöp et al., 1997; Salustri et al., 1989). Hyaluronic acid organises into a cross-linked matrix with other scaffolding proteins to gain a viscoelastic state, and absorbs water to detach oocyte and cummulus cells and expand the COC (Fülöp et al., 2003; Salustri et al., 1999; Salustri et al., 2004). FSH-mediated cAMP modulates the cumulus expansion (Dekel and Phillips, 1980).

During ovulation, matrix metalloproteinase 2 degrades posterior follicle cells, which causes follicle and ovarian epithelium rupture and the release of COC into the oviduct (Deady and Sun, 2015). The sticky hyaluronic matrix allows cells within the COC to remain in place, and is essential for its pick-up and transport by the cilliated surface of the oviduct (Mahi-Brown and Yanagimachi, 1983). The COC travels through the oviductal ampulla during its viable period and is sustained by the progesterone produced by the corpus luteum, thecal cells from the remainder of the follice remaining in the ovary (Deady and Sun, 2015; Young and McNeilly, 2010).

Should a spermatozoon pass through the hyaluronic matrix and the zona pellucida, its sperm surface Izumo protein will bind the Juno receptor on the oocyte surface (Bianchi et al., 2014). Gamete fusion ensues, which triggers the release of intracellular oocyte calcium (Fig. 1.5) (Stricker, 1999). Sperm-specific phospholipase C isoform (PLCζ) hydrolyzes phosphatidylinositol biphosphate (PIP_2) to inositol trisphosphate (IP_3). IP_3 induces multiple calcium spikes that prevent the entry of more spermatozoa into the oocyte (Stith et al., 1993; Stricker, 1999; Swann and Parrington, 1999; Swann and Yu, 2008; Whitaker, 2006).

Calcium release also induces Emi2 phosphorylation, which causes the inactivation of MPF cyclin B1 and so releases the egg from its metaphase II arrest (Fig. 1.5) (Chang et al., 2009; Madgwick et al., 2005). The resulting zygote contains two haploid pronuclei (paternal and maternal) that need to fuse their genetic information to initiate the embryonic development. First and second polar bodies degenerate (Fig. 1.5) (Gilbert, 2000).

1.5 Stem Cells in Animals

Stem cells are long-standing undifferentiated cells capable of maintaining their own population in a tissue. The clone progeny may sustain self-renewal or undergo

differentiation and maturation to perform certain functions in said tissue. The stem cell system is modulated by factors and conditions that compound a specific tissue microenvironment (Schofield, 1983). In summary, stem cells are characterised by their unspecificity, self-renewal, longevity, production of a large differentiated progeny and the requirement of a tissue niche to depelop their functions.

1.5.1 Classification and History of Stem Cells

In animals, three types of stem cells can be classified upon their ability to differentiate into a number of specialised cells.

Totipotency is characteristic of the fertilised egg, the zygote and the blastomeres present in embryos up to the 8-cell stage. They are capable of differentiating into the trophectoderm (TE), which forms the extraembryonic tissues, and the inner cell mass (ICM), which forms the future embryo, just before compaction and implantation in the endometrium of the uterus (Kelly, 1977). In recent years, however, 30% of blastomeres at 4-cell stage embryos have been observed to contribute solely to the TE in long-term cell labelling reporter mice (Fujimori et al., 2003; Tabansky et al., 2013). This has led to question whether the TE/ICM developmental bias is a result of the heterogenicity in epigenetical modulators or the cell division pattern and position within the embryo, without clear conclusions (Chazaud and Yamanaka, 2016).

Pluripotency is typical of embryonic stem cells (ESCs) from 16-cell stage embryos until the formation of the ICM and the epiblast, which contains epiblast-derived ESCs (EpiESCs). They can differentiate into all three embryonic germ layers (ectoderm, mesoderm and endoderm) and the PGCs, but not the TE (Jaenisch and Young, 2008). Furthermore, ESCs can give rise to teratocarcinomas, polyclonal noncancerous tumours that derive from all three embryonic germ layers and produce tissue foreign to the area in which they exist (Lewis, 2000; Stevens, 1970). High expression of the anti-apoptotic oncofoetal survivin may be the major cause of ESC-derived teratomas in humans (Blum et al., 2009). Interestingly, EpiESC pluripotency is described as a transient stage, with early EpiESCs presenting a naïve or uncommited pluripotency sustained by global DNA hypomethylation and expression of *Pou5f1/Oct4* and *Nanog* (Nichols and Smith, 2009; Santos et al., 2002), that develops into a primed or more restricted pluripotency modulated by axis development, inductive factors from the extraembryonic tissues, and epigenetic restrictions from E5.5 in the mouse (Beddington and Robertson, 1999; Nichols and Smith, 2009). Importantly, *in vivo* ESCs from the ICM do not self-renew (Santos et al., 2002),

whereas they are immortalised if isolated from the embryo and cultured *in vitro* (Meissner et al., 2008).

Multipotency and unipotency are characteristic of germline stem cells (PGCs and GSCs), adult or somatic stem cells and extraembryonic stem cells, such as those from the TE. These cells have a limited differentiating ability and usually reside among differentiated cells of a specific tissue. TE stem cells are the precursors of differentiated placental cells and derive from CDX2-positive outer blastomeres of 8-cell and 16-cell stage embryos (Lu et al., 2008). They present limited self-renewal similar to their ICM counterparts (Roberts and Fisher, 2011; Tanaka et al., 1998). Somatic stem cells can be found in all adult tissues, with relevance in the amnion and amniotic fluid (Dobreva et al., 2010), umbilical cord (Weiss and Troyer, 2006), bone marrow (Becker et al., 1963; Morstyn et al., 1980; Sutherland et al., 1990), skin (Rochat et al., 1994; Taylor et al., 2000; Watt, 1998), intestinal epithelium (Potten, 1998), liver (Haele and Roskams, 2017) and skeletal muscle (Seale et al., 2001). Male and female germline stem cells are a particular case of unipotent stem cells, since they can give rise to teratocarcinomas upon migration to organs other than the gonads during embryonic development or upor parthenogenesis in adult stages (Andrews et al., 2001; Marshak et al., 2001).

The existence of stem cells in animals was firstly described in the 19th century. Pluripotent stem cells from teratocarcinomas were the first to be isolated and cultured *in vitro* (Hogan, 1976; Martin and Evans, 1975), as well as the first to produce derived organisms after being injected into blastocysts (Mintz and Illmensee, 1975). In the early 20th century it was discovered that many adult tissues, such as the haematopoietic system, contained stem cells that would regenerate aged and damaged parts. This knowledge led to the first bone marrow transplantations to treat patients with immunological deficiencies in 1968 (Bach et al., 1968; Gatti et al., 1968). Since the first isolation of stem cells from the ICM of a mouse embryo and its culture *in vitro* (Evans and Kaufman, 1981; Martin, 1981), the aim of the stem cell techniques has been to understand developmental processes, cellular aging and clinical outcomes. Hence the interest in creating stem cell lines (Thomas and Capecchi, 1987; Thomson et al., 1995; Thomson et al., 1998), and genetically modified animals as experimental models for human illnesses (Bradley et al., 1984; Campbell et al., 1996; Koller et al., 1989; Robertson et al., 1986; Thomas et al., 1992).

1.5.2 *In Vivo* Pluripotency/ Differentiation Balance in Stem Cells

In vivo embryonic and somatic stem cell fates are tightly regulated by the stem cell niche, the microenvironment in which they reside (Scadden, 2006), and morphogens, molecules that govern the pattern of tissue development in a dose-dependent manner (Christian, 2012).

The fate and potential of a stem cell are defined by the characteristics of the stem cells and the nature of their niche (Scadden, 2006). It is yet not well understood how stem cell niches established during embryo development. However, once formed, nonstem cells in the niche keep the stem cells undifferentiated and attached to this compartment through direct physical interaction (Fuchs et al., 2004). Cadherins and caterins form adherens junctions (Song et al., 2002), whereas integrins mediate cell adhesion to the basal lamina of the extracellular matrix (Watt and Hogan, 2000). For example, male and female GSCs in *Drosophila* initiate meiosis and gamete differentiation when they lose adhesion with the somatic cells at the apical tip of the germarium (Fuchs et al., 2004). A niche can also attract and retain stem cells by synthesising attractant molecules (Whetton and Graham, 1999). This ‘homing’ process has already been seen in the migration of PGCs towards the genital ridges (see Section 1.2.3), and also applies to the principles of bone marrow transplantation.

Signalling molecules also modulate stem cell proliferation and fate specification in the niche, as does transmembrane receptor Notch. The self-renewal/differentiation cellular decision is individual of each cell but can be transmited to neighbouring stem cells in an inductive wave (Maillard et al., 2008). The most dramatic effect of Notch signalling is the anterior-to-posterior somite patterning during embryo development (Feller et al., 2008). BMPs are also involved in the cellular developmental fate mainly through the activation of the SMAD signalling cascade (see Section 1.2.1), and in other secondary signalling pathways depending on cellular context (Walsh et al., 2010). Some of them involve signal transducer and activator of transcription 3 (STAT3) cascades in cooperation with leukaemia inhibitory factor (LIF) (see Section 1.5.4) (Hirai et al., 2011). Also interesting is the Wnt signalling pathway in cooperation with foetal and embryonic growth factors (FGF and EGF). Wnt proteins bind to cell surface tyrosine kinase receptors in stem cells in order translocate ß-catenin into the nucleus and activate pluripotency target genes. FGF and EGF use this same signalling pathway to promote proliferation of stem cells in the meantime (Nusse, 2008).

Some of the previously reviewed signalling molecules are morphogens, substances capable of difussing through fields of cells in a dose-dependent manner to develop spatial

patterns of tissues, organs and, finally, a fully functional organism (Christian, 2012; Turing, 1952). The amount of morphogen that reaches a certain position determines the level of activation of the corresponding ligand and downstream intracellular signalling cascade (Christian, 2012). Morphogens can act locally in a stem cell niche, such is the case of the retinoic acid gradient that activates an anterior-to-posterior meiotic wave in the mouse embryonic ovary (see Section 1.4.1) (Koubova et al., 2014) but also an inside-to-outside temporal meiotic wave in the adul testis (Endo et al., 2015).

Most importantly, morphogen gradients induce stem cell niche formation and fate specification of the cells within in places far from its original site of synthesis. It happens with the differentiation of PGC-like cells by the ExE-expressed BMP4 and BMP8b (Matsui and Okamura, 2005) and the VE-expressed BMP2 (Lawson et al., 1999) (see Section 1.2.1), or the anterior-to-posterior somite patterning by Notch (Feller et al., 2008). Morphogens are transported by binding heparan sulfate proteoglycans (Filmus et al., 2008; Marjoram and Wright, 2011), lipids that perform post-translational modifications on them (Steinhauer and Treisman, 2009) and soluble partners that drive diffusion towards a certain direction or cell type (Christian, 2012). Morphogen gradients can also arise by transcytosis or endocytosis followed by intracellular trafficking and exocytosis in the receiving cells (Steinhauer and Treisman, 2009)

BMPs are also at the basis of the dorso-ventral patterning of the early embryo. Low-to-high BMP signalling gradients determine the ectoderm, mesoderm, and endoderm germ layers (Bier and Robertis, 2015). Further into the differentiation of the ectoderm, low BMP levels produce the central nervous system, whereas high levels produce the epidermis. During the differentiation of the mesoderm, low BMP gives rise to the notochord and high BMP produces blood (Bier and Robertis, 2015). This patterning programme is tightly regulated by BMP antagonists noggin, gremlin, FGF and chordin among others (Khokha et al., 2005; Walsh et al., 2010). Antagonists bind BMPs to form an extracellular heterocomplex that prevents recognition by cell surface receptors, but can also inhibit signalling cascades through intracellular disruption (Walsh et al., 2010).

1.5.3 Methods to Derive Embryonic Stem Cell Cultures

Pluripotent cell lines are usually obtained through isolation of ESCs from the ICM in pre-implantational human and mouse embryos (Evans and Kaufman, 1981; Martin, 1981; Thomson et al., 1998) or EpiESCs by excising the epiblast in *in vitro*-grown mouse embryos (Brons et al., 2007; Tesar et al., 2007). Murine and human PGCs (Matsui et al.,

1992; Resnick et al., 1992; Shamblott et al., 1998) and adult spermatogonial stem cells (Kanatsu-Shinohara et al., 2003; Kanatsu-Shinohara et al., 2004) can also revert into pluripotency. Many organisms have already been used to derive ESC cultures but the mouse is the most used in mammalian research because its cells easily colonise the germline, despite a heavy reliance on its genetic background (Nagy et al., 2003). The 129S6/SvEvTac 129 inbred mouse substrain contains the least genetic contamination from other mouse strains, and is therefore advised to be used in ESC derivation. On the other hand, the C57BL/6 mouse strain-derived cell cultures have problems to maintain germline potential, with the better strategy being the use of a 129-C57BL/6-derived F1 progeny (Takahashi and Yamanaka, 2006). Nonpermissive mouse strains, on the other hand, are better to derive EpiESC-like cell colonies (Hanna et al., 2009).

Three problems arise during the ESC culture derivation. First, female-derived cell cultures present two X active chromosomes that difficult their stability and propagation (Rastan and Robertson, 1985), whereas XY-derived cell cultures only retain male imprinting signature which compromises its safety for clinical use (Ko et al., 2009). Second, primate ESC cultures have not yet been long-term established and validated (Ko et al., 2010). Third and most important, ethical issues on the destruction of viable embryos prohibit the creation of human embryos for the sole harvesting of human ESCs and PGCs (Takahashi and Yamanaka, 2006), although they can be obtained from embryos discarded and donated after IVF treatments.

It is also possible to derive ESC cells by parthenogenetic activation of oocytes with 7% ethanol or cytochalasin-D (Kaufman et al., 1983; Robertson et al., 1983). Their DNA undergoes duplication without division and provides with diploid parthenogenetic ESC cell colonies. Another technique is to transfer the nucleus of a somatic cell into enucleated oocytes either by microinjection (The Honolulu method) (Wakayama et al., 1998; Wilmut et al., 1997) or electrofusion (Ogura et al., 2000), or to fuse said somatic cell with ESCs (Cowan et al., 2005; Tada et al., 2001). The oocyte and the ESC contain reprogramming factors trat provide the transferred somatic cell with pluripotency abilities (Takahashi and Yamanaka, 2006).

Also important in the last years has been the possibility of reprogramming adult somatic cells into induced pluripotent stem cells (iPSCs) by vector-based overexpression of the key pluripotent genes *Pou5f1*, *Sox2*, *cMyc*, and *Klf4* (Takahashi and Yamanaka, 2006) and injecting the resulting cells into blastocysts. Overexpression of *Nanog*, *Lin28* and other pluripotency genes have also rendered good results (Ichida et al., 2009; Yu et al., 2007).

Murine iPSCs have been derived so far from adult fibroblasts, hepatocytes and pancreatic cells (Aoi et al., 2008; Danner et al., 2007; Imamura et al., 2010; Okita et al., 2007; Zhao et al., 2009). They share all defining characteristics of *in vitro* ESCs, including pluripotency, reactivation of both X chromosomes, and teratoma formation if injected into an organism. However, the F1 generation showed increased incidence of tumours (Okita et al., 2007) and high perinatal death (Okita et al., 2007; Zhao et al., 2009).

1.5.4 *In Vitro* Maintenance of Pluripotency, Proliferation and Self-renewal

In vitro stem cell cultures take modulating factors directly from the medium to maintain pluripotency, self-renewal and germline potential. Otherwise, they undergo differentiation or acquire mutations unsuitable for the production of healthy progeny. A precise cocktail of said factors and culturing conditions are needed, and may vary depending on the species and morphological origin of the stem cell cultures (Nagy et al., 2003).

Most usually, the basis for the murine ESC culture medium is Dulbecco´s modified Eagle´s medium (DMEM). It is a bicarbonate-buffered culture medium that maintains a pH of 7.2-7.4 in a humidified atmosphere of 5% CO2 and 95% air at 37°C (Thermo Fischer, technical bulletin). Its optimised knockout DMEM (KO-DMEM) provides an osmolarity that approximates that of the mouse embryonic tissue (Nagy et al., 2003). The DMEM needs further supplementation to enhance proliferation and stability in the cell culture. L-glutamine is an unstable essential amino acid that transports nitrogen to the cells; is degraded for the production of energy in cells with a poor intake of glucose; and is used in the synthesis of the vitamins nicotinamide adenine dinucleotide (NAD) and nicotinamide adenine dinucleotide phosphate (NADP), purine nucleotides, cytidine triphosphate (CTP) and asparagine (Sigma-Aldrich, technical bulletin). Also needed is supplementation with non-essential amino acids (NEAA) that improve *in vitro* growth and viability of propagating cells (Sigma-Aldrich, technical bulletin). Another essential supplement is β-mercaptoethanol, an unstable reducing agent that prevents toxic levels of oxygen radicals in *in vitro* cell cultures (Thermo Fischer, technical bulletin). Sodium pyruvate and antibiotics are optional but advisable. Sodium pyruvate is a carbon source in addition to glucose, however, some cell cultures make sodium pyruvate as an intermediate metabolite in the glycolysis pathway and will not need this supplement (Thermo Fischer, technical bulletin).

Serum-supplementation provides with a rich variety of proteins, hormones, growth factors, lipids and vitamins that promote cell survival, growth, and proliferation

(Gstraunthaler, 2003). Foetal bovine serum (FBS) is the most common in ESC cultures, however, its composition is not fully defined and may include unidentified components that could alter the ESC culture. Serum-free supplementation is a chemically defined replacement that provides a standardised alternative to FBS (Gstraunthaler, 2003).

Leukaemia inhibitory factor (LIF) is a cytokine that maintains self-renewal of murine ESC cells *in vitro* by binding its cell surface LIF receptor, which immediately forms a heterodimer with the membrane protein gp130. This heterodimer phosphorylates and activates Janus kinase (JAK), which in turn phosphorylates gp130 and creates a binding site for signal transducer and activator of transcription 3 (*Stat3*) (Niwa et al., 1998). STAT3 is bound to gp130 and homodimerized by JAK, which allows this transcription factor to translocate to the nucleus and activate target genes involved in self-renewal (Hirai et al., 2011; Niwa et al., 1998). Another signalling pathway activated by JAK is the LIK/PI3K/ATK, where phosphoinositide 3-kinase (PI3K) is phosphorylated to activate the protein kinase B (ATK). This serine/threonine kinase in turn inhibits glycogen synthase kinase 3β (GSK3β), which increases the levels of NANOG and c-MYC, and induces self-renewal of ESCs (Bechard and Dalton, 2009; Hirai et al., 2011). Although *in vivo* stem cells produce and diffuse low amounts of LIF to maintain a small undifferentiated population, *in vitro* ESC cultures require supplementation to avoid differentiation of those cells that receive less amount of LIF from their neighbours (Hirai et al., 2011).

LIF is not enough to maintain pluripotency in murine ESC cultures, and requires serum-based supplements (Hirai et al., 2011). Combined LIF and BMP4 activate STAT3 to induce the upregulation of pluripotency genes and the downregulation of differentiation genes (Ying et al., 2003). Furthermore, BMP4 activates expression of inhibitor of differentiation 1 (*Id-1*) gene to sustain pluripotency (Romero-Lanman et al., 2011; Ying et al., 2003).

Interestingly, human ESCs do not require LIF to maintain their pluripotency (Dahéron et al., 2004; Humphrey et al., 2004) and BMP4 induce their differentiation into trophoblasts (Xu et al., 2002). Instead, they necessitate supplementation with Activin A, Nodal, foetal growth factor 2 (FGF2) and insulin-like growth factor (IGF) (Romito and Cobellis, 2016). Activin A/Nodal and FGF2 cooperate in promoting upregulation of pluripotency markers via SMAD2/3 signalling (James et al., 2005; Xu et al., 2005a) and the MEK/ERK pathway (Xu et al., 2008; Yu et al., 2011). FGF2 also inhibits BMP4-derived differentiation of *in vitro* human ESCs by upregulating *Nanog* (Yu et al., 2011).

IGF collaborates with FGF2 and Activine A in promoting upregulation of pluripotency (Bendall et al., 2007; Romito and Cobellis, 2016).

Another specification in ESC cultures is that a monolayer of feeder cells is compulsory for the growth of human ESC cultures, not of mouse. Feeder cells provide attachment of cells, release growth factors to the culture media, synthetise extracellular matrix proteins and detoxify the culture medium (Namba et al., 1982). Feeder cells are usually mitotically inactive mouse embryonic fibroblasts (MEFs) or SIM Thioguanine/Ouabain-resistant (STO) mouse fibroblasts, being the former the preferred. Despite mouse ESCs efficiently growing in feeder-free in vitro cultures, the expression of pluripotent markers is higher if MEFs are present (Park et al., 2015). On the other hand, human ESCs heavily rely on the MEF-derived FGF2 to maintain pluripotency (Llames et al., 2015). This has led to concerns over MEF-derived zoonosis that would ultimately affect the clinical applications of human ESCs (Llames et al., 2015).

1.5.5 *In Vitro* Differentiation of Embryonic and Induced Pluripotent Stem Cells

Supplementation with LIF or fibroblast growth factor 4 (FGF4) can lead lineage differentiation upon activation of the SHP2/MAPK signalling pathway (Hirai et al., 2011; Kunath et al., 2007). Here, JAK phosphorylates protein-tyrosine phosphatase 2C (SHP2), which in turn activates the Ras/RAF/MEK/ERK cascade through the Grb2-SOS (growth-factor-receptor-bound protein 2 – son of sevenless) complex (Hirai et al., 2011; Schiemann et al., 1997). The Ras/RAF/MEK/ERK cascade downregulates pluripotency genes *Tbx3* and *Nanog* and induces differentiation of ESCs (Hamazaki et al., 2006; Niwa et al., 1998). FGF4 can also activate the Mek/Erk/Klf2 differentiating pathway (Yeo et al., 2014).

The 2i cell culture medium was therefore engineered to include inhibiting kinases of the Mek/Erk/Klf2 pathway, which led to more genetically stable ESC cultures (Romito and Cobellis, 2016) and germline differentiation (Hanna et al., 2009; Nichols et al., 2009). An easy method to differentiate mouse ESCs into EpiESCs cells is to replace 2i supplemented with LIF with a combination of FGF2 and activin A. Similarly, dedifferentiation of primed pluripotent stem cells and production of iPSCs can be achieved by culturing the cells in LIF and 2i (Hirai et al., 2011).

1.5.6 Oocyte-like cells from Embryonic and Induced Pluripotent Stem Cells

Considering the absence of ovarian GSCs in the postnatal ovary and the gradual loss of follicles during the fertile life of women, deriving oocytes from other totipotent and pluripotent cells has become a strategy to combat female infertility in addition to techniques currently used in assisted reproduction clinics

Embryonic stem cells (ESCs) were the first to be derived *in vitro* into PGC- and oocyte-like cells in human (Clark et al., 2004; Park et al., 2009; Tilgner et al., 2008; West et al., 2008) and mouse (Hubner et al., 2003; Matsui et al., 2014; Nicholas et al., 2009; Qing et al., 2007; Resnick et al., 1992; Salvador et al., 2008). ESCs showed formation of embryoid bodies and expression of germline-specific genes, with a preference for *Ddx4* (Clark et al., 2004; Hubner et al., 2003). This germline differentiation improved when co-culturing the ESCs with granulosa cells (Qing et al., 2007), supplementing with growth factors (Koshimizu et al., 1996; Resnick et al., 1992; Salvador et al., 2008; West et al., 2008), and especially after transplantation under the kidney capsule (Nicholas et al., 2009). Only one study obtained parthenogenetic embryos (Hubner et al., 2003) but no offspring, therefore implying that the oocyte-like cells were immature and not meiotically competent. Mouse litters have been reported to be derived from ESCs by applying a complex protocol that involved: a double induction of ESCs into PGC-like cells, four changes of culture medium and transplantation under the kidney capsule. Oogenesis in the transplants was around 30–40%, although the majority of the embryos produced contained 3 pronuclei and some type of polyploidy (Hayashi and Saitou, 2013; Hayashi et al., 2012b).

Only one study reported differentiating oocyte-like cells from iPSCs *in vitro* by manipulating the key pluripotent genes *Pou5f1*, *Sox2*, *cMyc*, and *Klf4* (Takahashi and Yamanaka, 2006), but without offspring (Imamura et al., 2010). Other studies have focused on the differentiation of male gametes, as female iPSC predominantly express male-like genes (Eguizabal et al., 2011).

1.6 Germ Stem Cells in the Adult Mammal Ovary

1.6.1 Early Studies on *De Novo* Oogenesis

Whether the postnatal mammal ovary renews its follicle pool has been a topic of discussion since the late 19th century. In 1870 Waldeyer-Hartz was the first to propose that oogenesis occurs during the foetal life of female mammals and produces a finite number of oocytes that are exhausted during her lifespan. On the contrary Pflüger, Schrön and Paladino in the 19th century, Kingery (1917), Arai (1920) and Allen (1923) noted increased

numbers of young oocytes in the ovarian epithelium – by then called germinal epithelium – preferentially during human menstruation and the oestrus of mice, cats and rabbits (for a review see Swezy, 1933). All these studies were based on follicle counting of ovarian slides stained with haematoxylin-eosin which, as Arai (1920) criticised, were scarce or came from too few animals to allow for a correct calculation of the total number of oocytes in the ovary.

Interestingly, Arai (1920) discussed whether *de novo* oogenesis arose from existing PGCs or from epithelial cells in the germinal epithelium. According to his results on 39 Wistar rats aged 1 to 947 days, the ovary presented two waves of folliculogenesis (Arai, 1920): from 4 to 23 dpp (birth to puberty) the number of oocytes rapidly decreased given the degeneration of PGCs; then from 23 to 63 dpp neo-oogenesis took place in the germinal epithelium and would balance the loss of PCGs. In the end, the ovary would solely ovulate oocytes produced by this germinal epithelium. These conclusions were in line with those presented by Kingery (1917) in the white mouse from birth to 60 dpp: "… *The primordial germ cells probably degenerate, playing no part in the development of the definitive ova; the primitive germ cells develop to a certain point and then degenerate before puberty; none of these cells take part in the formation of the definitive ova; the definitive germ cells develop by a process of growth and differentiation from cells of the germinal epithelium between birth and puberty; this potentiality of the cells of the germinal epithelium is lost and after sexual maturity no more egg cells or follicle cells are derived from the epithelium.*" Allen (1923), however, concluded that postnatal oogenesis also happened in the post-pubertal mice during hyperaemia of the ovary, by studying six adult mice with one ovary removed before puberty and nine mice with one ovary removed after puberty: "*A cyclical proliferation of the germinal epithelium gives rise to a new addition of young ova to the cortex of the adult ovary at each normal oestrous period*".

Aside from *de novo* oogenesis in the healthy female mouse, others reported the regeneration of the ovarian function after X-rays irradiation and total ovariectomy (Butcher, 1927; Davenport, 1925; Gerard, 1920; Parkers et al., 1927). Such results were challenged by Hill and Parkes (1931) when they could not recover oocyte production in female mice ovariectomized or exposed to X-rays after treatment with gonad-stimulating principle of the anterior pituitary body (the name given to FSH and LH before their complete identification).

1.6.2 Early Mathematical Models of Follicular Dynamics

The primitive research techniques did not provide definitive results until Zuckerman (1951) reviewed his 20 years of work on whether postnatal oogenesis occurs and whether the germinal epithelium is its source (Breward and Zuckerman, 1949; Green and Zuckerman, 1946; Mandl and Zuckerman, 1950; Mandl and Zuckerman, 1951a; Mandl and Zuckerman, 1951b; Mandl and Zuckerman, 1951c). He argued that quantitative studies of changes in follicle numbers were inaccurate on the grounds of (Zuckerman, 1951): few experimental animals used; subjective identifications of oocytes; multiple counting of the same oocyte and inadequate classification of oocytes into atretic/non-atretic and follicular stages, with primordial follicle numbers underestimated; as well as considerations on the species, strain, age, cycling stage and individual variations of the animal studied. He also argued that the cyclical proliferation of the germinal epithelium could not be proved as long as no methods to track these cells and their derived oocytes existed or the researchers did not include meiotic prophase as a *de novo* oogenesis marker in the postnatal ovary (Zuckerman, 1951) – by then, the general belief was that meiosis was not essential in oocyte formation (reviewed in Greenfeld and Flaws, 2004).

In his dissertation, Zuckerman (1951) suggested mathematical methods for follicle counting to overcome the observed difficulties, which had been successfully adopted in his lab after application of new histological techniques (Mandl and Zuckerman, 1950) and knowledge on the cycling female sexual hormones in Wistar rat (Bourne and Zuckerman, 1940a; Bourne and Zuckerman, 1940b; Breward and Zuckerman, 1949) and Rhesus monkey (Green and Zuckerman, 1946; Zuckerman, 1940).

He suggested that follicle counting should be based on the clear identification of the nucleolus rather than the oocyte nucleus to avoid multiplication. Furthermore, 1 in 10 or 20 10-µm slides counted would provide a fairer estimate of follicle numbers than the usual 1 in 5. He also included a correction factor of double counting (Mandl and Zuckerman, 1950; Zuckerman, 1951):

$$P = \frac{10\mu m\ (section\ thickness)}{10\mu m\ (section\ thickness) + 10\mu m\ (nuclear\ diameter)} \cdot \frac{1}{2}$$

P being the nuclear population of the slide counted.

Additionally, Zuckerman (Mandl and Zuckerman, 1950; Zuckerman, 1951) observed that plots of follicle counting vs age of animal drew a curve that resembled an exponential relationship for statistical significance and comparison:

$$y = ax^b$$

y being the total number of oocytes, *x* the age of the animal and *a* and *b* two constants resulting from a fit to experimental data.

This equation allowed him to conclude that the oocyte population in the Wistar rat declined rapidly at first, then slowly and continuously until death, bearing no evidence of postnatal oogenesis (Mandl and Zuckerman, 1950; Zuckerman, 1951). His studies on thirteen sexually matured Rhesus monkeys (Green and Zuckerman, 1946) and 36 Wistar rats aged 60 to 262 days (Mandl and Zuckerman, 1950) conveniently grouped at all cycling stages showed that the number of follicles did not fluctuate throughout the menstrual cycle. Therefore, no postnatal oogenesis existed in oestrus stage, as suggested before (Allen, 1923; Arai, 1920; Kingery, 1917). Zuckerman (1951) also highlighted that removal of the germinal epithelium in 50 Wistar rats by chemical (tannic acid) or physical (calcium alginate gauze) means did not dramatically reduce follicle numbers (Mandl and Zuckerman, 1951a; Mandl and Zuckerman, 1951b), as would have happened should new oocytes arise from this epithelium (Allen, 1923; Arai, 1920; Kingery, 1917). Additionally, no ovarian and oocyte regeneration were observed in rats where the ovary had been deprived of blood supply, X-irradiated, or partially or totally removed (Mandl and Zuckerman, 1951c; Zuckerman, 1951).

Zuckerman’s data accumulated over two decades reinforced the notion of sole production of oocytes during the foetal life (Breward and Zuckerman, 1949; Green and Zuckerman, 1946; Green and Zuckerman, 1951; Green et al., 1951; Mandl and Zuckerman, 1950; Mandl and Zuckerman, 1951a; Mandl and Zuckerman, 1951b; Mandl and Zuckerman, 1951c; Mandl and Zuckerman, 1951d; Mandl and Zuckerman, 1952; Mandl and Zuckerman, 1956a; Mandl and Zuckerman, 1956b). He is considered to have established the dogma of the non-renewal of oocytes due to the complete differentiation or atresia of female germ stem cells in modern times.

Concerns over Zuckerman's conclusions resulted in a study on sexually matured Rhesus monkeys (Vermande-Van Eck, 1956) that developed mathematical models of follicular dynamics under new variables: the total number of oocyte-containing follicles, the incidence of follicle loss via atresia, and the rate of clearance of atretic follicles (Powell,

2007; Tilly et al., 2009; Woods and Tilly, 2013a). The incidence of atresia in the ovary of Rhesus monkeys at 4 years old was of 4.5% after 2 weeks. This would mean that the initial ovarian reserve of 60,000 follicles would only guarantee fertility up to eight years of age. The female Rhesus monkey is fertile up to 25 years of age, therefore the author concluded that this fertility could only be explained if a renewal of the follicle reserve existed (Vermande-Van Eck, 1956; Woods and Tilly, 2013a).

1.6.3 Modern Mathematical Models of Follicular Dynamics

Vermande-Van Eck´s experiment was recently repeated in mice with the aim of studying the suspected adult oocyte renewal (Bristol-Gould et al., 2006; Faddy et al., 1987; Johnson et al., 2004; Kerr et al., 2006; Lei and Spradling, 2013; Liu et al., 2007).

Johnson et al. (2004) performed follicle counting of one fifth of ovarian slides from C57BL/6, CD1 and AKR/J mice, the latter being a mouse strain deficient in DNA repair that causes high oocyte atresia. In C57BL/6 mice, the atresia rate was low up to 20 dpp, but it dramatically increased by 30 dpp and reached a peak at 42 dpp, with a daily loss of 1,200 follicles that was maintained until the end of reproductive life. At this point, one-third of immature follicles had been lost in the ovary of young adults.

However, Johnson et al. (2004) observed that the non-atretic follicles had declined by only 36% between 4 and 42 dpp and suggested a gain of 77 follicles. CD1 mice showed 4% decline in the same period, whereas in AKR/J mice the population of atretic follicles had increased by 20%. This did not match the rate of postnatal follicle depletion expected from the ratio of atretic oocytes eliminated in this window of time. In other words, a gain of non-atretic follicles existed in the postnatal ovary in mice regardless of the strain.

The explanation for this gain was to be found in the presence of large ovoid cells in the ovarian epithelium surface that stained positive for the germline specific DDX4 (Johnson et al., 2004). These cells were not enclosed in follicular structures and were mitotically active given the large incorporation of 5-bromodeoxyuridine (BrdU) into their nuclear genome, a sign of active DNA replication and mitosis. mRNA transcripts of zygotene and pachytene meiotic markers (*Sycp3*, *Spo11* and *Dmc1*) were similarly found in the ovary and were linked to *de novo* postnatal oogenesis in the ovarian epithelium, although the study lacked confirmation that these markers were specifically expressed in these DDX4-positive cells.

In two final experiments, the authors tested the ability of these DDX4-positive cells to recover the ovarian function. First, mice received a dose of busulfan at 25 and 35 dpp and their ovaries were collected 10 days later. Busulfan is an alkylating antineoplastic agent that causes DNA damage. Upon observation, busulfan-treated ovaries contained less than 5% of the primordial follicle pool present in the control group. But rather than being sterilised, they had healthy maturing follicles and growing oocytes. Second, GFP-positive ovarian fragments were transplanted into ovaries of wild type mice, and after 3–4 weeks the authors recovered GFP-positive oocytes engrafted in well vasculated GFP-negative granulosa. These experiments suggested an initiation of folliculogenesis in the postnatal ovary, which was linked to the presence of these mitotically active DDX4-positive cells (Johnson et al., 2004).

The presumptive DDX4-positive germ stem cells were called oogonial stem cells (OSCs) (Johnson et al., 2004) and soon led to much debate. High rates of atretic primordial follicles were linked to a harsh formalin fixation and inaccurate identification, and it was put into question whether busulfan did actually kill all primordial oocytes (Greenfeld and Flaws, 2004). On the other hand, it was noted that GFP-negative oocytes enclosed in GFP-positive granulosa had not been reported as would have been expected, therefore the results observed would be an aberration or due to a different allelic expression of GFP in oocytes (Albertini, 2004; Greenfeld and Flaws, 2004).

Many groups were unable to observe follicle replenishment in adult mice (Begum et al., 2008; Bristol-Gould et al., 2006; Lei and Spradling, 2013; Liu et al., 2007), but rather reported a curve of follicle dynamics where the initial pool of oocytes was not supplemented with *de novo* oogenesis (Bristol-Gould et al., 2006). Bristol-Gould et al. (2006) proposed two differential equations of ovarian dynamics: a pool of primordial follicles as the only follicle source (fixed pool model) and a pool of primordial follicles postnatally supplemented by GSCs (stem cell model). They counted all types of follicles in 41 fixed ovaries of CD1 mice from 6 dpp to 12 months old, and concluded that the fixed pool model better fitted the kinetics parameters for the follicle counting. The stem cell model did not explain the follicle dynamics observed, even with the suggested new 77 non-atretic follicles formed (Johnson et al., 2004). Importantly the fixed pool model showed two separate time periods: 6 to 20 dpp and 20 dpp to 12 months old, which would be explained by the arousal of sexual maturity (Bristol-Gould et al., 2006).

Liu et al. (2007) examined 12 ovaries from women aged 28 to 53 years old for the expression of meiotic markers (*SPO11*, *PRDM9*, *SYCP1*, *SYCP3*, *DMC1*, *NOBOX*, *MSH5*,

REC8) and genes for germ cell proliferation (*TERT*, *OCT4*, *DDX4*, *MLH1*, *PLZF*) via conventional PCR. They were unable to retrieve positive bands for any of the markers and, importantly, no cells in the ovarian epithelium surface stained for PCNA, a marker of PGCs (Liu et al., 2007).

Last, Lei and Spradling (2013) lineage-labelled a mouse model that presented Cre recombinase and oestrogen receptor expression ubiquitously. However, upon Tamoxifen injection at 28 dpp, a stop cassette located within ROSA-YFP was excised and activated YFP expression in a few cells and all its descendants. This method proved to be very sensitive and showed mitotically active YFP-positive GSCs in all 94 embryo ovaries analysed, but not in the adult ovary in 40 mice between 24 hours and 16 weeks post-busulfan treatment. Similarly after depletion of primordial and primary follicles with busulfan in 16 mice, no YFP-positive GSCs or their derived oocytes were observed, therefore concluding that the adult mammal ovary under no circumstances can produce new oocytes (Lei and Spradling, 2013).

However, despite these studies evidenced that adult ovaries did not contain mitotically active GSCs (Bristol-Gould et al., 2006; Lei and Spradling, 2013; Liu et al., 2007), they did not invalidate the presence of dormant DDX4-positive GSCs in the ovary (Abban and Johnson, 2009).

1.7 The Bone Marrow as a Source of Germ Stem Cells

The reported postnatal oogenesis observed in mouse by Johnson et al. (2004) was briefly associated with the extragonadal origin of GSCs in circulating bone marrow and peripheral blood cells (Johnson et al., 2005). In this study, a small cluster of cells expressing the germline-specific marker *Ssea1* was found in the ovarian medulla of 6 to 9 week-old C57BL/6 mice. Upon fluorescence-activated cell sorting (FACS) these cells also expressed *Dppa3*, *Ddx4*, *Dazl* and *Pou5f1*, but not the oocyte-specific *Sycp3*, *Hdac6*, *Gdf9* and *Zp3*. The authors concluded that these *Ssea1*-positive cells were GSCs. However, such small population could not be responsible of the spontaneous regeneration of the immature follicle pool in mice treated with the germline toxicant doxorubicin within 36 hours post-treatment.

Therefore, Johnson et al. (2005) tested whether a GSC reservoir would exists in the bone marrow, given that PGCs and haematopoietic stem cells originate in the embryonic proximal epiblast (Lawson and Hage, 1994), and that the mesenchymal stem cells within

the bone marrow present tissue plasticity (Grove et al., 2004). Certainly, bone marrow from adult female mice (number, age and type of bone used not disclosed) showed expression of *Dppa3*, *Ifitm3*, *Ddx4*, *Dazl*, *Pou5f1* and *Nobox*, whereas cryopreserved bone marrow from four women donors aged 24 to 36 years old showed expression of *Dppa3* and *Dazl*. Bone marrow *Ddx4* expression was showed to be 9.52-fold higher at metestrus than at oestrus in the cycling mouse via RT-PCR, and coincided with peaks of 800 primordial follicles in the ovary compared with the oestrus. Ovariectomized mice did not express bone marrow *Ddx4*. Suspected bone marrow GSCs were cultured after FACS-sorting and removal of other haematopoietic cell types: after 6 weeks in culture, the FACS-negative fractions still expressed *Dppa3*, *Ifitm3*, *Ddx4*, *Dazl* and *Nobox*, but no direct evidence was provided on the colocalization of these markers in the presumptive GSCs.

In a second set of experiments, Johnson et al. (2005) used C57BL/6 bone marrow transplantation to prove that it rescued the ovarian function of the hosts via intravenous injection. Cyclophosphamide and busulfan-sterilised C57BL/6 female mice and ataxia telangiectasia (*Atm*) knockout female mice – which are deficient in early meiotic progression and completely lack oocytes (Giacomo et al., 2005) – recovered their pool of oocytes at all stages one to seven days post-transplantation, as well as corpora lutea indicative of ovulation. Eleven months post-transplantation such animals still maintained growing oocytes, but the study did not disclose if mating and pregnancy occurred. Second, *Pou5f1*-GFP-expressing female mice were used as donors in peripheral blood cell transplantation again in fertile, chemically sterilised wild type and *Atm* knockout female mice (9 mice per group). In all three hosts, around 13 GFP-positive oocytes enclosed in primordial follicles were recovered per ovary within 30 hours post-transplantation, and expressed *Ddx4*, *Hdac6*, *Nobox* and *Gdf9*. The study concluded that bone marrow would be a source of GSCs that sustained postnatal oogenesis, and that they would arrive into the ovary via peripheral blood circulation (Johnson et al., 2005).

However, other studies soon rejected the hypothesis of an extragonadal origin of postnatal oogenesis. Eggan et al. (2006) created parabiotic pairs by surgically joining wild type and GFP-expressing C57BL/6 mice at 28 to 56 dpp by the skin of their knee and elbow joints (Kamran et al., 2013). The mice developed a common circulatory system within 3 days and showed continuous and rapid exchange of blood components. The four pairs created remained joined for 6 to 8 months. This long-term shared blood circulation allowed observing high blood chimerism, but not GFP-positive oocytes in the ovaries of

the wild type females, even if the mouse had been previously sterilised with cyclophosphamide and busulfan (Eggan et al., 2006).

Begum et al. (2008) transplanted 28 dpp ovaries from 129/SvJ mice into the kidney capsule or ovarian bursa of transgenic CAG::H2B-EGFP host females. In these hosts, ovarian cells were all GFP-positive in the nucleus with the exception of granulosa cells. Some 129/SvJ mice donors were irradiated with X-rays to remove all primordial follicles within 24 hours, although the total number of experimental animals was not disclosed. The transplanted ovaries were monitored after 2, 4 and 8 weeks, and of 819 oocytes examined none expressed GFP. Furthermore, there was an absence of primordial and primary follicles. Therefore, this study concluded that *de novo* postnatal oogenesis did not occur due to circulating GSCs (Begum et al., 2008).

Reizel et al. (2012) used an algorithm for cell lineage tree construction based in somatic mutations accumulated in microsatellites, which would estimate the lineage relationship between different cell types and the cell depth, that is, the number of cell divisions since the zygote. Such an algorithm had been already used by the same group in normal (Frumkin et al., 2005; Reizel et al., 2011; Wasserstrom et al., 2008) and tumorigenic tissues (Frumkin et al., 2008) with good *in silico* predictions. In their study, mice knocked-out in the mismatch-repair (MMR) protein MLH1 were used because they present high microsatellite mutation rates (Baker et al., 1996) and increase the precision of the cell depth predictions. DNA from cells was amplified over a panel of 81 microsatellite loci, and the cell depth was given as number of microsatellite repeats at each locus. In the first experiment GV oocytes, mesenchymal stem cells, spleen lymphocytes, thymus and lymph nodes, and cumulus cells were collected from 17 female mice at ages 12 dpp to 1 year old. Clustering results in all animals showed that the PGC lineage and haematopoietic progenitor cells were derived from different embryonic populations and not contributed by them (Reizel et al., 2012). In a second experiment, GV oocytes from 9 mice at the same window of age as before showed that oocyte depth increased with age, from 13 divisions at 12 dpp to 18 divisions at 1 year old. Such observation was not the cause of mutations accumulated during meiotic arrest, and would be consistent with the ‘production-line’ hypothesis where the order of oocyte ovulation follows the order of meiotic onset in GSCs (Henderson and Edwards, 1968). Another explanation considered would be that a population of progenitor GSCs exist in the postnatal ovary and give rise to those oocytes with the higher cell depth in adult life (Reizel et al., 2012).

Further papers have subsequently detached bone marrow transplantation from postnatal oocyte production in the mouse using colour coat-mismatched donors and receptors (Lee et al., 2007), immunodefficient (PU.1 and SCID) mice (Santiquet et al., 2012) and GFP-expressing donors (Selesniemi et al., 2009), where the derived offspring always arouse from the host mouse. However, bone marrow seemed to rescue chemotherapy-based long-term ovarian failure (Lee et al., 2007; Santiquet et al., 2012; Selesniemi et al., 2009). Lee et al. (2007) observed that 70% of the chemotherapy-sterile females achieved six pregnancies after bone marrow transplantation, compared to three or less in the control group. Selesniemi et al. (2009) observed that 52% females transplanted at 3 months old were still fertile at 14.5 – 17.5 months old, compared to 31% females in the control group. Although fecundity decreased in both groups, higher offspring survival occurred in the aged transplanted group (71%) compared with the control group (33%).

Ghadami et al. (2012) suggested that the rescue of ovarian failure is a consequence of the restoration of ovarian physiology and hormone synthesis. They transplanted bone marrow of C57BL/6 female donors into FORKO (follitropin receptor; *Fshr*) knockout mice, which do not present folliculogenesis and have elevated FSH and decreased oestrogen levels. After one day, serum FSH had decreased to 40–50% and estrogen had increased 4–5.5 times in transplanted animals. mRNA *Fshr* transcripts were also found in these ovaries, and it was suggested that bone marrow stem cells had differentiated and expressed FSHR receptor, making the ovary responsive to FSH and activating folliculogenesis, given the presence of growing oocytes. Lack of evidence of fertility restoration in women after cancer treatment and bone marrow transplantation has been raised as evidence to reject this hypothesis (Oktay and Oktem, 2007; Powell, 2007; Telfer et al., 2005; Tilly et al., 2009).

1.8 Oocytes Obtained from Adult Oogonial Stem Cells

1.8.1 *Ddx4*-based Method for OSCs Isolation

Claims that a small group of *Ddx4*-positive cells were responsible for postnatal oogenesis (Johnson et al., 2004) soon led to an interest in isolating them from the adult ovary for further studies and characterisation. Whether through magnetic-activated cell sorting (MACS) (Zou et al., 2009; Zou et al., 2011) or through fluorescence-activated cell sorting (FACS) (Grieve et al., 2014; Imudia et al., 2013; Park et al., 2013; White et al., 2012; Woods and Tilly, 2013b) using a commercial antibody to a cell surface C-terminal

domain of DDX4, 50 to 1,000 10-µm diameter oogonial stem cells (OSCs) could be isolated from murine, human, rat, bovine and Rhesus monkey ovarian cell suspensions – approximately 1 in 10,000 cells of the total ovary (Vogel, 2012).

Murine OSCs have been the most studied, with cells isolated from C57BL/6 and CD-1 strains (White et al., 2012; Zhang et al., 2011; Zou et al., 2009). Whereas the Chinese team led by Ji Wu (Zhang et al., 2011; Zou et al., 2009) employed 9 to 12 5-dpp mice and 6 to 8 2-week-old mice, the team led by Jonathan Tilly recommended to use two 6-8-week-old mice since their ovaries were easier to digest with collagenase.

The *in vitro* OSC cultures expressed primitive and secondary germline markers (*Prdm1*, *Dppa3*, *Ifitm3*, *Ddx4*, *Dazl*) and presented high telomerase and alkaline phosphatase activity, normal karyotype (Pacchiarotti et al., 2010; Zhou et al., 2014; Zou et al., 2009), maternally imprinted *Igf2r* and *Peg10* regions, and paternally imprinted *H19* and *Rasgrf1* regions (Zou et al., 2009; Zou et al., 2011). The *in vitro* OSC cultures rapidly formed clusters after isolation and seeding (White et al., 2012; Zou et al., 2009), and maintained this morphology and expression pattern after 6 months in culture (Imudia et al., 2013; Zou et al., 2009). The OSCs soon expressed meiotic- (*Stra8*, *Dmc1*, *Sycp3*, *Ybx2*) and oocyte-specific markers (*Nobox*, *Lhx8*, *Gdf9*, *Zp1*, *Zp2*, *Zp3*) (Imudia et al., 2013; Park et al., 2013; White et al., 2012; Zou et al., 2009), and an haploid population was observed via FACS-based ploidy analysis with propidium iodide fluorescence (White et al., 2012). However, immunofluorescence showed inconclusive results for homologous recombination and chromosome annealing and segregation: DMC1 presented a wild type-like punctuated distribution, but SYCP3 failed to acquire a fibrillar conformation and the chromatin had not condensed as expected (White et al., 2012; Zou et al., 2009). The oocyte-like cells were therefore immature (White et al., 2012).

Interestingly, only one group reported having obtained offspring from isolated adult OSCs, only after intraovarian transplantation. Zou et al. (2009) sterilised 15 host adult female mice at 60 dpp with busulfan and cyclophosphamide, and injected 10,000 GFP-expressing purported OSCs into their ovaries. Two months later, 80% of the host females produced offspring, with 28% GFP-expressing pups, compared with the control group of fertile females injected with DMSO. In a similar experiment, Zhang et al. (2011) transfected OSCs with vectors carrying *Dnaic2*-GFP, a novel gene with an unknown role in the oocyte. Two months after intraovarian injection of chemically-sterilised host females, 90% gave birth, with 36% of the offspring bearing the *Dnaic2* gene. White et al. (2012) also obtained eight GFP-expressing oocytes six months post-injection of GFP-

expressing OSCs into the ovaries of five fertile host mice. The oocytes were IVF-fertilised and the resulting embryos progressed *in vitro* up to hatching blastocyst.

Furthermore, 100,000 OSCs were subcutaneously injected in BALB/c mice, with no teratoma formation after 8 weeks (Zou et al., 2009). Similarly, 10,000 OSCs were transplanted into the rear haunch of three nonobese diabetic-severe combined immunodeficient (NOD/SCID) mice, with no sign of tumor formation after 24 weeks (White et al., 2012). It was therefore suggested that these OSCs were pluripotent stem cells different from other pluripotent cell lines previously described in the ovary. These observations should however be taken with cautiousness. In a conference, Woods et al. (2012a) acknowledged that OSCs produced tumours in NOD/SCID mice 3 weeks post-transplantation when injected outside the ovaries. They suggested that the ovarian environment could supress this tumorigenic potential and induce *de novo* oogenesis instead (Woods et al., 2012a; Woods et al., 2012b).

However, these results were controversial on the grounds that DDX4 has always been considered a cytoplasmic protein in stem cells and oocytes (Castrillon et al., 2000; Fujiwara et al., 1994), not a cell surface protein (Abban and Johnson, 2009; Gura, 2012; Telfer and Albertini, 2012). The sorting would therefore have isolated oocytes, the antibody would have not been specific to DDX4, or the sorted cells would have been an artefact of the FACS sorting, as other groups found difficulties in isolating these ovarian cells (Gura, 2012; Vogel, 2012). This irreproducibility of results is common in the field of stem cells (Check, 2007).

To counter these allegations, White et al. (2012) suggested an explanation based on the migrating nature of DDX4 during female germline development. In GSCs the protein would contain a cell surface C-terminal domain, which would be translocated into the cytoplasm with the onset of meiosis and oogenesis. However, this hypothesis has never been proved (Gura, 2012) other than with *in silico* transmembrane domain prediction (Abban and Johnson, 2009; Zou et al., 2009). Such justification was initially obtained by Zou et al. (2009) with the online transmembrane helix predictor TMPred (Hofmann and Stoffel, 1993) and repeated in Abban and Johnson (2009) with similar conclusions: a transmembrane domain in DDX4 would exist between two motifs responsible for RNA helicase activity. However, these results were just mentioned and never shown in detail. Interestingly, Abban and Johnson (2009) claimed to having performed this transmembrane analysis of DDX4 with many other sequence analysis tools, but the tools used and the results obtained were not disclosed.

1.8.2 *Ifitm3*- and *Pou5f1*-based Methods for OSCs Isolation

Two more studies have replicated the OSCs isolation based on less controversial germline markers.

IFITM3 (FRAGILIS) is a cytoplasmic protein with two transmembrane domains that leave the COOH and the NH_2 termini on the cell surface. It has been used to MACS-sort cells in 5 dpp CD-1 mouse (Zou et al., 2011), with more than 1,000 *Ifitm3*-positive cells recovered from 20 digested ovaries, which helped to establish *in vitro* culturing of these cells much quicker than through the DDX4 antibody. These cells expressed the germline markers *Ddx4*, *Dazl* and *Pou5f1* after two weeks in culture, and the maternally imprinted *Igf2r* and *Peg10* regions after three weeks in culture (Zou et al., 2011). Similarly, 300 *Ifitm3*-positive cells were MACS-sorted from 20 digested ovaries in Sprague Dawley albino rats (Zhou et al., 2014). The freshly sorted cells expressed germline markers (*Prdm1*, *Ifitm3*, *Ddx4*, *Dazl*, *Pou5f1*), maintained a stable diploid karyotype and presented partial methylation on the maternally imprinted *Igf2r* and *Peg10* regions and demethylation on paternally imprinted *H19* and *Rasgrf1* regions. After 29 days in culture, the rat *Ifitm3*-positive cells expressed meiosis- (*Sycp1*, *Sycp2*, *Sycp3*) and oocyte-specific markers (*Zp3*), and some cells had grown to 55 – 60 µm, with 10% of oocyte-like cells resembling GV oocytes. Furthermore, GFP-expressing *Ifitm3*-positive cells were injected into the ovaries of six host rats previously sterilised with busulfan and cyclophosphamide (Zhou et al., 2014), where 66% produced healthy offspring two months post-transplantation, and bore 28% GFP-positive pups.

White et al. (2012) claimed to have replicated this IFITM3-based isolation method with success, but the data has not been published so far.

Pacchiarotti et al. (2010) used a germline-restricted *Pou5f1*-GFP reporter mouse. FACS-sorted GFP-positive cells from 5 dpp and adult mice showed expression of pluripotency and germline markers (*GCNA*, *Nanog*, *Ddx4*, *cKit*, *Pou5f1*), as well as high telomerase activity, normal karyotype and no teratoma formation seven months post-transplantation into *Pou5f1*-GFP mice. *In vitro Pou5f1*-positive cell cultures formed embryoid bodies representative of pluripotent stem cells, with some cells in the centre resembling 60-µm GV oocytes, expressing oocyte-specific markers (*BicD1*, *Ybx2*, *Gdf9*, *ZP1*) and forming lectin-enriched cytoplasmic granules usual in immature oocytes (Pacchiarotti et al., 2010). Such oocyte-like cells also achieved *in vitro* follicle formation after being cultured overnight with granulosa cells from neonatal ovaries.

This *Pou5f1*-based sorting technique was discouraged by Woods and Tilly (2013b) on the grounds that *Pou5f1* is downregulated in the germline between meiotic onset and first meiotic arrest, contrary to the continuous expression of *Ddx4*. Furthermore, many *Pou5f1*-positive cell populations could be observed, including small tetraploid oocytes (Pacchiarotti et al., 2010), that would make difficult the sorting of adult germ stem cells (Woods and Tilly, 2013b). Lastly, many germline marker-expressing cells present in the *Pou5f1*-negative fraction (Pacchiarotti et al., 2010) would be discarded, including cell surface *Ddx4*-positive cells (Woods and Tilly, 2013b). Upon FACS-sorting of dissociated *Pou5f1*-GFP ovaries immunostained with the DDX4 antibody, Woods and Tilly (2013b) recovered few *Pou5f1*-GFP-expressing *Ddx4*-positive cells, whereas *Pou5f1*-GFP-negative *Ddx4*-positive cells generated *Pou5f1*-GFP-expressing oocyte-like cells in transplanted host ovaries (Woods et al., 2012c). Since *Pou5f1*-GFP-expressing cells present some characteristics of the OSCs, both cell types would be at different developmental stages (Woods and Tilly, 2013b).

1.8.3 Studies Not Supporting the Existence of OSCs

At the start of my thesis, critisism over the existence of OSCs focused on the isolation methodology and the many interpretations of the results, including a lack of information on cellular, genetic and epigenetic markers in these oocyte-like cells, the possibility that GFP-expressing OSCs had fused with wild type oocytes during transplantation, and the unknown effects of sex reassignation treatment in the ovaries of those women that donated their ovarian tissue for experimentation (Abban and Johnson, 2009; Telfer and Albertini, 2012; Vogel, 2012). Only one group had rejected the existence of OSCs cells via a published study (Zhang et al., 2012b).

Zhang et al. (2012) used a Rosa26rbw/+;*Ddx4*-Cre multifluorescent reporter mouse to trace the proliferation and meiotic entrance of *Ddx4*-positive ovarian cells *in vitro* and *in vivo*. This mouse is obtained after mating males bearing a Cre recombinase whose expression is driven by a *Ddx4* promoter, with females bearing a Rainbow cassette that contains four open reading frames encoding four different fluorescent proteins in series (Red-Horse et al., 2010; Rinkevich et al., 2011). In this multifluorescent reporter mouse initially all tissues express GFP, but when activated, the *Ddx4* promoter stimulates the Cre recombinase to induce recombination in the Rainbow cassette causing a switch to random expression of red, orange or cyan fluorescent proteins only in those *Ddx4*-positive cells.

Zhang et al. (2012) initially transplanted GFP-expressing GSCs from E12.5 Rosa26rbw/+ foetuses into the ovaries of fertile or chemically-sterilised (busulfan and cyclophosphamide) 2-months-old wild type mice. Four weeks post-transplantation GFP-expressing follicles could be observed in these host ovaries, therefore concluding that the adult ovary supports *de novo* oogenesis only if provided with the essential GSCs.

Next, Zhang et al. (2012) disaggregated gonads from 8 dpp and adult Rosa26rbw/+;*Ddx4*-Cre male and female mice, and followed the mitotic division of RFP-expressing cells *in vitro*. After 72 hours in culture the male RFP-positive cells indeed proliferated, and were considered spermatogonial stem cells. None of the female RFP-positive cells had proliferated during this time, but most had died, therefore they were considered immature oocytes. Interestingly, some female GFP-positive cells formed colonies and oocyte-like cells *in vitro*, as OSCs do (White et al., 2012; Zou et al., 2009), but they did not express pluripotency or germline markers (*Sox2*, *Dppa3*, *Ddx4*, *Pou5f1*) or formed follicles upon transplantation into host ovaries (Zhang et al., 2012b).

This study was highly criticised on the grounds that OSCs and immature oocytes in the recombined Rosa26rbw/+;*Ddx4*-Cre mouse would bear a same fluorescence pattern, therefore this reporter mouse would not be specific in the identification and isolation of germ stem cells (Woods and Tilly, 2013b; Woods et al., 2012c). Furthermore, no test was performed to establish whether the *Ddx4*-Cre reporter mouse experienced leakiness and maintenance of recombined fluorescence in cells with *Ddx4* expression downregulated, and whether the senescent female RFP-positive cells were oocytes (Woods and Tilly, 2013b; Woods et al., 2012c). Last, Zhang et al. (2012) did not attempt to FACS-sort these multifluorescent cells with antibody-based methodology, or to assess if the observed oocyte-like cells expressed oocyte-specific markers (Woods et al., 2012c).

1.9 Thesis Aims

1.9.1 Do OSCs exist?

Despite reports on the existence of germ stem cells in the adult mammalian ovary (White et al., 2012; Zou et al., 2009), little has been published on the replication of results by other groups. The only study that has been opposed to the idea of OSCs did not actually replicate the original DDX4 antibody-based FACS sorting experiments, but rather relied on a *Ddx4* reporter mouse that possibly led to the isolation of oocytes given the size of the

isolated female *Ddx4*-positive cells (Zhang et al., 2012b). Therefore, it was of importance to examine in detail the antibody-based FACS sorting and cell culturing performed in White et al. (2012) for a more accurate comparison of results. Furthermore, it was important to perform more extensive *in silico* transmembrane analysis on DDX4 to critically test that done previously (Abban and Johnson, 2009; Zou et al., 2009), which had been used to justify the FACS protocol. Therefore in Chapters 3, 4 and 6 I explore the specificity of the DDX4 antibody in germline cells in both sexes, and whether an epitope of DDX4 exists on the cell surface based on an extensive *in silico* transmembrane analysis of the mouse protein, and on the FACS-sorting of cells from the ovary, testis and non-germline tissues. The expression of *Ddx4* and other germline markers in the FACS-sorted cells is performed in Chapters 5 and 6.

1.9.2 Can they provide us with oocytes?

FACS-based ploidy and gene and protein expression analysis support the activation of meiosis markers and oocyte progression in *in vitro* OSC cultures. Onset of meiosis reportedly happened up to three days after cell passage (Imudia et al., 2013; Park et al., 2013; White et al., 2012). However, it is not known if the OSCs are pre-disposed to this meiotic ability immediately after being FACS-sorted or as a result of being cultured. Furthermore, it would be interesting to see how the order of meiosis and oogenesis events is achieved in such a brief window, and whether oocytes arise from germline cysts, as it happens in physiological conditions (Mork et al., 2012a). Therefore in Chapters 5 and 7 I explore the onset of meiosis and oogenesis in these presumed OSCs both morphologically and via gene expression analysis with and without the addition of meiotic enhancers and at early and middle growth passages.

1.9.3 Are these oocytes meiotically competent cells?

Despite evidence for meiotic markers in oocyte-like cells (Imudia et al., 2013; Park et al., 2013; White et al., 2012; Zou et al., 2009), a further understanding of meiotic and oogenesis progression is missing. It would be interesting to see if all known pathways for meiotic onset take place, and whether or not proteins responsible for chromosome chiasma and spindle formation are present. Furthermore, it is possible that these oocyte-like cells do not have all the required oocyte-specific genes active, which would indicate a truncated oogenesis. Therefore, in Chapter 7 I explore an extensive selection of genes essential for the correct onset and progression of meiosis and oogenesis, including those involved in

homologue recombination (*Meiob*), sister chromatids cohesion (*Rec8*), oocyte maturation (*Sohlh2* and *H1foo*) and follicle formation (*Figα*). Activation of these genes is explored in the presence or absense of meiotic enhancers at early and middle growth passages.

Chapter 2

General Materials and Methods

2.1 Mice

2.1.1 Ethics

All experimental procedures were performed in compliance with the local and UK government regulations on the use of animals in research, and were reviewed and approved by the Ethics Committee of the Faculty of Natural and Environmental Sciences, University of Southampton.

2.1.2 Mice

All experiments in this thesis were performed using 3-to-4-week-old females, 5-to-20-week-old males and E13.5–18.5 embryos from the C57BL/6 mouse strain (Charles Rivers UK, Biomedical Research Facility at Southampton General Hospital). Mice of the same sex were caged together and housed in the Holding Room Facility at the Faculty of Natural and Environmental Sciences, University of Southampton, previous to be used. They were fed and given water *ad libitum*.

2.1.3 Hormonal Priming

To increase the yield of oocytes obtained per animal and to reduce the number of animals used in each experiment, females were injected with 10IU of Pregnant Mare Serum Gonadotropin (PMSG-Intervet; Centaur Services, UK) (Appendix B) 44–48 hours prior to collection of GV oocytes. For the induction of ovulation and collection of MII oocytes, females were further primed with 10IU of human Chorionic Gonadotropin (hCG-Chorulon; Centaur Services, UK) (Appendix B) 44–48 hours after PMSG injection and terminated 14–16 hours later. Females were immobilised by the skin of their neck and turned over to access their abdomen, then injected in the peritoneal cavity with a 27-gauge and ½ inch needle (#NN-2713R, Terumo, UK).

2.1.4 Tissue Collection

Cervical dislocation was used as the terminal method for the adult mice. Embryos were obtained after the pregnant female had been exposed to a lethal inhalation of CO_2. Adult mice were placed face up and the abdomen was sprayed with 70% ethanol prior to dissection. The abdomen skin was then cut with a pair of surgical scissors, and confirmation of death was performed by exsanguination of the body via the puncture of the heart through the rib cage. Ovaries with oviducts attached, testes, livers, kidneys and abdominal skin explants were removed with a pair of surgical spring scissors, cleansed of surrounding adipose tissue and placed on ice cold Dulbecco´s Phosphate Buffered Saline (DPBS; #14190-086, Gibco, UK). Testes were then cleansed of their epididymis and tunica albuginea. Ovaries and oviducts for oocyte collection were specifically placed into warm M2 medium (#GSM-5120, Globalstem, UK) supplemented with 0.5mM milrinone (#M4659, Sigma, UK) to maintain the meiotic arrest of oocytes. Mouse embryos were previously placed on ice cold DPBS and deprived from their head for neurobiology research purposes. Their abdominal cavity was sectioned and emptied of red organs with tweezers. The kidneys were removed with a pair of surgical spring scissors, cleansed off the ureter and placed on ice cold DPBS.

2.2 Oocyte Handling and Collection

2.2.1 Manufacture of Mouth Pipetting System

Handling pipettes were made from 150-mm glass pipettes (#FB50251, Fisherbrand, UK) that were heat-pulled. The thin part next to the neck of the pipette was heated over a Bunsen burner until it became incandescent. The glass pipette was pulled gently in opposite directions, separated from the flame and pulled again quicker in opposite directions. Levels of speed and pulling strength allowed obtaining handling pipettes with different diameters. The excess glass was broken so that the pipette conserved the majority of the pulled edge.

The handling pipette was mounted for its use onto a mouth pipetting system consisting on a mouthpiece, a flexible plastic tube and a filter piece where the handling pipette was inserted. Handling pipettes and mouthpieces were discarded after one use. The plastic tube was cleansed with 70% ethanol and stored after each use.

2.2.2 GV Oocyte Handling and Collection

All oocyte handling and collections were performed under a stereo microscope (#SZ40, Olympus, Japan) with variable zoom ratio, equipped with a stage (#MATS-U4020WF, Tokai Hit, Japan) heated to 37°C to mimic *in vivo* physiological temperature. GV oocytes were obtained by puncturing ovaries from culled mice with a hypodermic 30-gauge and ½ inch needle (#NN-3013R, Terumo, UK) in order to release Cumulus-Oocyte Complexes (COCs) into M2 medium covered with mineral oil (#M8410, Sigma, UK) to avoid evaporation and pH changes. The edge of a pulled pipette was cut to an appropriate diameter (~80–90µm), and the COCs were moved in and out the pipette quickly 5–10 times until the oocyte had been stripped of all the surrounding granulosa cells. The oocytes were then transferred with a handling pipette of a larger diameter (~100–120µm) to a new drop of M2 medium.

2.2.3 MII Oocyte Handling and Collection

MII oocytes were obtained by tearing the middle part of oviducts from hCG-primed female mice, and releasing ovulated COCs into 300IU/ml hyaluronidase (#H4272, Sigma-Aldrich) (Appendix B). The COCs were allowed 10–15 seconds in the hyaluronidase to release the oocytes from the cumulus mass. The edge of a pulled pipette was cut to an appropriate diameter (~80–90µm) and the oocytes were moved in and out the pipette quickly 5–10 times until the remaining surrounding granulosa cells had been removed. The oocytes were then transferred with a handling pipette of a larger diameter (~100–120µm) to a drop of M2 medium.

2.2.4 Enzymatic Digestion of Organs

Organs of interest (ovary, testis, oviduct, liver and kidney) were washed twice in Hank's Balance Salt Solution without calcium and magnesium (HBSS; #14175, Gibco, UK) for five minutes and tightly minced in 3ml of 800U/ml warmed collagenase (#CLS4, Worthington Biochemical Corporation, USA) in HBSS, supplemented with 1:1,000 (vol/vol) of 1mg/ml DNase I (#04536282001, Roche, USA) (Appendix B). The fragments were then collected into a 15-ml conical tube and incubated in an orbital shaker (#SSM1, Stuart, UK) mounted inside an oven at ~37°C, twice for 15 min at 300 r.p.m. The fragments were dispersed in between with a 5-ml borosilicate disposable pipette. The resulting cell suspension was filtered through a 100-µm nylon mesh (#04-004-2328, Partec

Celltrics, UK) and washed twice with 10ml of warmed HBSS for 5 minutes at 300g in a centrifuge with the brake off (#5804R, Eppendorf, UK).

2.3 Gene Expression Analysis

2.3.1 Total RNA Extraction from Oocytes

GV oocytes extracted from undamaged COCs and bigger than 70µm, or MII oocytes with a visible polar body were transferred to Tyrode´s solution drops (#T1788, Sigma, UK) to remove the zona pellucida, and then washed in 1% polyvinylpyrrolidinone (PVP; #P0930, Sigma, UK) in home-made PBS (Appendix B). Groups of 50–70 treated oocytes were transferred to a lysis buffer containing 10% (vol/vol) Triton (#X-100, Sigma, UK) and 1M dithiothreitol (DTT; #43816, Sigma, UK) (Appendix B). They underwent three cycles of freezing-thawing-vortexing-spinning to mechanically lyse them.

2.3.2 Total RNA Extraction from Tissue and Cell Suspensions

RNA from tissues of interest (ovary, testis, flushed oviduct, liver and kidney) was isolated by adding TRIzol (#15596-026, Ambion, UK) onto the tissue, then homogenising it with a pestle and incubating for 5 minutes at room temperature. RNA from cell suspensions and plated cells was extracted by adding TRIzol onto the cells, then pipetting up and down to lyse them. Wasted culture medium was incorporated to the RNA extraction in case that it contained floating oocyte-like cells.

Then, 1:5 (vol/vol) of chloroform (#288306, Sigma, UK) was added to the sample and shaken vigorously by hand for 20 seconds. The sample was further incubated for 3 minutes at room temperature, and then it was centrifuged at 12,000g for 15 minutes at 4°C. The upper aqueous phase was removed and placed in a new tube, then mixed with 2µl of 20mg/ml glycogen (#39766.01, Amsbio, UK), 1:10 (vol/vol) of sodium acetate 3M buffer (#S7899, Sigma, UK) and 1ml of 100% ethanol (#E7023, Sigma, UK). The sample was left overnight at –20°C to allow the glycogen to scavenge as much total RNA as possible.

The next day, the pellet was alcohol-precipitated by washing it in 75% ethanol twice, resuspended in nuclease-free water (#W3513, Sigma, UK) and heated at 60°C to eliminate any secondary structures in the RNA. The RNA was then placed on ice and its quantity and quality measured with spectrophotometry (NanoDrop, USA).

2.3.3 Complementary DNA Synthesis

The desired quantity of total RNA was taken from the stock sample and placed on two new tubes named ‘Sample’ and ‘RT⁻’ on ice. Similarly, some nuclease-free water was placed in a ‘Blank’ tube. The protocol was then performed as follows to obtain 50µl of cDNA (all reagents from Promega, UK). The resulting cDNA was stored at –20°C (Promega, 2014).

Table 2.1. Complementary DNA synthesis.

STEP	SAMPLE TUBE	RT⁻ TUBE	BLANK TUBE
Oligo(dT)15 primer (#C1101)		2µl	
Heat-denature at 70°C and cool on ice for 5 minutes each			
5X M-MLV reaction buffer (#M1705)		10µl	
10 mM dinucleotide triphosphate (#U1420)		12µl	
M-MLV Reverse Transcriptase (#M1705)	2µl		2µl
Top up to 50µl and incubate at room temperature for 10 minutes			
Incubate at 37°C for 50 minutes			

2.3.4 Real-Time Polymerase Chain Reaction

A 20-µl working solution was prepared for each gene and sample of interest following the manufacturer´s instructions: 1X GoTaq green reaction buffer (M300), 10mM PCR nucleotide mix (C1141), 1µl of template cDNA, 1.25 units of GoTaq DNA Polymerase (M300) (all from Promega, UK), 1µl of upstream 10µM primer, 1µl of downstream 10µM primer (Sigma, Eurofins) and nuclease-free water.

The RT-PCR conditions were: one cycle at 95°C for 2 minutes; 40 cycles at 95°C for 30 seconds, 60°C or 52°C (*Ifitm3*, *Ddx4*, *Stra8*) for 30 seconds, and 72°C for 1 minute; one cycle at 72°C for 5 minutes.

Table 2.2. Primer sequences used for RT-PCR.

Gene	Accesion no.	Primer sequences (F, forward; R, reverse)	Size (bp)
Rps29	NM_009093.2	F: GAAGTTCGGCCAGGGTTCC R: TCGGTTCCACTTGGTAGTAGTC	180
Bmpr1A	NM_009758.4	F: AGGATTCACCGAAAGCCCAG R: TACCAACCTGCCGAACCATC	393
Bmpr2	NM_007561.4	F: GGGGTTCTGGATCGTTTGGT R: GCCATCTTGTGTTGACTCACCT	246
Rara2	NM_001177302.1	F: CAAGAACTCCCCCATCCTCAA G: GAGCTGGTCTTCAGGGTATCA	186
Rarg2	NM_001042727.2	F: GGGGAGGAGGGGGAATGG R: ATAGACCCGAGGAGGTGGTG	298
Prdm1	NM_007548.3	F: CGGAAAGCAACCCAAAGCAATAC R: CCTCGGAACCATAGGAAACATTC	483
Dppa3	NM_139218.1	F: CCCAATGAAGGACCCTGAAAC R: AATGGCTCACTGTCCCGTTCA	354
Ifitm3	NM_025378	F: GTTATCACCATTGTTAGTGTCATC R: AATGAGTGTTACACCTGCGTG	151
Ddx4	NM_001145885.1	F: GGAAACCAGCAGCAAGTGAT R: TGGAGTCCTCATCCTCTGG	212
Dazl	NM_010021.4	F: GTGTGTCGAAGGGCTATGGAT R: ACAGGCAGCTGATATCCAGTG	328
Pou5f1	NM_013633.3	F: TCTTTCCACCAGGCCCCCGGCTC R: TGCGGGCGGACATGGGGAGATCC	223
Lin28A	NM_145833.1	F: GAAGCCTCAAGGAGGGTGAG R: CTAGCCCACCGCAGTTGTAG	183
Utf1	NM_009482.2	F: GGATGTCCCGGTGACTACGTCTG R: GGCGGATCTGGTTATCGAAGGGT	344
Zfp296	NM_022409.2	F: CCATTAGGGGCCATCATCGCTTTC R: CACTGCTCACTGGAGGGGGCTTGC	307
Stra8	NM_009292.1	F: GCCAGAATGTATTCCGAGAA R: CTCACTCTTGTCCAGGAAAC	651
Rec8	NM_020002.3	F: AAGAATGCTCAGACAAAGGCCA R: CGATCTCGCTCAGAGCTTCAGT	107
Meioc	NM_001127576.2	F: ATGATGCTGACCGGCTCG R: TTGATGAGGAGAGTGGAGTGC	100
Meiob	NM_029197.1	F: GGCCCGGAAGTATCCGATTT R: CGAGCGGATGTAGTCCTCAC	253
Sycp3	NM_011517	F: AGCAGAGAGCTTGGTCGGG R: TCCGGTGAGCTGTCGCTGTC	100
Ybx2	NM_016875	F: CCTCCCCACTTTCCCATAAT R: AATGGGTGGGGAAGAAAAAC	235
Sohlh2	NM_028937.3	F: GCCCAGGTTACAGAAGCCAT R: TGGAATACACGTTCAGGCCC	178
Nobox	NM_130869	F: CCCTTCAGTCACAGTTTCCGT R: GTCTCTACTCTAGTGCCTTCG	379
Figα	NM_012013.2	F: GCTACTCCACCACGGATGAC R: TGTGGTAGAAACGGCACCAG	133
H1foo	NM_138311.3	F: TTCTGGATCATGTGGGCTCC R: GTCCACTGTCGGGTACTTGT	187
Gdf9	NM_008110	F: TGCCTCCTTCCCTCATCTTG R: CACTTCCCCCGCTCACACAG	709
Zp3	NM_011776	F: CCGAGCTGTGCAATTCCCAGA R: AACCCTCTGAGCCAAGGGTGA	183

2.3.5 Agarose Gel Electrophoresis

A 2% (wt/vol) agarose gel was prepared by dissolving agarose powder (#MB1200, Melford, UK) in 1X tris-acetate EDTA (TAE) buffer (Appendix B) with heat. After cooling down, 1:20,000 (vol/vol) of GelRed (#41003, Biotium, UK) was spiked in and homogenised. The solution was poured into a gel cast with combs and left to solidify for at least 30 minutes.

1X TAE buffer was poured into the gel cast until covering it. Combs were removed and 5µl of a 100bp DNA ladder (0.13µg/µl) (#G2101, Promega, UK) dissolved in 1X Green GoTaq buffer were added in the first and last wells. Then, 4µl of each sample were added into each well. Gels were run at 55–120V depending on their size, until the yellow bands resulting from the dissociation of the Green GoTaq buffer had reached the edge of the gel. The resulting bands were photographed under UV light with a ChemiGenius imaging system and GeneSnap software (all from Syngene).

2.4 Western Blot

2.4.1 Protein Extraction and Measurement

Samples were homogenised on ice in tissue lysis buffer (Appendix B) with a pestle, and centrifuged at 4ºC for 20 minutes at full speed. The supernatant was collected, and an aliquot was diluted 1:10 in water and incubated with Bio-Rad Reagents A and B (#5000113 and #5000114, Bio-Rad, UK) to measure its protein concentration on a Nanodrop spectrophotometer at A_{280}.

2.4.2 SDS-PAGE Gel Running

SDS-PAGE gels were made by pouring 10% acrylamide resolving gel (Appendix B) between two glass plates firmly secured by a casting frame. A couple of minutes later the 4% acrylamide stacker gel (Appendix B) was added on top and wells were made with a comb. The gel cast was inserted into an electrophoresis module, and the assembled module was put inside a tank. The tank was filled with running buffer (Appendix B).

Then 100µg of protein from each sample were top up to 10µl by adding protein lysis buffer, and 10µl of 2x Laemmli buffer (#S3401, Sigma, UK) were mixed with the diluted

sample by pipetting. The solution was heated at 100ºC for 5 minutes and loaded into the SDS-PAGE gel together with a protein ladder (#26621, Life Technologies, UK). The gel was run at 15mA for 90 minutes.

2.4.3 Transfer of Proteins to Nitrocellulose Membranes

The SDS-PAGE gel was carefully removed from the glass plates and placed over a filter carton in a tray with transferring buffer (Appendix B). A nitrocellulose membrane (#16201, Bio-Rad, UK) was placed on top of the SDS-PAGE gel and covered with soaked filter paper (#1650962, Bio-Rad, UK). The sandwich was placed between soaked sponges in an electrophoresis module, with care to orientate the nitrocellulose membrane towards the red electrode and the SDS-PAGE gel towards the black electrode. The electrophoresis module was placed into a tank filled with transferring buffer and run at 200mA for 2 hours.

2.5 Cell Culture

2.5.1 Control Culture Medium (CM)

Control culture medium was prepared under sterile conditions by adding, in order, 10% foetal bovine serum (FBS) (#FCS-SA/50, Labtech, UK), 1X penicillin-streptomycin (#15140-122, Gibco, UK), 1X L-glutamine (#25030-024, Gibco, UK), 1X non-essential aminoacids (#11140-050, Gibco, UK) and 0.1mM β-mercaptoethanol (#M3148, Sigma, UK) to Dulbecco´s minimum essential medium (MEM) containing pyruvate and high glucose (#41966-029, Gibco, UK).

Control culture medium was filter sterilised with a 0.22-µm sterile syringe filter unit (#SLGP033RS, Millex, UK) into 15ml Falcon tubes and stored parafilmed in the fridge at 4°C. Control medium was warmed in the incubator with the lid loose half an hour before use. Control culture medium was prepared every two weeks.

2.5.2 OSC Culture Medium (OSCM)

OSC culture medium was prepared under sterile conditions by adding to MEM-α supplemented with GlutaMax (#32561-029, Gibco, UK) the following supplements in order: 10% embryonic stem cell-qualified FBS (#16141-061, Gibco, UK), 1mM sodium pyruvate (#S8636, Sigma, UK), 1X penicillin-streptomycin (#15140-122, Gibco, UK), 1X

L-glutamine (#25030-024, Gibco, UK), 1X non-essential aminoacids (#11140-050, Gibco, UK), 0.1mM β-mercaptoethanol (#M3148, Sigma, UK), 1X N-2 MAX media supplement (#AR009, R&D Systems, USA), 10^3 U/ml human recombinant leukemia inhibitory factor (#AMS-263-10, Amsbio, UK), 10ng/ml epidermal growth factor (#AMS-060-100, Amsbio, UK), 1ng/ml basic fibroblast growth factor (#AMS-480-10, Amsbio, UK) and 40ng/ml glial-derived neurotrophic factor (#4097-10, Amsbio, UK).

OSC culture medium was filter sterilised with a 0.22-µm sterile syringe filter unit (#SLGP033RS, Millex, UK) into 15ml Falcon tubes and stored parafilmed in the fridge at 4°C. OSC culture medium was warmed in the incubator with the lid loose half an hour before use. OSC culture medium was prepared every two weeks.

2.5.3 MEF Growth Culture Medium

Embryonic fibroblasts proliferated in a MEF growth culture medium that was prepared under sterile conditions by adding 10% FBS (#FCS-SA/50, Labtech, UK) to Dulbecco´s minimum essential medium (MEM) containing pyruvate and high glucose (#41966-029, Gibco, UK).

MEF growth culture medium was filter sterilised with a 0.22-µm sterile syringe filter unit (#SLGP033RS, Millex, UK) into 15ml Falcon tubes and stored parafilmed in the fridge at 4°C. MEF growth culture medium was warmed in the incubator with the lid loose half an hour before use. MEF growth culture medium was prepared every two weeks.

2.5.4 Coating of Culture Dish Surfaces for Fibroblast Expansion

Approximately 2ml of pre-warmed 2% (wt/vol) gelatine type B (#G1393, Sigma, UK) were poured into a 25-cm^2 flask (#431463, Corning, UK), with gentle rotation until the solution had covered the entire surface. The surface was allowed to dry for 2 hours before introducing cells and medium.

2.5.5 Initial Plating

Cells were centrifuged at 300g for 5 minutes at room temperature, and FACS-sorting medium or HBSS/DPBS buffers were removed from the sample with a plastic pipette. The

supernatant was discarded and the cell pellet was resuspended in 1ml of pre-warmed cell culture medium.

Putative OSCs and FACS-sorted cells from testis, liver and kidney were divided into two wells in 24-well dishes, then completed with 0.5ml of OSC culture medium. To avoid a high evaporation rate, 12 empty wells were filled with 1ml of DPBS. Fibroblasts were seeded into two 25-cm^2 flasks, and then completed with 10ml of fibroblast culture medium. Cells were placed in an incubator at 37°C with 5% CO_2.

2.5.6 Feeding of Cells

Cells were fed every Monday and Wednesday by adding drops of cell culture medium. On Friday, half of the spent medium was removed and new pre-warmed cell culture medium was added in the same quantity.

2.5.7 Passage of Cells

Cells were allowed to reach 90% confluence. The spent cell culture medium was removed and kept aside in the incubator. Wells were washed once with cold HBSS to remove traces of FBS, then 0.1ml of 0.05% (vol/vol) trypsin-EDTA solution (#25300, Gibco, UK) were added to each well containing the cells. The dish was kept in the incubator for 5 minutes maximum, with sporadic and gentle bottom tapping to help the cells to detach. The trypsin was then neutralized with the FBS in the wasted cell culture medium. The cell suspension was collected with a 5-ml borosilicate disposable pipette and centrifuged at 300g for 5 minutes at room temperature. The supernatant was discarded and the cell pellet was resuspended in 1ml of pre-warmed cell culture medium, and pipetted up and down until no clusters of cells were visible. Cells were then counted (see Section 2.5.6) and divided in a 1:2–1:3 proportion into new wells (average density of 2.5×10^4 cells) then completed by adding more cell culture medium.

2.5.8 Cell Counting with Neubauer Chamber

A Neubauer chamber with its coverglass was used in cell counting. A sample of 10µl of resuspended cells of interest was stained with 10µl of Trypan Blue (#93595, Sigma, UK). Then 10µl of the solution were expelled with a 20-µl pipette between the coverglass and the chamber carefully not to make bubbles. The Neubauer chamber was placed on a

microscope stage and observed with a 10X objective. Cells found in 4 large corner squares were counted (Fig. 2.1) and the cell density (cells per ml), total number of cells and required volume (based on the desired cell density) were calculated as follows.

$$\text{Average cells per square} = \frac{\text{Total counted live cells}}{\text{Number counted squares}}$$

$$\text{Cell viability} = \frac{\text{Total counted live cells}}{\text{Total counted live+dead cells}}$$

$$\text{Cell density} = \frac{\text{Average live cells per square} \cdot \text{Dilution factor}}{\text{Square volume (ml)}} = \text{Cells per ml}$$

The dilution factor is always 1, and the square volume is always 0.0001ml.

$$\text{Total number of cells} = \text{Cell density (cells per ml)} \cdot \text{Total volume (ml)}$$

$$\text{Required volume} = \frac{\text{Total counted live cells}}{\text{Desired cell density (cells per ml)}}$$

Figure 2.1. Cell counting with a Neubauer chamber.

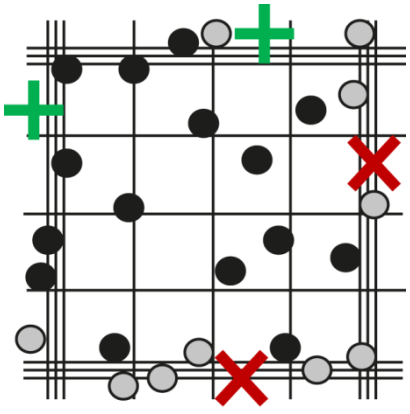

2.5.9 Cryopreservation and Thawing

After trypsinization and centrifugation, the cell pellet was resuspended in 1ml of cold cryopreservation medium (Appendix B). The suspension was stored into an appropriately labelled 2-ml cryovial (#V4757-500EA, Nalgene, UK) placed into a small polystyrene box, which was transferred to a –80°C freezer and left overnight. The next day, the cryovial was transferred to a liquid nitrogen storage container.

For the thawing of cells of interest, the cryovial was removed from liquid nitrogen storage and quickly placed in a 37°C water bath until only a small ice crystal remained. The thawed cells were slowly pipetted dropwise into 5ml of prewarmed cell culture medium in a 15-ml conical tube, with gentle agitation to distribute the cells. The tube was then centrifuged once at 200g for 5 minutes at room temperature. The supernatant was discarded and the cell pellet was resuspended in 2ml of pre-warmed cell culture medium. The cells of interest were distributed in 2 wells in a 24-well dish or 2 25-cm^2 flasks. The cell culture medium was entirely changed after 24 hours to remove any cryoprotectant left.

2.5.10 Mitotic Inactivation of Embryonic Fibroblasts

Embryonic fibroblasts (kindly provided by Dr Neil Smyth, Biological Sciences, University of Southampton) were cultured until Passage 3–4. When the cells had reached 90% confluence, they had the MEF culture medium discarded. The cell culture was then washed twice with 10ml of pre-warmed HBSS. Last, pre-warmed MEF culture medium was mixed with 10µg/ml of mitomycin C (#M4287, Sigma, UK) (Appendix B), and the solution was added to the fibroblasts of interest. The fibroblasts were inactivated for 2–3 hours in an incubator at 37°C with 5% CO_2. After this time, the inactivating medium was aspirated from the flask, and the inactive fibroblasts were typsinized (as seen in Section 2.5.5) and cryopreserved (as seen in Section 2.5.7).

2.5.11 Meiosis Enhancement

As putative OSCs were cultured into Passages 3 and 10, they were divided into 8 wells: 2 to maintain the cell line proliferation (Fig. 2.2A) and 6 for meiotic enhancement experiments in a separate 24-well dish (Fig. 2.2B). 24 hours post-seeding, the basic (Fig. 2.2, in blue) and OSC (Fig. 2.2, in pink) culture media were removed and replaced with control (Section 2.5.1) or OSC culture medium (Section 2.5.2) supplemented with one of the following (Fig. 2.2B) (Appendix B): 100ng/ml of bone morphogenetic growth factor 4 (BMP4; #TP723042, Amsbio, UK) for 48 hours; 6µg/ml of all-trans retinoic acid (RA; #R2625, Sigma, UK) for 48 hours; combined 100ng/ml of BMP4 and 6µg/ml of all-trans RA for 48 hours; 5 days in 100ng/ml of BMP4, then 15 days in 6µg/ml of all-trans RA.

Figure 2.2. Meiotic enhancement of putative OSC lines in 24-well dishes. (A) Cell culture dish for cell stock and proliferation and **(B)** meiotic enhancement. Basic medium is represented in blue. OSC medium is represented in pink.

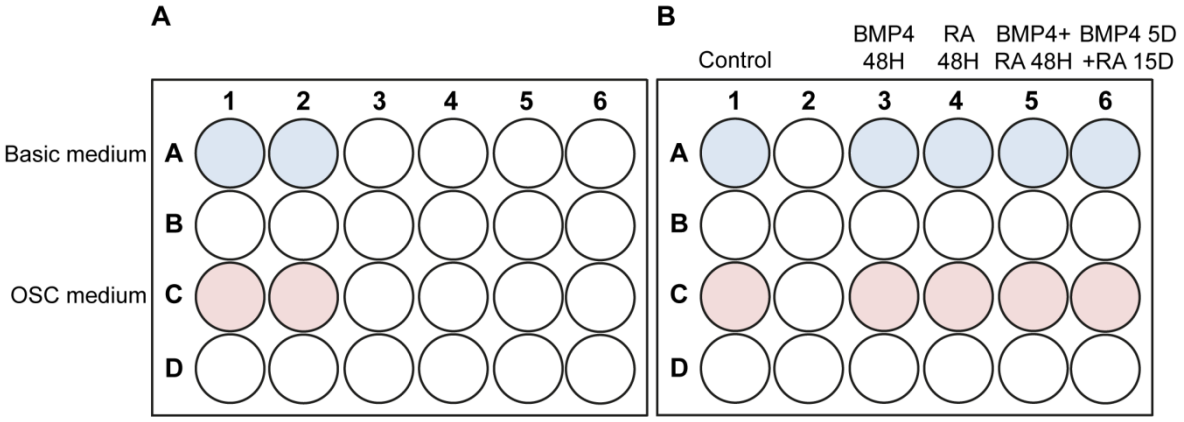

2.6 Tissue Fixation and Permeabilisation

2.6.1 Oocyte Fixation and Permeabilisation

Only GV oocytes stripped from intact COCs and bigger than 70µm, or MII oocytes with a visible polar body were transferred with a handling pipette into 200µl of 1X PHEM (Appendix B), and washed three times for 5 minutes. The oocytes were then transferred to 4% (vol/vol) formaldehyde (ref: 252549, Sigma, UK) in 1X PBS (Appendix B) for 30 minutes at room temperature. Oocytes were then washed in 1X PBS and permeabilised in 0.1% (vol/vol) Triton X-100 in 1X PBS solution (Appendix B) for 15 minutes at room temperature. Permeabilisation was avoided should the experiment test the presence of externalised DDX4 protein.

2.6.2 Organ Fixation and Paraffin Embedding

Ovaries and oviducts from at least 3 female mice, one testis, and kidneys from at least 3 embryos were separately fixed in 4% (vol/vol) formaldehyde in 1X PBS overnight at 4°C (Appendix B). The next day they were washed twice in 70% (vol/vol) ethanol in nuclease-free water for 5 minutes. Oviducts and kidneys were briefly stained with 1% (vol/vol) eosin (#212954, Sigma, UK) in 70% (vol/vol) ethanol in nuclease-free water for 2 hours given their small size. Samples were transported to the Histochemistry Research Unit (Southampton General Hospital) in 70% (vol/vol) ethanol in nuclease-free water in sealed tubes, where they were embedded in paraffin by staff at the Histochemistry Research Unit, Southampton General Hospital.

2.6.3 Tissue Sectioning and Mounting onto Glass Slides

Tissue sections were required to be mounted onto polylysine-coated glass slides to promote attachment of the cells. Poly-L-lysine solution (50μg/ml) (P4707, Sigma, UK) was poured into a 100-mm Petri dish (#430167, Corning, UK) in a fume hood. Microscope slides (#BS7011/2, Menzer-Gläser, Germany) were immersed in poly-L-lysine solution and incubated for 2 minutes at room temperature. The microscope slides were then air dry for 1 hour, and stored in a box at least 2 days before being used, to allow the polylysine to completely adhere to the glass.

For the tissue sectioning a paraffin rotary microtome (Leica, UK) was used. Precautions were taken to firmly adjust the specimen block in the specimen holder with the clamps provided by the manufacturer. The horizontally-fixed microtome knife was inspected and replaced if required in order to avoid notches in the cutting edge. The specimen holder was aligned in parallel with the cutting edge of the microtome knife. The thickness knob was adjusted to 4-μm and tissue sections were produced by moving the paraffin block up and down the microtome knife with a handwheel. The thin tissue section was carefully held with a small paint brush during the cutting, transferred with tweezers to a water bath and allowed to flatten for a couple of minutes at 37–40°C. The tissue sections were fished with the polylysine-coated slides and placed vertically in a glass slide box to allow drying for 2 days.

2.6.4 Dewaxing and Antigen Retrieval of Tissue Sections

Glass slides containing tissue sections were put in a glass slide holder into a stain bath (#258-4095-000, Evergreen Scientific, USA) twice for 5 minutes at room temperature in xylene (#534056, Sigma, UK) to remove the paraffin. The glass slides were then transferred with tweezers in a sequence of 100%, 90% and 70% (vol/vol) ethanol solutions for 20 seconds each at room temperature to allow rehydration of the tissue. Last, the dewaxed glass slides were washed twice in double-distilled water (ddH_2O) for 5 minutes with agitation at 15 r.p.m. at room temperature in a mechanical agitator (Stuart, UK).

Antigen retrieval was performed by completely immersing the slides in the glass slide holder in 0.01M citrate buffer (Appendix B) in a stain bath. The stain bath was covered with transparent film and allowed to boil 4 times in the microwave for 5 minutes each, topping up the buffer with ddH_2O after each boiling. Samples were allowed to cool in the citrate buffer for at least 20 minutes at room temperature before proceeding to the next step.

To remove background noise caused by blood, tissue slides in the glass slide holder were blocked with 3% H_2O_2 (#H1009, Sigma, UK) in methanol (#M/4000/17, Fisher Scientific, UK) (Appendix B) for 30 minutes at room temperature with agitation at 15 r.p.m. in a mechanical agitator.

2.6.5 Permeabilisation of Tissue Sections

Glass slide holders containing tissue sections were put into a stain bath twice for 5 minutes in 1% Triton X-100 in PBS (Appendix B) at room temperature, with agitation at 15 r.p.m. in a mechanical agitator to allow permeabilisation of the tissues.

2.6.6 Fixation and Permeabilisation of Cells Growing onto Coated Fluorodishes

Cells of interest were seeded in 200µl of OSC medium (Appendix B) in 35-mm imaging dishes (#P35G-1.0-14-C, MatTek, USA) (Fig. 2.3, in yellow) where the glass bottom was coated in poly-D-lysine (#P7886, Sigma, UK), with the evaporation controlled by attaching drops of DPBS to the sides of the dish (Fig. 2.3, white ovals). Dishes were placed into a humidified tissue culture incubator at 37°C, 5% CO_2 until the cells of interest had achieved confluence.

Figure 2.3. Seeding of cells in coated imaging dishes. The cells of interest were resuspended in OSC medium and were seeded only within the coated area (in yellow). DPBS drops were added to the sides of the dish (white ovals).

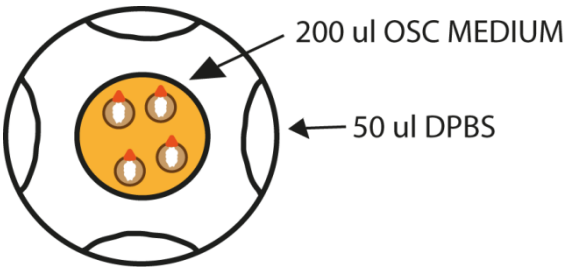

Imaging dishes with cells growing were then washed twice in ice cold PBS for 5 minutes, and the cells were fixed in 4% formaldehyde in PBS (Appendix B) for 20 minutes at room temperature. Then the devices were washed twice in ice cold PBS for 5 minutes, and the cells were permeabilised in 0.1% Triton X-100 in PBS (Appendix B) for 15 minutes at room temperature. Permeabilisation was avoided should the experiment test the presence of externalised DDX4 protein.

2.7 Immunohistochemistry

2.7.1 Immunohistochemistry Procedure to Isolate DDX4^{C25}-positive Cells

All FACS sortings required the previous immunostaining of cell suspensions in conical tubes. The cell pellet was resuspended in blocking solution (Appendix B) to prevent non-specific binding and background staining, and was incubated 20 or 40 minutes on fresh not-melting ice in an ice bucket to avoid cell damage and internalisation of the epitope of interest into the cytoplasm. The cell suspensions were then washed 3 times in ice cold HBSS at 300g for 5 minutes, and incubated in 1:10, 1:30, 1:100 and 1:300 DDX4^{C25} antibody (Table 2.4) adjusted to a concentration of 1mg/ml for 20 minutes on ice. The cell suspensions were washed as seen before and incubated in 1:250 IgG antibody conjugated to Alexa Fluor 633 or allophycocyanin (Table 2.5) adjusted to a concentration of 2mg/ml for 20 minutes on ice. This step required the samples to be in a dark environment to avoid photobleaching of the secondary antibody by covering the ice bucket in aluminium foil. The cells were washed as seen before and resuspended in FACS buffer (Appendix B) on ice with care to keep the cells in the dark until the FACS isolation took place.

2.7.2 Immunohistochemistry Procedure in Oocytes

All immunostaining procedures were performed using 96-well plates, where oocytes were transferred with a handling pipette through the wells. These wells contained 200µl of different solutions as required. The oocytes were incubated in blocking solution (Appendix B) for 1 hour at room temperature, and immediately after this they were transferred to 1:400 primary antibody (Table 2.4) overnight at 4°C. The next day the oocytes were washed 3 times in washing solution (Appendix B) for at least 5 minutes, and were transferred to 1:1,000 secondary antibody (Table 2.5) for 1 hour at room temperature. This incubation took place in a dark environment by wrapping the 96-well plates in aluminium foil. The oocytes were then washed as seen before and counterstained with 4',6-diamidino-2-phenylindole (DAPI, 20µg/ml; #D9542, Sigma, UK) diluted in PBS for 5 minutes.

To mount oocytes, 2µl of Vectashield Hard Set Mounting Medium (#H-1400, Vector Laboratories, UK) were placed in the centre of wells in 12-well 5.2mm numbered diagnostic microscope slides (#ER-202W-CE24, Thermo Scientific, UK). The oocytes were then collected with a handling pipette in minimal medium and transferred to the drop of Vectashield. The coverslip was carefully pressed down on the oocytes and it was fixed

to the microscope slide with nail varnish. Slides were stored horizontally in the dark overnight at 4°C, and the next day they were observed.

2.7.3 Immunohistochemistry Procedure in Tissue and Cell Culture Slides

All immunostaining procedures were performed using a home-made humid chamber, where paper tissue was soaked in PBS to prevent the different solutions added to the tissue slides from drying. The tissue and cell culture slides were incubated in blocking solution (Appendix B) for 1 hour at room temperature, and immediately after this the solution was removed by slightly touching it with a piece of paper tissue. The tissue slides were then incubated in 1:200 primary antibody, whereas the cell culture slides required a 1:400 dilution (Table 2.4) overnight at 4°C. The next day the tissue and cell culture slides were washed 3 times in washing solution (Appendix B) for at least 5 minutes, and were added 1:500 secondary antibody (Table 2.5) for 1 hour at room temperature. This incubation took place in a dark environment by wrapping the humid chamber in aluminium foil. The tissue and cell culture slides were washed as seen before and counterstained with DAPI diluted in PBS for 5 minutes. A final wash in PBS was performed.

To mount tissue and cell culture slides, the microscope slides were dried with a paper tissue with care not to touch the samples. Then 10µl of Vectashield Mounting Medium were placed over the sample, and a coverslip was carefully pressed down on it, which was then fixed to the microscope slide with nail varnish. Slides were stored vertically in the dark overnight at 4°C, and the next day they were observed.

2.7.4 Immunohistochemistry Procedure in Western Blot

All immunostaining procedures were performed using an opaque plastic container that was covered with plastic film during incubations and washes. The nitrocellulose membrane was incubated in blocking solution (Appendix B) for 1 hour at room temperature with agitation at 15 r.p.m. Immediately after this the primary antibody was spiked in the blocking solution to a 1:1,000 dilution (Table 2.4) and left overnight with agitation. The next day the membrane was washed 3 times in washing solution (Appendix B) for at least 5 minutes with agitation at 15 r.p.m., and was transferred to 1:5,000 secondary antibody (Table 2.5) for 1 hour at room temperature with agitation. This incubation took place in a dark environment by wrapping the plastic container in aluminium foil. The membrane was

washed as seen before and allowed to dry in an oven for at least 2 hours at 37°C before visualisation.

Table 2.3. Primary antibodies used in this study.

SOURCE	TARGET	DILUTION IN BLOCKING SOLUTION
Rabbit polyclonal	DDX4^{C25} (#13840, Abcam, UK)	1:10–1:300 for FACS 1:400 for oocytes and cells 1:200 for tissue slides 1:1,000 for Western Blot
	DAZL (#34139, Abcam, UK)	1:400 for oocytes and cells 1:200 for tissue slides
	DDX4^{351} (#17545-1-AP, ProteinTech, UK)	
	DPPA3 (#19878, Abcam, UK)	
	IFITM3 (#19878, Abcam, UK)	
	PRDM1 (#PA5-20310, Thermo Scientific, UK)	

Table 2.4. Secondary antibodies used in this study.

SOURCE	CONJUGATED TO	DILUTION IN BLOCKING SOLUTION
Goat anti-rabbit IgG	Allophycocyanin (#111-136-144, Jackson ImmunoResearch, USA)	1:250 for FACS
	Alexa Fluor 633 (#A21070, Life Technologies, UK)	1:250 for FACS 1:1,000 for oocytes and cells 1:500 for tissue slides
	IRDye 800CW (#926-32211, LiCor, UK)	1:5,000 for Western Blot

2.8 Fluorescence Analysis

All immunostaining procedures described here (confocal microscopy, FACS sorting, Western blot) are based on the ability of a fluorophore to emit fluorescence. A fluorescent substance can absorb light at a certain wavelength to excite its electrons to a higher energy level, with the excited electrons in turn emitting photons of light at a higher wavelength. In biological research fluorophores can be fluorescent dyes such as DAPI and propidium iodide (PI), proteins such as GFP, and synthetic dyes such as Alexa Fluor 633, allophycocyanin (APC) and IRDye 800CW. Such compounds have specific excitation and

emission wavelengths (Table 2.5) that require specific lasers, mirrors and detectors to be analysed.

Table 2.5. Maximum absorbance and emission of fluorophores.

FLUOROPHORE	EXCITATION MAXIMUM (nm)	EMISSION MAXIMUM (nm)
PI	351	617
DAPI	357	461
Alexa Fluor 633	631	647
Allophycocyanin	652	660
IRDye 800CW	776	792

2.8.1 Confocal Microscopy

In confocal microscopy the laser beams rapidly scan across the sample to create an image. In the confocal microscope used here detailed images are created by a method called Acousto-optical Beam Splitting (AOBS), where a tellurium dioxide crystal diffracts light of different wavelengths depending on its density. This density of the crystal can be altered through mechanical radiofrequency waves. Thanks to this mechanical wave, the desired excitation colour is selected and fed through the objective lens to the sample. Once the sample emits a signal from the fluorophore, this light travels through the crystal and is collected by the detector. The detector in turn passes the information to the imaging programme and creates an image pixel by pixel. Clearer and more detailed images are obtained by passing the emitted light through a pinhole before reaching the detectors. The pinhole blocks out of focus light that could smear the final image. Last, a photo-multiplier tube (PMT) detector collects visible light to produce a bright-field image of the sample.

Fixed samples were imaged using the 60X oil immersion objective on a Leica SP8 confocal microscope fitted with hybrid detectors. Single stack was taken at 1024x1024 pixel resolution. DAPI and Alexa Fluor 633 were imaged sequentially to prevent spillage of fluorescence (Table 2.6).

Table 2.6. Path configuration used to image fluorophores on a Leica SP8 microscope.

FLUOROPHORE	LASER TYPE AND WAVELENGTH (nm)	DETECTOR
DAPI	Solid state, 405	Hybrid HyD1
Alexa Fluor 633	Air-cooled Helium-Neon 633	Hybrid HyD2

2.8.2 Fluorescence-Activated Cell Sorting

Fluorescence-activated cell sorting (FACS) is a flow cytometry technique that simultaneously determines yield, physical characteristics and expression of various external and internal markers of interest in single cells using an optical-to-electronic coupling system, which can also record these data for subsequent analysis. Despite being a slow cytometry method requiring trained professionals to operate it, it allows for a high sensitivity and resolution in the sample analysis and reaches up to 95% purity in isolated populations, contrary to the 75% purity obtained by magnetic-activated cell sorting (MACS). MACS is a magnetic-bead-based separation method that is quick, cheap, portable and avoids hazardous reagents, therefore causing less stress to live cells. However, during the OSC isolation by MACS, positive fractions were contaminated with oocytes, possibly caused by a reactivity of cytoplasmic DDX4 in damaged oocytes or a carryover during column washing (White et al., 2012). Therefore, for my project, FACS was selected as the most efficient OSC isolation method and cell sorting was performed in BD Biosciences FACSAria I and II (Beckton Dickinson, UK).

FACS are made up of three systems: fluidics, optics and electronics (Fig. 2.4). The fluidics system divides the cell suspension into individual particles in a stream towards the laser beam for interrogation (Fig. 2.4A). This process is known as hydrodynamic focusing. To accomplish this in a FACSAria, the cell suspension is driven into a fully closed flow chamber based on a quartz cuvette that injects the sample into a stream of buffer called shearth fluid (Fig. 2.4A). By maintaining both streams unperturbed and unmixed, the cell suspension is accelerated, which pressure-forces it to narrow into a stream of single 0.2–100µm particles. The maximum size of the particles can be selected by a ceramic nozzle tip (Fig. 2.4A). At the same time, this sample stream is moved through the centre of the flow chamber and emerges into open air (Fig. 2.4A), where it perfectly aligns with the laser beam and collection optics (Fig. 2.4B).

The optics system consists of: light sources that illuminate the particles in the sample stream, optical filters that direct the resulting photons or light signals to appropiate detectors, and the detectors that communicate with the electronics system (Fig. 2.4B). In a FACSAria the light sources are lasers (Table 2.7). This allows to focus a high beam of monochromatic light in a small volume of sample thanks to the small spot size of the laser, and to obtain maximum excitation from a single cell. These characteristics minimise the probability of finding more than one cell in the laser beam and produce purer population analysis. The photons emmited by the sample are refined by long-pass dichroic mirrors

placed at different angles with respect to the light (Fig. 2.4B, green rectangles), which allows them to select out light above certain wavelenghts. The splittered photons are further narrowed by a barrier filter (Fig. 2.4B, orange rectangle) which selects wavelenght within a certain range. This is ultimately the light collected by the PMT receptors (Fig. 2.4B, grey rectangle).

Table 2.7. Lasers available in the FACSAria at the University of Southampton.

LASER	WAVELENGHT	TYPE AND POWER
Violet	407 nm	396 mW Diode Point Source Solid State laser. Min. power 10mW.
Blue	488nm	Coherent Sapphire Solid State laser. Min. power 13mW.
Red	635 nm	626 mW Diode JDS Uniphase HeNe Air-cooled laser. Min. power 11mW.

The path configuration in the FACSAria at the University of Southampton starts with the 488nm laser. Light is initially scattered deppending on the size and internal complexity of the particle. Forward-scattered light (FSC) measures diffracted light in the forward direction and gives information on the cell surface area (Fig. 2.4B). Side-scattered light (SSC) measures refracted and reflected light occuring at cellular intervals in an angled direction and gives information on the internal complexity of the cell. FSC and SSC do not require mirrors, but are further narrowed by different barrier filters, and are collected by different detectors (Table 2.8). Next, DAPI is excited with a 407nm laser. The light emitted by DAPI is narrowed by a dichroic mirror that removes wavelenghts above 502nm and by a 450/40 filter, so that the light arriving at the PMT1 receptor is within the 410–490nm range (Table 2.8). Last, Alexa Fluor 633 is excited with a 633nm laser, and its emitted light is narrowed by a dichroic mirror that removes wavelengths above 735nm and by a 660/20 filter, therefore the light arriving at the PMT3 receptor is within the 640–680nm range (Table 2.8).

Initial FACS analyses were performed with PI and a secondary antibody conjugated to APC. In this case, PI was excited with the 488nm laser, and the emitted light was processed with a dichroic mirror allowing light below 595nm and a 610/20 filter. The final detected light was in the 590–595nm range (Table 2.8). Arrangements to excite and detect APC-emitted light were the same as for Alexa Fluor 633 (Table 2.8).

Table 2.8. Path configuration for cell sorting in a FACSAria.

LASER	FILTERS		DETECTORS	
	DICHROIC MIRROR	BARRIER FILTER		EMISSION FROM
407 nm	502 Long Pass	450/40 Band Pass	PMT1	DAPI
488 nm			FSC	Forward Scatter
	595 Long Pass	610/20 Band Pass	PMT2	Side Scatter PI
635 nm	735 Long Pass	660/20 Band Pass	PMT3	Alexa Fluor 633 APC

The electronics system modulates the laser intensity and the amplitude and frequency of the streath stream. Furthermore, when the particle is at the centre of the laser beam the electronics system converts the detected photons into voltages that are assigned a channel number on a data plot in logarithmic scale (Fig. 2.4C). In a FACSAria such electronics system is governed by the FACS Diva programme, which decides on the sorting by charging and deflecting particles. To perform this charging, the streath stream firstly passes the laser beam and analysis on the emitted light takes place. The flow chamber contains a piezoelectric transducer that vibrates vertically at a frequency between 20 and 60kHz, and causes the analysed streath stream to break into droplets and to positively charge the droplets of interest at 50–150V (Fig. 2.4C). The gap between droplets is controled by the electronics system. The steam of droplets then passes through a pair of plates charged at ~ 5000V, and only the positively charged droplets are deflected and collected in a given container (Fig. 2.4C).

Live immunostained cells resuspended in FACS buffer (Appendix B) were analysed with FACSAria I and II governed by the FACS Diva programme. The cell suspensions were injected in a fully closed flow chamber with a 100-µm nozzle tip. The path configuration (Table 2.8 and 2.9) was maintained in all experiments. ‘No antibodies’ and ‘secondary antibody only’ controls were analysed with the addition of PI or DAPI to gate viable $DDX4^{C25}$-negative populations. Samples were then gated for live $DDX4^{C25}$-positive populations as a result of events appearing above certain logarithmic scale on a data plot, by comparison with the control samples. Populations of interest were sorted with high purity. Amplitude of the vibrations and frequency of the droplet creation were adjusted in each experiment. Positive and negative populations were collected in M2 medium with 20% FBS (Appendix B) and transported to the laboratory in a portable incubator at 37°C.

Figure 2.4. FACSAria analysis and sorting of DDX4^{C25}-positive cells.

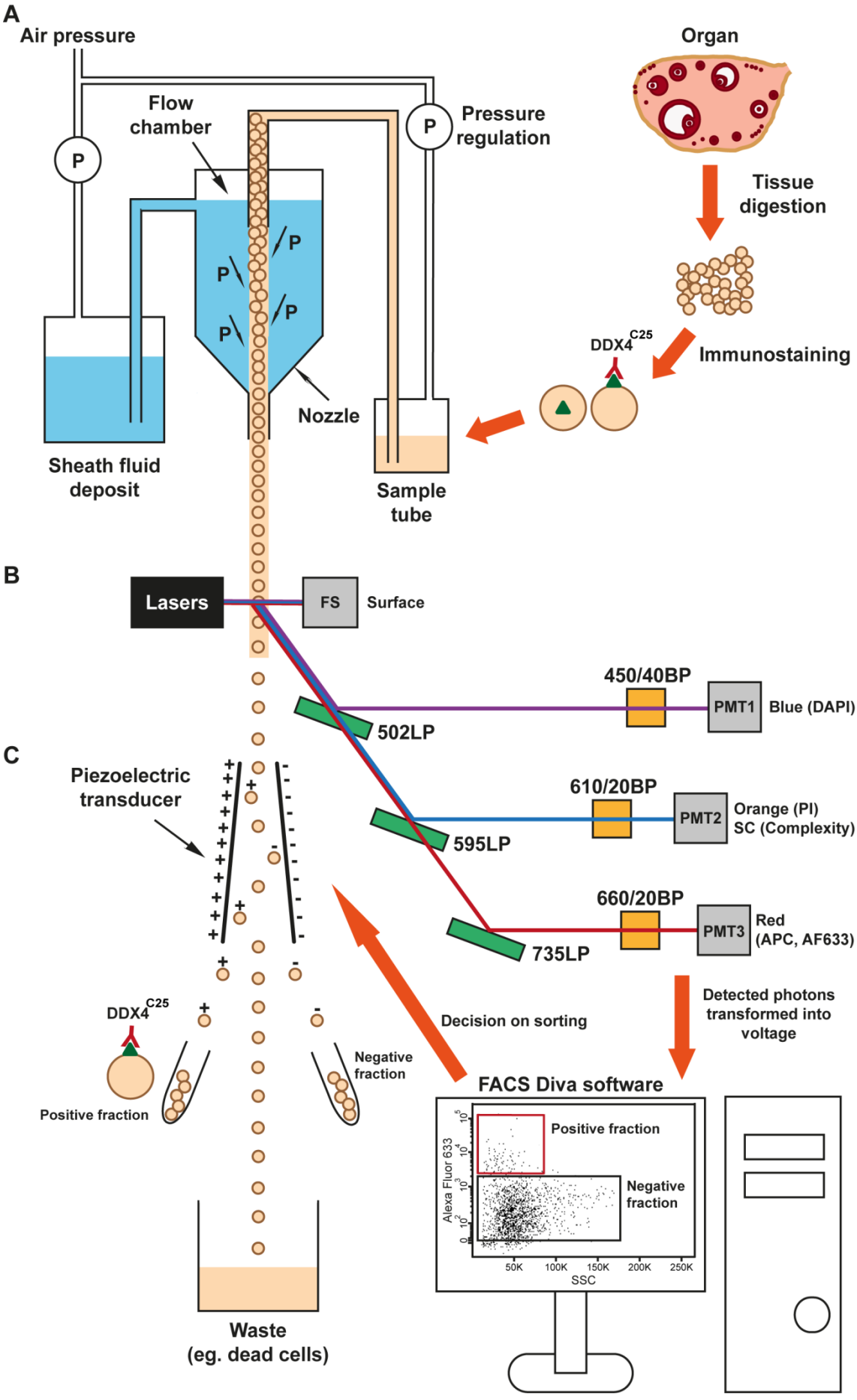

2.9 Protein *In Silico* Modelling

2.9.1 Sequence Detection

The National Center for Biotechnology Information (NCBI) Protein Database (www.ncbi.nlm.nih.gov/protein) was used to obtain human and mouse reported DDX4 isoform sequences (Appendix B) by selecting from a list of 'DDX4' the following results:

- Probable ATP-dependent RNA helicase DDX4 isoform 1 [*Mus musculus*],
- Probable ATP-dependent RNA helicase DDX4 isoform 2 [*Mus musculus*],
- Probable ATP-dependent RNA helicase DDX4 isoform 1 [*Homo sapiens*],
- Probable ATP-dependent RNA helicase DDX4 isoform 2 [*Homo sapiens*],
- Probable ATP-dependent RNA helicase DDX4 isoform 3 [*Homo sapiens*],
- Probable ATP-dependent RNA helicase DDX4 isoform 4 [*Homo sapiens*].

Protein alignment and similarity comparison with the epitopes recognized by the $DDX4^{C25}$ and $DDX4^{351}$ antibodies were performed on NCBI Protein-to-protein Basic Local Alignment Search Tool (BLASTp) (https://blast.ncbi.nlm.nih.gov/Blast.cgi). The last 25 or 351 residues of the C-terminal domain of each DDX4 isotype were selected, then they were run as query sequences against the last 25 residues of the carboxyl domain of human DDX4 isotype 1 (the epitope recognized by the $DDX4^{C25}$) or the last 351 residues of the carboxyl domain of human DDX4 isotype 1 (the epitope recognized by the $DDX4^{351}$) after selecting the 'Align two or more sequences' option.

2.9.2 Sequence Comparison

Potential mouse proteins aligning to the $DDX4^{C25}$ epitope were searched through BLASTP. The last C-terminal 25 or 351 residues of the human DDX4 isotype 1 were selected as the query sequence for the entire proteome of *Mus musculus* using the blastp algorithm. Two databases were used because they retrieved different aligning proteins (Appendix C):

- UniProtKB/SwissProt (SwissProt),
- Reference Sequence (RefSeq).

2.9.3 Transmembrane Modelling

For the detection of transmembrane domains in the human and mouse DDX4 isoforms

retrieved from BLASTp (Appendix C), eleven online transmembrane protein prediction methods (Table 2.9) were selected based on the following characteristics: developed by reliable institutions, free of charge to use, programmed by a combination of a statistical model and a discriminative analysis of protein topology (Table 2.9).

Table 2.9. Selected computer-based predictors of transmembrane domains.

		STATISTICAL MODEL			
		Hidden Markov	**Neural Networks**	**Support Vector Machines**	**Wimley-White**
ANALYSIS	**TM helix vs beta barrel TM**		MEMSAT3		MPEx
	TM helix vs signal peptides	Phobius		MEMSAT-SVM	
	TM helix vs re-entrant regions	OCTOPUS			
	Experimental derived TM helix	HMMTOP TMHMM TopPred TMpred	PredictProtein		
	TM helix vs globular		PRED-CLASS MEMSAT3		

2.10 Statistics Analysis

All experiments were replicated at least twice. Statistics were performed with GraphPad Prism (GraphPad, USA). Quantitative data were expressed as means ± s.e.m. Two-tailed Fisher test determined the likelihood of $DDX4^{C25}$ staining being present in the nucleus of germinal vesicles with surrounded nucleolus organisation. A P-value of 0.05 or smaller was considered statistically significant.

Chapter 3

In silico modelling and initial immunohistochemical analysis of an antibody to DDX4

3.1 Introduction

OSCs have been sorted (using FACS or MACS) from ovarian tissue in most studies with an antibody to DDX4 (DEAD box polypeptide 4) (Ding et al., 2016; Hernandez et al., 2015; Imudia et al., 2013; Khosravi-Farsani et al., 2015; Park and Tilly, 2014; Park et al., 2013; White et al., 2012; Zhang et al., 2011; Zou et al., 2009). DDX4 is a germline-specific RNA helicase, containing a DEADc ATP hydrolysis domain and a HELICc RNA unwinding domain that are common to all members of the DEAD box protein family (Cordin et al., 2006; Hickford et al., 2011; Linder and Lasko, 2006). Adding to the continuing controversy over the existence of OSCs is that DDX4, as an RNA binding protein, was hitherto believed to be cytoplasmic (Castrillon et al., 2000; Fujiwara et al., 1994) rather than membrane-bound. As such, it is unclear how an antibody raised against it can be effective in sorting live cells.

The inconsistency in isolating live cells by means of a cytoplasmic protein has been rationalised by invoking a differentiation-dependent externalisation of the C-terminus domain of DDX4 in germ stem cells only, not oocytes (White et al., 2012). However, this has never been proved experimentally. Hence, concerns have arisen around the specificity of the FACS-specific antibody to DDX4 (Abban and Johnson, 2009; Hernandez et al., 2015; Vogel, 2012; Woods and Tilly, 2015; Zhang et al., 2015).

My aim in this Chapter is to elucidate further the DDX4 antibody used in the previous FACS/MACS studies – here called $DDX4^{C25}$ antibody – before attempting any FACS analysis myself. I wanted to explore more fully the *in silico* evidence for a membrane-bound DDX4, and additionally perform immunohistochemistry in male and female germ cells.

3.2 Results

3.2.1 Human and mouse DDX4 isoforms identified by database analysis

Human and mouse DDX4 isoforms – different sequence forms codifying for the same protein by alternative splicing of mRNA (Buratti et al., 2012) – were identified by the NCBI Protein Database.

In human, four DDX4 isoforms were retrieved: isoform 1 (724 aa), isoform 2 (690 aa), isoform 3 (704 aa) and isoform 4 (575 aa) (sequences in Appendix C). Isoform 1 is thought to be the mature protein expressed in the human germline (Castrillon et al., 2000; Hickford et al., 2011; Noce et al., 2001). Two mouse isoforms were retrieved: isoform 1 (728 aa) and isoform 2 (702 aa) (sequences in Appendix C). Mouse isoform 1 is thought to be the mature protein expressed in the germline (Castrillon et al., 2000; Fujiwara et al., 1994; Hickford et al., 2011; Olsen et al., 1997).

Although only one DDX4 isoform has been observed by Western and Northern blot analysis in testes and germ stem cells in mouse (Fujiwara et al., 1994) and human (Castrillon et al., 2000; Medrano et al., 2012), no information is available on whether it is the same isoform present in the OSCs. Furthermore, it is not known if any of the variants contain external domains. Therefore, all human and mouse isoforms were selected for further bioinformatics analysis.

3.2.2 *In silico* analysis of the DDX4^{C25} antibody specificity

The DDX4^{C25} antibody used in the OSC FACS and MACS sorting is raised against the C-terminal domain of human DDX4. As stated by Abcam, the company producing this antibody, the epitope is within residues 700 to the COOH-terminus of the human DDX4. The epitope therefore spans the C-terminal 25 residues of the mature protein sequence, and would be predicted to detect all four human DDX4 isoforms.

The DDX4^{C25} epitope was subjected to sequence alignment with the mouse DDX4 on BLAST Protein, using the SwissProt and RefSeq databases. The programme found a 92% correlation with the C-terminus of both mouse isoforms, with just two mismatching residues: serine to histidine, and phenylalanine to isoleucine (Figure 3.1).

SwissProt and RefSeq databases were also interrogated for any significant alignment between the human DDX4^{C25} epitope and a sequence in the mouse proteome not belonging to DDX4, which would potentially cause cross-reactivity of the antibody for DDX4 (Appendix C).

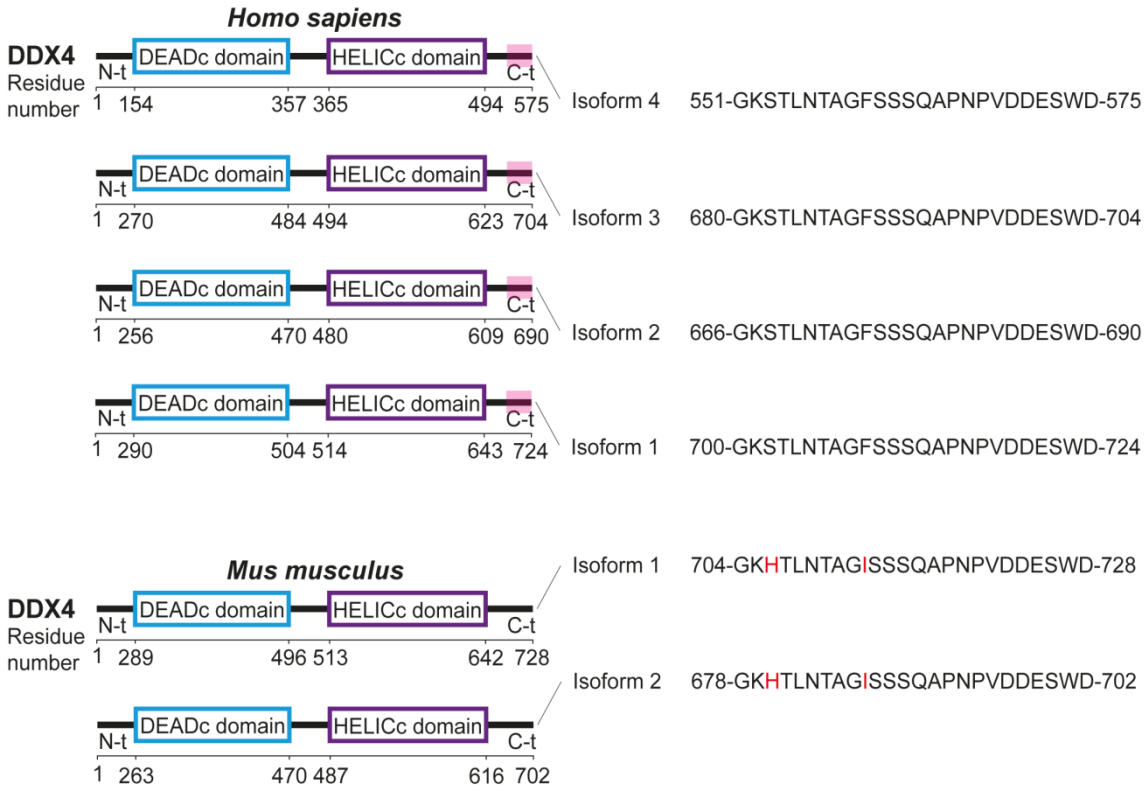

Figure 3.1. The epitope used to generate the DDX4^{C25} antibody is highly conserved for all DDX4 isoforms in mouse and human. Diagram representing the functional domains of the human and mouse DDX4 isoforms and the C-terminal domain sequence. The antibody used for the isolation of the OSCs targets the last 25 residues of the COOH-terminus (C-t, in pink) of the human DDX4 protein. In the mouse, this C-terminus differs in two residues (highlighted in red).

The DDX4^{C25} sequence did not entirely align to any other murine protein, but did partially align to three cell surface receptors: ATP-binding cassette subfamily C member 12 (ABCC12, also known as MRP9), receptor-type protein tyrosine phosphatase H (PTPRH) and neurogenic locus notch homolog protein 3 (NOTCH3) (Fig. 3.2A). ABCC12 is a protein involved in multidrug resistance that contains 12 transmembrane domains (Kruh et al., 2007). It aligns to the DDX4^{C25} epitope in seven residues and is ubiquitously expressed (Fig. 3.2A, B), but the aligned sequence is located near the N-terminal domain, which is intracellular (Fig. 3.2C). PTPRH presents ten residues aligned (Fig. 3.2A, B), with the alignment in an extracellular chain domain close to a signal peptide that allows the recognition and transmembrane transport of molecules (Fig. 3.2C). Interestingly, this protein is highly expressed in the testis, but also in a handful of other tissues, where it is involved in cell differentiation (Fig. 3.2B) (Matozaki et al., 1994). NOTCH3 also has an alignment in its cell surface domain, between the EGF-like 25 and 26 domains (Fig. 3.2C), with nine residues aligned here (Fig. 3.2A, B). Although it helps in cell fate and differentiation pathways, its expression is not restricted to the reproductive system (Fig. 3.2B) (Bellavia et al., 2008). The cellular localization of those residues involved in the partial alignment to the DDX4^{C25} epitope suggests that only PTPRH and NOTCH3 would be recognized by the DDX4^{C25} antibody in non-permeabilised cells (Fig. 3.2C).

Taking these results together, the alignment of the human C-terminal sequence of DDX4 against the mouse proteome shows only a strong alignment with the epitope in DDX4 itself. Considering only the protein primary structure, the polypeptide chain, binding of the antibody to a cell surface protein other than DDX4 is remote, based on the low number of aligned residues (Fig. 3.2A), and on E-values higher than one that point to a non-biological, random alignment (Fig. 3.2B) in the two membrane-bound receptors that it could potentially recognize. Secondary and tertiary structures, as well as post-translational modifications should be studied to fully determine the specificity of the DDX4^{C25} antibody for DDX4.

3.2.3 *In silico* analysis of transmembrane domains in human and mouse DDX4

For the detection of transmembrane domains in the human and mouse DDX4 isoforms retrieved in Section 3.2.1, 11 transmembrane protein prediction methods were applied by combining four statistical models with five discriminative analysis of protein topology.

In *Homo sapiens*, only three methods predicted a transmembrane domain, and this was for all the human isoforms. However, in each case it was in an outside-to-inside orientation

A

Human DDX4	700	GKSTLNTAGFSSSQAPNPVDDESWD	724
Mouse ABCC12	42	--------------APNPVDD----	48
Mouse PTPRH	149	---TLNT-----S-APNPV------	159
Mouse NOTCH3	992	--------GFTGSQCQNPVD---W-	1004

B

PROTEIN	SEQUENCE MATCH	E-VALUE	LOCALIZATION	FUNCTION
ABCC12	7/25	1.3	All tissues	Multidrug resistance
PTPRH	10/25	5.5	Brain, liver, testis	Differentiation, mitotic cycle
NOTCH3	9/25	3.6	All tissues	Differentiation, renewal, fate determination

C

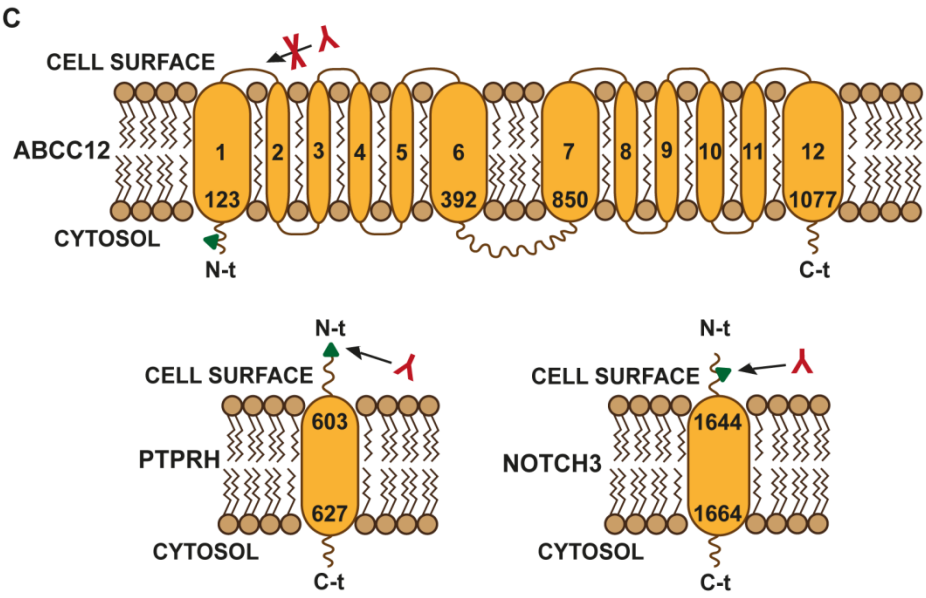

Figure 3.2. Partial alignment of human DDX4^{C25} epitope to three cell surface receptors. (A) Alignment of mouse cell surface proteins with the human DDX4^{C25} epitope. **(B)** Aligned residues, tissue distribution and functional characteristics of the candidate mouse cell surface proteins that may be bound by the DDX4^{C25} antibody. **(C)** Cellular localization of those residues involved in the partial alignment to the DDX4^{C25} epitope (green triangle) and binding by DDX4^{C25} antibody (red Y) in non-permeabilised cells.

that would place the C-terminus in the cytoplasm, rather than on the cell surface (Fig. 3.3A, B, C, D) (Appendix C). The transmembrane sequence would be between 15 and 18 residues long, formed towards the C-terminus in MEMSAT3 (Fig. 3.3A, B, C, D; first column), and within the DEADc domain for MEMSAT-SVM and TopPred (Fig. 3.3A, B, C, D; second and third columns).

For *Mus musculus*, again three methods identified a transmembrane domain in an outside-to-inside orientation, with the C-terminus in the cytoplasm (Fig. 3.4A, B) (Appendix C). As with the human modelling, between 15 and 18 residues would be contained in this transmembrane sequence. Similar to the human prediction, MEMSAT3 placed the transmembrane domain near the C-terminus (Fig. 3.4A, B; first column), whereas for MEMSAT-SVM and TopPred it was placed inside the DEADc domain (Fig. 3.4A, B; second and third columns). TMpred was the only method to suggest a cell surface C-terminus in two different conformations: a strong double-transmembrane domain prediction that included an externalised N-terminus (Fig. 3.4A, B; fourth column), and a weaker single-transmembrane domain prediction (Fig. 3.4A, B; fifth column). Therefore, given that the C-terminal domain of DDX4 would only be external in mouse, these predictions would state that live cell sorting of OSCs by FACS would only be possible in mouse, not human.

3.2.4 Performance of the DDX4^{C25} antibody in ovarian and testicular cells

The transmembrane domain prediction for DDX4 performed in Sections 3.2.1-3.2.3, suggests that live cell sorting of OSCs by FACS via a membrane-bound C-terminus DDX4 is only viable in mouse ovarian cell suspensions. Before attempting to perform this FACS-sorting, I wanted to examine the ability of the DDX4^{C25} antibody to recognize DDX4 protein within the germline.

As would be predicted based on its known function as an RNA-binding protein (Linder and Lasko, 2006), immunohistochemical DDX4^{C25} staining on permeabilised fully-grown GV and MII oocytes revealed a cytoplasmic distribution (Fig. 3.5A). A similar result was found in male germline cells from testicular cell suspensions (Fig. 3.5C). As observed previously (Toyooka et al., 2000), different cell stages during spermatogenesis were distinguishable thanks to a reduction in the distribution of DDX4 and the formation of membraneless organelles called chromatoid bodies (Fig. 3.5E). In early meiotic stages, from spermatogonia to leptotene spermatocytes, DDX4 was distributed all over the cytoplasm. As meiosis progressed, DDX4 became concentrated in perinuclear granules, at

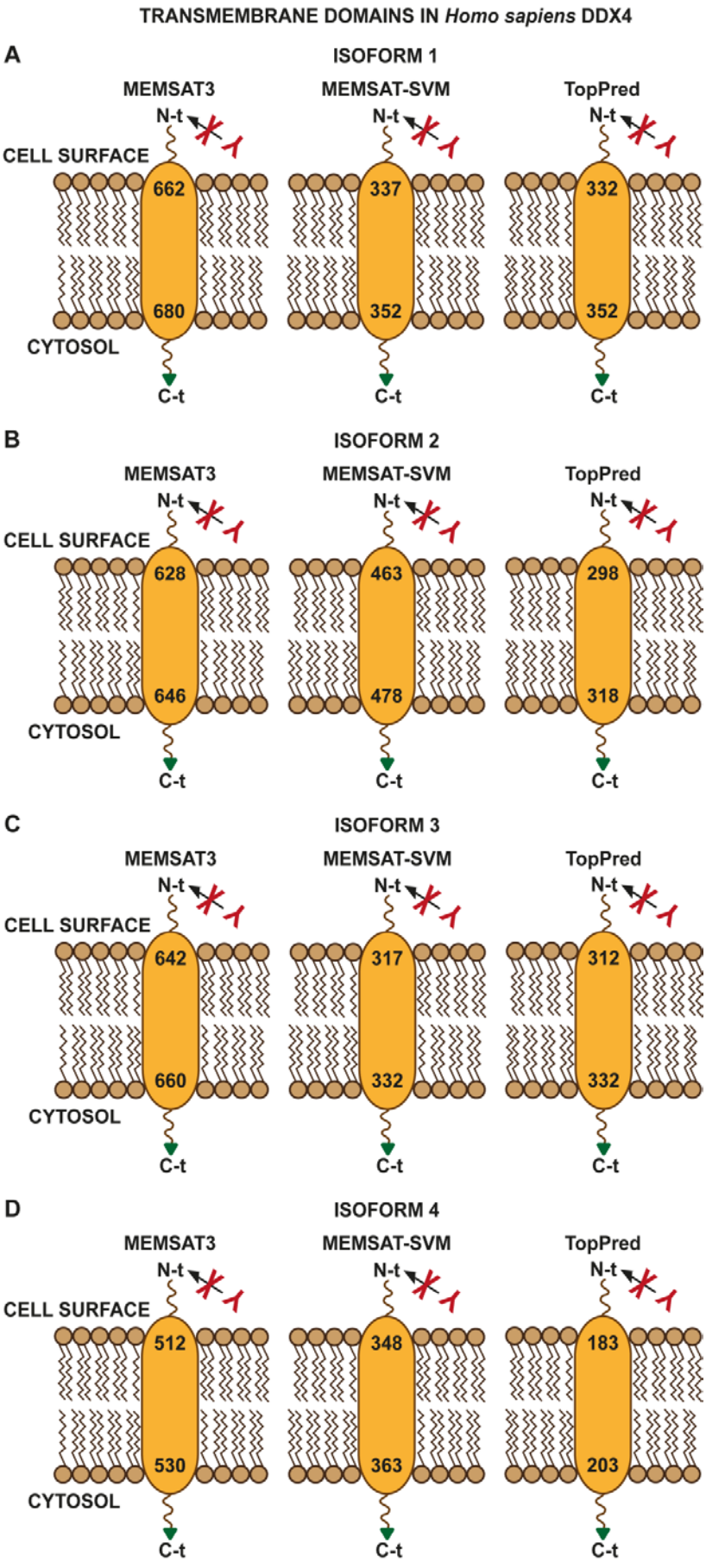

Figure 3.3 (continues)

Figure 3.3. *In silico* prediction of transmembrane domains in *H.s.* DDX4. Diagram of the single-transmembrane domains predicted in human DDX4 isoform 1 **(A)**, isoform 2 **(B)**, isoform 3 **(C)** and isoform 4 **(D)** by three transmembrane protein prediction methods.

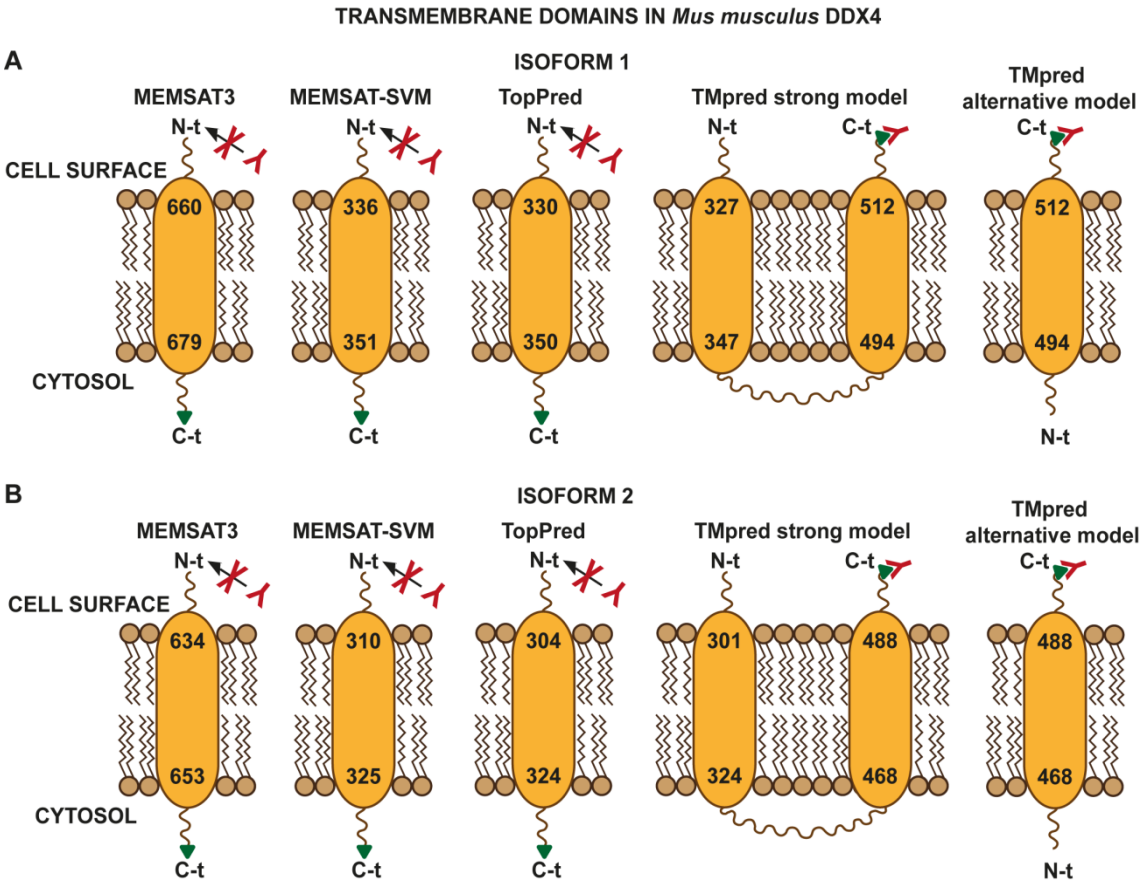

Figure 3.4. *In silico* prediction of transmembrane domains in *M.m.* DDX4. Diagram of the transmembrane domains predicted in mouse DDX4 isoform 1 **(A)** and isoform 2 **(B)** by four transmembrane protein prediction methods.

first in increased numbers in zygotene spermatocytes and reduced to 3–5 granules in pachytene to diplotene stages. Finally, after meiosis was complete, DDX4 was concentrated in a perinuclear chromatoid body in round spermatids at stages I to VI. DDX4 disappeared as these spermatids elongated their nucleus at later stages (VII to VIII), and was absent from the mature sperm and from supporting somatic cells.

The cytoplasmic distribution of DDX4 was absent in non-permeabilised oocytes, with no evidence of any surface staining (Fig. 3.5B). There was positive immunostaining of DDX4 in the polar body of MII oocytes (Fig. 3.5B and insert), which may be because plasma membrane permeabilisation had taken place as part of the polar body apoptosis, resulting in the $DDX4^{C25}$ antibody gaining access to the cytoplasm, without prior permeabilisation step therefore being needed.

As expected of a germline-specific protein (Fujiwara et al., 1994), DDX4 appeared absent from ovarian somatic cells, a mixture of granulosa, stromal and epithelial cells, independent of their permeabilisation status (Fig. 3.5B). Interestingly, non-permeabilised testicular cells (Fig. 3.5D) gave the same DDX4 distribution as permeabilised cells (Fig. 3.5C), with clear staining of the perinuclear granules. I believe this is in an artefact of preparation, as the spreading of these cells onto the slide is likely to have compromised their membrane integrity, allowing the $DDX4^{C25}$ antibody to enter the cytoplasm. These circumstances, however, do not alter the resulting conclusion that no $DDX4^{C25}$-positive cells were observed in the ovarian cell suspension (Fig. 3.5A, B). This absence suggests that if present, OSCs are a scarce population in the mouse ovary, and that live oocytes will not be a source of false positives in the FACS-sorting of OSCs.

3.2.5 Observed inclusion of DDX4 in the nucleus of SN-stage GV oocytes

In the experiments described in Section 3.2.4., high $DDX4^{C25}$ immunostaining was observed in the nucleus of GV oocytes that presented a condensed chromatin. GV oocytes are arrested at the diplotene stage of the first meiosis. Meanwhile, as part of maturation, their chromatin is remodelled for the control of gene expression and meiotic competence (De La Fuente, 2006; Lodde et al., 2007). From an initial decondensed chromatin that does not surround the nucleolus (non-surrounded nucleolus organisation, NSN), oocytes progress to a condensed ring of chromatin around the nucleolus (surrounded nucleolus organisation, SN), that is associated with transcriptional quiescence (Bouniol-Baly et al., 1999), changes in metabolic activity (Ma et al., 2013) and a greater meiotic maturation and

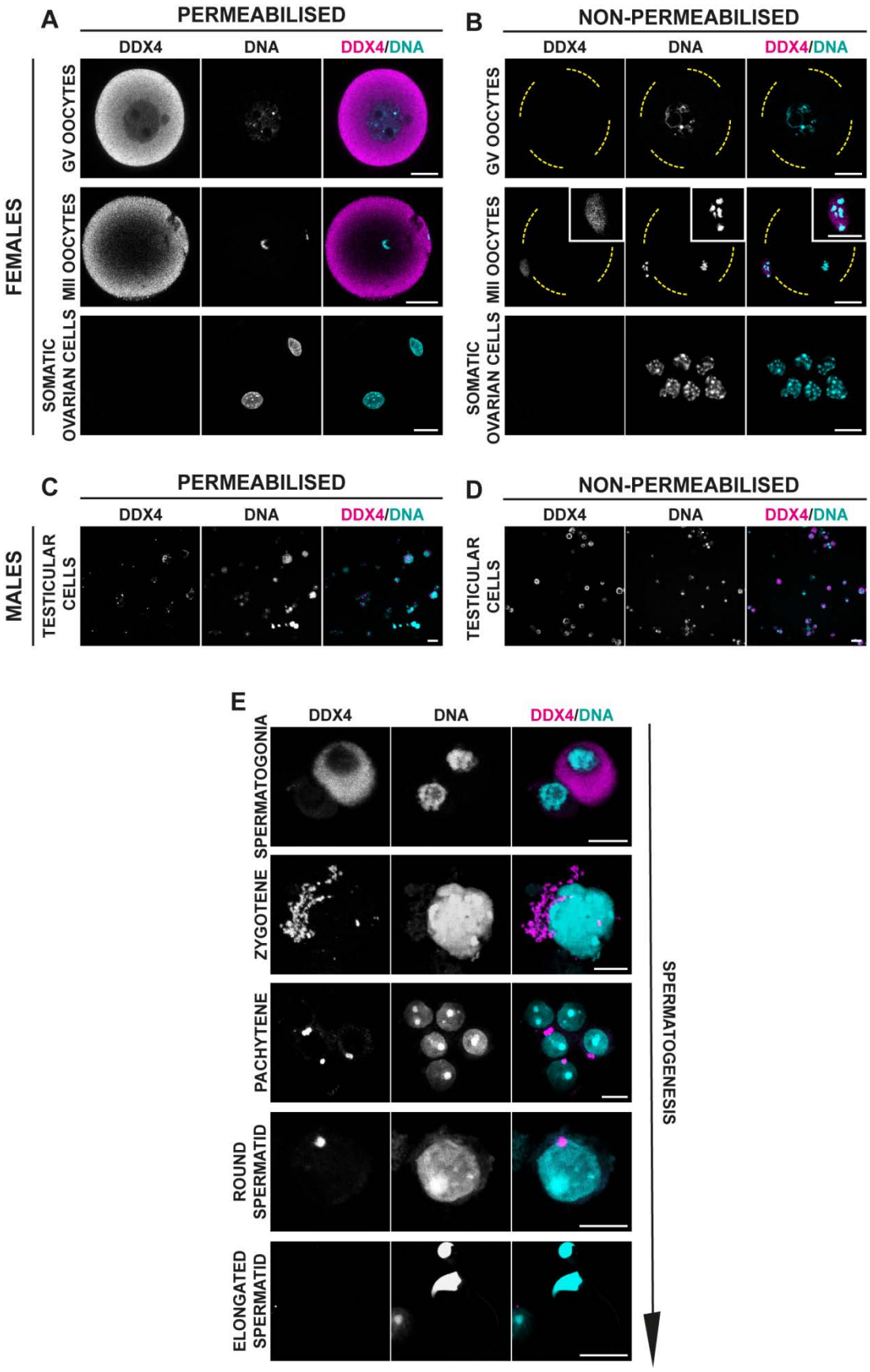

Figure 3.5. DDX4^{C25} antibody immunostaining of fully-grown oocytes and male germ cells. (A, B) DDX4^{C25} immunostaining in permeabilised **(A)** and non-permeabilised **(B)**

fully-grown oocytes and ovarian somatic cells (a mixture of stroma and granulosa cells). **(C, D)** DDX4^{C25} immunostaining in permeabilised **(C)** and non-permeabilised **(D)** testicular cells (a mixture of somatic and germline cells). **(E)** DDX4 distribution in the male germline as spermatogenesis progresses. In total 93 oocytes and 500 somatic cells taken from 14 ovaries, and 750 male cells taken from 2 testes were analysed. Chromatin was stained with Hoechst 33342. Scale bar: 20 µm, insert 10 µm.

developmental competence following fertilisation (Inoue et al., 2008; Liu and Aoki, 2002; Wickramasinghe et al., 1991; Zuccotti et al., 2002). However, this nuclear distribution in SN GV oocytes has not previously been described, nor was expected. DDX4 performs post-transcriptional modifications in the mRNA in the cytoplasm, not the nucleus. Furthermore, it is thought to be dispensable for oocyte meiotic progression, with knockout mouse females having an uncompromised fertility (Tanaka et al., 2000). Therefore, nuclear increase of DDX4 would be without reason in a transcriptionally-silent GV oocyte preparing to exit meiosis I.

Therefore, to determine if the entry of DDX4 in the nucleus was being achieved only in completely condensed chromatin, the staining of permeabilised GV oocytes with the $DDX4^{C25}$ antibody was repeated, and the oocytes were sorted into four different groups depending on the chromatin condensation stage and the low or moderate/high presence of DDX4 from their nucleus: NSN-low, NSN-high, SN-low, SN-high.

Virtually all NSN GV oocytes had DDX4 immunostaining predominantly in the cytoplasm, with only low nuclear presence (Fig. 3.6A, B). In contrast, the majority of SN GV oocytes positively stained for DDX4 in the nucleus, either at the same level (Fig. 3.6A, B), or higher than in the cytoplasm (Fig. 3.6A, B). No high nuclear DDX4 NSN GV oocytes were observed. Despite the low number of oocytes studied, there is a clear tendency of DDX4 to be included in the nucleus of GV oocytes as they prepare to exit the first meiosis (P-value < 0.0001). But why is it so, given the transcriptional quiescence of GV oocytes and the non-meiotic role of DDX4, is unknown.

3.3 Discussion

This study has shown that the primary technique for isolating adult germline stem cells from the ovary of mammals is possibly based on a false assumption: the existence of a cell surface DDX4 allowing live cell-sorting by FACS. Here I have demonstrated that, although the $DDX4^{C25}$ antibody may have specificity for DDX4, the externalisation of its C-terminal domain through a transmembrane domain is not very likely.

3.3.1 The $DDX4^{C25}$ antibody is specific of DDX4 in the germline

Given their functions in RNA metabolism, the DEAD-box RNA helicase family including DDX4, are generally regarded as being cytoplasmic (Cordin et al., 2006; Linder and Lasko, 2006; Nott et al., 2015). Known exceptions are *Lactobacillus* aggH,

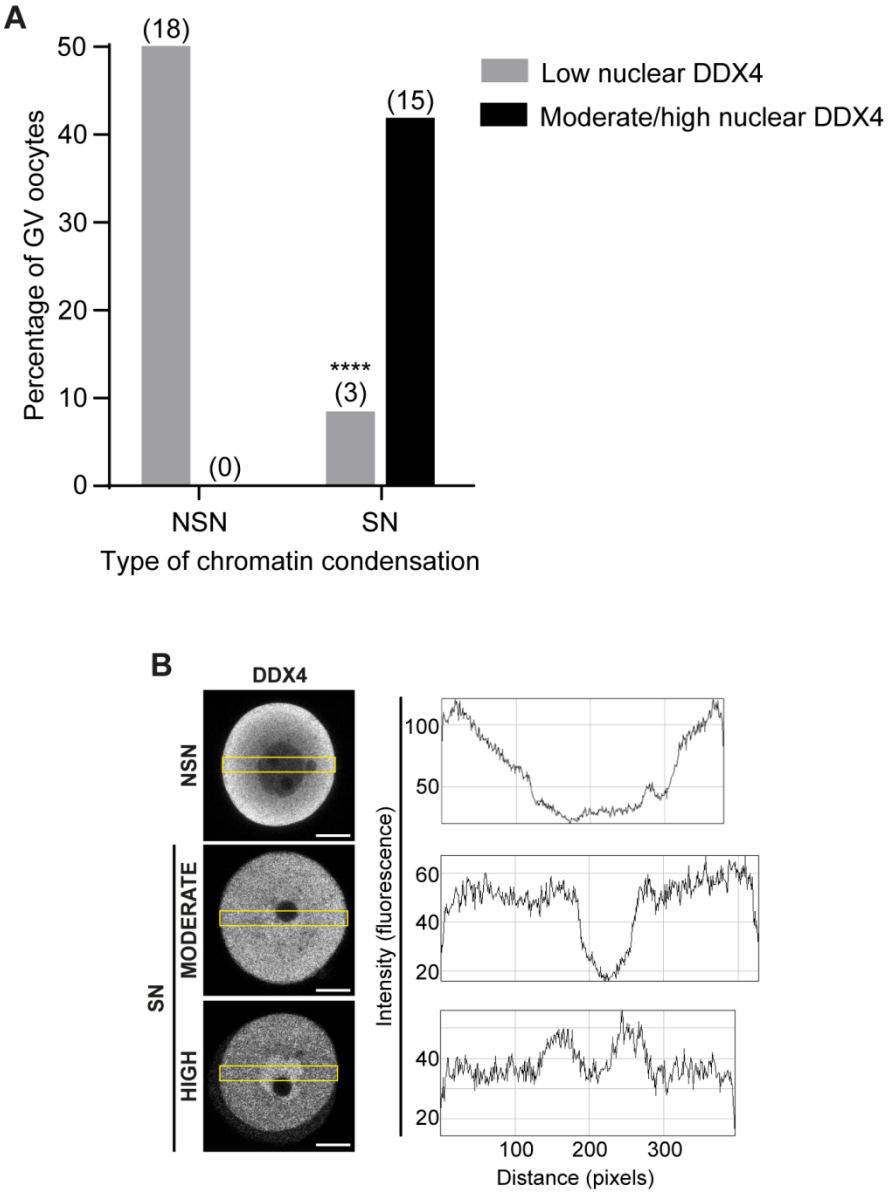

Figure 3.6. Distribution of DDX4^{C25} immunostaining in NSN- and SN-type GV oocytes. (A) Nuclear DDX4^{C25} immunostaining distribution in permeabilised GV oocytes with uncondensed (NSN, grey bars, 18 oocytes) or condensed chromatin (SN, black bars, 18 oocytes). In total I analysed 36 GV oocytes from 12 ovaries with a two-tailed Fisher's exact test (P-value < 0.0001). **(B)** DDX4 fluorescence intensity histograms for NSN- and SN-stage GV oocytes. Scale bar: 20 µm.

which contains a cell surface domain for bacterial aggregation (Roos et al., 1999), and mouse HEL-T in immature thymocytes, the only known example of development-dependent cell surface expression of an RNA/DNA helicase (Miazek et al., 1997).

Consistent with this cytoplasmic localization were my observations on permeabilised male germ cells, which through stage specific meiotic changes provided evidence that immunostaining was indeed DDX4: meiosis progression stage was easily determined by dynamic change of the protein from an homogeneous cytoplasmic distribution in spermatogonia to a concentration in perinuclear granules and chromatoid bodies in round spermatids (Kotaja et al., 2006; Toyooka et al., 2000). These granules are membraneless cytoplasmic organelles that capture and store RNA by direct contact with the nucleus, perform post-transcriptional gene regulation, and prevent the deleterious activity of transposable elements in the RNA interference pathway during spermatogenesis (Kotaja and Sassone-Corsi, 2007). Here, the RNA-silencing pathway of the male germline differentiation depends on the interaction between N-terminus DDX4 and C-terminus Dicer, another helicase with an RNase motif (Bernstein et al., 2001; Kotaja et al., 2006).

3.3.2 *In silico* analysis does not support a cell surface DDX4 model

Considering the well-established cytoplasmic expression of DDX4 (Castrillon et al., 2000; Cordin et al., 2006; Linder and Lasko, 2006; Nott et al., 2015; Toyooka et al., 2000), the existence of a membrane-bound C-terminus DDX4 in germ stem cells but not oocytes to justify the FACS-sorting of OSCs has generated controversy, as it is solely sustained by *in silico* topology predictions (Abban and Johnson, 2009; Zou et al., 2009). Transmembrane proteins are thought to make 20–25% of the proteome, and perform bidirectional communication between the cell and its environment, which makes them excellent pharmacological targets (Ahram et al., 2006; Krogh et al., 2001; Wallin and von Heijne, 1998). Experimental detection of these transmembrane proteins is however difficult, and only 2% of their presumed numbers are known (Berman et al., 2000). Statistical topology prediction methods determine the best candidates presenting this conformation, which can then be pursued by more direct experimental confirmation (Tusnády and Simon, 2010). The hydrophobic transmembrane helix and increased cytoplasmic protonated residues that can be differentiated from regular loops are at the core of the *in silico* transmembrane prediction methods (Claros and von Heijne, 1994). The eukaryotic protein chains adopt α-helix structures to pierce the plasma membrane: low free energy conformations where polar amino and carbonyl groups are embedded in the lipid

bilayer to confer hydrophobicity (Granseth et al., 2005), accompanied of positively charged residues remaining in the cytoplasm in what is called the 'positive inside rule' (von Heijne, 1986). Improvements for the topology prediction include statistical optimisation of programming algorithms to present the optimal topology (Jones, 2007; Viklund and Elofsson, 2004), and machine-learning methods that align problem sequences with known transmembrane proteins (Krogh et al., 2001; Tusnady and Simon, 1998). Despite none of the available *in silico* transmembrane prediction methods is 100% accurate (Chen et al., 2002), those model-based and alignment-based methods are more efficient (Chen et al., 2002; Ikeda et al., 2002; Viklund and Elofsson, 2004) and were used in this DDX4 analysis.

The absence of DDX4 staining in non-permeabilised reproductive cell suspensions and the computational analysis of transmembrane domains in DDX4 both support a cytoplasmic expression, and lend little evidence for a membrane-bound C-terminal domain that can be used for the FACS-sorting of OSCs. The TMpred model that has previously justified the OSC-sorting technique (Abban and Johnson, 2009; Zou et al., 2009) reports the externalisation of the C-terminus only in mouse, not human, DDX4 and brings into question its reported ability to sort human OSCs (Fakih et al., 2015; White et al., 2012). Furthermore, the predicted mouse double-transmembrane conformation, which allows the externalisation of the C-terminus should be regarded as doubtful, because this also necessitates a membrane-bound N-terminal domain that was previously thought not to exist (White et al., 2012). This leaves an alternative C-tail-anchored conformation (Borgese and Fasana, 2011) to explain the mouse OSC sorting.

A further criticism on the predictions made by TMpred in mouse is that both the double and single conformations hinder the RNA unwinding and coordination of HELICc over the ATP hydrolysis and RNA binding performed by DEADc (Fig. 3.7A, B). In the double prediction, the DEAD-box domain is truncated: Q motif for ATP binding on the cell surface; motif I (Walker A) for ATP binding embedded in the plasma membrane; and in the cytoplasm, motifs Ia and Ib for RNA binding and motifs II (Walker B) and III for ATP binding and hydrolysis (Fig. 3.7A) (Cordin et al., 2006). When considering the C-tail-anchored prediction, both the DEADc and HELICc domains remain intact, but are physically separated by the plasma membrane (Fig. 3.7B). Although both domains contain motifs with suspected repeated functions – motifs Ia and Ib in the DEADc domain are structurally similar to VI and V in the HELICc domain (Story et al., 2001) –, it is worth thinking how the HELICc domain can bind and modify RNA in the extracellular matrix

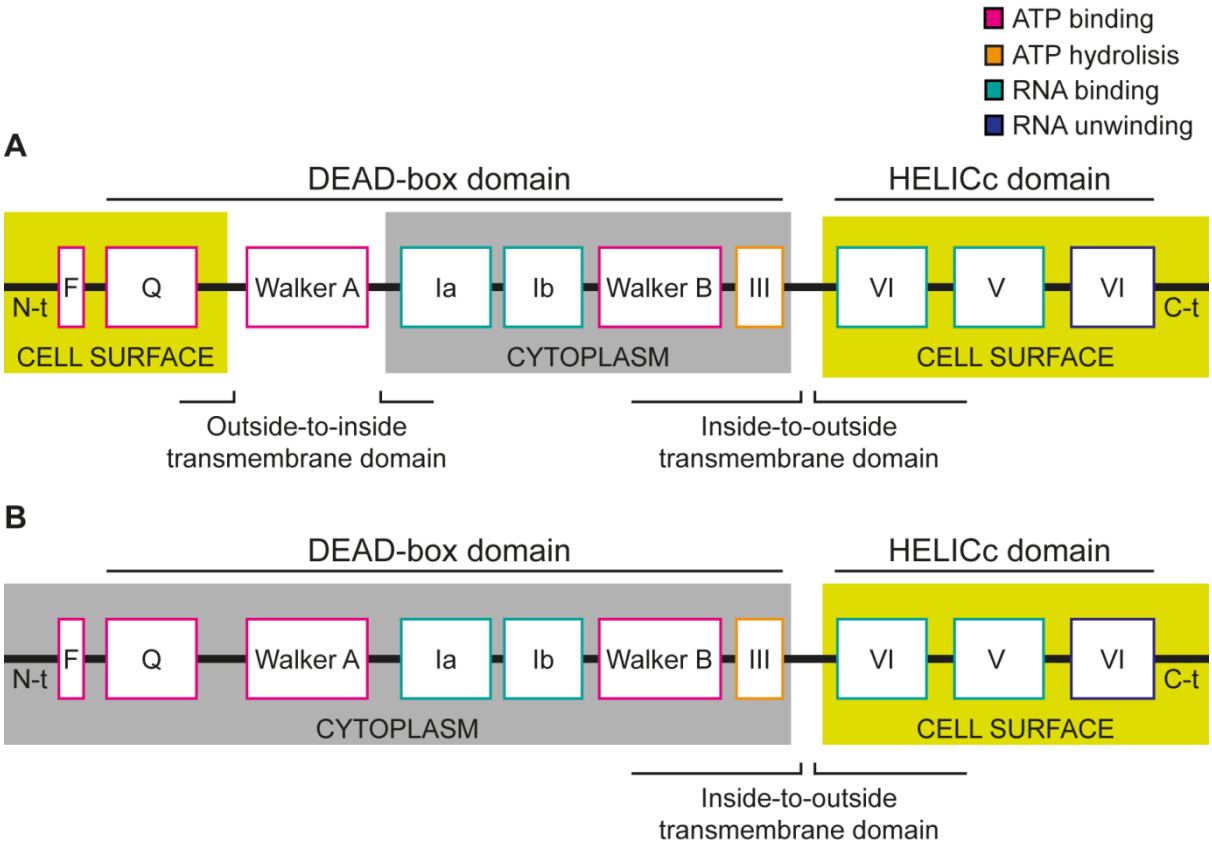

Figure 3.7. Functional motifs affected by externalisation in *M.m.* DDX4 following TMpred transmembrane prediction. Disruption of the functional motifs in mouse DDX4 isoform 1 based on predictions of a strong double-transmembrane model **(A)** and a weaker single-transmembrane model **(B)** through TMpred.

when this molecule is prone to quickly degrade. The proposed C-tail-anchored DDX4 (Abban and Johnson, 2009; Zou et al., 2009), if existing, would not be functional under these circumstances.

Aside from the *in silico* transmembrane prediction methods, it is difficult to clearly predict whether the C-terminal domain of DDX4 is externalised in PGCs and OSCs in physiological conditions or as a truncated isoform. This C-terminus is predicted to be intrinsically disordered and, therefore, hard to anticipate in structure and folding (Forman-Kay and Mittag, 2013). Some crystallisation has been done in *Drosophila*: the last residues within this C-terminal domain are important for the translation factor elF5B binding, but they also interact with the N-terminus to form an interdomain cleft were ATP is embedded and RNA runs (Sengoku et al., 2006). DDX4 is an evolutionary well-conserved protein, and these models should help to clarify the C-terminus function in physiological conditions in mouse and human. The necessity of N- and C-termini interaction once again points to an entire cytoplasmic localization of the latter.

3.3.3 The DDX4^{C25} antibody may bind to membrane-bound receptors

The DDX4^{C25} antibody may potentially bind to a cell surface domain in another protein. My proteomic predictions point to the possibility of binding the membrane-bound receptor-type protein tyrosine phosphatase H (PTPRH) and the neurogenic locus notch homolog protein 3 (NOTCH3). Both evolutionary-conserved proteins are involved in cell differentiation (Bellavia et al., 2008; Matozaki et al., 1994), which makes them candidates to explain the OSCs potential to develop into oocyte-like cells in culture. These findings, however, should be considered as illustrative rather than definitive: the expected overall extent of alignment is low with both of them, and their high E-values suggest a non-biological random match between sequences. The expression of these two receptors is not germline-restricted, but distributed throughout a number of tissues. They also do not directly take part in oogenesis. PTPRH has been linked to MLH1, essential for meiotic spindle dynamics (Santucci-Darmanin et al., 2000), but it is not to be found in oogenesis in Drosophila (Fitzpatrick et al., 1995). In mouse oogenesis, the NOTCH signalling pathway is involved in the epigenetic methylation maintenance of *Stra8* for stimulation by retinoic acid and in the meiosis I progression (Feng et al., 2014), and later in the primordial follicle assembly between pregranulosa cells and the immature oocyte, with high rates of oocyte apoptosis in the presence of Notch inhibitors (Trombly et al., 2009). However, NOTCH3-deficient female mice show normal oogenesis, which indicates that this candidate is not

essential for germ stem cell differentiation (Krebs et al., 2003). The ubiquitous expression of PTPRH and NOTCH3 would explain why a number of laboratories can obtain DDX4^{C25}-positive cells from non-reproductive tissues such as liver or kidney (Hernandez et al., 2015; Zhang et al., 2015), but not the scarcity of these populations and its absence from my granulosa and stromal ovarian cells immunocytochemistry preparations.

Taking together the sequence binding analysis and the immunohistochemistry of reproductive tissues, the DDX4^{C25} antibody seems to show specificity to DDX4, but a weak likelihood to bind a cell surface DDX4 epitope. The staining in male and female germline cells but not in surrounding somatic cells likely corresponds to DDX4. There are, however, issues that require further consideration before rejecting the existence of a cell surface DDX4. One is the possibility that OSCs contain a non-functional C-tail-anchored DDX4. The other is the unavailability of *in silico* and experimental crystallization of the mouse and human C-terminal DDX4, which refrain from predicting the level of specificity of the DDX4^{C25} antibody for the secondary and tertiary structures of the mouse DDX4, or after post-translational modifications, as well as its binding to other proteins with a similar folding.

3.3.4 A membrane-bound DDX4 may behave similarly to HEL-T

Another approach to ascertain whether a membrane-bound DDX4 is non-functional is by comparing it to the DEAD-box helicase HEL-T. As explained before, this protein is maturation-dependent externalised in thymocytes, and the only known membrane-bound DNA/RNA helicase in metazoans (Miazek et al., 1997). HEL-T has been speculated to be a molecular supervisor of immunity maturation in the αβ ($CD4^+8^+$) and γδ ($CD4^-8^-$) lineages. The externalisation of an unidentified epitope would allow the V(D)J recombinase to rearrange T-cell antigen-specific receptor (TCR) α, β, γ and δ genes in immature thymocytes, whereas its TCR-mediated internalisation would inhibit the V(D)J recombinase through helicase activity and end the T-cell maturation. Northern blot analysis of mRNA revealed that post-translational-dependent modification would mediate this epitope externalisation, rather than being the effect of different isoforms (Miazek et al., 1997). However, as the authors of this study report, it is not clear whether membrane-bound HEL-T is non-functional or actively allowing the activity of the V(D)J recombinase (Miazek et al., 1997). Therefore, HEL-T comparison to DDX4 does not solve the functionality of the protein in OSCs.

3.3.5 DDX4 could help to detect meiotically competent GV oocytes

Also interesting is the accumulation of DDX4^{C25} in the nucleus of SN stage GV oocytes only after chromatin condensation and just before germinal vesicle breakdown. Aside from its decreased cytoplasmic concentration as the oocyte gains meiotic competence (Castrillon et al., 2000; Fujiwara et al., 1994), and its condensation in the Balbiani body in non-murine primordial oocytes (Castrillon et al., 2000) – a membraneless organelle enriched in mitochondria (De Smedt et al., 2000) that has a role in early oocyte specification (Lei and Spradling, 2016; Pepling et al., 2007) – the role of DDX4 in oocytes is unknown. I speculate that it may have a role in GV oocytes that are highly competent to exit the meiosis I dictyate arrest.

Unlike males, female mammals do not require DDX4 for meiosis entry and progression, and are still fertile in the absence of DDX4 (Reynolds et al., 2005; Shibata et al., 2004; Sugimoto et al., 2009; Tanaka et al., 2000). A deletion between residues 328 and 338 (corresponding to the Walker A motif) in *Ddx4* formed a stop codon that prevented synthesis of the full length protein. In homozygous knockout male mice this led to reduced numbers of PGCs and no spermatogenesis beyond the zygotene stage, associated with high apoptosis rates (Tanaka et al., 2000). It is possible that their female counterparts conserve other RNA helicases that compensate for the absence of DDX4 during PGC proliferation and oogenesis (Tanaka et al., 2000). Alternatively, oogenesis may also differ from spermatogenesis at this key postmeiotic stage.

Another possibility to explain why DDX4 is essential in males, but not female mammals, is the different Dicer isoforms active in both gametes. The N-terminus DDX4 and the C-terminus Dicer interact in the RNA silencing pathway in spermatogenesis (Kotaja et al., 2006). The somatic and spermatogenic Dicer, known as Dicer^{S}, are different from the oocyte-specific Dicer^{O} isoform, in which the protein lacks the N-terminal domain (Flemr et al., 2013; Stein et al., 2015). It may be that this domain contains essential flanking sequences that confer specificity to bind DDX4, and hence the female DDX4 is no longer needed for meiotic progression.

These hypotheses, however, still do not explain the reason for the nuclear accumulation observed in SN GV oocytes, when the cell is transcriptionally silenced, and no mRNA is produced to necessitate such large quantities of RNA helicase. With such scarce information known about pathways operating at this time, it is difficult to venture what DDX4 is doing in the nucleus.

In summary, in this Chapter I have applied *in silico* transmembrane domains predictors and immunohistochemistry to provide evidence of the DDX4^{C25} antibody specificity for DDX4, and also to conclude that the externalisation of its C-terminal domain through a transmembrane domain is not very likely. This possibility however cannot be ruled out because the implications of post-transcriptional modifications of the protein could not be analysed, although it is known that they exist and produce isoforms (Hickford et al., 2011). Furthermore, functional DNA/RNA helicases with external domains have been reported in physiological conditions. And last, there is an *in silico* transmembrane domains predictor that does predict an external C-terminal domain in DDX4.

Given the lack of absolute certainty in the cellular localization of DDX4, I have determined to attempt live cell-sorting of adult germline stem cells from the mouse ovary by FACS and DDX4^{C25} antibody, and then culture them. This set of experiments will be performed and discussed in the next Chapter.

Chapter 4

Isolation by FACS of ovarian cells using a DDX4 antibody

4.1 Introduction

OSCs were initially sorted from murine and human live ovarian cell suspensions through FACS or MACS, using a DDX4^{C25} antibody raised against its C-terminus (White et al., 2012; Zou et al., 2009). Based on the DNA quantity contained in the freshly sorted cells, the number of OSCs has been estimated to be 1 in 10,000 cells of the whole adult mouse ovary (Vogel, 2012; White et al., 2012).

Controversy over the FACS-sorting methodology has focused on the lack of a membrane-bound DDX4 and the non-specificity of the DDX4^{C25} antibody employed in the FACS sorting (Abban and Johnson, 2009; Telfer et al., 2005; Vogel, 2012; White et al., 2012; Woods and Tilly, 2013b; Zhang et al., 2012b; Zou et al., 2009). DDX4 is believed to be cytoplasmic due to its RNA unwinding functions (Castrillon et al., 2000; Fujiwara et al., 1994), despite suggestions of a differentiation-dependent externalisation of the C-terminus domain of DDX4 in female germ stem cells (Abban and Johnson, 2009; White et al., 2012).

In Chapter 3 I concluded that the DDX4^{C25} antibody was specific to the primary sequence of the protein, and that by immunohistochemistry it was localised to the cytoplasm of oocytes. Furthermore, the *in silico* transmembrane modelling of DDX4 by TMpred predicted a C-tail-anchored conformation that provided a small possibility to isolate murine OSCs. Based on these results, in this Chapter I have attempted to obtain putative OSCs by adapting the original FACS-sorting protocol.

4.2 Results

4.2.1 FACS-sorting of DDX4^{C25}-positive ovarian cells with a DDX4/APC/PI protocol

One protocol for the FACS isolation of OSCs uses DAPI (Kapuscinski, 1995) as a viability dye (Woods and Tilly, 2013b). However, flow cytometers equipped with 375 nm or 405 nm lasers that would have maximally excited DAPI were initially unavailable at the University of Southampton. Instead, propidium iodide (PI) was chosen as the live/dead discriminator because of its previous use in the detection of DDX4^{C25}-positive ovarian cells (Fig. 4.1A) (White et al., 2012). A BD FACSAria was therefore arranged as follows for the excitation and collection of PI and allophycocyanin (Fig. 4.1B):

- PI (max. excitation: 351 nm, max. emission: 617 nm (Jaroszeski, 1998)) was excited with a 488 nm laser and detected with a 610/20 nm filter, which accounts for 41.4% of the total dye excitation and 20% of the total dye emission. However there was some bleedthrough of PI emission into the signal collected for APC,

- APC, allophycocyanin, an algae-derived fluorochrome (MacColl, 2004) (max. excitation: 652 nm, max. emission: 660 nm (MacColl, 2004)) was excited with a 635 nm laser and detected with a 660/20 nm filter, which accounts for 73.7% of the total dye excitation and 40.2% of the total dye emission.

Background autofluorescence and non-specific binding were removed during the screening analysis of the ‘No antibodies’ and ‘APC secondary antibody only’ control samples (Fig. 4.2A). Approximately 4% ± 1.2% DDX4^{C25}-positive cells (range 0.2%–11.6%) were sorted from the total live ovarian cell suspension, with 549 ± 222 cells recovered (range 55–2,268 cells) (Fig. 4.2B) (n = 10 independent FACS).

Despite the FACSAria settings being constant, the percentage of positive fractions was variable between experiments (Fig. 4.2A, B). Furthermore, few cells initially plated in culture, and they showed slow growth and low cell survival. It could be that the bleedthrough of PI into the APC collection (Fig. 4.1B, in red) had contaminated the putative OSCs with false-positive DDX4^{C25}-cells and also dead cells. Hence the reduced cell survival rate observed, and the variability in the percentages of putative OSCs that would not correlate with the real OSC population numbers.

4.2.2 FACS-sorting of DDX4^{C25}-positive ovarian cells with a DDX4/Alexa Fluor 633/DAPI protocol

As explained in Section 4.2.1, the overlapping PI and APC spectra necessitated the employment of a different immunofluorescence protocol for the detection of DDX4^{C25}-

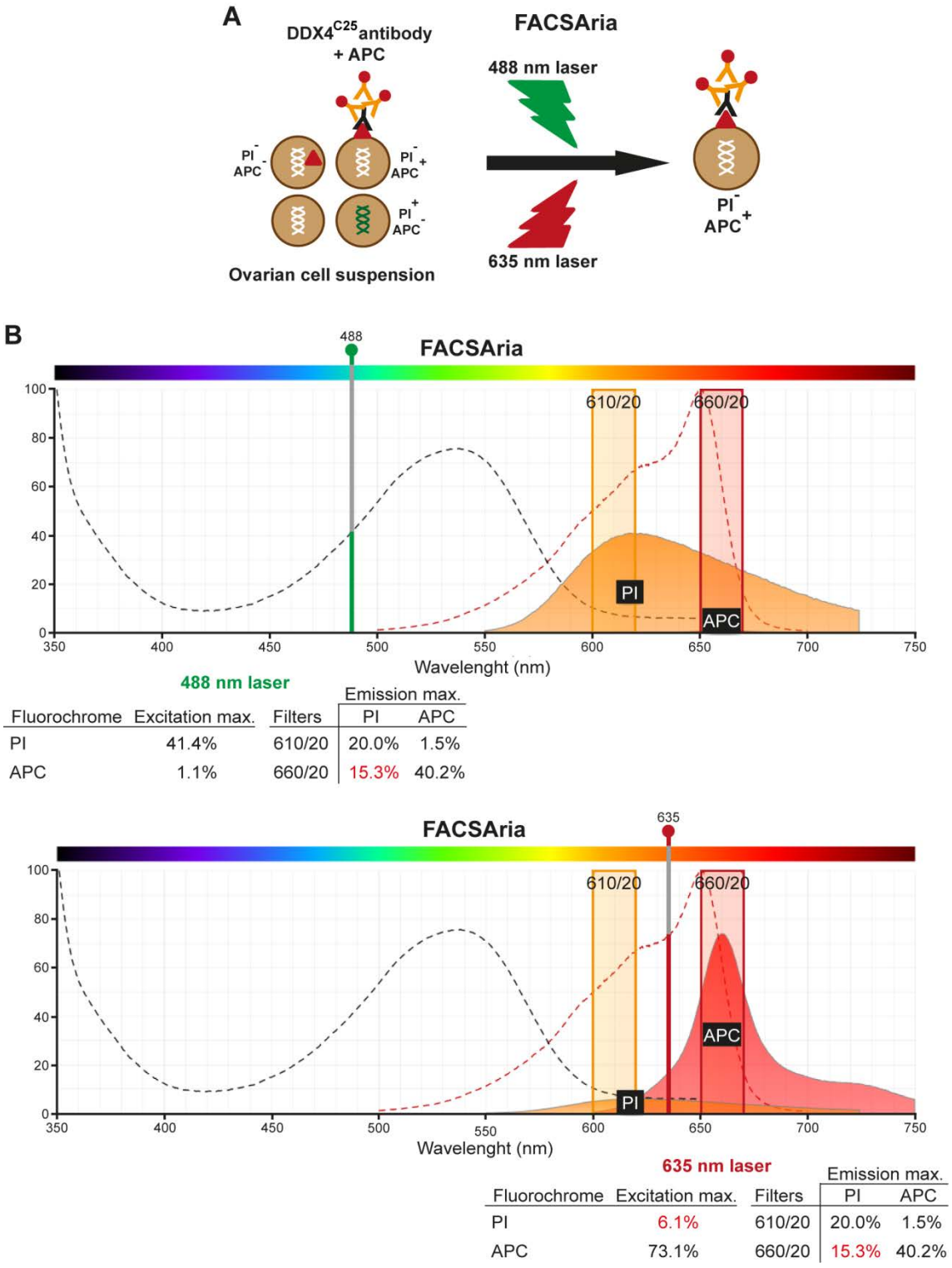

Figure 4.1. DDX4/APC/PI immunofluorescence protocol applied to the detection of DDX4^{C25}-positive cells. (A) Diagram representing the DDX4/APC/PI immunostaining protocol and detection of cells by a FACSAria. **(B)** University of Southampton´s FACSAria settings of lasers and filters for the detection of PI and APC. Discontinuous lines represent the excitation spectra and continuous lines represent the emission spectra. Note the spillover of PI during the detection of APC.

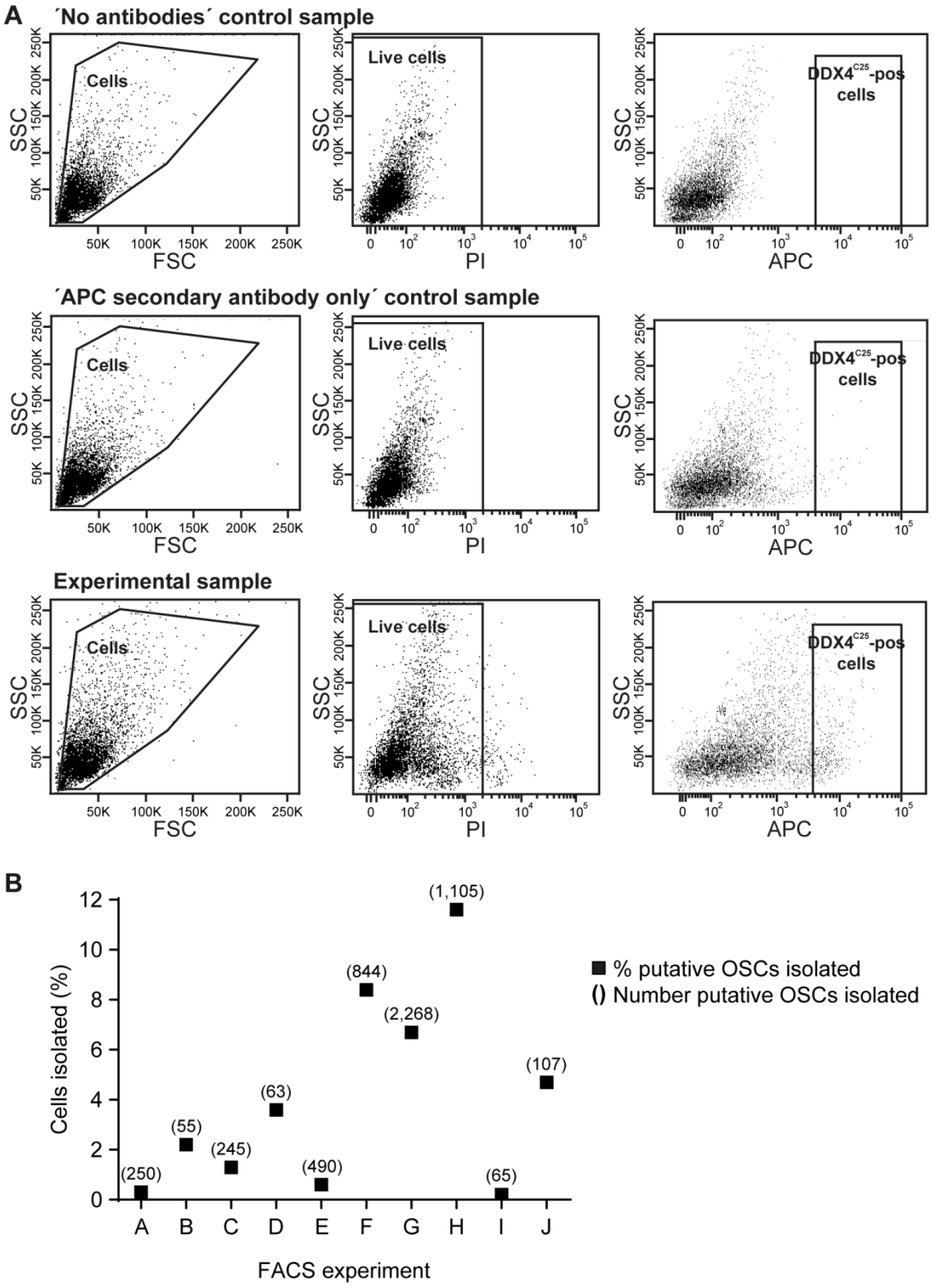

Figure 4.2. Detection of PI-negative DDX4^{C25}-positive ovarian cells. (A) Screening analysis of viable, APC-positive cells in 'No antibodies', 'APC secondary antibody only' and experimental samples. **(B)** Percentages and numbers of DDX4^{C25}-positive cells isolated from the total viable ovarian cell suspensions. N = 10 independent FACS.

positive cells. This was problematic because of a reduced selection of viability dyes that did not cause spectra overlapping with the 635 nm laser, as well as the short shelf life of the secondary antibody conjugated to APC, which was less than 6 months.

The second immunofluorescence protocol used a secondary antibody conjugated with Alexa Fluor 633, which has similar optical characteristics to APC (Berlier et al., 2003; Life Technologies, personal communication). Furthermore, a FACSAria equipped with a 407 nm laser became available at the University of Southampton, and allowed for the use of DAPI as the viability discrimination reagent, despite its reduced excitation with this laser. A DDX4/Alexa Fluor 633/DAPI selection protocol was therefore designed (Fig. 4.3A), and the BD FACSAria was arranged as follows (Fig. 4.3B):

- DAPI (max. excitation: 357 nm, max. emission: 461 nm (Kapuscinski, 1995)) was excited with a 407 nm laser and detected with a 450/40 nm filter, which accounts for 5.6% of the total dye excitation and 36.9% of the total dye emission,
- Alexa Fluor 633 (max. excitation: 631 nm, max. emission: 647 nm (Berlier et al., 2003)) was excited with a 635 nm laser and detected with a 660/20 nm filter, which accounts for 96.9% of the total dye excitation and 34.4% of the total dye emission,

This time, 2.5% ± 0.4% DDX4^{C25}-positive cells (range 0.1%–6.6%) were detected in the total live ovarian cell suspension, corresponding to 2,226 ± 628 cells sorted (range 23–8,281 cells) (Fig. 4.4A, B) (n = 17 independent FACS).

A high variability in the percentages of DDX4^{C25}-positive cells isolated remained with the new protocol (Fig. 4.4A, B), despite the same settings used throughout. This could not have been attributed to variation between mice as the number and age of the female mice were constant, as was the concentration of DAPI and the FACS settings.

It may be that the percentage of the OSC population is more variable than previously reported, or that the DDX4^{C25} antibody is binding to a highly variable cell surface protein not identified by my *in silico* analysis.

4.2.3 Strategies to improve reproducibility in isolating DDX4^{C25}-positive cells

The variability in the percentages and number of cells isolated by FACS could be explained by the binding of the DDX4^{C25} antibody to a protein other than DDX4, either because the antibody is non-specific or because the enzymatic digestion alters the cell surface epitopes of non-OSCs (Albertini and Gleicher, 2015). This possibility could pose an overestimation of the real numbers of OSCs in the adult ovary. Therefore, strategies

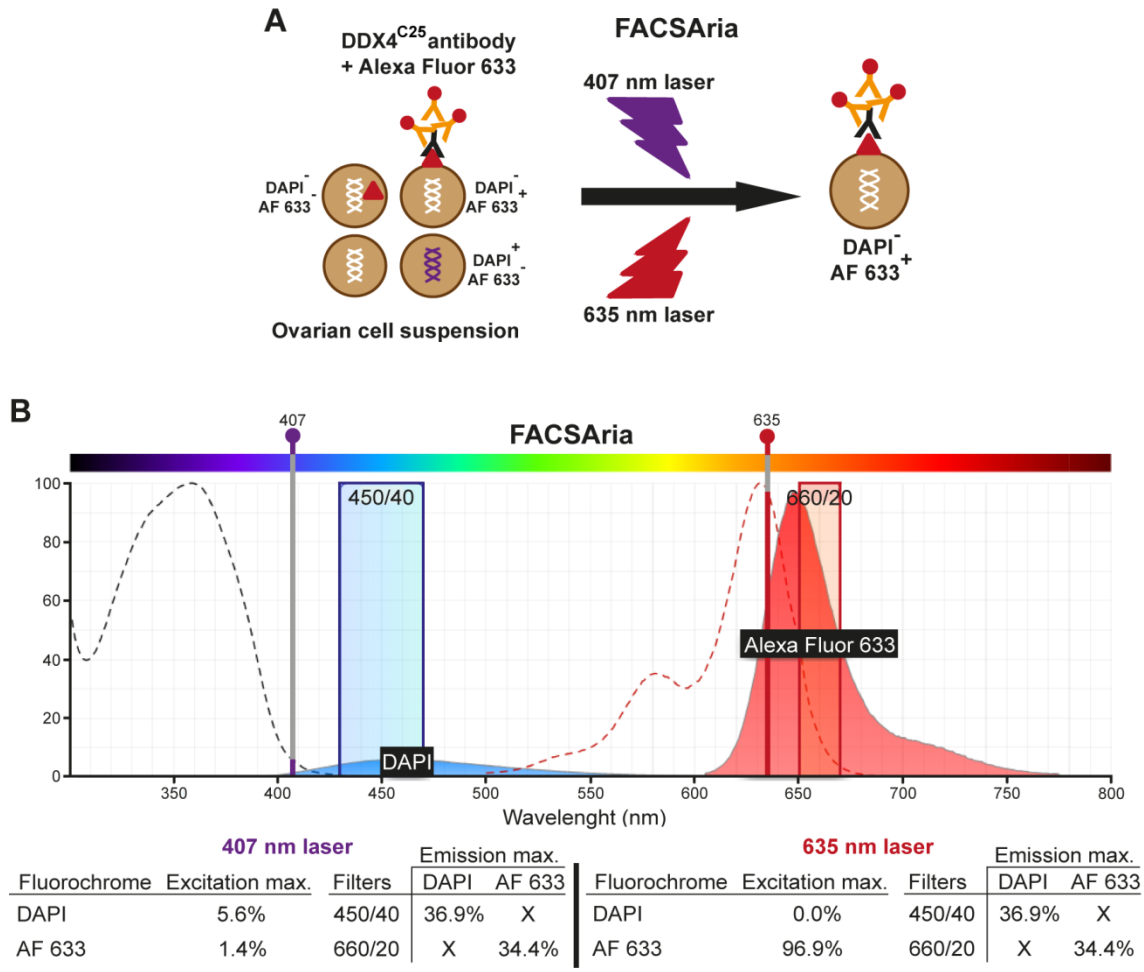

407 nm laser			Emission max.		635 nm laser			Emission max.	
Fluorochrome	Excitation max.	Filters	DAPI	AF 633	Fluorochrome	Excitation max.	Filters	DAPI	AF 633
DAPI	5.6%	450/40	36.9%	X	DAPI	0.0%	450/40	36.9%	X
AF 633	1.4%	660/20	X	34.4%	AF 633	96.9%	660/20	X	34.4%

Figure 4.3. DDX4/Alexa Fluor 633/DAPI immunofluorescence protocol applied to the detection of DDX4^{C25}-positive ovarian cells. (A) Diagram representing the DDX4/Alexa Fluor 633/DAPI immunostaining protocol and detection of cells by a FACSAria. **(B)** University of Southampton´s FACSAria settings of lasers and filters for the detection of DAPI and Alexa Fluor 633 in a FACSAria I. Discontinuous lines represent the excitation spectra and continuous lines represent the emission spectra.

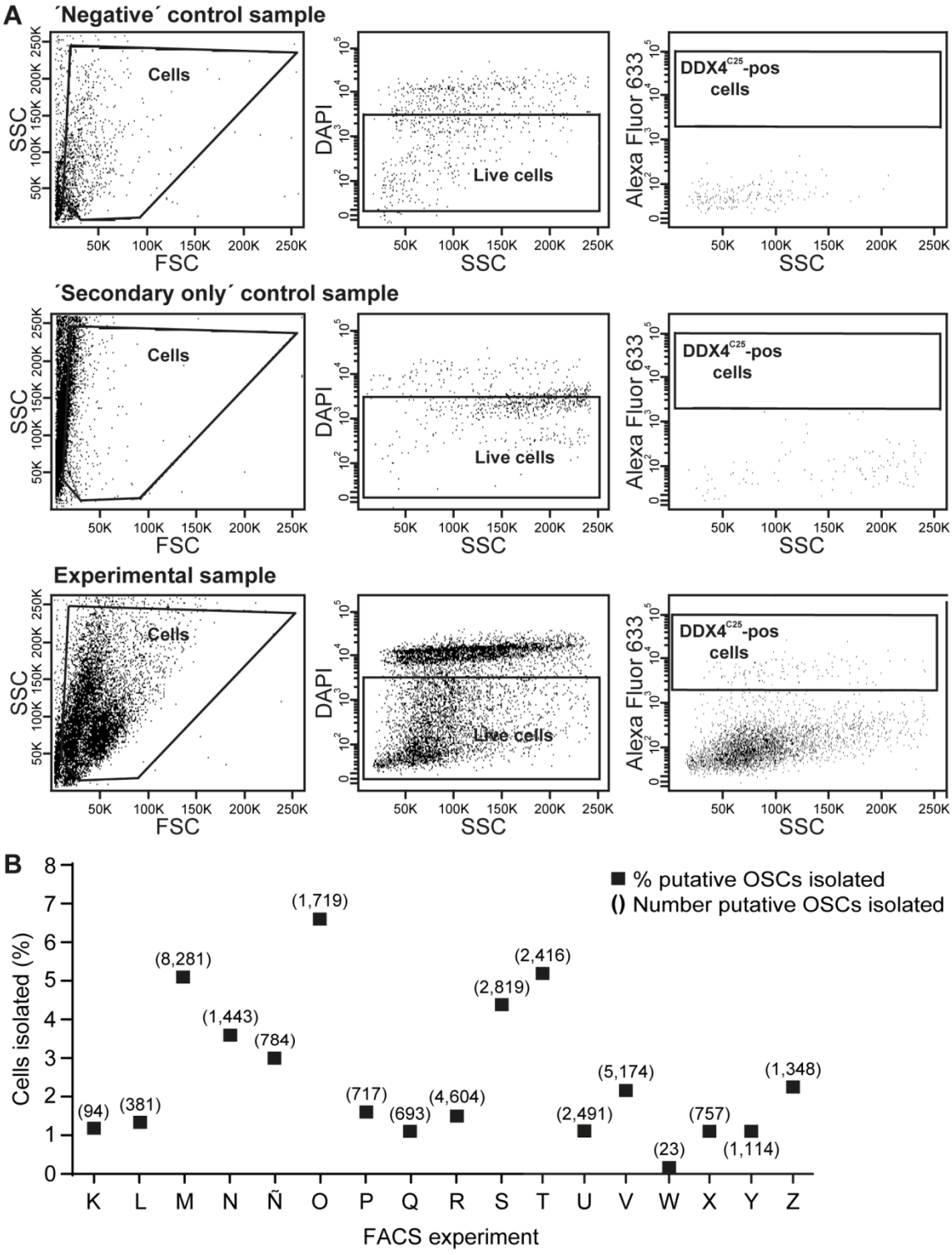

Figure 4.4. Detection of DAPI-negative DDX4^{C25}-positive ovarian cells. (A) Screening analysis of viable, Alexa-Fluor-633-positive cells in 'No antibodies', 'Alexa Fluor 633 secondary antibody only' and experimental samples. **(B)** Percentages and numbers of DDX4^{C25}-positive cells isolated from the total viable ovarian cell suspensions. N = 17 independent FACS.

recommended by Woods and Tilly (2013) were adopted to produce a more pure FACS-positive fraction.

An important point to consider in FACS analysis is the antigen biology; specifically when, where and how much is the epitope of interest expressed (Srivastava, 2015). To overcome the lack of knowledge on antigen density here, that is, if the cell surface DDX4^{C25} epitope is abundant or scarce, samples require to be incubated in a 1:10 dilution of the stock primary antibody (Srivastava, 2015). However, adding too much DDX4^{C25} antibody, for example, could saturate the ovarian cell suspension and lead to non-specific binding. Therefore, four samples of the same ovarian cell suspension from 12 ovaries were incubated with a logarithmic decreased dilution (1:10, 1:30, 1:100 and 1:300) of the stock DDX4^{C25} antibody for 20 minutes (n = 1 each independent FACS).

Consistent with previous FACS, a 1:10 anti-DDX4^{C25} dilution resulted in 1.4% DDX4^{C25}-positive cells being isolated of the total live ovarian cell population (corresponding to 2,491 cells; Fig. 4.5A). A 1:30 anti-DDX4^{C25} dilution (1% and 205 cells sorted) and 1:100 anti-DDX4^{C25} dilution (1.8% and 599 cells sorted) also provided with similar levels of isolation (Fig. 4.5A). Only the 1:300 anti-DDX4^{C25} dilution showed a noticeable reduction in the DDX4^{C25}-positive population (0.6% and 212 cells sorted) (Fig. 4.5A). Despite the 1:100 anti-DDX4^{C25} FACS run providing the highest percentage of putative OSCs (Fig. 4.5A), these cells did not grow in culture. It is possible that this FACS-positive fraction contained many more autofluorescent cells and debris that led to an absence of growth.

Other points to consider in FACS sorting are the protein concentration of the blocking solution and the time applied during the blocking step to promote only specific binding of the primary antibody (Srivastava, 2015). In the OSC protocol this is achieved with a 2% goat serum and 2% BSA blocking solution incubation for 20 minutes. However, it could be that this is sub-optimal and so fails to entirely remove non-specific binding. Protein concentrations greater than 10% serum are generally discouraged because it promotes the formation of clumps and clogging of the flow cytometer (Salk Institute for Biological Studies, unpublished communication). Therefore, only the incubation time in blocking solution was modified, and doubled as suggested by Woods and Tilly (2013). An ovarian cell suspension was divided into two tubes and incubated one for 20 minutes (control group) and the other for 40 minutes, and the same FACS-gating were maintained (n = 2 independent FACS).

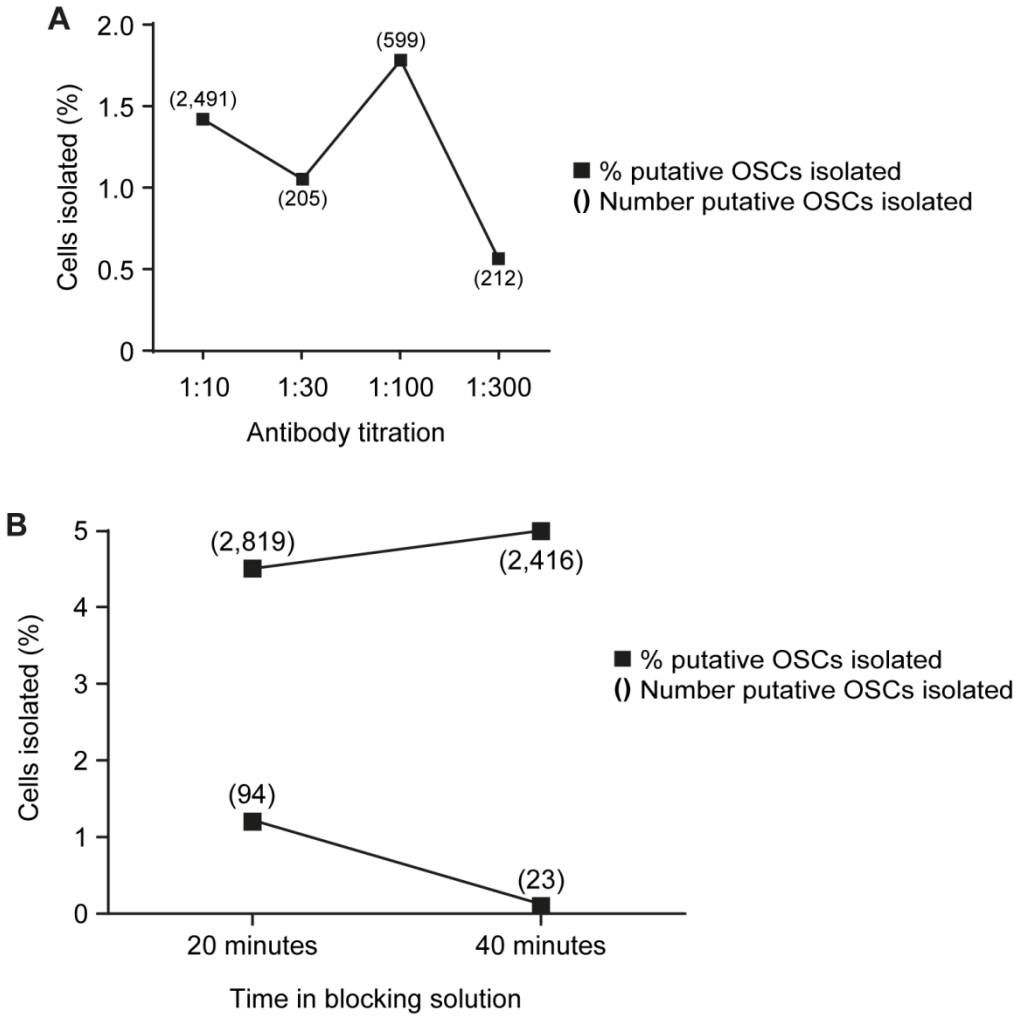

Figure 4.5. Strategies to affect the percentage of DDX4^{C25}-positive cells recovered by FACS. Percentages and numbers of DDX4^{C25}-positive cells isolated from the total viable ovarian cell suspensions after **(A)** titration of the DDX4^{C25} antibody and **(B)** doubling of the incubation time in blocking solution. N = 1 **(A)** and 2 **(B)** independent FACS.

In keeping with previous FACS sortings, the 20-minutes control group produced 1.2% and 4.5% DDX4^{C25}-positive cells. However, results for the 40-minutes experimental groups were different, with 0.3% and 5% DDX4^{C25}-positive cells recovered (Fig. 4.5B). No differences were observed between the control and experimental samples in percentages of cells isolated (Fig. 4.5B).

Therefore, neither the recommended titration of the DDX4^{C25} antibody nor the expansion of the incubation time in blocking solution led to the isolation of a better purified FACS-positive fraction by overcoming the suspected non-specific binding of the primary antibody. On the contrary, the maintenance of similar percentages of cells isolated may be indicative that the DDX4^{C25} antibody reacts specifically with an epitope on the cell surface, this being either DDX4 or another unknown protein(s).

4.2.4 Use of testicular cells for FACS-gating of DDX4^{C25}-positive cells

Postnatal pig, mouse and Rhesus monkey testes have been reported to contain DDX4^{C25}-positive cells by FACS, although they did not belong to the germline (Kakiuchi et al., 2014; Yuan et al., 2013). Since testes contain more cells than the ovary and the majority are germ stem cells, I hypothesized that it may be possible to isolate large numbers of mouse DDX4^{C25}-positive cells within the testicular cell suspension. This FACS detection protocol if successful could then be applied to isolate DDX4^{C25}-positive ovarian cells.

Gonads from six 3-to-4-week-old female mice and one 20-week-old male mouse were enzymatically digested and immunostained (n = 1 independent FACS). As expected, upon FACS, 1.2% DDX4^{C25}-positive ovarian cells were found (Fig. 4.6A). However, only 0.2% DDX4^{C25}-positive testicular cells of the total viable testicular cell suspension were obtained using the same FACS-gating protocol (Fig. 4.6A). Interestingly, the histogram for the fluorescence of Alexa Fluor 633 in male cells was concentrated between 10^{-2} and 10^{2} units of fluorescence, whereas the female cells seemed to be more reactive to the DDX4^{C25} antibody (Fig. 4.6B), possibly enhanced by the presence of autofluorescence from NADH contained in oocytes (Perfetto et al., 2004; Perfetto et al., 2006). Furthermore, the testicular cell suspension registered a greater live cell population than its ovarian counterpart (Fig. 4.6C). This could be indicative of a higher resistance of male testicular cells, or a vulnerability of oocytes, to tissue digestion and immunostaining on ice.

The low yield of male DDX4^{C25}-positive cells isolated by FACS discouraged further use of testicular cells for the development of a FACS-gating protocol for the isolation of

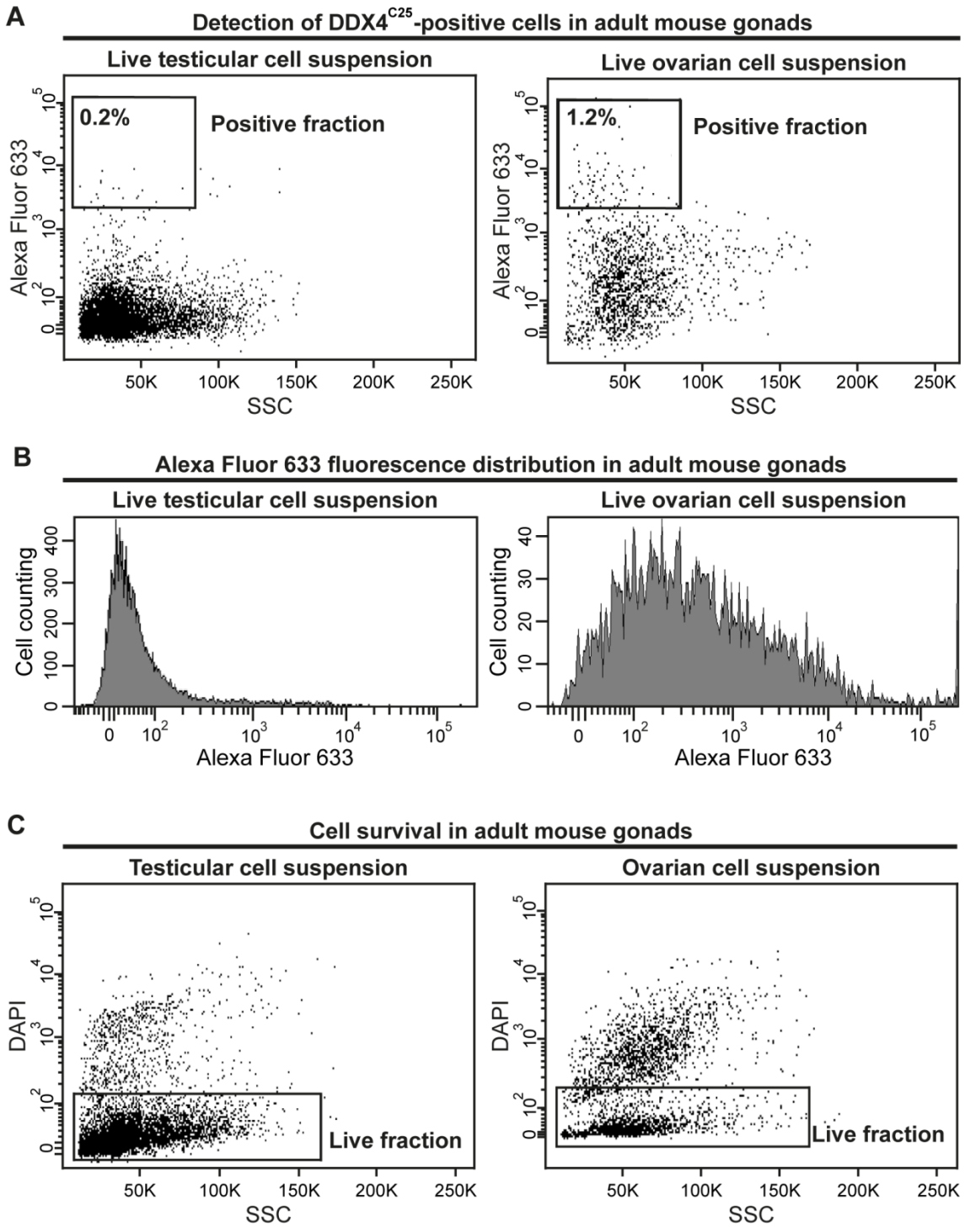

Figure 4.6. Detection of live DDX4^{C25}-positive cells in testicular and ovarian cell suspensions in adult mice. (A) DDX4^{C25}-positive cells detected in testicular and ovarian cell suspensions by means of the same gating protocol for DDX4-Alexa-Fluor-633 fluorescence. **(B)** Histogram for the DDX4-Alexa-Fluor-633 fluorescence FACS plot shown in (A). **(C)** Cell viability in testicular and ovarian cell suspensions by means of the same gating protocol for DAPI fluorescence. N = 1 independent FACS.

putative OSCs.

4.3 Discussion

Here I have isolated a small population of ovarian cells by FACS from mouse adult ovaries by means of a rabbit polyclonal antibody to the C-terminus of DDX4 (DDX4^{C25}). The FACS isolation protocol however required modifications and gave high variability percentages of putative OSCs obtained that could not be corrected.

4.3.1 DDX4-positive cells can be sorted by FACS using the DDX4^{C25} antibody

Consistent with previous reports (Hernandez et al., 2015; Imudia et al., 2013; Park and Tilly, 2014; Park et al., 2013; White et al., 2012; Woods and Tilly, 2015; Zhang et al., 2011; Zou et al., 2009), I could isolate DDX4^{C25}-positive cells from mouse ovarian cell suspensions with a DDX4^{C25} antibody (White et al., 2012; Zou et al., 2009), through the detection of fluorescence from APC or Alexa Fluor 633.

The percentages of putative mouse OSCs that I obtained with APC (4% ± 1.2%) and Alexa Fluor 633 fluorescence (2.5% ± 0.4%) were very similar to those previously reported by White et al. (2012) (1.5% ± 0.2%), Park and Tilly (2014) (1.83% ± 0.14%) and, more recently, Zhang et al. (2015) (3.83% ± 1.08%). However, overall the percentage recovery fluctuated, as did the number of DDX4^{C25}-positive cells sorted in each experiment, which varied between 2 and 828 per mouse ovary. These numbers differed from the reportedly consistent 250 to 1,000 cells per ovary in one other study (White et al., 2012).

Many other researchers have reported disparate percentages of recovered putative OSCs (Hernandez et al., 2015; Zhang et al., 2015), which they associate to methodological weaknesses in the protocol to FACS-sort these cells (Albertini and Gleicher, 2015), with the specificity of the DDX4^{C25} antibody at its core (Hernandez et al., 2015; Telfer and Albertini, 2012; Zhang et al., 2015). Interestingly, despite an attempt here to address methodological weakness by titrating the DDX4^{C25} antibody and doubling the time in blocking solution, the variation in the percentage of FACS-positive populations could not be reduced even within the same lot of antibody. Leaving aside this specificity, which was discussed in Chapter 3, the other suspected reason for such variation is the harsh enzymatic digestion of ovaries that would produce an antibody

cross-reaction through cell surface protein damage and release of cytoplasmic DDX4 (Albertini and Gleicher, 2015).

4.3.2 Absence of FACS-sorted testicular DDX4^{C25}-positive cells

I tried to use live testicular cell suspensions as a positive control to detect cell surface DDX4-expressing germ stem cells, but I could not retrieve any by FACS. This is a similar finding to experiments reported by Kakiuchi et al. (2014) but contrary to results from Yuan et al. (2013). Kakiuchi et al. (2014) performed their enzymatic digestion with trypsin, whereas Yuan et al. (2013) and I performed ours with collagenase, hence the method of digestion is not the reason for the disparity.

In their protocol, Woods and Tilly (2013, 2016) advise not to use trypsin for enzymatic disaggregation of ovaries because it can cause protein turnover and damage to the cell surface epitope of DDX4, and to use instead a collagenase compatible with receptor integrity.

Certainly, trypsin is an extracellular serine protease that degrades externally exposed protein epitopes by attacking positively charged lysine or arginine residues in the carbonyl carbon of the peptide bond that is to be cleaved (Voet and Voet, 2011). As long as the membrane proteins of interest contain trypsin cleavage sites, this enzymatic degradation can be applied in cell surface protein localization (Besingi and Clark, 2015) for the discovery of potential targets for: antibiotics (Solis et al., 2010); therapeutic drugs in cancer cells (Vit and Petrak, 2016); distinction between healthy and pathogenic cells; and identification by proteomic techniques (Griffin and Schnitzer, 2011). However, proteolysis with trypsin negatively perturbs *in vivo* and *in vitro* cells (Carney and Cunningham, 1977; Sefton and Rubin, 1970; Yamada et al., 1975; Yamada et al., 1976; Zetter et al., 1976) and, importantly, reduces cell surface epitope density and associated fluorescence in FACS analysis (Zhang et al., 2012a).

In applying collagenase in this work, I corroborated previous observations by Kakiuchi et al. (2014) that cell surface DDX4^{C25}-positive cells do not exist in the adult testis. These results prove that a harsh enzymatic digestion with collagenase or trypsin could not have been responsible for the degradation of cell surface proteins in non-germline cells, which has been proposed as the cause for the non-specific binding of the DDX4^{C25} antibody and the large variation of isolated putative OSCs (Albertini and Gleicher, 2015; Woods and Tilly, 2015). The absence of isolated DDX4^{C25}-positive testicular cells also dismissed the

hypothesis that enzymatic digestion could break the cell membrane of germ stem cells and release cytoplasmic DDX4, which in turn would adhere to the cell surface of somatic cells and produce false live DDX4^{C25}-positive cells (Albertini and Gleicher, 2015).

However, it could be that collagenase behaves differently in the ovarian cell suspension and does cause collapse of the oocyte cell membrane. Certainly fully-grown oocytes are hardly ever observed in the FACS-negative fractions, which suggest that they are easily destroyed at some point during the disaggregation and staining of the ovarian cell suspension or the FACS analysis and sorting. However, to prove this hypothesis, ovaries completely devoid of oocytes would be required, and at present there is no knockout model that can reliably be used.

4.3.3 Individual differences could explain the variability in FACS percentages

Could variations in the number of OSCs between mouse strains explain different rates of cell recoveries from ovaries?

This seems unlikely given only C57BL/6 mice have been used in past studies (Faustino et al., 2012; Hernandez et al., 2015; Park and Tilly, 2014; White et al., 2012; Zhang et al., 2012b; Zhang et al., 2015; Zou et al., 2009) and mine here.

The age of the mice could be a source of OSC variability. It is uncertain whether numbers of OSCs decrease or are maintained with maternal age (Faustino et al., 2012; Wang et al., 2012). However, no clear differences were observed between my 3-week-old mice and those of 6-8 week-old (Woods and Tilly, 2013b) and 2-3 month-old (Hernandez et al., 2015).

It remains possible that this fluctuation in number of OSCs has an environmental basis (e.g. general animal health, pathogen free status etc.) which currently has not been discovered.

4.3.4 The FACS-sorting protocol is difficult to adopt between laboratories

Gate drawing as part of the FACS methodology is a subjective exercise, and two difficulties were identified in the setting up of the FACSAria. First, the lack of information on the laser path configuration (e.g. power laser, filter sets and detectors) of the FACSAria used by labs that report on successful isolation of OSCs (e.g. the Tilly group). Second, the uncertainty in where to gate this population within the ovarian cell suspension.

The majority of researchers wishing to validate cytometric results of other groups simply manually replicate the lasers and dot plots published in the methods and subjectively gate populations of interest (Davies, 2015; Finak et al., 2016). However, for a faithful, objective and comparable cross-study the power laser, filters and detectors need also to be published (Davies, 2015; Finak et al., 2016; Perfetto et al., 2004). High power laser leads to the formation of very fluorescent cell groups in the graphs margins, which are considered an artefact of the FACS instrument and excluded from the sorting. Similarly, low power laser may not allow the human eye observation of defined positive and negative groups. In both cases, the presence and numbers of positive populations may be underestimated (Davies, 2015).

Furthermore, fluorescent staining looks significantly different depending on the lasers, filters and detectors in place. Although DAPI is excited with a 405 nm laser, PI with a 488 nm laser, and APC with a 633 nm laser (White et al., 2012; Woods and Tilly, 2013b), and similar lasers have been used in this project, the lack on information on how much laser intensity to apply and which detector collects the emitted fluorescence prevents faithful replication of the OSC isolation in its most critical step. For this reason, past and future studies performed on the detection of OSCs (Dunlop et al., 2014; Hernandez et al., 2015; Khosravi-Farsani et al., 2015; Zarate-Garcia et al., 2016; Zhang and Wu, 2016; Zhang et al., 2012b; Zhang et al., 2015) cannot be considered to having cross-centre replicated White et al. (2012), unless more information on the FACS configuration is disclosed. I put in place an internally standardised protocol as described previously (Finak et al., 2016; Perfetto et al., 2004) and all FACS analysis in this project were performed with the same laser paths, resulting in in-site comparability, however, not in cross-laboratory replication of the original report of OSC isolation (White et al., 2012).

Recently the use of calibrated beads, 2–15 μm in diameter, before the proper FACS analysis of stained live ovarian cell suspensions has been adopted to facilitate gating putative OSCs (Navaroli et al., 2016), which are reportedly small (White et al., 2012; Zou et al., 2009). However, without further disclosure of the laser path configuration of the FACSAria, the application of calibrated beads would be in vain.

Could the differences in the FACSAria path configuration have caused the variations in OSCs percentages? Certainly, I believe that it is part of the problem in the inter-laboratory replication. But it does not explain my internal variation, given that the FACSAria used here underwent quality control before each sorting in order to reduce the coefficient of variation to a minimum and to optimise the capture and quantitation of positive signals, as

recommended by the manufacturer. The variation reported here is therefore not caused by the machine itself.

In summary, in this Chapter I have applied immunohistochemistry with a DDX4^{C25} antibody and flow cytometry cell sorting on mouse live ovarian cell suspensions to isolate DDX4^{C25}-positive cells. These results are in line with the *in silico* prediction of an external C-terminal domain in the murine DDX4 in Chapter 3, and with reports from other groups that also isolated presumptive murine OSCs (Hernandez et al., 2015; Imudia et al., 2013; Park and Tilly, 2014; White et al., 2012; Zou et al., 2009). The large variation in the percentages of putative OSCs however confirms the difficulties that other groups had in replicating these experiments, both in the same lab and between different labs. It also puts in question the entire FACS-sorting protocol (Albertini and Gleicher, 2015), which some groups claim to be evidence that these cells do not express *Ddx4* nor any other germline marker (Hernandez et al., 2015; Zhang et al., 2015).

Given the controversial germ stem cell nature of these cells, I have attempted *in vitro* cell culture and germline marker expression analysis on these DDX4^{C25}-positive cells by gene expression analysis and protein immunohistochemistry. These experiments will be detailed and discussed in the next Chapter.

Chapter 5

Evaluation of the germline potential of DDX4^{C25}-positive cells

5.1 Introduction

OSCs isolated from the ovary by live-cell sorting methods using the germ cell marker DDX4 have some reported germline markers (Imudia et al., 2013; Park and Tilly, 2014; White et al., 2012; Zou et al., 2009). More importantly, they express meiotic markers and produce oocyte-like cells when cultured (White et al., 2012; Zou et al., 2009), and also assemble into follicles when transplanted into *in vivo* and *in vitro* ovaries (White et al., 2012; Zhang et al., 2011; Zou et al., 2009). Lastly, OSCs form early embryos when fertilised (White et al., 2012), with only one group reporting live, healthy pups (Zhang et al., 2011; Zou et al., 2009).

However, the stem cell and germ cell characteristics of OSCs remain disputed, as other groups using similar methods of isolation have reported to culture cells that senescence and were non-germline in origin, consequently not expressing DDX4 (Zhang et al., 2012b).

Previously in this thesis, I concluded that live OSC-like cells could be isolated by FACS from the adult mouse ovary using a DDX4^{C25} antibody, despite the absence of a good *in silico* modelling to support the existence of a surface-bound DDX4. In this Chapter, isolated FACS-positive fractions were cultured *in vitro* to evaluate pluripotency and germline potential, differentiation into oocyte-like cells, and expression of a surface-bound DDX4.

5.2 Results

5.2.1 *In vitro* growth of DDX4^{C25}-positive cells

DDX4^{C25}-positive cell cultures developed into well-defined colonies with round cells apparent in the first days of culture (Fig. 5.1A). However, by the end of the primary culture phase – the time between the initial plating and the first passage – they had lost compaction, and had instead spread into a monolayer (Fig. 5.1B) of fusiform cells with

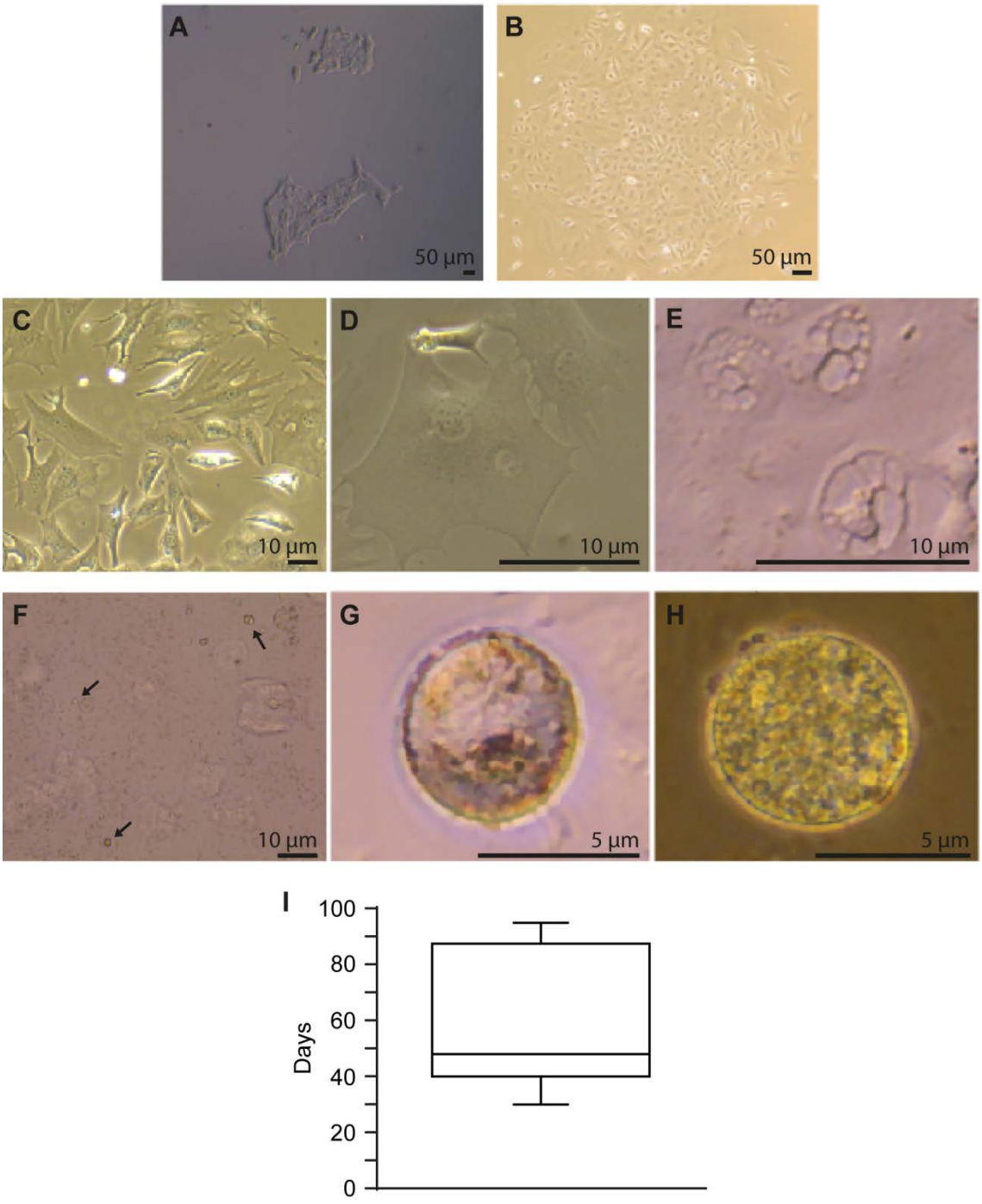

Figure 5.1. DDX4^{C25}-positive cells in culture. DDX4^{C25}-positive cell colonies **(A)** on day 3 and **(B)** 7 post-FACS isolation. **(C)** Cells on day 7 post-FACS isolation, some of them **(D)** binucleated or **(E)** vacuolated. **(F, black arrows; G, H)** Small floating oocyte-like cells. **(I)** Survival time of *in vitro* DDX4^{C25}-positive cell cultures analysed. N = 12 independent cell cultures (except I, n = 9).

little nuclei and extensive cytoplasm (Fig. 5.1C). This cell colony morphology was maintained. Both in early and late passages many cells were observed to be binucleated (Fig. 5.1D), whereas others appeared vacuolar, and by inference undergoing cell death (Fig. 5.1E).

In vitro oogenesis in mouse OSCs has been reported to reach its peak within 24–48 hours after each passage (White et al., 2012). On the contrary, in the putative OSC cultures studied here some floating round cells could be observed as cells gained confluence (Fig. 5.1F, black arrows; G, H). Despite resembling small oocytes with a zona pellucida (Fig. 5.1G, H), they never reached a diameter above 10 µm, contrasting with the reported 35–50 µm oocyte-like cells in one study (White et al., 2012).

The putative OSCs survived *in vitro* for 2–3 months (60.6 ± 8.3 days in culture, range 30 to 95 days), with decreasing mitotic rates (Fig. 5.1I) (n = 9 independent cell cultures).

5.2.2 Cell death of DDX4^{C25}-positive cells co-cultured with MEFs

I wanted to test whether plating the putative OSCs onto a feeder layer of mitotically-inactive embryonic fibroblasts (MEFs) would solve the reduced cell growth and lack of colonies with pluripotent characteristics observed in Section 5.2.1, as MEFs can ease the initial plating of freshly sorted putative OSCs (Woods and Tilly, 2013b). Putative OSCs were therefore sorted as usual and seeded onto tight MEF monolayers upon arrival at the lab (n = 2 independent FACS).

On the first day after the initial seeding, rounded cells identified as the putative OSCs were observed on top of the MEF monolayer. Despite the inability to tell apart proliferative DDX4^{C25}-positive cells from MEFs, given that both cell types were fusiform, a high number of dying cells were observed after four days post-sorting (Fig. 5.2A and B, black arrows and insert), compared with previous DDX4^{C25}-positive cell cultures seeded without MEFs. Furthermore, no colony formation was found on top of the MEFs (Fig. 5.2A, B). The cell culture was kept for 14 days, as suggested by Woods and Tilly (2013), but I could not record cell growth improvement or colony formation. The cell cultures were finally discarded. No further experiments with MEF monolayers were performed on the DDX4^{C25}-positive cells.

5.2.3 Characterisation of germline markers in GV oocytes

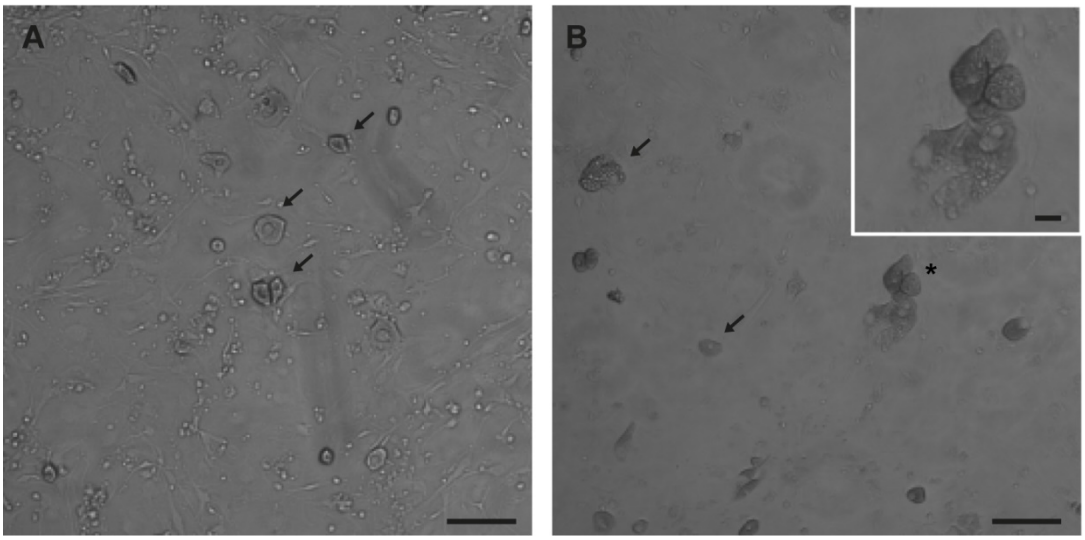

Figure 5.2. Culture of freshly sorted DDX4^{C25}-positive cells onto MEF monolayers. DDX4^{C25}-positive cells undergoing cell death **(A and B, black arrows and insert)** on day 4 post-FACS isolation. Scale bar: 50 μm. N = 2 independent FACS.

Freshly sorted OSCs should be positive for a number of well-known germline markers: PRDM1 (BLIMP1; PR domain containing 1, with ZNF domain), DPPA3 (STELLA; developmental pluripotency-associated 3), IFITM3 (FRAGILIS; interferon induced transmembrane protein 3) and DAZL (deleted in azoospermia-like). Initially I wanted to examine the ability of antibodies for these markers to recognize the corresponding proteins within the adult female germline, before performing immunostaining in DDX4^{C25}-positive cells.

As would be predicted based on its known function as a zinc finger-containing protein (Turner et al., 1994), immunohistochemical PRDM1 staining on permeabilised fully-grown GV oocytes showed a cytoplasmic distribution (Fig. 5.3A). Although the role and distribution of IFITM3 have not been reported in oocytes to my knowledge, a punctated staining for this protein was observed in the oocyte cytoplasm (Fig. 5.3B). As reported previously (Sato et al., 2002), DPPA3 staining was found in the cytoplasm (Fig. 5.3C), but only in surrounded nucleolus-stage GV oocytes did it seem to enter the nucleus (Fig. 5.3C), in line with its role as a maternal factor required for the developmental competence of the oocyte (Zuccotti et al., 2009a). DAZL was found mainly in the cytoplasm with low level nuclear staining (Fig. 5.3D), consistent with its function in RNA-binding (Ruggiu et al., 1997).

5.2.4 Analysis of protein expression of germline markers in DDX4^{C25}-positive cells

All five antibodies against germline markers (DDX4^{C25} antibody, Section 3.2.4; PRDM1, IFITM3, DPPA3 and DAZL, Section 5.2.3), were tested on freshly sorted DDX4^{C25}-positive cells.

In non-permeabilised primary cultures of DDX4^{C25}-positive cells there was a homogeneous cell surface immunostaining using the DDX4^{C25} antibody (Fig. 5.4), whereas the same remained absent from the ovarian somatic cells that had been isolated as DDX4^{C25}-negative cells during FACS analysis. This finding is consistent with the FACS methodology, in being able to sort cells that have an epitope against the DDX4^{C25} antibody on their cell surface.

DPPA3 or DAZL could not be detected in the DDX4^{C25}-positive cells (Fig. 5.5C, D). However, these cells positively stained for PRDM1 (Fig. 5.5A) and IFITM3 (Fig. 5.5B).

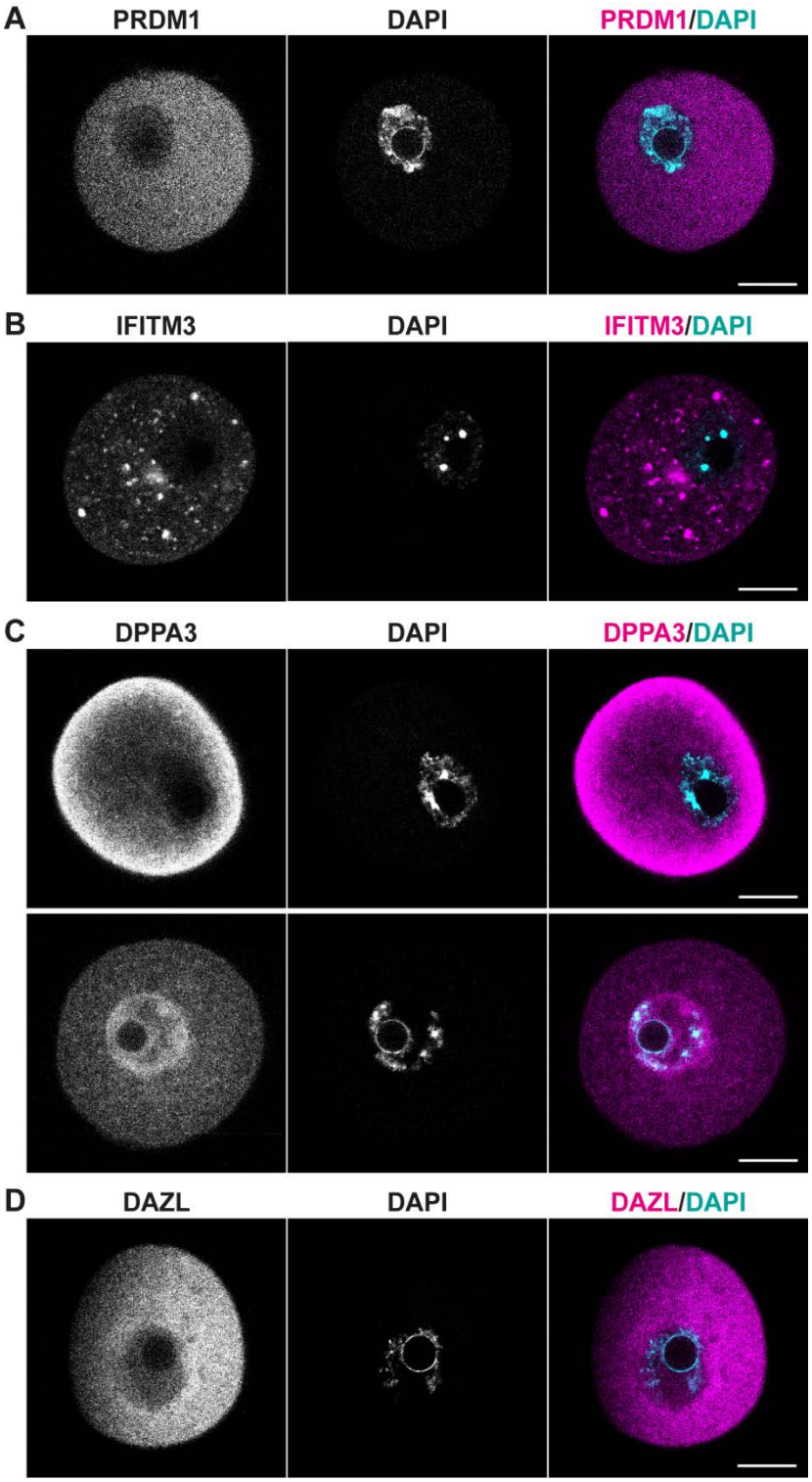

Figure 5.3. Immunostaining for germline markers in fully-grown oocytes. Immunohistochemical **(A)** PRDM1, **(B)** IFITM3, **(C)** DPPA3 and **(D)** DAZL staining in permeabilised fully-grown GV oocytes. In total 126 oocytes taken from 14 ovaries were analysed. Chromatin was stained with DAPI. Scale bar: 20 µm.

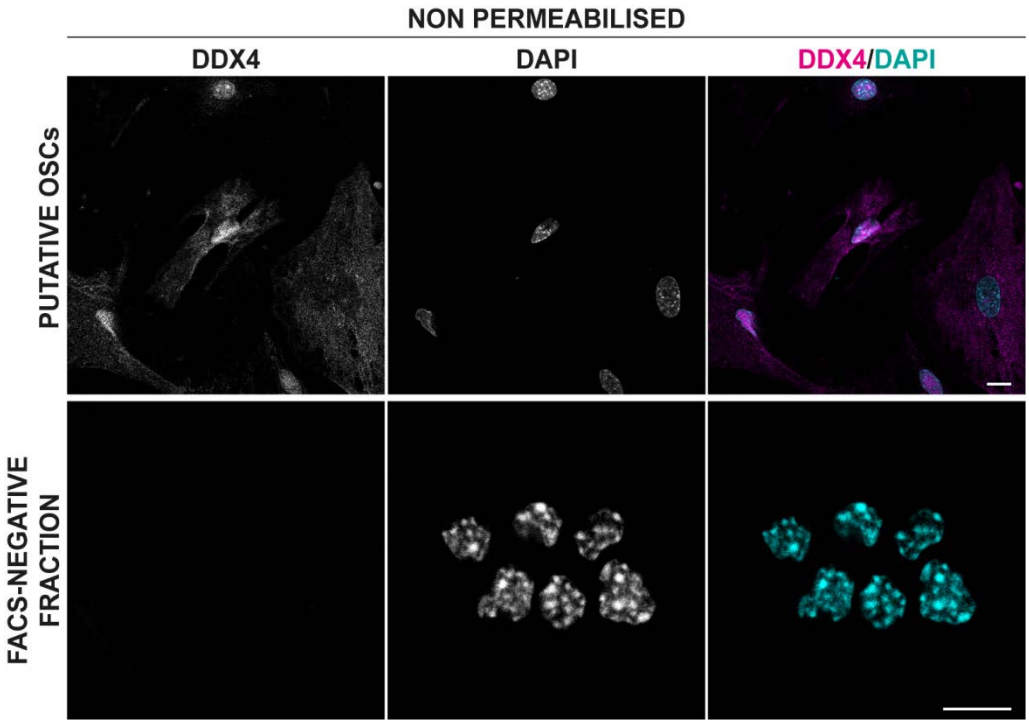

Figure 5.4. DDX4 immunostaining in non-permeabilised DDX4^{C25}-positive cells. DDX4^{C25} immunostaining in non-permeabilised putative OSCs. In total 70 DDX4^{C25}-positive cells and 250 DDX4^{C25}-negative cells taken from 3 independent FACS sorting were analysed. Chromatin was stained with DAPI. Scale bar: 20 μm.

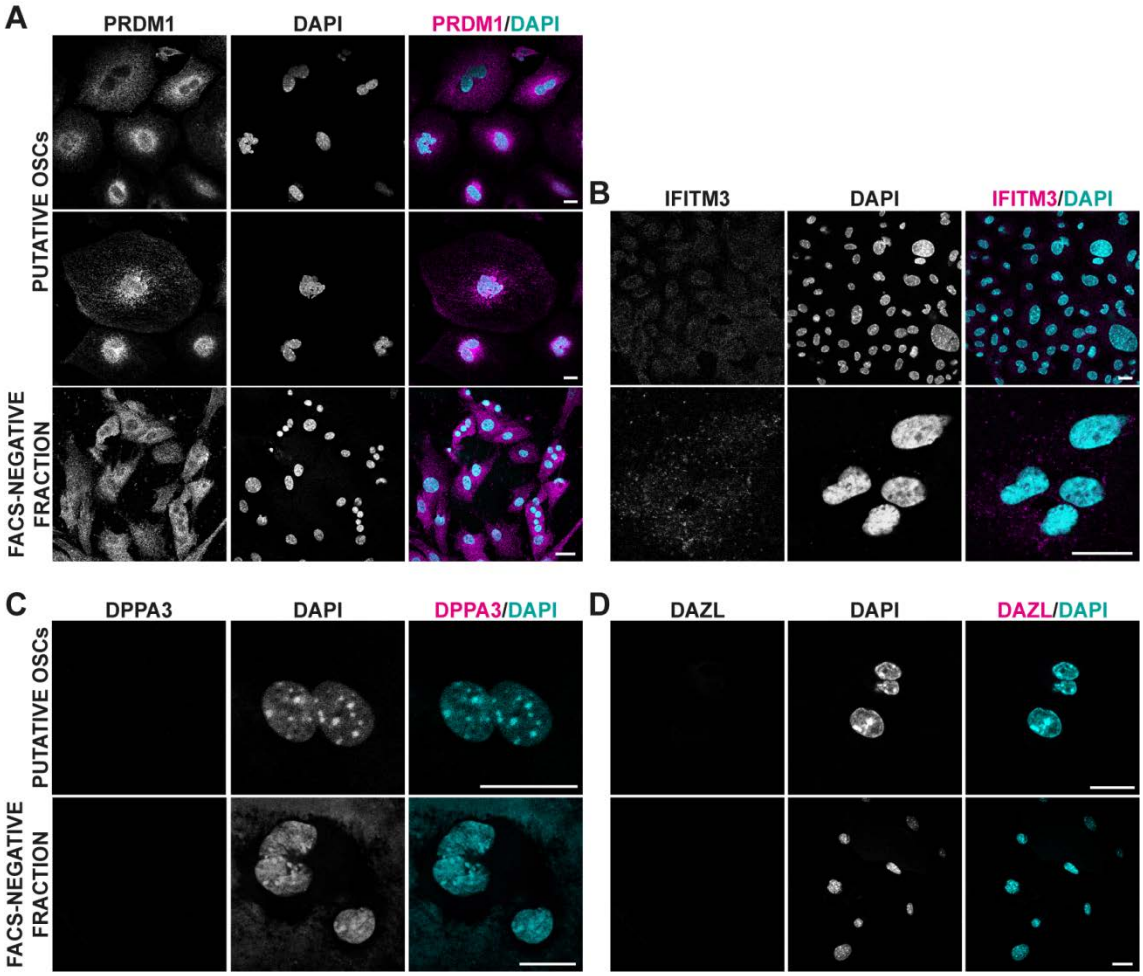

Figure 5.5. Germline marker immunostaining in DDX4^{C25}-positive cells. Immunohistochemical **(A)** PRDM1, **(B)** IFITM3, **(C)** DPPA3 and **(D)** DAZL staining in permeabilised DDX4^{C25}-positive and negative cells. In total 758 DDX4^{C25}-positive cells and 326 DDX4^{C25}-negative cells taken from 3 independent FACS sortings were analysed. Chromatin was stained with DAPI. Scale bar: 20 µm.

Interestingly, PRDM1 was found in the nucleus as well as in the cytoplasm of freshly sorted DDX4^{C25}-positive cells from the same cell cultures. IFITM3 gave the same punctated cytoplasmic distribution as in oocytes. However, DDX4^{C25}-negative ovarian somatic cells also stained positively for PRDM1 and IFITM3 (Fig. 5.5A, B), but not for DPPA3 and DAZL (Fig. 5.5C, D). Therefore both PRDM1 and IFITM3 are not specific germline markers as they appear to be present in many ovarian cells.

It could be that the levels of DPPA3 and DAZL were too low to be detected by immunofluorescence. Therefore, confirmation of these results was needed by a more sensitive method, and this was explored next.

5.2.5 Gene expression analysis of germline markers in adult reproductive tissues

I wanted to perform a gene expression analysis on the DDX4^{C25}-positive cells, in order to determine if at the level of mRNA they were expressing germline markers. Immunostaining had shown expression of some of these markers (Section 5.2.4), but it was unclear if the antibodies were specific, or if the level of expression was too low. Here I needed to establish the validity of my germline markers in cells known to be positive and negative for expression.

I specifically examined for germline markers (*Prdm1*, *Dppa3*, *Ifitm3*, *Ddx4*, *Dazl*), pluripotency markers (*Pou5f1*/*Oct4*, POU domain, class 5; *Zfp296*, Zinc finger protein 296; *Utf1*, undifferentiated embryonic cell transcription factor 1), meiosis markers (*Stra8*, stimulated by retinoic acid gene 8; *Rec8*, meiotic recombination protein REC8 homolog; *Ybx2*/*Msy2*, Y-box-binding protein 2; *Sycp3*, synaptonemal complex protein 3) and oocyte markers (*Nobox*, NOBOX oogenesis homeobox; *Gdf9*, growth differentiation factor; *Zp3*, zona pellucida glycoprotein 3). *Rps29* (ribosomal protein S29) was used as a positive control for each cDNA preparation (de Jonge et al., 2007).

Fully-grown GV oocytes and ovary were used as a positive control for all of the germline, pluripotency and oocyte markers, as well as meiotic markers with the exception of *Stra8*. Testis was used as a positive control for all of the germline, pluripotency, and meiosis markers, and as a negative control for oocyte markers. Granulosa cells isolated from fully-grown COCs and fibroblasts from skin explants were used as a negative control for all markers, with the exception of the housekeeping gene *Rps29*.

As expected, all germinal cell lines (oocytes, ovary and testis) proved to have all the

germline markers (Fig. 5.6A, B, C, in blue), as well as the pluripotency markers *Pou5f1*, *Zfp296* and *Utf1* (Fig. 5.6A, B, C, in red) and the meiosis markers *Sycp3* and *Ybx2* (Fig. 5.6A, B, C, in purple). The oocyte-specific markers *Zp3* and *Nobox* could only be detected in GV oocytes and whole ovaries (Fig. 5.6A, B, in green), and as expected they were absent from the testis (Fig. 5.6C, in green). *Zp3* is an oocyte-specific extracellular protein that forms part of the zona pellucida (Dean, 2002), and as such would be absent from the testis, as is *Nobox*, which is an oocyte-specific homeobox protein (Rajkovic et al., 2004). *Gdf9* is another oocyte-specific marker expressed in oocytes and whole ovaries (Fig. 5.6A, B, in green), where it allows for the formation and maintenance of multi-layered COCs (Dong et al., 1996; Su et al., 2004). It is also expressed in male round spermatids for the modulation of Sertoli cell functions, where it seems to regulate tight junction functions (Nicholls et al., 2009), but it was only detected in one of the three testis explants studied here (Fig. 5.6C, in green) .

The meiosis markers *Stra8* and *Rec8* were present in testis (Fig. 5.6C, in purple), but not ovaries (Fig. 5.6B, in purple). *Stra8* is associated with entry into meiosis but not oocyte maturation, and as such would be predicted to be absent from the adult ovary, which already contains meiosis-committed immature oocytes (Baltus et al., 2006; Dokshin et al., 2013). REC8 is a key component of the meiotic cohesion complex, and it is required for the maintenance of cohesion between sister chromatids and for the synapsis between homologous chromosomes (Xu et al., 2005b) but, interestingly, it could not be detected in the ovary or GV oocytes,. It could be that its mRNA levels are too low to be detected, or that it peaks in a very brief window in the female germline.

Also notable was the expression of *Utf1*, found in ovary and testis (Fig. 5.6B, C, in red). This pluripotency marker is involved in embryonic stem cell differentiation (van den Boom et al., 2007) and in spermatogonia A self-renewal (van Bragt et al., 2008). UTF1 is present in the nucleoplasm of spermatogonia (Kristensen et al., 2008; van Bragt et al., 2008), and it has been utilised by Imudia et al. (2013) to justify an early preparation to enter meiosis in OSCs. Its presence in ovaries is disputed (Kristensen et al., 2008; Okuda et al., 1998) but its expression could provide evidence of pre-meiotic cells in the adult ovary.

As expected, granulosa cells and fibroblasts were negative for the expression of germline, pluripotency, meiosis and oocyte markers (Fig. 5.6D, only granulosa represented). Critically, they showed presence of *Prdm1 and Ifitm3* (Fig. 5.6D, in blue), and granulosa was positive for *Zfp296* (Fig. 5.6D, in red). It could be that these markers are

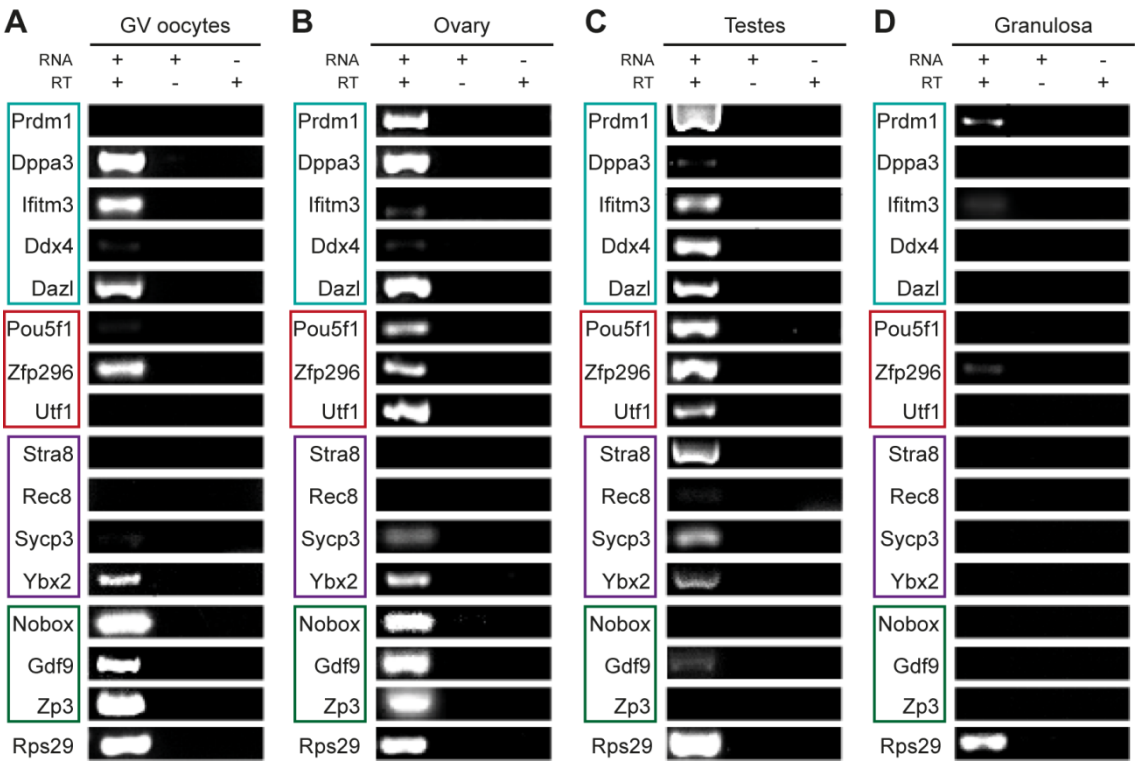

Figure 5.6. Expression of germline markers in adult reproductive tissues. Profile expression for germline (*Prdm1*, *Dppa3*, *Ifitm3*, *Ddx4* and *Dazl*, in blue) pluripotency (*Pou5f1*, *Zfp296* and *Utf1*, in red), meiosis (*Stra8*, *Rec8*, *Sycp3* and *Ybx2*, in purple) and oocyte-specific markers (*Nobox*, *Gdf9* and *Zp3*, in green) on **(A)** fully-grown oocytes, **(B)** whole adult ovary, **(C)** adult testis and **(D)** granulosa cells isolated from adult ovaries. Representative of 3 independent runs.

not exclusive of the germline, as previously suggested in Section 5.3.4, but are rather involved in pluripotency in somatic tissues.

5.2.6 Gene expression analysis of germline markers in putative OSCs

In Section 5.2.4 I had concluded that the primary cultures of putative OSCs had a cell surface DDX4^{C25} epitope, and were also immunopositive for PRDM1 and IFITM3 in their cytoplasm. However I could not detect DPPA3 and DAZL, which are key markers in the maintenance of the germline and the competency to enter into meiosis. Protein levels may have been too low to detect. Therefore here I examined gene expression, having validated the primers to be used (Section 5.2.5).

Gene expression analysis was performed on freshly sorted and 2-month-old putative OSCs to detect *Dppa3* and *Dazl*, and other germline markers. However, the lower levels of total RNA extracted from these DDX4^{C25}-positive cells obliged me to limit the analysis to a few, main markers. Specifically I examined for the germline markers *Prdm1*, *Dppa3*, *Ifitm3*, *Ddx4* and *Dazl*, the pluripotency marker *Pou5f1*, the meiosis marker *Stra8* and the oocyte markers *Nobox* and *Zp3*. To calibrate the sensitivity of my detection, RNA from total ovarian cell extracts was used at various concentrations (0.1 to 30 ng). Testis was used as a positive control for all of the germline, pluripotency, and meiosis markers, whereas fibroblasts from skin explants were used as a negative control for all of the markers studied. The ribosomal gene *Rps29* was again used as a positive control for each cDNA preparation.

The gene expression profile of germline, pluripotency and oocyte-specific markers in the ovary and testis were all as expected (Fig. 5.7). The testis expressed all markers except the oocyte-specific *Zp3* and *Nobox* (Fig. 5.7). Freshly sorted putative OSCs only expressed *Ifitm3* (Fig. 5.7), which confirms the immunostaining (Fig. 5.5). However, although often used as a germline marker, *Iftm3* was also observed in explants of dermal mouse fibroblasts (Fig 5.7). No *Prdm1* mRNA could be detected, which contradicted the immunostaining (Fig. 5.5). It could be that the antibody for PRDM1 is non-specific for this protein, or that the gene was not expressed at the time of the mRNA extraction. Even though OSCs were isolated on the basis of their cell surface DDX4^{C25}-positive antigen, they were negative for *Ddx4*. Furthermore these cells were negative for all the other germline, pluripotency and oocyte-specific markers (Fig. 5.7).

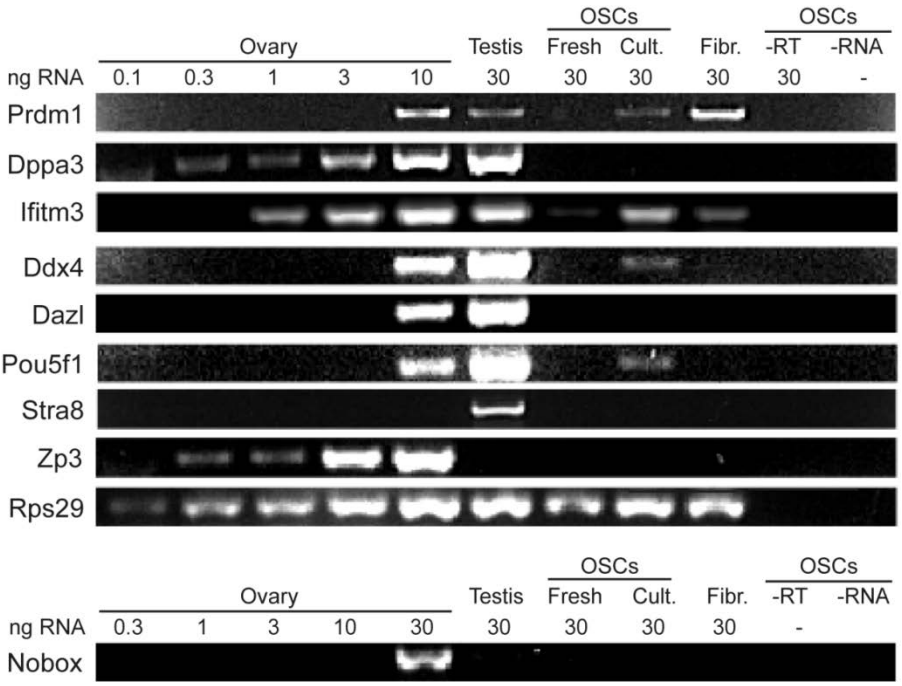

Figure 5.7. Expression of germline markers in freshly sorted and cultured DDX4^{C25}-positive cells. Gene expression in freshly sorted and 2-month-old cultured DDX4^{C25}-positive cells (the 'OSCs'), ovary, testis or fibroblasts for *Prdm1, Dppa3, Ifitm3, Ddx4, Dazl, Pou5f1, Stra8, Nobox* and *Zp3*. Representative of 8 independent runs.

These data suggest that although freshly isolated putative OSCs are categorised as DDX4^{C25}-positive cells by being FACS-sorted using a DDX4^{C25} antibody, they do not express detectable *Ddx4* and furthermore show no characteristics that would appear to give them a hallmark of being germ stem cells.

Interestingly, after 2 months in culture the putative OSCs also started to express *Prdm1*, *Ddx4* and *Pou5f1* (Fig. 5.7). However, it is difficult to conclude only on this expression profile that such cells are stem cells, given dermal fibroblasts were also positive for *Prdm1*. Furthermore there was no commitment to meiosis or oogenesis, judged by the lack of *Stra8*, *Nobox*, and *Zp3* (n = 8 independent FACS).

5.3 Discussion

This chapter has shown that the putative OSCs isolated by means of their affinity to a DDX4^{C25} antibody do not appear to show germ stem cell characteristics when initially isolated. However, they appear to take on some characteristics of OSCs following culture, although I have identified some 'germ cell' markers that appear not really to be germ cell specific. In culture, the DDX4^{C25}-positive cells can produce rounded cells that superficially resemble small oocytes, but critically they failed to develop recognisable mature oocyte-like cells or possess oocyte-specific markers. Furthermore the FACS sorted cells were not immortal and instead died after a few months.

5.3.1 FACS-sorted putative OSCs appear not to belong to the germline

The stem cell and germ cell characteristics of OSCs freshly isolated from the ovary remain disputed. Some groups have reported a germline identity (Ding et al., 2016; Dunlop et al., 2014; Hernandez et al., 2015; Imudia et al., 2013; Khosravi-Farsani et al., 2015; Park and Tilly, 2014; White et al., 2012; Woods and Tilly, 2015; Zhang and Wu, 2016; Zou et al., 2009) and the ability to enter meiosis and to produce oocyte-like cells (Ding et al., 2016; Grieve et al., 2014; Park et al., 2013; White et al., 2012; Zhang and Wu, 2016; Zhang et al., 2011; Zou et al., 2009).

However, other groups using similar methods of isolation have reported to culture cells that were non-germline in origin, consequently not expressing DDX4 (Yuan et al., 2013; Zhang et al., 2012b; Zhang et al., 2015).

In my experiments, only *Prdm1* and *Iftm3*, often regarded as germline markers (Hayashi et al., 2007), were present in freshly isolated ovarian cells following FACS with DDX4^{C25} antibody.

Prdm1 is a key regulator of PGCs in the embryo (Ohinata et al., 2005) but it has also been linked to stem cell pluripotency and maturation in non-germline cells (Chang et al., 2000; Horsley et al., 2006; Kim, 2015; Martins et al., 2006; Miyauchi et al., 2012; Muncan et al., 2011; Parfitt et al., 2015; Robertson et al., 2007; Turner et al., 1994), and it is expressed at low and medium levels in all human tissues (The Human Protein Atlas, www.proteinatlas.org/ENSG00000057657-PRDM1/tissue). Critically, here it was not a specific marker of the germline as it could be detected in dermal fibroblasts and granulosa cells. Therefore, expression of *Prdm1* in itself conveys no message of germ line identity.

Interestingly, PRDM1 was found in the nucleus as well as in the cytoplasm of freshly sorted DDX4^{C25}-positive cells (Fig. 5.4). PRDM1 has been described as a nuclear transcriptional regulatory factor that recruits epigenetic modifiers of chromatin for the controlling of gene silencing (Bikoff et al., 2009). Its presence in the nucleus of adult and embryonic somatic and germline cells has been assessed by Western blotting (Turner et al., 1994), immunofluorescence (Chang et al., 2000; Chang et al., 2002; Horsley et al., 2006; Muncan et al., 2011; Parfitt et al., 2015) and vector-expressing cells (Chu et al., 2011). However, a study has reported that in E11.5 PGCs, PRDM1 binds to the arginine methyltransferase Prmt5 and both translocate from the nucleus to the cytoplasm, which leads to the loss of histone H2A/H4 R3 methylation as part of the epigenetic reprogramming of PGCs (Ancelin et al., 2006). It would be reasonable to think that germline-specific epigenetic modifications are occurring in the DDX4^{C25}-positive cells as soon as they are subjected to *in vitro* cell culturing.

Ifitm3 is also involved in the differentiation of the first PGCs in the embryo (Tanaka and Matsui, 2002) but has also been reported in somatic tissues to mediate immune responses to viruses, either preventing the cytosolic entry (Feeley et al., 2011) or restricting the early replication of influenza A and flaviviruses (Brass et al., 2009). Interestingly, some groups have used the double-transmembrane-domain IFITM3 to MACS-sort OSCs instead of DDX4 (Lu et al., 2016; Woods and Tilly, 2013b; Zhou et al., 2014; Zou et al., 2011). The ubiquitous expression that has been observed here in the ovary, granulosa cells and skin suggests that this is not an ideal method, and may additionally isolate somatic cells. Furthermore, as Navaroli et al. (2016) have suggested, the N-terminal millieu of IFITM3 that is bound during the MACS sorting is poorly conserved throughout evolution (Yount et

al., 2011), and the sorting protocol necessitates the utilisation of species-specific antibodies to IFITM3$^{N\text{-}t}$, which avoids inter-species comparison and is time and money consuming.

In contrast to *Prdm1* and *Ifitm3*, I have found that *Dppa3*, *Ddx4* and *Dazl* have no somatic expression. They refine the functionality of PGCs to produce oocytes: *Dppa3* helps to maintain pluripotency (Saitou et al., 2002), whereas *Ddx4* and *Dazl* maintain the proliferation of GSCs (Haston et al., 2009; Tanaka et al., 2000) and cause entry into meiosis (Koubova et al., 2014; Medrano et al., 2012; Reynolds et al., 2005). Therefore, expression of *Prdm1* and *Ifitm3* should not be correlated with an adult GSC identity in the absence of corroborative markers such as *Dppa3*, *Ddx4* and *Dazl*.

Since some pre-meiotic markers, including *Ddx4*, were activated in cultured OSCs it may be that culture has some effect on the ability of the OSCs to self-reprogram. This has been proposed previously by Hernandez et al. (2015). Critically, despite this suspected self-reprogramming and the presence of small oocyte-like cells, the putative OSCs proved unable to enter into meiosis and to express the oocyte markers *Nobox* and *Zp3*.

5.3.2 The OSC culture medium may reprogram somatic ovarian cells

Long-term exposure to a highly enriched cell culture medium has been suspected to reprogram *in vitro* FACS-sorted ovarian cells towards a germline-like identity (Hernandez et al., 2015). Stable proliferating mouse OSCs are attained 12 weeks post-FACS isolation (White et al., 2012), after which time meiotic and oocyte markers activate and oocyte-like cells are observed (Park et al., 2013; White et al., 2012; Woods and Tilly, 2013b). The dynamics of OSCs during these first 3 months in culture remains unreported, but given that cultured OSCs have shown tumorigenic potential (Woods et al., 2012b), it is reasonable to think that reprogramming takes place once outside of a controlled ovarian niche (Scadden, 2006).

The cell culture medium recommended to grow FACS-sorted OSCs (Woods and Tilly, 2013b) contains a large amount of growth factors and hormones (see Section 2.5.2) whose purpose has not been reported. Furthermore, no explanations have been given on the chosen concentrations of said supplements. Therefore, the activity of these supplements in *in vitro* OSCs can only be guessed from their actions *in vivo* and *in vitro*.

The basis of the OSC culture medium is MEM-α, which is a modification of MEM without nucleosides that contains lipoic acid and vitamins B_{12}, C and biotin to protect cell cultures against oxidative stress and mitochondrial apoptosis (Sigma-Aldrich, technical

bulletin). Serum-supplementation is provided by FBS specially formulated for ESC culture to achieve higher upregulation of pluripotency markers and downregulation of differentiation markers (Thermo Fischer, technical bulletin, undisclosed markers). Another important supplement is LIF, which induces self-renewal and undifferentiation in stem cells through three different signalling pathways governed by STAT3 (see Section 1.5.2) (Hirai et al., 2011; Niwa et al., 1998).

Initially, the OSC culture medium resembles those used in the derivation of mouse ESCs and iPSCs (Nagy et al., 2003), however, it is further supplemented with growth factors and hormones that may be already present in the FBS.

Combined supplementation of FGF and EGF upregulate proliferation of pluripotent stem cells at the same time that some differentiation takes place (Lee et al., 2006). Glial-derived neutrophilic factor (GDNF) is a chemoattractant synthesised by the Sertoli cells in to modulate fate decision in GSC (Meng et al., 2000), as well as differentiating migration within the seminiferous tubules (Dovere et al., 2013). As for the hormones supplemented to the medium, insulin, transferrin, putrescine, selenite and progesterone all enhance cell proliferation by upregulating the cellular metabolism (Sigma-Aldrich, technical bulletin).

In summary, these supplements would provide with proliferation in some undifferentiated stem cells as well as dose-dependent differentiation in others, importantly, without a specific germline fate. It is important to note the duplicated adition of certain supplements (White et al., 2012; Zou et al., 2009) that would likely be present in the FBS, therefore rising to final unknown concentrations with uncertain results. It is surprising that the OSC culture medium develops into such an uncontrolled medium, given that the entire process of FACS-sorting and culturing OSCs precises such specific steps and protocols. Uncontrollable conditions during in vitro OSC culturing may well account for the low reproducibility and differentiation results in other groups, and rises the possibility that these cells self-reprogram not only towards germline, but also other unnoticed cell types.

5.3.3 Growth of DDX4^{C25}-positive cells does not correlate with pluripotent colonies

FACS can be an aggressive technique that produces irreparable damage on part of the sorted cells (Davies, 2007). Adding to the observed delicacy of OSCs in culture (Woods and Tilly, 2013b), slow *in vitro* growth and a high death ratio during the first passages were expected. However, it seems unlikely that FACS-induced cell damage could explain

the total extinction of the OSC cultures after four months post-isolation. Furthermore, colony formation in putative OSCs did not resemble that reported by other groups (White et al., 2012; Zou et al., 2009), but was instead very similar to that of DDX4^{C25}-negative ovarian stromal cells. This gives the idea that these cells are neither germ stem nor pluripotent cells, but common somatic ovarian cells with a limited lifespan.

Interestingly these DDX4^{C25}-positive cells activated the pluripotency marker *Pou5f1 in vitro*. It could also be that cells expressing *Pou5f1* were already present in the DDX4^{C25}-positive sorted fraction, as it has been previously reported (Ding et al., 2016; Imudia et al., 2013; Pacchiarotti et al., 2010; Zhang and Wu, 2016; Zou et al., 2009) and that they gained preponderance as other non-pluripotent cells died in culture. Although expression of *Pou5f1* in the adult ovary has been linked solely to oocytes (Scholer et al., 1989; Zuccotti et al., 2009a), there is certainly at least one study reporting the existence of POU5F1-expressing adult stem cells (Gong et al., 2010). However, the POU5F1-expressing cells formed embryoid-like bodies in culture (Gong et al., 2010), whereas my DDX4^{C25}-positive cells grew as a monolayer. It is likely that my cells are a different cell type. Single-cell gene expression analysis would be required, combined with the detection of other cell-type-specific markers, but based on my initial analysis fully-grown COCs and fibroblasts can be discarded given that they do not express *Pou5f1*. However, regardless of the already present or acquired nature of *Pou5f1* expression, this did not seem to alter the limited lifespan of cells.

I seeded freshly sorted DDX4^{C25}-positive cells onto MEF monolayers with the aim of enhancing the plating and formation of pluripotent colonies, as in Woods and Tilly (2013). However, the presence of MEF seemed to increase the death rate in the DDX4^{C25}-positive cells. The reason for this is uncertain; I have found no reports of the detrimental effect of MEFs on other cells. It is unlikely that traces of the mitosis inhibitor mitomycin C or the cryoprotectant DMSO were left in the MEF monolayer, since MEFs had been washed several times according to the protocol by Lin and Talbot (2011).

Using MEFs with putative OSCs as in Woods and Tilly (2013) was found to be challenging. They prohibit passaging OSCs until 90% confluence, which in the initial growth phase can take several weeks. However, MEF monolayers need to be changed every 2 weeks at the most, because they have a limited lifespan (Lin and Talbot, 2011; Thermo Fischer, personal communication). It is uncertain how these events can be overcome in the establishment of *in vitro* OSC lines on MEF monolayers, with such differences in the cell lifespans.

5.3.4 *Utf1* and *Zfp296* are not germline-specific markers

Utf1 and *Zfp296* expression are linked to pluripotency in PGCs (Chuva de Sousa Lopes et al., 2005; Fischedick et al., 2012). They have been used in OSCs to suggest a PGC-like development (Imudia et al., 2013). Interestingly, *Utf1* was detected in ovary explants, and *Zfp296* in granulosa cells from COCs.

Utf1 is a transcriptional repressor with histone-like properties (van den Boom et al., 2007) that is involved in pluripotency in ESCs and PGCs (Chuva de Sousa Lopes et al., 2005; Kristensen et al., 2008; Okuda et al., 1998; van Bragt et al., 2008). In the adult mammal, *Utf1* is expressed in the male germline, especifically in early A spermatogonia (van Bragt et al., 2008), where it enhances cell renewal and cell differentiation by self-regulating (Okuda et al., 1998) or through chromatin compaction and summoning of chromatin-remodelling proteins (van den Boom et al., 2007). Okuda et al. (1998) is the only study to have reported *Utf1* expression in post-partum ovaries, although no further studies followed on whether pre-meiotic cells existed in the adult female gonad.

Nuclear *Zfp296* is a pluripotency factor that allows differentiation of ESCs by repressing *Klf4* (Fujii et al., 2013). It also contributes to self-renewal of ESCs, PGCs and GSCs by upregulating *Pou5f1* and *Nanog* and downregulating differentiation markers (Fischedick et al., 2012). Last, *Zfp296* may play a role in tumour suppression (Li et al., 1999).

In conclusion, *Utf1* has been scarcely studied in the ovary (Kristensen et al., 2008; Okuda et al., 1998), and *Zfp296* can also be found in stem cells in the spleen, liver, skin, brain and many other organs (Dear, 2000; Fischedick et al., 2012). It is therefore a surprise that Imudia et al. (2013) establishes a strong link between these two pluripotency markers and a resemblance to PGCs in OSCs. Rather, these are non-specific germline markers, similar to *Prdm1* and *Ifitm3*. *Zfp296* may be needed for the differentiation of granulosa layers. It could also be activated to avoid tumour formation during the cumulus-oocyte growth. *Utf1* could be expressed in granulosa stem cells or in yet uncharacterised ovarian pluripotent cells, similar to those found in the adult testis (Kanatsu-Shinohara et al., 2004).

In summary, in this Chapter 5 I conclude that OSCs isolated using the DDX4^{C25} antibody are a subpopulation of somatic ovarian cells that contain a reactive uncharacterised epitope – this may be a member of the DEAD-box family but is unlikely to be DDX4. These cells can establish DDX4 expression in culture, but die without developing germline markers. It is possible that such expression is a product of continued

culture, rather than an inherent property of the cells themselves, which turns on DDX4 expression. It is highly unlikely that these putative OSCs play any physiological role in maintaining any adult oocyte pool as first reported (Johnson et al., 2004), and when isolated show no redeeming features to suggest they have stem cell capacity.

Given the probability that these cells are isolated by a protein other than DDX4, I will attempt to characterise this epitope in these and other mouse tissues reactive to the $DDX4^{C25}$ antibody. This set of experiments will be performed and discussed in the next Chapter.

Chapter 6

Examination of DDX4^{C25} antibody immunostaining in non-germline tissues

6.1 Introduction

One of the main issues over whether DDX4^{C25}-positive cells can be isolated from the adult mammalian ovary has been based on the specificity of the DDX4^{C25} antibody during FACS sorting (Abban and Johnson, 2009; Telfer et al., 2005; Vogel, 2012; White et al., 2012; Woods and Tilly, 2013b; Zhang et al., 2012b; Zou et al., 2009)

In this thesis, I have described the isolation of presumed germ stem cells by FACS from the adult mouse ovary using the DDX4^{C25} antibody. In culture, the freshly sorted cells were indeed reactive to this same DDX4^{C25} antibody on their cell surface, but critically did not express DDX4 or any other germline marker when examined by gene and protein expression analysis. I have therefore concluded in Chapter 5.2.4–5.2.5 that freshly isolated DDX4^{C25}-positive cells are not germ stem cells, and are being isolated by cell surface expression of protein(s) different from DDX4.

In this Chapter I have studied the use of the DDX4^{C25} antibody on non-germline tissues under FACS and non-FACS conditions, to further analyse the specificity of this antibody.

6.2 Results

6.2.1 FACS-sorting of DDX4^{C25}-positive cells in kidney and liver

Based on the results from Section 5.2.6, I hypothesized that the suspected non-specificity of the DDX4^{C25} antibody was an effect of the FACS-sorting conditions. To explore this possibility, I tried to FACS-sort cells reacting to the DDX4^{C25} antibody in non-germline tissues, which would not be expected to express the germline-specific DDX4. Therefore, postnatal mouse kidneys, livers and ovaries from six 3-to-4-week-old female mice were enzymatically digested and immunostained, and the same FACS settings were used on all three tissues (n = 6 independent FACS per tissue).

As expected, upon FACS, 2.1% ± 0.5% DDX4^{C25}-positive ovarian cells were found (range 757–5,174 cells) (Fig. 6.1A). Interestingly, 11.3% ± 2% DDX4^{C25}-positive kidney cells were sorted (range 1,979–102,696 cells) (Fig. 6.1A, B white rectangles) and 16.7% ± 4% DDX4^{C25}-positive cells were sorted from liver (range 4,224–105,155 cells) (Fig. 6.1A, B black rectangles). Similar to the observations in Sections 4.2.1–4.2.2 a high variability in the percentages of DDX4^{C25}-positive cells isolated was found (Fig. 6.1B).

Cells isolated from liver and kidney presented higher levels of DAPI staining and appeared between 10^3 and 10^4 units of DAPI fluorescence. However, they did not plate in OSC culture medium and after 24 hours the cell culture was discarded.

The isolation of cells from non-germline tissues adds support to the hypothesis that the DDX4^{C25} antibody is binding to cell surface protein(s) different from DDX4 under FACS conditions. The sorted cells were kept for further gene and protein expression analysis.

6.2.2 Analysis of DDX4^{C25} expression of germline markers in oviduct and kidney

It could be that the non-specificity of the DDX4^{C25} antibody is inherent to the antibody, rather than an artefact of the FACS conditions. I therefore studied the reactivity of the DDX4^{C25} antibody in germline (adult ovary and testis) and non-germline (adult oviduct and embryonic kidney) tissue sections by immunohistochemistry. Oocytes in the ovary and male GSCs in the testis were used as a positive control for DDX4, as was previously done in Section 3.2.4. Stromal ovarian and testicular cells, and spermatozoa served as negative control (n = 3).

As expected, only oocytes and male GSCs stained positive with the DDX4^{C25} antibody in their cytoplasm (Fig. 6.2A, and inserts) (Castrillon et al., 2000; Fujiwara et al., 1994). Primordial follicles were easily identifiable because they were located near the outer ovarian cortex and presented few, flat granulosa cells (Fig. 6.2A insert) (Fortune et al., 2000; McGee and Hsueh, 2000; Peters, 1969). The strongest expression of DDX4 was observed in primary oocytes, with staining reduced in fully-grown oocytes (Fig. 6.2A). Therefore DDX4 expression seems to decrease during oocyte growth, consistent with a previous report (Toyooka et al., 2000).

In the testis, DDX4-expressing cells were restricted to the spermatogonia and spermatids in seminiferous tubules (Fig.6.2A, marked as S). As reported previously (Tanaka et al., 2000), and similarly to the observed in Section 3.2.4, spermatogonia presented with a large nucleus and homogeneous cytoplasmic DDX4 staining (Fig.6.2A,

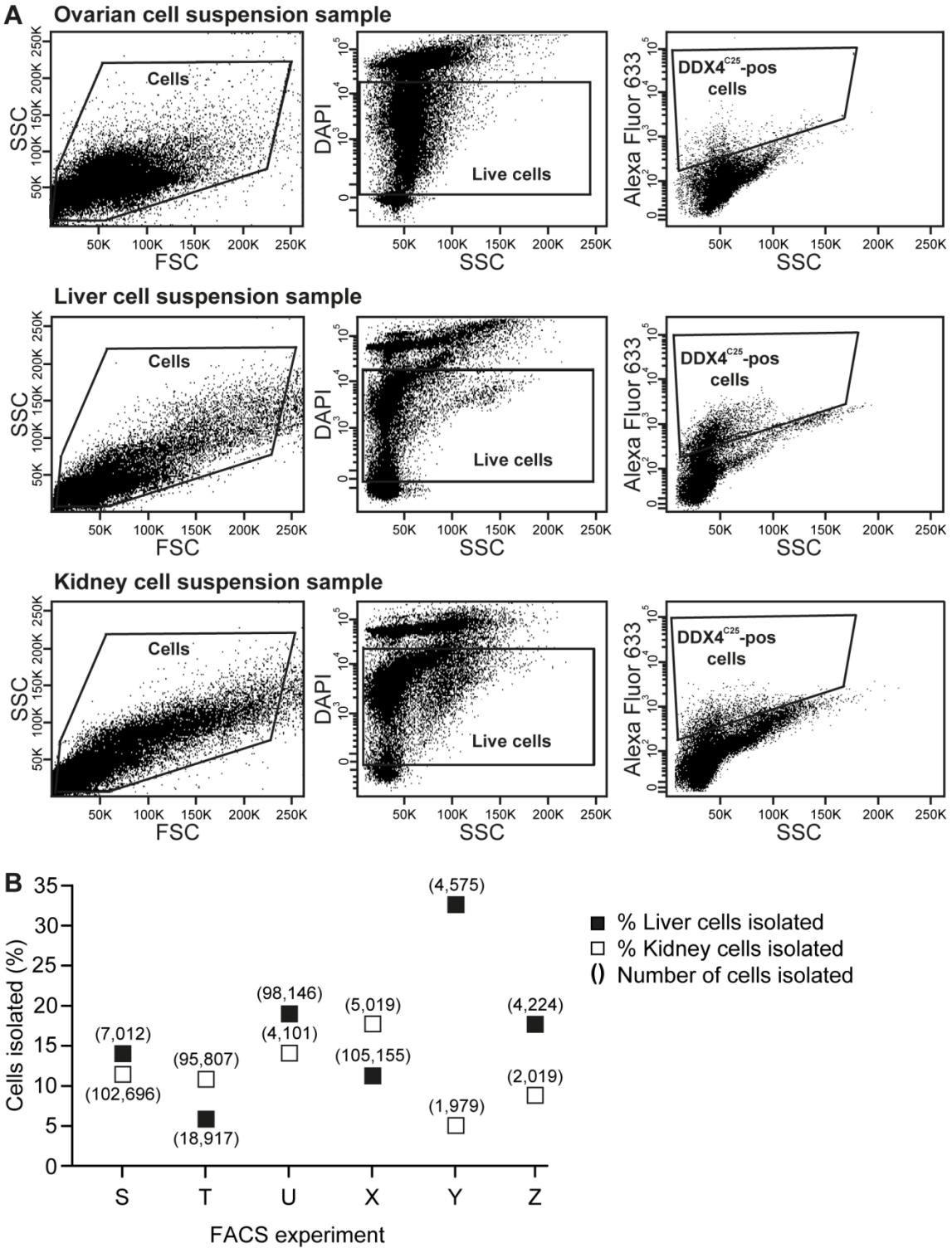

Figure 6.1. FACS-sorting of DDX4^{C25}-positive cells in non-germline tissues. (A) Screening analysis of viable, Alexa-Fluor-633-positive cells in ovarian, liver and kidney cell suspensions. **(B)** Percentages and numbers of DDX4^{C25}-positive cells isolated from the total viable cell suspensions in kidney and liver. N = 6 independent FACS.

red arrow, and insert), whereas spermatids had a compact chromatin and their chromatoid bodies stained strongly for DDX4 (Fig. 6.2A, orange arrow and insert). No staining was observed in stromal ovarian and granulosa cells (Fig. 6.2A), in connective tissue out of seminiferous tubules (Fig. 6.2A, marked as C) or in spermatozoa in the lumen of these tubules (Fig. 6.2A, marked as L).

Oviduct showed a positive staining for DDX4^{C25} in the cytoplasm of permeabilised, individual cells (Fig. 6.2B), but not in non-permeabilised cells (Fig. 6.2B). DDX4^{C25} staining on tissue slides showed that this cytoplasmic staining was mostly present in the oviductal epithelium (Fig. 6.2C, marked as E, and insert), with minor staining in the surrounding muscular mucosa (Fig. 6.2C, marked as M). Interestingly, although I had FACS-sorted DDX4^{C25}-positive kidney cells in Section 6.2.1, no positive staining was recovered from kidney tissue sections.

6.2.3 Analysis of protein expression of germline markers in oviduct and kidney

Staining of permeabilised oviductal epithelium and FACS-sorting of kidney cells with the DDX4^{C25} antibody could indicate that germline cells exist in these somatic tissues. To further analyse this hypothesis, I stained oviduct sections of pre-pubertal mice and embryonic kidney sections with antibodies to PRDM1, IFITM3, DPPA3 and DAZL. Oocytes in ovary sections were used as a positive control for DDX4, as was previously done in Section 5.2.3. Stromal ovarian cells served as negative control (n = 3).

PRDM1 and IFITM3 staining were observed in the ovary (Fig. 6.3), oviductal epithelium and kidney (Fig. 6.4A, B). PRDM1 staining was ubiquitously seen in oocytes, stromal and granulosa cells of the ovary (Fig. 6.3, and insert), in the epithelium and muscular mucosa of the epithelium (Fig. 6.4A, and insert), and in the tubules of the embryonic kidney (Fig. 6.4A, and insert). IFITM3 staining was also observed in oocytes and stromal cells of the ovary (Fig. 6.3, and insert), in those cell surfaces of the oviductal epithelium in contact with the lumen (Fig. 6.4B, marked as E, and insert), and in the cells next to the tubules in the embryonic kidney (Fig. 6.4B, and insert). This localization in somatic tissues further shows that IFITM3 and PRDM1 do not confer a germline identity, as was previously confirmed in Sections 5.2.4–5.2.6.

DPPA3 and DAZL were also present in oocytes at all stages of development (Fig. 6.3). Meiotically-competent GV oocytes accumulated DPPA3 in their nuclei, and DAZL was more abundant in fully-grown oocytes than in immature and growing oocytes (Fig. 6.3,

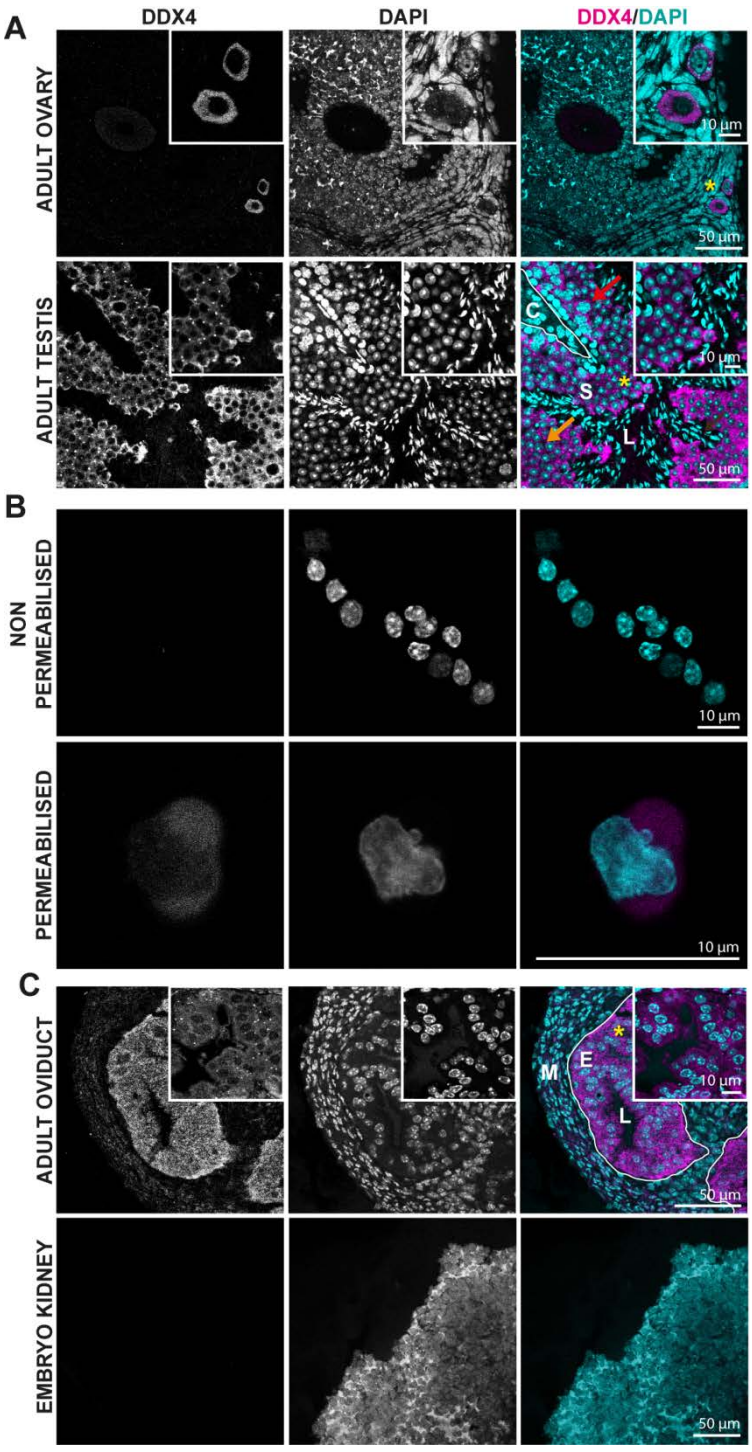

Figure 6.2. Immunostaining with DDX4^{C25} in germline and non-germline tissues. DDX4^{C25} immunostaining in **(A)** permeabilised ovarian and testicular tissue slides, **(B)** permeabilised and non-permeabilised oviductal cells (a mixture of mucosa and epithelial cells) and **(C)** permeabilised oviductal and kidney tissue slides. In total 16 ovaries and oviducts, 14 kidneys, 4 testes and 681 cells taken from 3 oviducts were analysed. Chromatin stained with DAPI. C = connective tissue; S = seminiferous tubule; E = epithelial cells; M = muscular mucosa; L = lumen (asterisks mark site of insert).

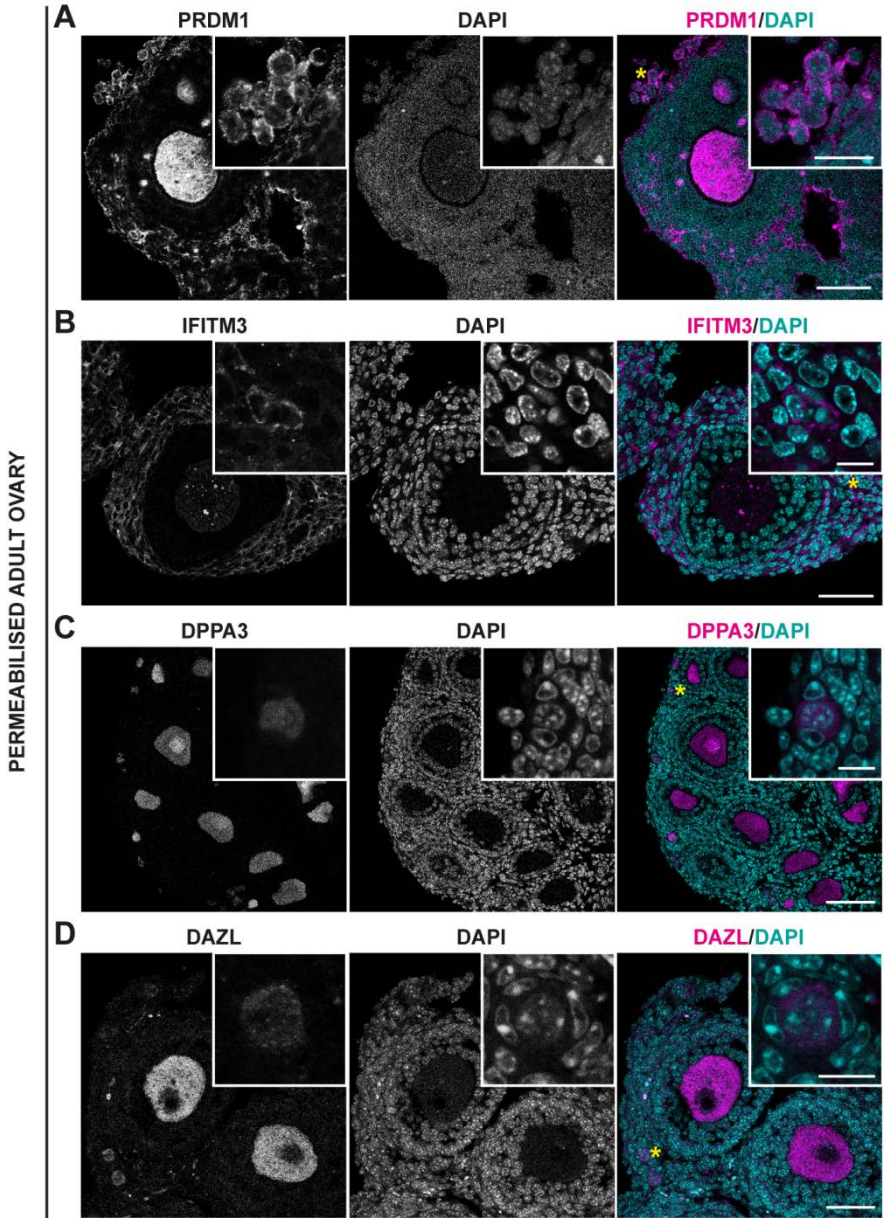

Figure 6.3. Immunostaining for germline markers in the ovary. Immunohistochemical **(A)** PRDM1, **(B)** IFITM3, **(C)** DPPA3 and **(D)** DAZL staining in permeabilised ovarian tissue slides. In total 16 ovaries were analysed. Chromatin was stained with DAPI. Asterisks mark site of insert. Scale bar: 50 µm, 10 µm inserts.

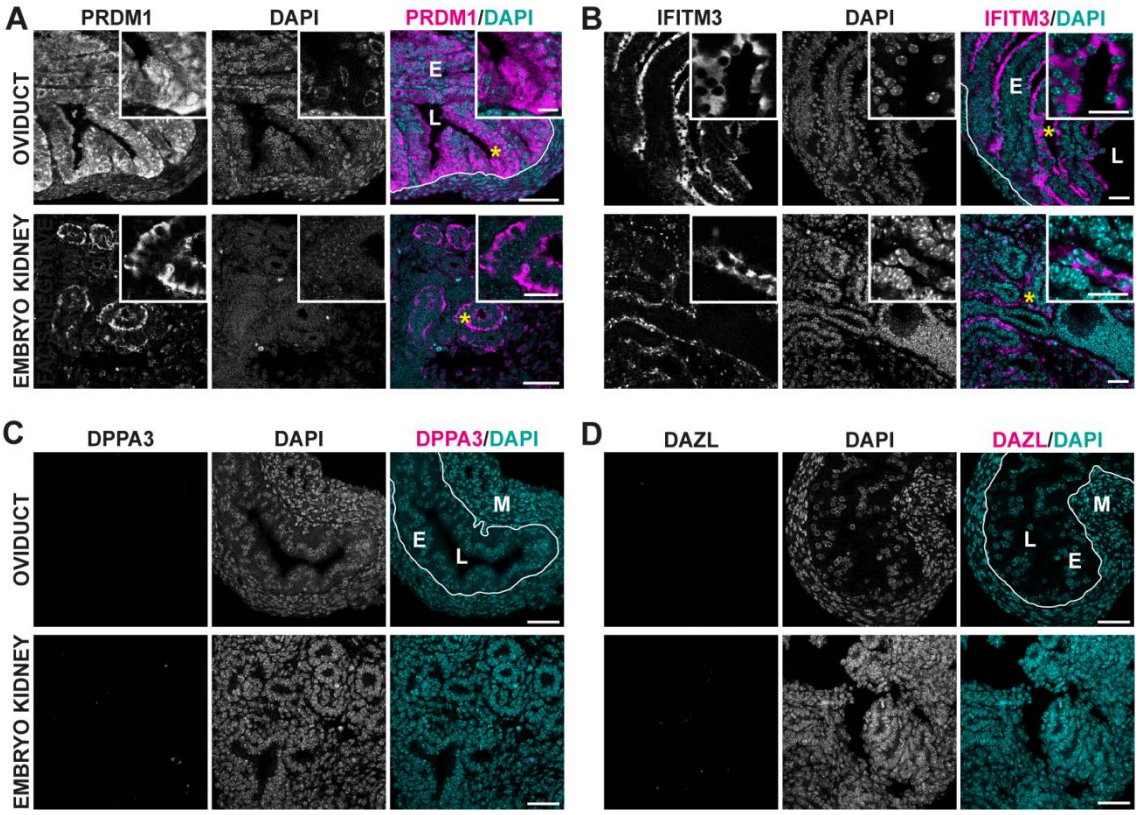

Figure 6.4. Immunostaining for germline markers in oviduct and kidney. Immunohistochemical **(A)** PRDM1, **(B)** IFITM3, **(C)** DPPA3 and **(D)** DAZL staining in permeabilised oviductal and kidney tissue slides. In total 16 oviducts and 14 embryonic kidneys were analysed. Chromatin was stained with DAPI. Asterisks mark site of insert. E = epithelial cells; M = muscular mucosa; L = lumen. Scale bar: 50 µm, 10 µm inserts.

and insert). Primordial follicles could be distinguished by a single layer of flat granulosa cells (Fig. 6.3 inserts). However, DPPA3 and DAZL were absent from the oviduct and the kidney (Fig. 6.4C, D). This absence of DPPA3 and DAZL from oviductal epithelia and kidney suggested that no GSCs existed in these tissues. However, it could be that DDX4 can be expressed in the absence of other germline markers.

6.2.4 Gene expression analysis of germline markers in oviduct and liver

The absence of DPPA3 and DAZL from oviductal epithelia suggested that this tissue was devoid of GSCs. However, DDX4^{C25} staining led me to think that either there were non-germline DDX4-expressing cells in the reproductive tract, or that the DDX4^{C25} antibody was not specific to DDX4 protein. The latter was my preferred hypothesis, given that the DDX4^{C25}-positive cells, isolated by FACS using DDX4^{C25} did not express DDX4 (see Section 5.2.6), and neither did the kidney even when DDX4^{C25}-positive cells could be isolated from it by FACS (see Sections 6.2.1–6.2.2).

To discriminate between the above two possibilities, I performed gene expression analysis on oviduct, flushed extensively to remove any ovulated oocytes that may lead to misinterpretation of results, and on freshly FACS-sorted cells from the liver, which had also reacted to the DDX4^{C25} antibody. I specifically looked for the germline markers *Prdm1*, *Ifitm3*, *Dppa3*, *Ddx4* and *Dazl*. *Nobox* and *Zp3* served as control markers for the cross-contamination of oviduct and liver with oocytes. *Rps29* was the housekeeping gene. Ovary and testis served as positive controls for the presence of germline cells. Fibroblasts from skin explants and DDX4^{C25}-negative liver cells served as negative control.

Confirming the immunofluorescence, *Prdm1* and *Ifitm3* were present in the oviduct (Fig. 6.5A) and DDX4^{C25}-positive liver cells (Fig. 6.5B), resembling the profile from primary fibroblasts and DDX4^{C25}-negative liver cells (Fig. 6.5A, B). This once again confirmed that these often used germline markers are not germline-specific when expressed on their own. The lack of *Zp3* and *Nobox* in oviductal epithelium (Fig. 6.5A) and DDX4^{C25}-positive liver cells (Fig. 6.5B) assured me that oocytes were indeed absent from both tissue preparations. Importantly the absence of *Ddx4* in oviductal tissue and in DDX4^{C25}-positive liver cells (Fig. 6.5A, B), where the DDX4^{C25} antibody had abundantly cross-reacted, suggested that this antibody hitherto used for DDX4 may readily cross-react with other proteins. This cross-reaction could be due to the inherent properties of the antibody and the FACS conditions, and would involve the unspecific binding to cell surface protein(s) in the ovary, liver and kidney.

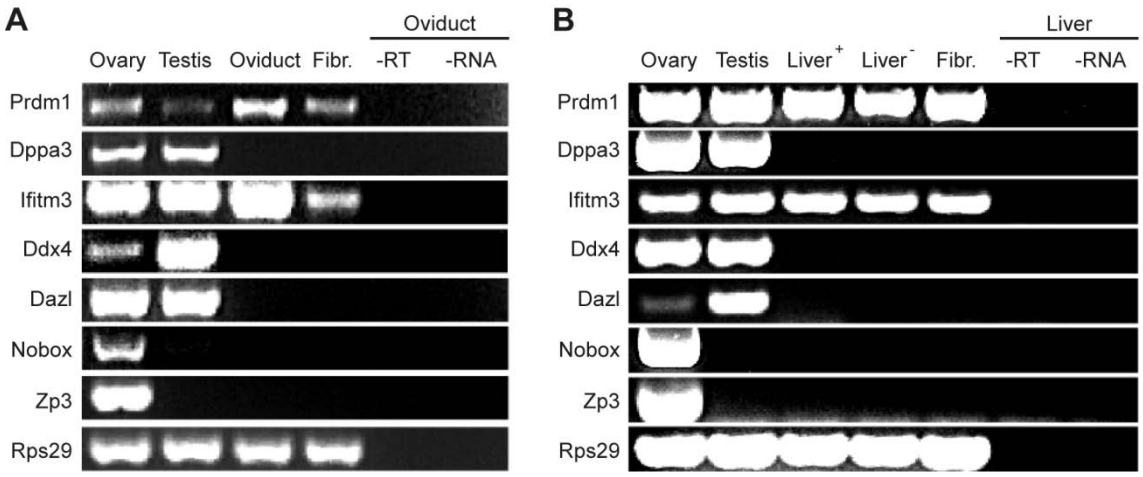

Figure 6.5. Expression of germline markers in oviduct and freshly sorted DDX4^{C25}-positive liver cells. Gene expression in **(A)** oviduct and **(B)** freshly sorted DDX4^{C25}-positive and negative liver cells, ovary, testis or fibroblasts for *Prdm1*, *Dppa3*, *Ifitm3*, *Ddx4*, *Dazl*, *Nobox* and *Zp3*. Representative of 3 independent runs.

6.2.5 *In silico* analysis of the DDX4^{351} antibody specificity

Sections 6.2.1–6.2.4 showed that the DDX4^{C25} antibody used in the DDX4^{C25}-positive cell FACS-sorting may not exclusively bind DDX4, but instead could be cross-reacting with other cytoplasmic and cell surface proteins in somatic cells from kidney, liver and oviduct. However, it could also be that DDX4^{C25}-positive ovarian cells express very low levels of *Ddx4* mRNA that could not be registered in Section 5.2.6.

I wanted to further examine for the presence of DDX4 in DDX4^{C25}-positive cells by immunohistochemistry using a second antibody against DDX4 that would recognise a larger C-terminal epitope of the protein. Therefore I used an antibody that was raised against an epitope within residues 373 to the COOH-terminus of the human DDX4 (Fig. 6.6A). As described by ProteinTech, the company manufacturing this antibody, the epitope spans the C-terminal 351 residues of the mature protein sequence, and would therefore be predicted to detect all four human DDX4 isoforms. Hereafter this second antibody is referred to as DDX4^{351}.

The DDX4^{351} epitope was subjected to sequence alignment with the mouse DDX4 on BLAST Protein, using the SwissProt and RefSeq databases. The programme found a 93% correlation with the C-terminus of both mouse isoforms, with just 24 mismatching residues (Fig. 6.6B).

SwissProt and RefSeq databases were also interrogated for any significant alignment between the human DDX4^{351} epitope and a sequence in the mouse proteome not belonging to DDX4, which would potentially cause cross-reactivity of the antibody for DDX4.

The DDX4^{351} sequence did not entirely align to any other murine protein, but did partially align to four proteins belonging to the DEAD-box protein family: DEAD-box helicase 3 X-linked (DDX3X, also known as FIN14), DEAD-box helicase 3 Y-linked (DDX3Y, also known as DBY), DEAD-box helicase 5 (DDX5, also known as p68), and DEAD-box helicase 17 (DDX17, also known as p72) (Appendix C). As I wanted to work on female tissue and DDX3Y is only present in male germ cells (Fig. 6.6C) (Ditton et al., 2004; Foresta et al., 2000), the protein was initially discarded as a source of cross-reactivity. DDX3X is a cytoplasmic protein involved in the G1/S cell cycle phase through regulating cyclin E1 expression (Lai et al., 2010). It is also part of the innate anti-viral immunity (Oshiumi et al., 2010), and for this reason it is the target of hepatitis B and C viruses, human immunodeficiency virus and poxviruses during viral invasion and replication (Schröeder, 2010). It aligns to the DDX4^{351} epitope in 227 residues and is

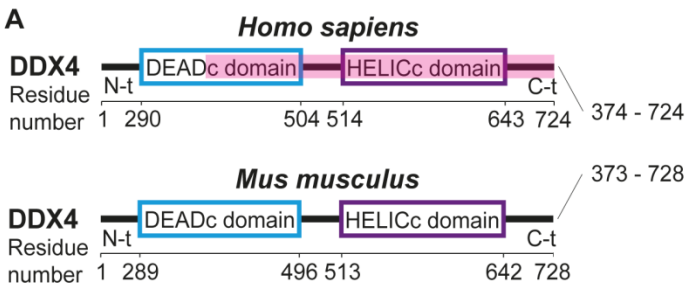

B

Human DDX4 374 TRELVNKIYLEARKFSFGTCVRAVVIYGGTQLGHSIRQIVQGCNILCATPGRLMDIIGKE
KIGLKQIKYLVLDEADRMLDMGFGPEMKKLISCPGMPSKEQRQTLMFSATFPEEIQRLAA
EFLKSNYLFVAVGQVGGACRDVQQTVLQVGQFSKREKLVEILRNIGDERTMVFVETKKKA
DFIATFLCQEKISTTSIHGDREQRERERQALGDFRFGKCPVLVATSVAARGLDIENVQHVI
NFDLPSTIDEYVHRIGRTGRCGNTGRAISFFDLESDNHLAQPLVKVLTDAQQDVPAWLEE
IAFSTYIPGFSGSTRGNVFASVDTRKGKSTLNTAGFSSSQAPNPVDDESWD 724

Mouse DDX4 373 TRELINQIYLEARKFSFGTCVRAVVIYGGTQFGHSVRQIVQGCNILCATPGRLMDIIGKE
KIGLKQVKYLVLDEADRMLDMGFGPEMKKLISCPGMPSKEQRQTLLFSATFPEEIQRLAG
DFLKSSYLFVAVGQVGGACRDVQQTVLQVGQFSKREKLVEILRNIGDERTMVFVETKKKA
DFIATFLCQEKISTTSIHGDREQRERERQALGDFRCGKCPVLVATSVAARGLDIENVQHVI
NFDLPSTIDEYVHRIGRTGRCGNTGRAISFFDTDSDNHLAQPLVKVLSDAQQDVPAWLEE
IAFSTYVPPSFSSSTRGGAVFASVDTRKNYQGKHTLNTAGISSSQAPNPVDDESWD 728

C

PROTEIN	SEQUENCE MATCH	E-VALUE	LOCALIZATION	FUNCTION
DDX3Y	242/351	1e-111	Testis	Early spermatogonial proliferation
DDX3X	227/351	3e-111	All tissues	S phase entry through Cyclin E1
DDX5	190/351	6e-67	All tissues	Pre-mRNA splicing, ribosomal DNA/RNA
DDX17	188/351	1e-65	All tissues	Endogenous miRNA biogenesis

Figure 6.6. The epitope used to generate the DDX4^{351} antibody is highly conserved in mouse but aligns to four cytoplasmic proteins. (A) Diagram representing the functional domains of the human and mouse mature DDX4 isoforms. The DDX4^{351} antibody targets the last 351 residues of the COOH-terminus (C-t, in pink) of the human DDX4 protein. **(B)** The human 351-residues domain sequence. In the mouse, this sequence differs in 24 residues (highlighted in red). **(C)** Aligned residues, tissue distribution and functional characteristics of the candidate mouse proteins that may be bound by the DDX4^{351} antibody.

ubiquitously expressed (Fig. 6.6C). DDX5 presents 190 residues aligned (Fig. 6.6C). This protein is expressed in the nucleus in all tissues (Rössler et al., 2000), where it is involved in pre-mRNA splicing (Lin et al., 2005), postmitotic nucleolar reassembly and ribosomal DNA/RNA transcription and processing during telophase (Fig. 6.6C) (Nicol et al., 2000). DDX17 also has 188 residues aligned (Fig. 6.6C). Though modulation by DDX5 (Jalal et al., 2007), DDX17 is involved in the biogenesis of endogenous miRNA (Connerty et al., 2016) and splicing programmes (Dardenne et al., 2014; Samaan et al., 2014) in the nucleus of cells in all tissues (Fig. 6.6C) (Lamm et al., 1996). DDX17 also acts in antiviral defence (Moy et al., 2014), but once a cell is infected with human immunodeficiency virus, DDX17 promotes the production of infectious particles (Lorgeoux et al., 2013).

Based on the large number of aligned residues (Fig. 6.6C), and on E-values lower than one that point to a biological, certain alignment (Fig. 6.6C), the alignment of the human DDX4^{351} epitope against the mouse proteome shows strong interaction with all the three predicted proteins in females. This was somehow expected, since the annealed residues match those conserved sequences in the DEAD-box helicases, such as the DEADc domain.

6.2.6 Performance of the DDX4^{351} antibody in DDX4^{C25}-positive and oviductal cells

The *in silico* analysis of the DDX4^{351} antibody specificity performed in Section 6.2.5 showed that this antibody was very specific to both mouse DDX4 isotypes. However, it could be that cross-reaction occurred with other proteins also belonging to the DEAD-box protein family. Therefore, I tested the ability of the DDX4^{351} antibody to recognize DDX4 protein within the germline.

Ovarian cells that had been positively FACS-sorted with the DDX4^{C25} antibody (Fig. 6.7A, red Y) by means of an externalised epitope (Fig. 6.7A, green triangle) were plated, fixed, permeabilised and immunostained with the DDX4^{351} antibody (Fig. 6.7A, blue Y) (n = 3 independent FACS). Permeabilised fully-grown GV oocytes in ovarian tissue slides or stripped from their COCs were used as positive controls. Negative controls for the presence of germline cells were permeabilised stromal, epithelial and granulosa cells belonging to the negatively FACS-sorted ovarian fraction and the ovarian tissue slides, as well as the oviductal tissue slides. Non-permeabilised fully-grown GV oocytes were used as a negative control for the presence of cell surface DDX4 immunostaining (n = 3).

Figure 6.7. Schematic analysis of DDX4 in FACS-sorted cells. (A) Ovarian cells FACS-sorted by means of an externalised epitope (green triangle) with a DDX4^{C25} antibody (red Y) are then permeabilised and immunostained using DDX4^{351} antibody (blue Y).

As expected of a cytoplasmic RNA-binding protein (Linder and Lasko, 2006), immunohistochemical DDX4^{351} staining on permeabilised fully-grown GV oocytes revealed a cytoplasmic distribution (Fig. 6.7B), with lower presence in the nucleus and none on the cell surface (Fig. 6.7B).

As would be predicted based of a germline-specific protein (Fujiwara et al., 1994), only oocytes showed cytoplasmic DDX4^{351} staining in ovarian tissue slides independent of their stage of growth (Fig. 6.8). DDX^{351} staining was highest in primary oocytes (Fig. 6.8, and insert). Staining decreased with oocyte growth development (Fig. 6.8), as has been reported previously (Toyooka et al., 2000).

As expected, DDX4 staining was absent from ovarian somatic cells in the ovarian tissue sections and FACS-negative fractions (Fig. 6.8). More importantly, neither oviduct nor DDX4^{C25}-positive ovarian cells were ever observed to be DDX4-positive (Fig. 6.8, and insert). This absence strongly supports my hypothesis that there is a cross-reaction of DDX4^{C25} antibody with other cell surface and cytoplasmic proteins, and suggests that DDX4^{C25}-positive ovarian cells do not express DDX4.

6.2.7 Western blotting of DDX4^{C25} in adult non-reproductive tissues

It could be that those proteins that cross-react with the DDX4^{C25} antibody in ovary, oviduct, and FACS-sorted kidney and liver cells could be identified through proteomics. With the aim of unravelling their identity, I first tried to isolate these proteins by Western blot. Whole ovaries and testes from adult mice were used as positive controls, whereas skin explants were used as a negative control for the presence of germline cells (n = 3). The presence of proteins in all lysed tissues was certified with electrophoresis-based measurement and staining of the nitrocellulose membrane.

Interestingly, although the ovary had stained positive with the DDX4^{C25} antibody (see Section 6.2.2), here it did only provide me with bands in one of the three samples analysed (Fig. 6.9). It is possible that the levels of DDX4 protein in 3-week-old ovaries were too low to be detected with this method. On the other side I always retrieved positive bands for the DDX4^{C25} antibody in all testis samples analysed (Fig. 6.9).

However, the remaining samples did not provide me with bands. This confirms that the antibody had cross-reacted, or was affected, under FACS conditions during the isolation of cells from ovary, liver and kidney, and also possibly during the immunostaining of oviduct. Furthermore, despite the expected size band for the antibody is 76 kD, two strong bands at

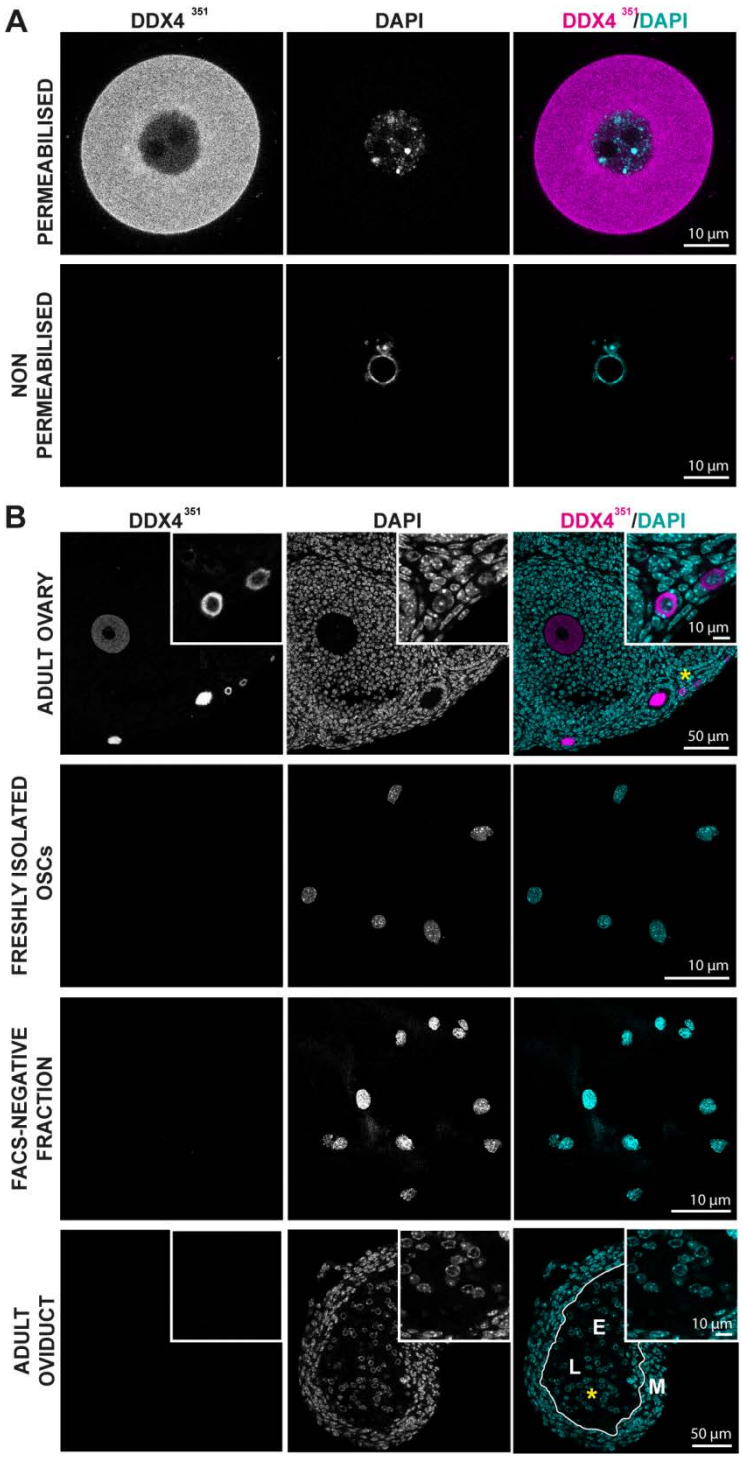

Figure 6.8. DDX4^{351} antibody immunostaining of germline and somatic cells. (A) Immunostaining for DDX4^{351} antibody in permeabilised and non-permeabilised fully-grown GV oocytes, and **(B)** permeabilised ovary and oviduct tissue slides and FACS-positive and negative cells. In total 166 fully-grown oocytes taken from 12 ovaries, 192 FACS-negative cells and 117 FACS-positive cells from 3 independent FACS runs, 16 ovaries and oviducts were analysed. Chromatin was stained with DAPI. Asterisks mark site of insert. E = epithelial cells; M = muscular mucosa; L = lumen.

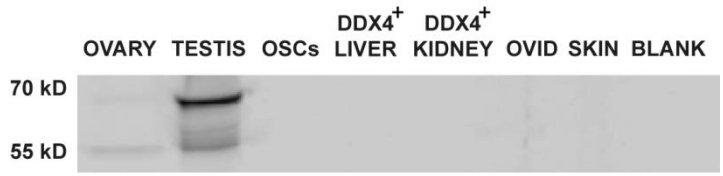

Figure 6.9. Western blotting the DDX4^{C25} antibody on germline and somatic cells. Western blot of an antibody against DDX4^{C25} on 100 µg of protein from adult ovary, testis, oviducts and skin, and DDX4^{C25}-positive FACS-sorted cells from ovary, liver and kidney. N = 3.

~55 and ~68 kD appeared in ovary and testis (Fig. 6.9). This strongly suggests that either the antibody cross-reacts with other proteins present in germline cells, or that post-translational modifications in DDX4 were detected.

6.3 Discussion

This study has showed that the same DDX4^{C25} antibody used for the isolation of mouse ovarian cells – which some studies claim to be germ stem cells but for my results they are not – also binds to epitopes in the cell surface of liver and kidney cells, and in the cytoplasm of the oviductal epithelia. Importantly, these tissues did not express *Ddx4* or were immunostained by a second independent DDX4 antibody (DDX4^{351}), whereas only oocytes at different stages of growth stained positive on account on the presence of DDX4 in their cytoplasm. The absence of reactive proteins in Western blotting made it unable to characterise this epitope through proteomics.

6.3.1 Cells from non-germline tissues can be sorted by FACS using the DDX4^{C25} antibody

Here I was able to isolate cells from mouse liver and kidney live cell suspensions with a DDX4^{C25} antibody through the detection of fluorescence from Alexa Fluor 633. This is consistent with very recent reports (Hernandez et al., 2015; Zhang et al., 2015). These two somatic tissues were analysed at the same time and with the same FACS settings as mouse ovarian samples, from which a small population of cells was isolated (See Chapter 4.2.2). However, as predicted for a non-germline tissue, these cells did not express *Ddx4* or any other germline-specific marker.

The percentages of cells that I recovered from mouse liver (16.7% ± 4%) were remarkably similar to those reported by Zhang et al. (2015) (16.17% ± 3.07%). Isolated kidney cells (11.3% ± 2%) were recovered by me at larger percentages than the reported by Zhang et al. (2015) (5.50% ± 1.23%) or Hernandez et al. (2015) (3.2%). DDX4^{C25}-positive ovarian cells isolated by FACS in this Chapter (2.1% ± 0.5%) were similar to those I reported earlier (Chapter 4.3.2) and similar to others: White et al. (2012) (1.5% ± 0.2%), Park and Tilly (2014) (1.83% ± 0.14%) and Zhang et al. (2015) (3.83% ± 1.08%).

Interestingly, the isolated cells from liver and kidney presented greater uptake of DAPI than those from ovary. It could be that the cells that I isolated were multinucleated and in a state of cellular senescence. Hepatocytes are binucleated, and cell polyploidy has been

found in the liver as a sign of terminal differentiation and cell death (Gupta, 2000). In kidney, multinucleated cells can be found in the podocytes of the glomerulus (Nagata et al., 1995). It is possible that some nuclei in these cell types were undergoing degradation and so absorbed more DAPI.

On the other hand the growth of kidney and liver cells require specific serum-free and growth factors-free formulations, and a preference for seeding onto coated flasks (Shen et al., 2012; Valente et al., 2011). Cell culture loss was therefore expected.

6.3.2 Oviductal epithelium staining with the DDX4^{C25} antibody

The oviductal epithelium of adult mice stained positive with the DDX4^{C25} antibody, consistent with a previous study (Hashimoto et al., 2008). However, *Ddx4* expression was observed to be absent. The staining here was in the cytoplasm, not the cell surface, and so I did not attempt FACS-sorting similar to ovarian cells.

Cells in the oviductal epithelia are the origin of the serous epithelial ovarian carcinoma, the most lethal of all ovarian cancers in women (Auersperg et al., 2001). They have been reported to be epithelial stem cells that express *Lgr5* in their cytoplasm (Capel, 2014; Ng et al., 2014) but little more is known about them. The affinity of the oviductal epithelium for this DDX4^{C25} antibody could be of use to detect and isolate cells prone to mutate and give rise to these ovarian carcinomas. However, the absence of bands for this tissue after Western blotting suggests that no particular epitope is involved in the binding under immunohistochemical procedures.

6.3.3 The DDX4^{C25} antibody is non-specific and binds to an unknown epitope(s)

A shared characteristic of DDX4^{C25}-positive cells observed in the oviductal epithelium and in FACS-sorted populations from mouse ovary, kidney and liver is that they did not express *Ddx4* (Hernandez et al., 2015; Yuan et al., 2013; Zhang et al., 2012b; Zhang et al., 2015). The absence of DDX4 was further proved when my oviductal epithelium sections and my freshly sorted ovarian cells isolated by means of the DDX4^{C25} antibody stained negative for a second DDX4^{351} antibody that was raised against a larger epitope of the C-terminal DDX4. This was in line with a recent report where a further independent monoclonal mouse antibody to DDX4 could not detect freshly sorted DDX4^{C25}-positive ovarian cells (Hernandez et al., 2015).

My observations strongly suggest that the DDX4^{C25} antibody is isolating cells through binding a non-related epitope on the cell surface of some ovarian cells, as has been suggested by many (Hernandez et al., 2015; Telfer and Albertini, 2012; Zhang et al., 2015). Concerns over irregular antibody design and synthesis have also been proposed (Albertini and Gleicher, 2015) but not tested.

6.3.4 DDX4^{C25}-positive cells in the ovarian cortex are primary oocytes

Those groups that support the existence of adult germ stem cells consider the ovarian surface epithelium as the anatomical reservoir of these cells (Grieve et al., 2015; Hanna and Hennebold, 2014; Johnson et al., 2004; Pacchiarotti et al., 2010; Woods and Tilly, 2012; Zou et al., 2009). Some reports have given evidence of this existence though localisation of DDX4^{C25}-positive cells in histological preparations of the murine ovarian cortex (Johnson et al., 2004; Pacchiarotti et al., 2010; Zou et al., 2009).

I too could observe DDX4^{C25}-positive cells in my histological preparations (see Section 6.2.3). They were around 10 µm long, consistent with the reported size of the putative OSCs (White et al., 2012; Zou et al., 2009). However, upon closer observation, it was clear that these cells were primordial follicles, consisting of oocytes enclosed by a single layer of half moon-shaped granulosa cells, which are known to locate in the outer layers of the ovary (Fortune, 2003; Peters, 1969).

6.3.5 DDX4 presents post-transcriptional modifications

More than one protein band for DDX4^{C25} were observed in ovary and testis during Western blotting: two strong bands ~55 and ~68 kD and a weaker band at ~58 kD specific of testis. These did not agree with the expected 76 kDa band size nor the secondary band at 28 kDa found in testis (www.abcam.com/ddx4--mvh-antibody-ab13840.html), and whose identity is unknown, which could be taken as a proof of post-transcriptional modifications in DDX4.

Ovarian post-translational modifications in DDX4 have not been characterised, but they are indispensable in testis for the interaction with SUMO1, PIWI, MIWI and TUDOR proteins to activate the meiotic onset and spermatogenesis progression (Kirino et al., 2010; Xiao et al., 2016; Zhang et al., 2008). It could be that the bands observed in my ovarian and testicular samples are post-translational modifications of the murine DDX4 required to perform the same or different function in both sexes. It could also be that the weak ~58 kD

band in testis is specific of spermatogenesis, and may be occurring in the C-terminal domain. Murine proteins truncated in their C-terminal epitope cannot interact with Dicer^{S} in the chromatoid body of round spermatids (Kotaja et al., 2006). Hence it may be that the C-terminus requires some post-translational modification to bind Dicer^{S} and perform essential functions only in certain cell types and moments during spermatogenesis.

In summary, in this Chapter 6 I have concluded that it is highly likely that the DDX4^{C25} antibody binds to an unknown reactive epitope(s) on the cell surface and cytoplasm of non-germline tissues when exposed to a variety of staining conditions. Furthermore, by using a second antibody to a larger C-terminal DDX4 epitope I have reinforced the conclusion that DDX4^{C25}-positive ovarian are not actually isolated by DDX4 nor they express the protein.

Given that the DDX4^{C25}-positive ovarian cells can establish a partial germline expression possibly as a product of continued culture, in the next Chapter I will culture them with meiotic enhancers to further characterise their transformation potential.

Chapter 7

Meiotic induction of DDX4^{C25}-positive ovarian cells

7.1 Introduction

Cells isolated from the ovary by live-cell sorting methods using the germ cell marker DDX4 have been reported to express meiotic markers and produce oocyte-like cells when cultured (White et al., 2012; Zou et al., 2009). According to Park et al. (2013), this oogenesis can be accelerated with the addition of BMP4 to the cell culture medium.

BMP4 is required for the early differentiation of ESCs into PGCs (Lawson et al., 1999), whereas retinoic acid (RA) has been described as the key activator of meiosis and oogenesis in mice (Anderson et al., 2008). Interestingly, the effect of RA in DDX4^{C25}-positive ovarian cells has not yet been characterised in any study.

Previously in this thesis, I concluded that ovarian cells that had been isolated by FACS using a DDX4^{C25} antibody did not belong to the germline. Despite this they acquired some germline characteristics in culture, but they did not enter into meiosis or produce oocytes. One explanation for these observations is that the enriched cell culture medium had reprogrammed these cells to express some germline markers, but importantly, not those required to differentiate into PGCs.

In this Chapter, isolated FACS-positive fractions were co-cultured *in vitro* with BMP4 and RA to evaluate if a complete PGC-like genetic profile could be activated, and meiosis and oogenesis achieved.

7.2 Results

7.2.1 Morphology of the DDX4^{C25}-positive cells after supplementation with BMP4 and RA

Oogenesis in *in vitro* cultured DDX4^{C25}-positive ovarian cells has been reported to peak for 48 hours after each passage spontaneously at 4 months post-sorting (White et al., 2012), and at passages 32–38 with the aid of exogenous BMP4 (Park et al., 2013). However, this could be a long-term reprogramming effect of the *in vitro* cell culturing, and

not an inner ability of the cells to enter into meiosis, as was previously observed in my cell cultures (see Section 5.2.6).

To test whether my DDX4^{C25}-positive cells had acquired a partial germline profile by means of a conditioned cell culture medium, freshly sorted FACS-positive fractions were split into two and cultured in two different media: a basic culture medium with only foetal bovine serum as supplement (control medium, CM from here onwards) and a growth factor-supplemented cell culture medium (Woods and Tilly, 2013b) (OSC medium, OSCM from here onwards) (Fig. 7.1).

In order to evaluate if meiotic commitment was innate or acquired in time though the feeding, cells growing in CM and OSCM were probed for meiotic and oocyte markers at early (passage 3, approximately one month post-sorting) and later stages (passage 10, approximately 4 months post-sorting) (Fig. 7.1).

I also wanted to measure the effect of meiotic supplements on these DDX4^{C25}-positive cells, on their own or when combined. For this reason CM and OSCM cells at passages 3 and 10 were split into wells that were individually conditioned with one of the following culture mediums (Fig. 7.1):

- 100 ng/ml of BMP4 for 48 hours (Park et al., 2013),
- 600 µg/ml of all-trans RA for 48 hours (Bahmanpour et al., 2015; Park et al., 2013),
- Combined 100 ng/ml of BMP4 and 600 µg/ml of all-trans RA for 48 hours,
- 5 days in 100 ng/ml of BMP4, then 15 days in 600 µg/ml of all-trans RA (Bahmanpour et al., 2015).

Around 250–300 floating medium-to-large oocyte-like cells per well have been reported within the first 16 hours post-treatment (Park et al., 2013). However, I could not observe any floating cell larger than 10 µm neither at passage 3 nor at passage 10, even at the end of the experiment, for any conditioned cell culture (Fig. 7.2A, B, C, D, E).

Interestingly, my DDX4^{C25}-positive cell cultures developed into compact colonies with oval cells that maintained a high nucleus:cytoplasm ratio (Fig. 7.2A, B, C, D, E). This cell morphology was contrary to what I previously observed (see Section 5.2.1) but similar to White et al. (2012). Only in those sequentially conditioned for BMP4 and then RA did the cells reach confluence (Fig. 7.2E), but this is likely due only to a longer time in culture rather than a greater proliferation.

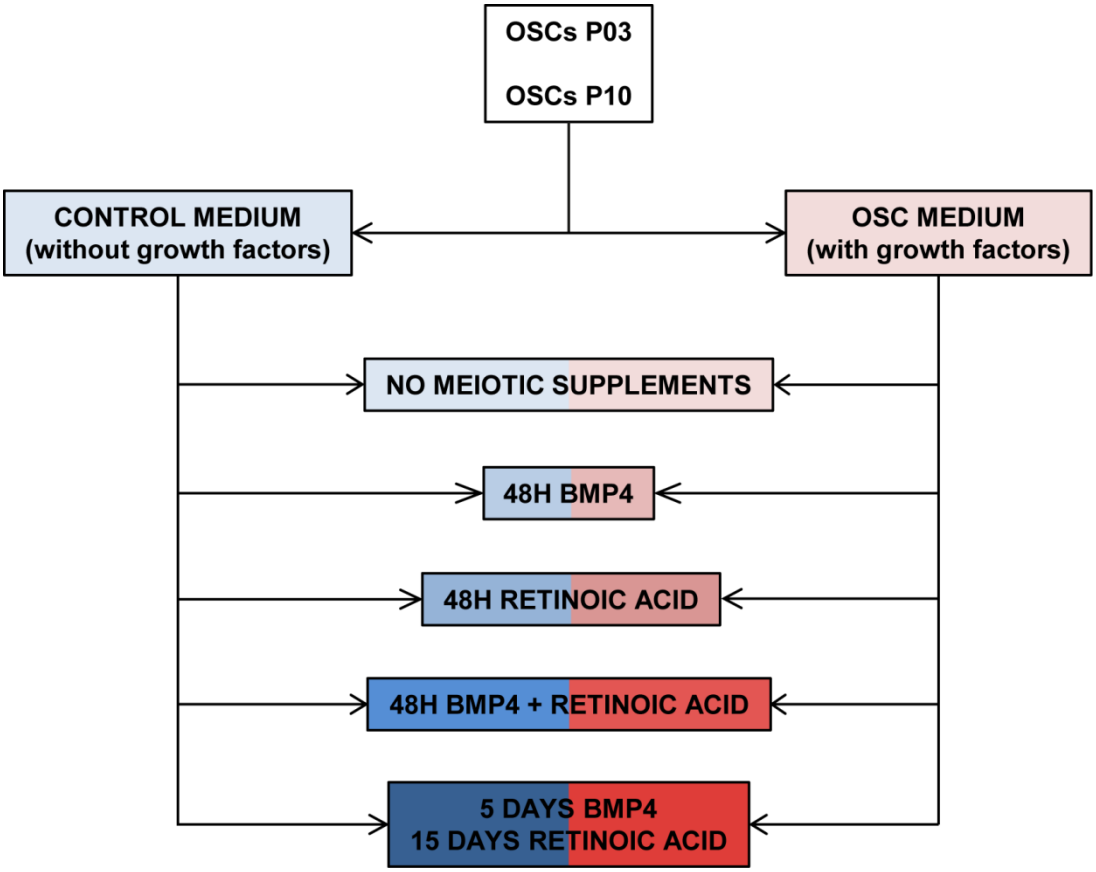

Figure 7.1. Evaluation of the meiotic ability of DDX4^{C25}-positive cells. DDX4^{C25}-positive cells were initially seeded into CM and OSCM culture media. At passage 3 and 10, the cell cultures were split into five wells and supplemented for 48 hours or 20 days with the meiotic enhancers BMP4, RA or a combination of both. N = 3 independent FACS sortings.

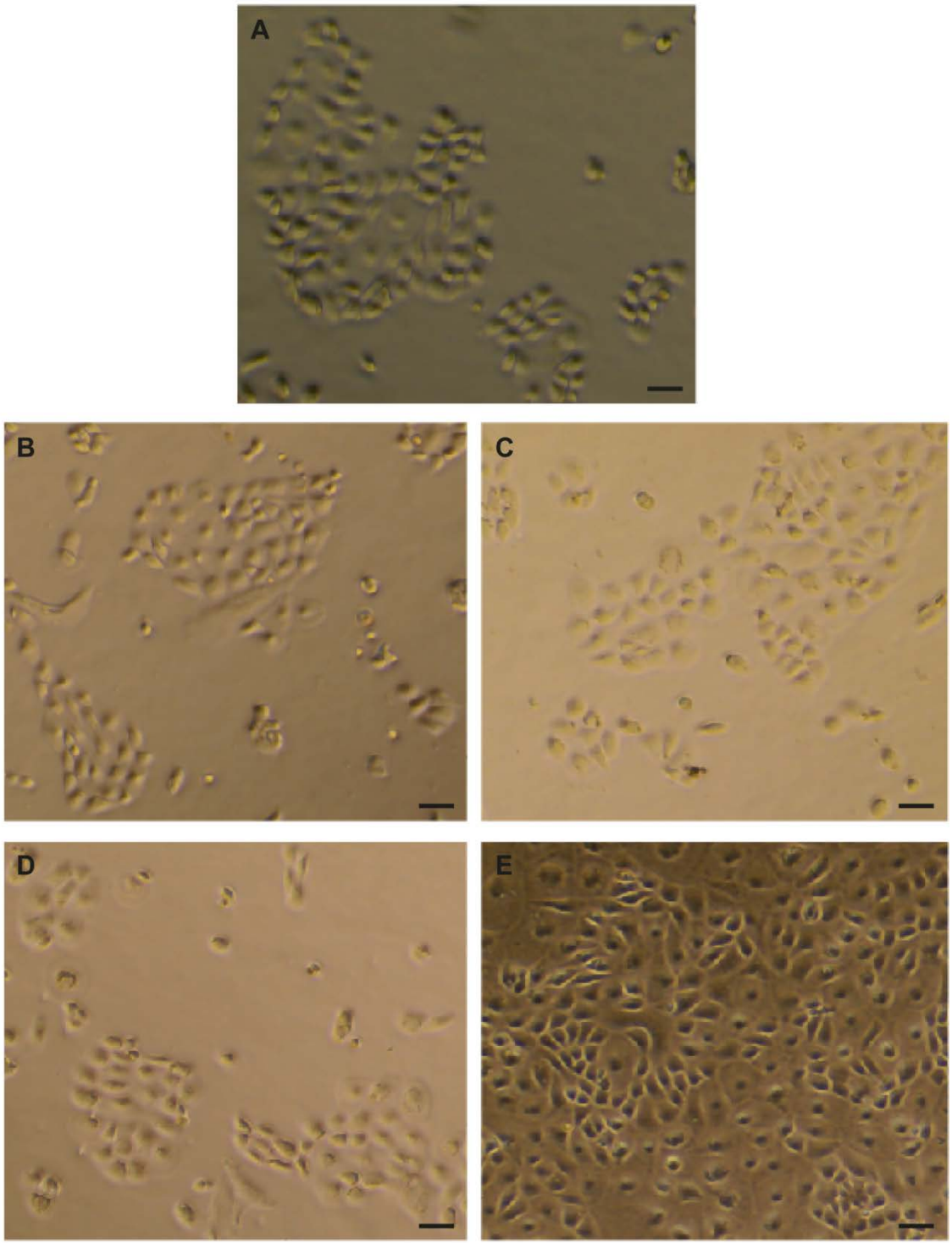

Figure 7.2. Growth of DDX4^{C25}-positive cells in OSCM. DDX4^{C25}-positive cell colonies at Passage 10 post-FACS isolation in **(A)** OSCM and OSCM conditioned with **(B)** BMP4, **(C)** RA, **(D)** a combination of both for 48 hours or **(E)** for 20 days. Scale bar: 50 µm. N = 3 independent cell cultures.

DDX4^{C25}-positive cell numbers growing in basic medium declined, and cells died shortly after passage 4. However those growing in OSC medium proliferated beyond passage 10. Therefore here I could observe the first evidence of medium-based conditioning of these cells. It is possible that those growth factors in the OSC medium had helped to develop some pluripotency ability in these cells.

7.2.2 Expression of receptors for BMP4 and RA in DDX4^{C25}-positive cells

It is important to know if DDX4^{C25}-positive cells in culture express the required receptors to bind either BMP4 or RA. DDX4^{C25}-positive cells at passage 32 - 38 have been reported to express the transmembrane receptors BMPR1A/ALK3, BMPR1B/ALK6 and BMPR2, which allows them to respond to exogenous BMP4 (Park et al., 2013). RA during meiosis activation on the other hand has been reported to bind to nuclear receptors RARα and RARγ (Gely-Pernot et al., 2012).

Ovary and testis were used initially to determine their usefulness as positive controls for mRNA to *Bmpr1a*, *Bmpr1b*, *Bmpr2*, *Raraα2*, *Rarγ1* and *Rarγ2*. However, of these isoforms, *Bmpr1b* and *Rarγ1* could not be found in either tissue, and therefore were removed from further analysis.

DDX4^{C25}-positive cells that had been cultured in CM or OSCM were interrogated for expression of *Bmpr1a*, *Bmpr2*, *Raraα2* and *Rarγ2* at passages 3 and 10 (Table 7.1A, B). Ovary, testis and skin explant were used as positive controls for the presence of germline cells. No negative controls could be included since these receptors are ubiquitous in *in vivo* tissues (Germain et al., 2006).

As expected, ovary and testis expressed all four transmembrane receptors (Fig. 7.3, Table 7.1A, B). Furthermore, fibroblasts from the skin were expressing all markers but *Rarγ2* (Fig. 7.3, Table 7.1A, B).

Cells at passage 3 that had been cultured with CM did not express or lost expression for all receptors (Fig. 7.3, Table 7.1A). This was also observed in cells with OSCM, except for one cell line that expressed *Bmpr1a*, *Bmpr2* and *Rarγ2* (Fig. 7.3, Table 7.1A). At passage 10, these same cell lines in OSCM all expressed *Bmpr2*, with *Bmpr1a* present in one line (Table 7.1B), and no evidence for *Raraα2* or *Rarγ2* (Table 7.1B).

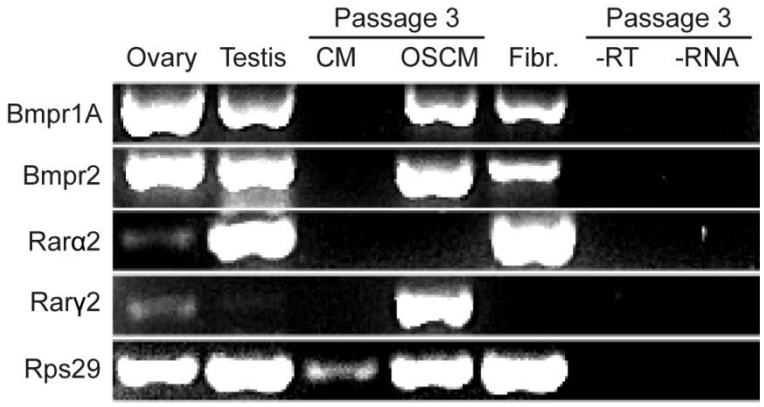

Figure 7.3. Expression of BMP4- and RA-binding receptors in DDX4^{C25}-positive cells. Expression of receptors for the recognition of BMP4 and RA in DDX4^{C25}-positive cells cultured in CM and OSCM at passage 3.

A

RECEPTOR / SAMPLE	*Bmpr1A*	*Bmpr2*	*Rarα2*	*Rarγ2*
OVARY	■	■	■	■
TESTIS	■	■	■	■
CM				
OSCM				
	■	■		■
SKIN	■	■	■	
	■	■		

B

RECEPTOR / SAMPLE	*Bmpr1A*	*Bmpr2*	*Rarα2*	*Rarγ2*
OVARY	■	■	■	■
	■	■	■	
TESTIS	■	■	■	■
	■	■		
OSCM	■	■		
		■		
		■		
SKIN	■	■	■	
	■	■		

Table 7.1. Summary of the expression of BMP4- and RA-binding receptors in DDX4^{C25}-positive cells. (A, B) DDX4^{C25}-positive cells cultured in CM and OSCM were interrogated at **(A)** passage 3 and **(B)** passage 10 for the expression of receptors that would bind to BMP4 or RA. N = 3 independent FACS sortings. Each cell line or tissue explant is represented as a row of coloured boxes, with grey meaning activation of a gene of interest and white meaning absence of activation.

Based on these findings, cells growing on CM would unlikely respond to BMP4 and RA because they were not expressing the required receptors. Cells cultured with OSCM may initially respond to both meiotic enhancers, but in long-term culture may lose the ability to respond to RA, which in turn could compromise the RA-dependent meiotic pathway, if active.

7.2.3 Gene expression analysis of germline markers in DDX4^{C25}-positive cells at passage 3

Here a gene expression analysis was performed on DDX4^{C25}-positive cells after the addition of BMP4 and RA, in order to determine if at the level of mRNA they were expressing any germline markers and more importantly if they had entered into meiosis.

Germline markers (*Dppa3*, *Ddx4*, *Dazl*), pluripotency markers (*Pou5f1*/*Oct4*; *Lin28A*, lin-28 homolog A), meiosis markers (*Stra8*; *Meioc*, meiosis-specific with coiled-coil domain; *Rec8*; *Meiob*, meiosis specific with OB domains; *Sycp3*; *Ybx2*/*Msy2*) and oocyte markers (*Sohlh2*, spermatogenesis and oogenesis specific basic helix-loop-helix 2; *Nobox*, *H1foo*, H1 histone family, member O, oocyte-specific; *Figla/Figα*, folliculogenesis specific basic helix-loop-helix; *Zp3*) were used. *Rps29* was used as a positive control for each cDNA preparation (de Jonge et al., 2007).

Ovary was used as a positive control for all of the germline, pluripotency and oocyte markers, as well as meiotic markers with the exception of *Stra8* and *Meioc*. Testis was used as a positive control for all of the germline, pluripotency, and meiosis markers, and as a negative control for oocyte markers with the exception of *Sohlh2*. Fibroblasts from skin explants were used as a negative control for all markers, with the exception of the housekeeping gene *Rps29*.

As expected, ovary and testis contained all the germline markers (Table 7.2, in yellow), as well as the pluripotency markers *Pou5f1* and *Lin28A* (Table 7.2, in orange), the meiosis markers *Rec8*, *Meiob*, *Sycp3* and *Ybx2* (Table 7.2, in purple) and the gamete-specific *Sohlh2* and *Figα* (Table 7.2, in green). *Figα* is responsible for the activation of the zona pellucida genes, although it is expressed in testes at lesser levels, with an unknown function (Liang et al., 1997). The oocyte-specific markers *Zp3* and *Nobox* could only be detected in ovaries (Table 7.2, in green), and as expected they were absent from the testis (Table 7.2, in green). *H1foo* is a well-conserved oocyte-specific linker histone that drives the epigenetic regulation of oogenesis and meiotic maturation (Hayakawa et al., 2012) and

that could be responsible of decondensing the sperm chromatin after fertilisation (Mizusawa et al., 2010). Despite *H1foo* being reported in GV and MII oocytes only, it was detected in one of the three testis explants studied here (Table 7.2, in green).

The meiosis markers *Stra8* and *Meioc* were present in testis (Table 7.2, in purple), but not ovaries (Table 7.2, in purple). MEIOC is a key component of the onset of meiosis, where it stabilizes meiotic transcripts in a RA-independent manner and prior to the activation of *Stra8* and *Rec8* (Abby et al., 2016). Therefore, it would be predicted to be absent from the adult ovary, which already contains meiosis-committed immature oocytes.

As expected, fibroblasts from skin explants were negative for the expression of germline, pluripotency, meiosis and oocyte markers (Table 7.2). Only on one occasion was low level expression of *Pou5f1* seen (Table 7.2, in orange). This may be expected given that this tissue contains pluripotent cells (http://www.proteinatlas.org/ENSG00000204531-POU5F1/tissue).

The analysis of $DDX4^{C25}$-positive cells cultured in CM suggests that none of the five cell culture conditions achieved a complete activation of germline, pluripotency, meiosis and oocyte markers (Table 7.2). The 'CM + BMP4' group showed some promising results, with *Dppa3*, *Dazl* and *Ddx4* activated in two of the cell lines studied (Table 7.2, in yellow). However, the 'CM + RA', 'CM + BMP4 + RA 48H' and 'CM + BMP4 5D + RA 15D' gave either weak or no activation at all (Table 7.2, in yellow). Cells cultured in CM had, therefore, not transformed into germ stem cells, and importantly, did not express *Dazl*, which is a prerequisite for the onset of meiosis. On the other hand, those cell lines in the 'CM' and 'CM + RA' groups had all activated the pluripotency marker *Pou5f1* (Table 7.2, in orange). However, none of the five diversified CM cultures presented the pluripotency marker *Lin28A* (Table 7.2, in orange). LIN28A is essential in the PGC differentiation and maintenance up to the onset of meiosis (Childs et al., 2012; West et al., 2009).

It is therefore not surprising that none of the CM cell cultures had activated any of the key activators of meiosis, that is, *Stra8*, *Rec8* and *Meioc*, or the meiotic recombination marker *Meiob* (Table 7.2, in purple). MEIOB ensures the proper maintenance of recombinases RAD51 and DMC1, and is indispensable for the homologous recombination and DNA double-strand break repair during prophase I of meiosis (Souquet et al., 2013). Although meiosis recombination was not taking place, it was surprising to observe activation of the synaptonemal component *Sycp3* in all lines in 'CM' and 'CM + RA' groups, whereas *Ybx2* activation was present in at least one line in 'CM', 'CM + BMP4'

and ‘CM + RA’ groups (Table 7.2, in purple). This could indicate that some characteristics of a meiotic cell were active. However, the absence of oocyte-specific markers *Sohlh2*, *Nobox*, *Figα* and *H1foo* confirmed that no oogenesis had taken place (Table 7.2, in green). Surprisingly, *Zp3* was heavily expressed in the “CM + RA” group (Table 7.2, in green).

Similarly, DDX4^{C25}-positive cells cultured in OSCM had not transformed into germ stem cells or oocyte-like cells (Table 7.2). *Dppa3* was expressed in all groups, importantly, in the same second cell line (Table 7.2, in yellow), which suggests that this activation had taken place earlier before the meiotic induction with BMP4 and RA. *Ddx4* was present in ‘OSCM’ and ‘OSCM + BMP4 5D + RA 15D’ groups (Table 7.2, in yellow), whereas *Dazl* was absent (Table 7.2, in yellow). Cells growing in OSCM had activated *Pou5f1* (Table 7.2, in orange) in a few cell lines but, importantly, the suggested pluripotency was not germline-specific, given the absence of *Lin28A* (Table 7.2, in orange).

As expected, the vast majority of the OSCM cell cultures were not expressing the meiotic-specific markers *Stra8*, *Rec8*, *Meioc* and *Meiob* (Table 7.2, in purple). The only exception was one cell line expressing *Rec8* (Table 7.2, in purple). Here again expression of the synaptonemal component *Sycp3* and *Ybx2* was recorded. Whereas *Sycp3* was always observed in the second cell line in all but ‘OSCM + BMP4 + RA 48H’ group (Table 7.2, in purple), *Ybx2* briefly expressed in two different cell lines in ‘OSCM’ and ‘OSCM + RA’ groups (Table 7.2, in purple).

The absence of oocyte-specific markers *Sohlh2*, *Nobox*, *Figα* and *H1foo* confirmed that no oogenesis had taken place in OSCM. Expression of *Zp3* was observed in all groups, which could explain the presence of small cells surrounded by a thick membrane in Section 5.2.1.

In summary, the DDX4^{C25}-positive ovarian cells had not developed into germline in these early stages of cell culture and supplementation with BMP4 and RA had not helped accelerating the process.

7.2.4 Gene expression analysis of germline markers in DDX4^{C25}-positive cells at passage 10

Despite the fact that DDX4^{C25}-positive cells had not transformed into germ stem cells at early stages after isolation, it could be that they needed more time in culture. I therefore performed the same experiment as in Section 7.3.4, this time at passage 10. Only cells in

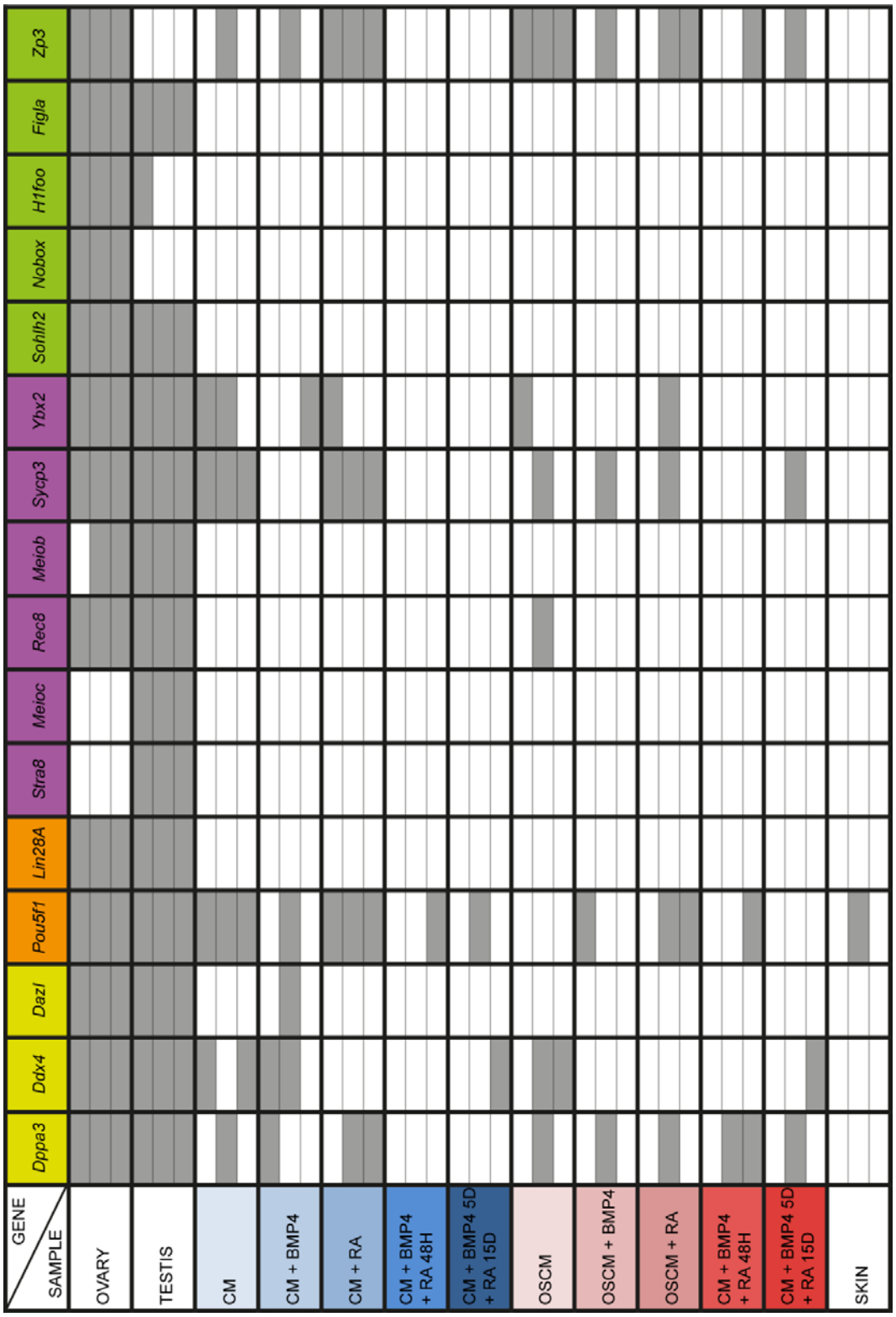

Table 7.2. Analysis of DDX4^{C25}-positive cells at Passage 3. Expression of germline, pluripotency, meiosis and oocyte markers in DDX4^{C25}-positive ovarian cells in the presence of CM and OSCM mediums supplemented with BMP4 or RA. N = 3 independent FACS sortings. Each cell line or tissue explant is represented as a row of coloured boxes, with grey meaning activation of a gene of interest and white meaning absence of activation.

OSCM were viable at this stage; cells in CM had enter into senescence shortly after passage 4, without further observation that the cells had transformed into oocyte-like cells.

I again examined for germline markers (*Dppa3*, *Ddx4*, *Dazl*), pluripotency markers (*Pou5f1*/*Oct4*; *Lin28A*), meiosis markers (*Stra8*; *Meioc*, *Rec8*; *Meiob*, *Sycp3*; *Ybx2*/*Msy2*) and oocyte markers (*Sohlh2*, *Nobox*, *H1foo*, *Figla/Figα*, *Zp3*). Ovary was used as a positive control for all of the germline, pluripotency and oocyte markers, as well as meiotic markers with the exception of *Stra8* and *Meioc*. Testis was used as a positive control for all of the germline, pluripotency, and meiosis markers, and as a negative control for oocyte markers with the exception of *Sohlh2*. Fibroblasts from skin explants were used as a negative control for all markers, with the exception of the housekeeping gene *Rps29*.

In passage 10 DDX4^{C25}-positive cells cultured in OSCM expression profiles were similar to the results in passage 3. *Dppa3* was expressed in all groups, and importantly in most of the cell lines (Table 7.3, in yellow). This could be considered promising for the development of a germline identity. However, neither *Ddx4* nor *Dazl* were present (Table 7.3, in yellow), and any previous expression observed at Passage 3 (‘OSCM’ , ‘OSCM + BMP4’, ‘OSCM + RA’, ‘OSCM + BMP4 + RA 48 H’, ‘OSCM + BMP4 5D + RA 15D’ had been lost. *Pou5f1* had also increased its presence, and was now expressed in almost all cell lines and groups (Table 7.3, in orange). Importantly, *Lin28A* was observed in a cell line in ‘OSCM + BMP4’ (Table 7.3, in orange), which suggested that some cells here would be able to activate a PGC-like differentiation should the supplementation continue.

None of the OSCM cell cultures were able to enter meiosis, given the absence of *Stra8*, *Rec8*, *Meioc* and *Meiob* (Table 7.3, in purple). However, *Sycp3* and *Ybx2* were randomly expressed in all OSCM groups and cell lines (Table 7.3, in purple), but this was not accompanied by expression of oocyte-specific markers *Sohlh2*, *Nobox*, *Figα*, *H1foo* and *Zp3* (Table 7.3, in green). Expression of this later gene had been completely lost compared to the profile in passage 3.

7.3 Discussion

This study has shown that a population of DDX4^{C25}-positive cells isolated from mouse ovaries, which were not GSCs in origin, acquire a partial germline profile in culture regardless of the supplementation of the cell culture medium with growth factors or meiotic enhancers – BMP4 and RA. This is the first study of the effects of BMP4 and RA in inducing oogenesis in early and middle passages of DDX4^{C25}-positive ovarian cells.

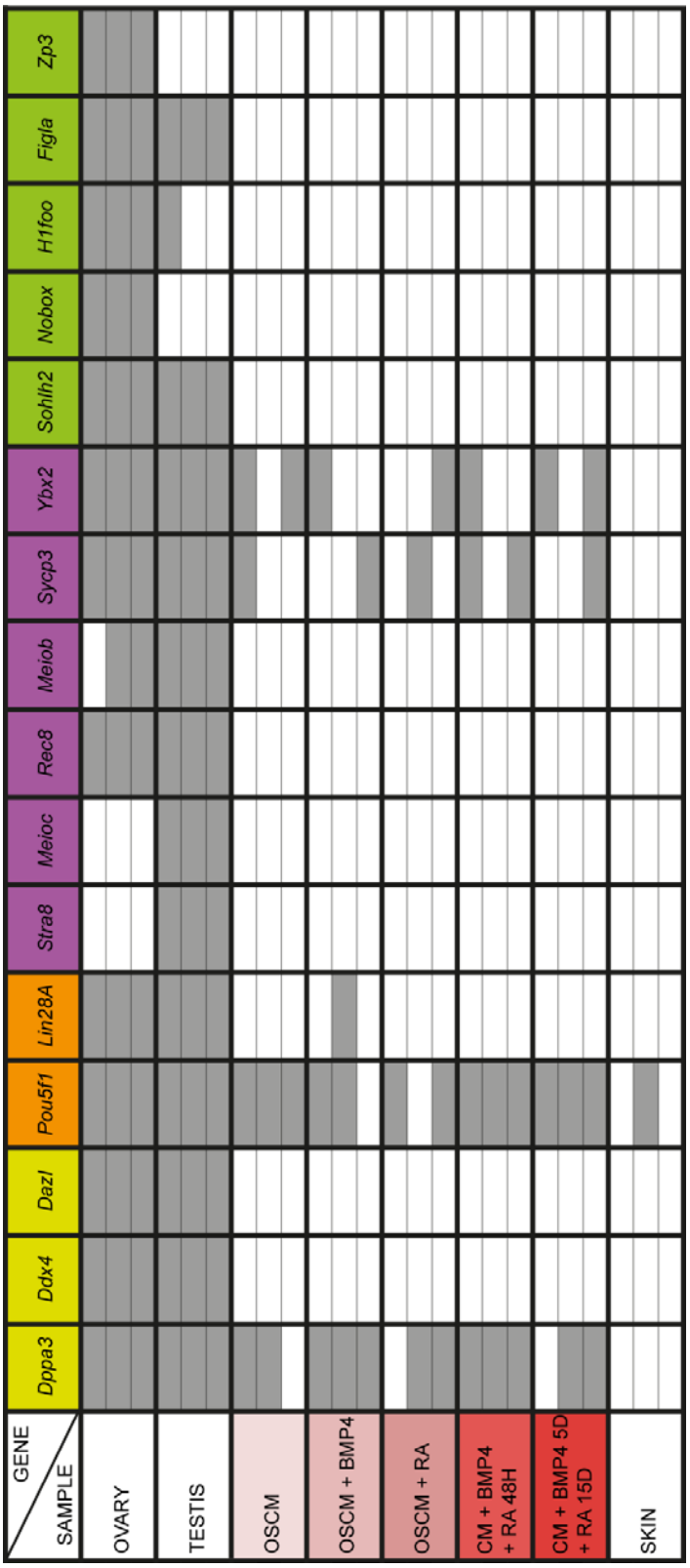

Table 7.3. Analysis of DDX4^{C25}-positive cells at passage 10. Expression of germline, pluripotency, meiosis and oocyte markers in DDX4^{C25}-positive ovarian cells cultured in OSC medium supplemented with BMP4 or RA. N = 3 independent FACS sortings. Each cell line or tissue explant is represented as a row of coloured boxes, with grey meaning activation of a gene of interest and white meaning absence of activation.

Furthermore, this is also the first time that these DDX4^{C25}-positive ovarian cells are cultured in basic cell culture medium without additional supplements to evaluate the potential effect that the cell culture media have over the suspected transformation of these cells.

Although the cells expressed some oocyte-specific markers early in culture, given the absence of *Stra8*, *Rec8*, *Meioc* and *Meiob* they would likely be unable to enter meiosis. They did have a partial germline profile, with expression in some lines of *Dppa3*, *Ddx4* and *Zp3*, but these were absent with further culture. My results suggest that cultured DDX4^{C25}-positive ovarian cells do not have the tendency to directly develop into germ stem cells. Their expression of a chaotic germline profile is promising but would require extensive research to learn how to direct it effectively.

7.3.1 DDX4^{C25}-positive cells have the ability to bind BMP4

Addition of BMP4 has been reported to enhance the formation of oocyte-like cells in DDX4^{C25}-positive ovarian cell cultures in a dose-dependent manner (Park et al., 2013). In that study cells at passage 32-38 were expressing *Bmpr1A*, *Bmpr1B* and *Bmpr2*. Such extended cell culture could have reprogrammed the cells and be the result of supplemented growth factors. Here only *Bmpr1A* and *Bmpr2* were expressed at passage 3 and 10, and only in cells growing in supplemented cell culture medium, not in basic medium.

The fact that *Bmpr1A* and *Bmpr2* are not specific markers for pre-meiotic cells was observed in this Chapter where both were expressed in skin explants. Actually, BMPR1A (http://www.proteinatlas.org/ENSG00000107779-BMPR1A/tissue) and BMPR2 (http://www.proteinatlas.org/ENSG00000204217-BMPR2/tissue) are ubiquitous in human adult tissues. Therefore, expression of *Bmpr1A* and *Bmpr2* in itself conveys no message of meiotic induction via BMP4; cells bind BMP4 for other signalling pathways.

7.3.2 DDX4^{C25}-positive cells and Retinoic Acid receptors

A very recent study has reported that human DDX4^{C25}-positive ovarian cells growing in medium supplemented with RA expressed *RARα* and increased their meiotic activation and oocyte development (Ding et al., 2016). However, these DDX4^{C25}-positive ovarian cells were not FACS-sorted, but MACS-sorted cells from human follicular aspirates. In my experiments, *Rarα2* and *Rarγ2* were not present, and therefore my DDX4^{C25}-positive cells would lack the necessary receptors to bind RA and activate meiosis.

Rarα and *γ* have important and redundant roles in GSC proliferation and differentiation in the testis (Gely-Pernot et al., 2012; Ikami et al., 2015; Kashyap et al., 2013; Law, 2013; Li et al., 1993; Lohnes et al., 1993; Lufkin et al., 1993). However, they modulate adult tissue homeostasis (Kastner et al., 1990; Zelent et al., 1989), and both *Rarα* and *Rarγ* gene expression distribution is ubiquitous in human tissues (see http://www.proteinatlas.org/ENSG00000131759-RARA/tissue for *RARα* and http://www.proteinatlas.org/ENSG00000172819-RARG/tissue for *RARγ*).

Critically, expression of *Rarα* and *Rarγ* were not specific to the germline and onset of meiosis in these DDX4^{C25}-positive ovarian cells, since their expression could be observed in the ovary and in skin explants; the latter only in the case of *Rarα* isoform 2. It could be that *Rarγ* isoform 2 is not abundantly expressed in the skin, or that its expression is not active or very low at the time that the tissue is collected.

7.3.3 DDX4^{C25}-positive cells express an incomplete germline profile regardless of the culture medium

Some groups have reported that DDX4^{C25}-positive ovarian cells broaden their early germline identity with the activation of meiosis and oogenesis (Ding et al., 2016; Grieve et al., 2014; Park et al., 2013; White et al., 2012; Zhang and Wu, 2016; Zhang et al., 2011; Zou et al., 2009). However, one study has suggested that these ovarian cells are not germline in origin, and that culture has some effect on the ability of the cells to self-reprogram (Hernandez et al., 2015).

In my experiments, I did not observe a specific type of culture medium leading to the highest germline reprogramming in cultured DDX4^{C25} positive cells following FACS. Activation of *Dppa3*, *Ddx4*, *Pou5f1*, *Sycp3*, *Ybx2* and *Zp3*, were generally observed at early passage, independent of BMP4 or RA. However, although *Ddx4* and *Zp3* appeared absent at later passage, *Dppa3*, *Pou5f1*, *Sycp3* and *Ybx2* increased their likelihood of expression in all cultures.

Dppa3 and *Ddx4* expression have been observed specifically in GSCs of both sexes and in oocytes (Fujiwara et al., 1994; Sato et al., 2002), although they are dispensable for oogenesis (Bortvin et al., 2004; Tanaka et al., 2000). On the other hand, female knockout mice for *Sycp3* and *Ybx2* are infertile, since the oocytes cannot progress beyond meiosis I (Yang et al., 2005; Yuan et al., 2000; Yuan et al., 2002). *Zp3* on the other hand is indispensable for the fertilisation of the oocyte (for a review see Dean, 2002). The

activation of these five germline-, meiosis- and oocyte-specific markers was promising and suggests at least some germline differentiation and meiotic entry had taken place.

However, my cell lines lacked activation of *Dazl,* an essential component of *Stra8*- and *Rec8*-dependent meiosis induction (Koubova et al., 2014; Soh et al., 2015). Despite three different routes for the onset of meiosis were interrogated – *Stra8, Rec8* and *Meioc* (Abby et al., 2016; Koubova et al., 2014) – without evidence of expression.

In conclusion, these DDX4^{C25}-positive cultured cells had not differentiated into GSCs or oocytes even under long-term exposure to BMP4 and RA. It is interesting to note that meiosis- and oocyte-specific proteins such as SYCP3 and ZP3 have been observed in the oocytes of *Stra8* knockout female mice (Dokshin et al., 2013), which do not enter into meiosis and are infertile. It could be that certain genes are prone to spontaneous activation *in vivo* and *in vitro*.

7.3.4 DDX4^{C25}-positive cells grow for longer in OSC culture medium

As found in Chapter 5, DDX4^{C25}-positive cells in all CM and OSCM cell lines expressed the pluripotency marker *Pou5f1*. However, improvement in cell survival and growth was observed only in DDX4^{C25}-positive cells fed with supplemented culture medium.

It is possible that this prolonged lifespan is very limited, given the absence of other pluripotency markers such as *Lin28A.* The loss at middle passages of markers that were activated early – *Ddx4, Zp3* – could be an indication of the decline of the DDX4^{C25}-positive cell lines and their near senescence.

In summary, cells isolated using the DDX4^{C25} antibody develop partial germline and meiotic characteristics as a product of continued culture, rather than because of a supplementation to the culture medium. It is highly unlikely that these DDX4^{C25}-positive ovarian cells can achieve complete oogenesis in culture, given the limited features of their stem cell capacity. Further research into how to manipulate their gene expression through the cell culture medium should be required.

This problem may have already been solved by Hikabe et al., (2016), who were able to transform fibroblasts from adult female mice into viable oocytes solely through the exposure of fibroblasts to different cell culture media and supplements.

Chapter 8

General Discussion

OSCs are described as female germline stem cells in the adult mammal ovary (Johnson et al., 2004; White et al., 2012; Zou et al., 2009). They have challenged the dogma of the fixed reserve of oocytes in mammals (Zuckerman, 1951), although their existence is still controversial (Albertini and Gleicher, 2015). At the starting point of this thesis freshly sorted OSCs reportedly expressed germline and pluripotent markers and underwent meiosis and oogenesis *in vitro* and *in vivo* (Imudia et al., 2013; White et al., 2012; Zou et al., 2009). One group claimed to have produced offspring from them (Zhang et al., 2011; Zou et al., 2009). However, only one group had reported that the experiments were not reproducible (Zhang et al., 2012b).

In my studies I did indeed isolate a small population of ovarian cells using the DDX4^{C25} antibody (Fig. 8A) following a protocol by White et al. (2013). This indicates that the antibody was recognising an epitope on the cell surface of these cells, possibly the germline-specific DDX4. However, protein and gene expression analysis showed that these freshly sorted DDX4^{C25}-positive cells were not germline in origin, and did not even express *Ddx4* (Fig. 8A). Interestingly, in culture they acquired some germline-, meiotic- and oocyte-specific markers, although the absence of essential components of meiosis and oogenesis pathways likely prevented these DDX4^{C25}-positive cells from developing into oocytes (Fig. 8A, B). Cell culture media supplementation with meiotic enhancers did not improve this transformation. Finally, although the cells expressed some pluripotency markers (Fig. 8A), they were not immortalised, but died within four months post-isolation. In short, these DDX4^{C25}-positive cells were somatic cells isolated by an unknown epitope and had some degree of germline differentiation *in vitro*, but it was not sufficient to consider them as functional germ stem cells (Fig. 8B).

My work and others have highlighted the difficulty in rationale and practicality of using DDX4^{C25}-positive cells for the differentiation of oocytes in a dish (Hernandez et al., 2015; Zarate-Garcia et al., 2016; Zhang et al., 2012b; Zhang et al., 2015): in my hands it currently appears impossible given the difficulties in isolating and replicating oogenesis. Despite protocols for the sorting and expansion of DDX4^{C25}-positive cells have been published twice (Navaroli et al., 2016; Woods and Tilly, 2013b), efforts should be made in

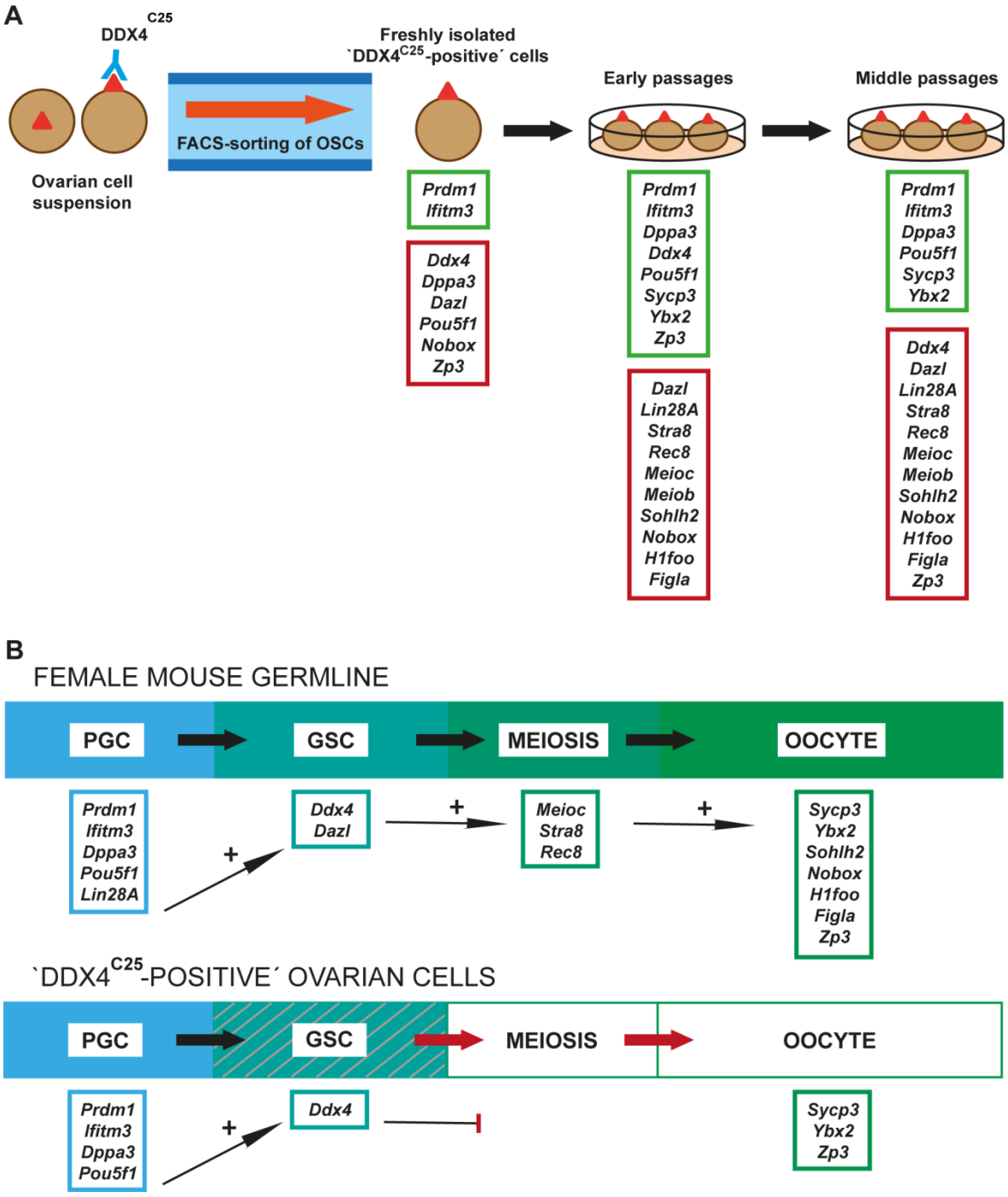

Figure 8. Germline potential of freshly sorted and cultured DDX4^{C25}-positive ovarian cells. (A) Overview of the isolation, culture and expression of germ stem cell, meiosis and oocyte markers in DDX4^{C25}-positive ovarian cells. Markers in green boxes were expressed, whereas markers in red boxes were absent. **(B)** Diagram comparing the development of the female germline from primordial germ cells to oocytes and the truncated differentiation (red arrows) in DDX4^{C25}-positive ovarian cells due to the lack of activation of key germline markers.

providing better access and explanation to the techniques used, and more specifically to the FACS-sorting set up that is the centrepoint of irreproducibility (Woods and Tilly, 2015). Other strategies should involve teaming up labs to perform experiments and compare results, as has been recently done (Zhang et al., 2015), and testing potential explanations that the reproductive biologists have raised for the observed germline potential of these cells (Albertini and Gleicher, 2015; Telfer and Albertini, 2012; Telfer et al., 2005).

A change in the isolation methodology should be agreed given that the current DDX4-based technique is irrational (Hernandez et al., 2015; Zarate-Garcia et al., 2016; Zhang et al., 2015). Similarly, the use of IFITM3-based isolation (Lu et al., 2016; Zhou et al., 2014; Zou et al., 2011) seems retrograde given it is a ubiquitous externalised protein (Brass et al., 2009). *Ddx4* reporter mouse models were poorly engineered and gave unreliable results (Park and Tilly, 2014; Zhang and Wu, 2016). Therefore, the *Ddx4* reporter mouse model should be improved or a new germline-specific marker selected, which requires further research on the expression of cell surface proteins in germ stem cells.

Once the reproducibility is solved, efforts should focus on improving the efficiency of oogenesis of these $DDX4^{C25}$-positive cells. Mature oocyte-like cells were scarce and appeared between 24 hours and 15 days post-meiotic induction (Ding et al., 2016; Park et al., 2013; White et al., 2012), which is shorter than physiological conditions (McGee and Hsueh, 2000). Future studies should elucidate if these cells present coordination between oocyte growth and meiosis progression or are a product of spontaneous activation of oocyte-specific genes, as it has been observed in my cell cultures. Also important would be to evaluate their paracrine and junctional communication ability, which could be acquired through the type of cell culture technique rather than the type of cell differentiated, as Hikabe et al. (2016) have reported after the succesful transformation of adult skin fibroblasts into a few competent oocytes – which should also be subjected to replication. Another big step in the improvement of oocyte differentiation would be to discover the factors provided by perinatal granulosa cells that allow a complete oocyte competency (Hikabe et al., 2016; Nicholas et al., 2009; White et al., 2012). Synthetic synthesis and dose knowledge would make the transforming protocol and replication of results easier.

Lastly, good oocyte quality should lead to good embryo quality. Fertilised oocyte-like cells block mainly during the activation of the embryo metabolism at the preblastocyst stage (White et al., 2012). This points to an insufficiency in the maternally inherited genes, but could also be indicative of a lack of genetic integrity due to aneuploidy and epigenetic imprinting.

Appendix A

Published works contained in this thesis

One publication was used in this thesis. My contributions to this publication is outlined below

Zarate-Garcia, L., Lane, S. I. R., Merriman, J. A., and Jones, K. T. (2016) 'FACS-sorted putative oogonial stem cells from the ovary are neither DDX4-positive nor germ cells', Sci Rep, 6:27991

This publication was published in June 2015 and corresponds to much of the work presented in Chapter 3, 4, 5 and 6 of this thesis. Experiments were planned by K.T.J., S.I.R.L. and L.Z.-G. L.Z.-G. performed all the experiments, statistically analysed the data and made all the figures for the data presented, as well as their corresponding figure legends. L.Z.-G. also contributed by writing the materials and methods, discussing the content of the results and discussion with the other authors of this paper and took part in the proof reading process. All authors contributed to data interpretation. The manuscript was drafted by K.J., with input from all other authors.

Appendix A

Appendix B

Considerations:

- ddH_2O refers to distilled water from a Milli-Q system (Milli-Q, USA) with a resistivity of 18.2 MΩ.cm at 25°C,
- Commercial Hank´s Balance Salt Solution (HBSS) and Dulbecco´s Phosphate Buffered Saline (DPBS) are used without calcium and magnesium,
- The home-made Phosphate Buffered Saline (PBS) contains calcium and magnesium
- Filter sterilising and filtering refer to the solution being pushed through a syringe filter with a pore diameter of 0.2µm (Nalgene/Thermo Fisher Scientific, USA),
- All solutions were prepared under sterile conditions except those described in Section C.5. Sterile conditions refer to the solution being prepared in a Class II cabinet with HEPA-filtered circulating air in a tissue culture laboratory.

B.1. Hormones

B.1.1. PMSG

The PMSG was prepared by dissolving 5000IU of lyophilised PMSG in 1ml of DPBS and mixing it gently to dissolve the hormone. The solution was further diluted in DPBS until obtaining a final concentration of 5IU/0.1ml. The PMSG solution was loaded into 1ml syringes which were frozen at -20°C until just prior to use, when the syringe was fitted with a 27 gauge 1/2 inch hypodermic needle and the hormone was gently warmed to room temperature.

B.1.2. hCG

The hCG was prepared by dissolving 1,500 IU of lyophilised hCG in 5ml of DPBS and mixing it gently to dissolve the hormone. The solution was further diluted in DPBS until obtaining a final concentration of 5IU/0.1ml. The hCG solution was loaded into 1ml syringes which were frozen at -20°C until just prior to use, when the syringe was fitted with a 27 gauge 1/2 inch hypodermic needle and the hormone was gently warmed to room temperature.

B.2. Enzymatic Digestion Solutions

B.2.1 Hyaluronidase

The hyaluronidase was prepared by dissolving lyophilised hyaluronidase type IV-S in 3ml of M2 medium containing 0.4% (wt/vol) BSA and mixing it gently to dissolve the hormone. The solution was further diluted in M2 supplemented with BSA until obtaining a final concentration of 300U/ml. The hyaluronidase solution was filter sterilised, divided into 2ml aliquots and stored in glass tubes then frozen at -20°C until just prior to use, when the enzyme was gently warmed to 37°C in a heat block.

B.2.2 Collagenase

The collagenase was prepared by dissolving lyophilised collagenase CLS 4 in commercial HBSS to a final concentration of 800 IU/ml (units of enzymatic activity specific of each lot). The collagenase solution was divided into 3ml aliquots and stored in 15ml Falcon tubes then frozen at -20°C until just prior to use, when the hormone was gently warmed to 37°C in a water bath.

B.2.3 DNase I

The DNase I was prepared by dissolving lyophilised DNase I in 20mM Tris-EDTA, 1mM $MgCl_2$ and 50% (vol/vol) glycerol in embryo-grade water to a final concentration of 10,000U/ml. The solution was divided into 50µl aliquots and snap-frozen in liquid nitrogen, then stored at -20°C until just prior to use, when the hormone was gently added to collagenase type IV at a 1:1,000 (vol/vol) final ratio.

B.3. Cell Culture Medium Supplements

All supplements were aliquoted and snap-frozen in liquid nitrogen, then stored at -20°C until just prior to use.

B.3.1 Bovine Foetal Growth Factor

Dissolved a vial of bFGF in 1ml embryo-grade water containing 0.1% (wt/vol) BSA to a final concentration of 10µg/ml.

B.3.2 Bone Morphogenetic Growth Factor 4

Dissolved a vial of BMP4 in 1ml embryo-grade water containing 20mM (vol/vol) Acetic Acid to a final concentration of 10µg/ml.

B.3.3 Epidermal Growth Factor

Dissolved a vial of EGF in 1ml embryo-grade water containing 0.1% (wt/vol) BSA to a final concentration of 100µg/ml.

B.3.4 Glial-Derived Neurotrophic Factor

Dissolved a vial of GDNF in 1ml embryo-grade water containing 0.1% (wt/vol) BSA to a final concentration of 10µg/ml.

B.3.5 Mitomycin C

Dissolved a vial of Mitomycin C in DPBS to a final concentration of 1mg/ml.

B.3.6 Retinoic Acid

Dissolved a vial of RA in 5ml DMSO to a final concentration of 10mg/ml.

B.4. Cell Culture Media

All cell culture media were filter sterilised into 15ml Falcon tubes and stored parafilmed in the fridge at 4°C. Cell culture media were warmed in the incubator with the lid loose half an hour before use. Cell culture media were prepared every two weeks.

B.4.1 MEF inactivation medium

DMEM	8,900ml
FBS	1ml
Mitomycin C	100µl

B.4.2 Cryopreservation medium

DMEM	7ml
FBS	2ml
DMSO	1ml

B.5 Buffers and Solutions

B.5.1 X50 TAE

Tris base	242g
Glacial acetic acid	57.1ml
0.5M EDTA	100ml

Dissolved in 600ml ddH_2O and top up to 1l with ddH_2O.

B.5.2 X1 TAE

X50 TAE	40ml
ddH_2O	1,800ml

B.5.3 2% Agarose Gel

X1 TAE	100ml
2% agarose	2g
1:20,000 (vol/vol) GelRed	5µl

Agarose was poured into X1 TAE and the solution was heated in a microwave until complete dissolving. GelRed was then added.

B.5.4 X25 PVP solution

Polyvinylpyrrolidone	2.5g

Dissolved in 10ml ddH_2O

B.5.5 X1 PVP-PBS

X25 PVP	1ml
PBS	24ml

B.5.6 X10 PBS

NaCl	80g
KCl	2g
Na_2HPO_4	14.4g
KH_2PO_4	2.4g

The pH was adjusted to 7.4 with XM HCl and KOH and top up to 1l with ddH_2O.

B.5.7 20% Triton X-100

Triton X-100	200µl
ddH_2O	800µl

B.5.8 1% Triton X-100

Triton X-100	0.1ml
ddH_2O	9.9ml

B.5.9 1% Tween-20

Tween-20	0.1ml
ddH_2O	9.9ml

B.5.10 0.05% Tween-20

1% Tween-20	1µl
ddH_2O	19µl

B.5.11 Oocyte Lysis Buffer

10% Triton X-100	10µl
1M DTT	5µl
Nuclease-free H_2O	985µl

B.5.12 1M NaCl

NaCl	2.922g

Dissolved in 50ml ddH_2O.

B.5.13 0.5M PIPES

PIPES	3.024g

Dissolved in 10ml KOH, pH to 7 and top up to 20ml with ddH_2O.

B.5.14 1M HEPES

HEPES	2.382g

Dissolved in 5ml KOH, pH to 7 and top up to 20ml with ddH_2O.

B.5.15 0.8M HEPES

HEPES	1.906g

Dissolved in 5ml KOH, pH to 7 and top up to 20ml with ddH_2O.

B.5.16 0.1M EGTA

EGTA	0.761g

Dissolved in 10ml KOH, pH to 7 and top up to 20ml with ddH_2O.

B.5.17 X3 PHEM

0.5M PIPES	3.600ml
0.8M HEPES	0.770ml
0.1M EGTA	3.000ml
0.8M $MgCl_2$	0.075ml
ddH_2O	2.555ml

B.5.18 X1 PHEM

X3 PHEM	1ml
ddH_2O	2ml

B.5.19 Tissue Lysis Buffer

ddH_2O	7,800ml
1M HEPES	500µl
20% Triton X-100	500µl
1M NaCl	500µl

P1 enzymatic cocktail	500µl
PIC II phosphatase cocktail inhibitor	100µl
PIC III phosphatase cocktail inhibitor	100µl

B.5.20 0.25M TRIS HCl

TRIZMA base	3g

Dissolved in 80ml ddH_2O, pH to 6.8 using HCl and top up to 100ml with ddH_2O.

B.5.21 TRIS 3M

TRIZMA base	36g

Dissolved in 80ml ddH_2O, pH to 8.8 using HCl and top up to 100ml with ddH_2O.

B.5.22 10% SDS

SDS	0.1g
ddH_2O	10ml

B.5.23 10% APS

APS	0.1g

Dissolved in 10ml ddH_2O, aliquoted into 1ml aliquots and stored at -20°C until use.

B.5.24 10% Acrylamide Resolving Gel

40% acrylamide	2.5ml
TRIS 3M	1.25ml
10% SDS	100µl
10% APS	50µl

ddH_2O	6.9ml
TEMED	10µl

B.5.25 4% Acrylamide Stacker Gel

40% acrylamide	0.5ml
0.25M TRIS HCl	1.875ml
10% SDS	50µl
10% APS	50µl
ddH_2O	7.525ml
TEMED	10µl

B.5.26 X10 Laemmli Buffer

Tris base	30.30g
Glycine	144.00g
SDS	10g
ddH_2O	650ml

Stir until solids are dissolved. Top up to 1l with ddH_2O.

B.5.27 Acrylamide Gel Running Buffer

X10 Laemmli buffer	100ml
ddH_2O	900ml

B.5.28 Acrylamide Gel Transferring Buffer

Methanol	100ml

X10 Laemmli buffer	100ml
ddH_2O	800ml

B.5.29 Amido Black Solution

0.1% Naphtol Blue Black	0.1g
7% acetic acid	7ml
ddH_2O	93ml

B.5.30 Oocyte Fixing Solution

X1 PHEM	200µl
37% Paraformaldehyde	21.62µl

B.5.31 Tissue Slide Fixing Solution

X1 PBS	1ml
37% Paraformaldehyde	108.1µl

B.5.32 Oocyte Permeabilisation Solution

X1 PVP-PBS	190µl
X1 Triton X-100	10µl

B.5.33 Tissue Slide Permeabilisation Solution

X1 PBS	495ml
X1 Triton X-100	5ml

B.5.34 0.1M Citrate Buffer

$HOC(COONa)(CH_2COONa)_2 \cdot 2H_2O$	29.41g

Dissolved in 800ml ddH_2O, pH to 6.2 and top up to 1l with ddH_2O.

B.5.35 Antigen Retrieval Buffer

0.1M citrate buffer	100ml
ddH_2O	900ml

B.5.36 3% H_2O_2

H_2O_2	7.5ml
ddH_2O	242.5ml

B.5.37 Oocyte Blocking Solution

X1 PBS	850µl
Goat serum	100µl
1% Tween-20	50µl

B.5.38 Tissue Slide Blocking Solution

Goat serum	2ml
BSA	0.5g
X1 PBS	10ml

B.5.39 FACS Blocking Solution

Fatty acid-free BSA	200mg
HBSS	9.8ml

Goat serum	200µl

B.5.40 Western Blot Membrane Blocking Solution

Skimmed milk	0.5g
Tween20	100µl
X1 PBS	10ml

B.5.41 Oocyte Washing Solution

X1 PBS	20ml
BSA	0.1g
0.05% Tween-20	1µl

B.5.42 Tissue Slide Washing Solution

X1 PBS	999ml
0.1% Triton X-100	1ml

B.5.43 FACS Buffer

FBS	10µl
HBSS	10ml

Appendix C

C.1 Protein Sequences

C.1.1 DDX4 isoforms in *Homo sapiens*

Isoform 1 (mature protein sequence) (NCBI ref. NP_077726.1)

```
  1 mgdedweaei nphmssyvpi fekdrysgen gdnfnrtpas ssemddgpsr rdhfmksgfa
 61 sgrnfgnrda gecnkrdnts tmggfgvgks fgnrgfsnsr fedgdssgfw ressndcedn
121 ptrnrgfskr ggyrdgnnse asgpyrrggr gsfrgcrggf glgspnndld pdecmqrtgg
181 lfgsrrpvls gtgngdtsqs rsgsgsergg ykglneevit gsgknswkse aeggessdtq
241 gpkvtyippp ppededsifa hyqtginfdk ydtilvevsg hdappailtf eeanlcqtln
301 nniakagytk ltpvqkysip iilagrdlma caqtgsgkta afllpilahm mhdgitasrf
361 kelqepecii vaptrelvnq iylearkfsf gtcvravviy ggtqlghsir qivqgcnilc
421 atpgrlmdii gkekiglkqi kylvldeadr mldmgfgpem kkliscpgmp skeqrqtlmf
481 satfpeeiqr laaeflksny lfvavgqvgg acrdvqqtvl qvgqfskrek lveilrnigd
541 ertmvfvetk kkadfiatfl cqekisttsi hgdreqrere qalgdfrfgk cpvlvatsva
601 argldienvq hvinfdlpst ideyvhrigr tgrcgntgra isffdlesdn hlaqplvkvl
661 tdaqqdvpaw leeiafstyi pgfsgstrgn vfasvdtrkg kstlntagfs ssqapnpvdd
721 eswd
```

Isoform 2 (NCBI ref. NP_001136021.1)

```
  1 mgdedweaei nphmssyvpi fekdrysgen gdnfnrtpas ssemddgpsr rdhfmksgfa
 61 sgrnfgnrda gecnkrdnts tmggfgvgks fgnrgfsnsr fedgdssgfw ressndcedn
121 ptrnrgfskr gdndldpdec mqrtgglfgs rrpvlsgtgn gdtsqsrsgs gserggykgl
181 neevitgsgk nswkseaegg essdtqgpkv tyipppped edsifahyqt ginfdkydti
241 lvevsghdap pailtfeean lcqtlnnnia kagytkltpv qkysipiila grdlmacaqt
301 gsgktaafll pilahmmhdg itasrfkelq epeciivapt relvnqiyle arkfsfgtcv
361 ravviyggtq lghsirqivq gcnilcatpg rlmdiigkek iglkqikylv ldeadrmldm
421 gfgpemkkli scpgmpskeq rqtlmfsatf peeiqrlaae flksnylfva vgqvggacrd
481 vqqtvlqvgq fskreklvei lrnigdertm vfvetkkkad fiatflcqek isttsihgdr
541 eqrereqalg dfrfgkcpvl vatsvaargl dienvqhvin fdlpstidey vhrigrtgrc
601 gntgraisff dlesdnhlaq plvkvltdaq qdvpawleei afstyipgfs gstrgnvfas
661 vdtrkgkstl ntagfsssqa pnpvddeswd
```

Isoform 3 (NCBI ref. NP_001160005.1)

```
  1 mgdedweaei nphmssyvpi fekdrysgen gdnfnrtpas ssemddgpsr rdhfmksgfa
 61 sgrnfgnrda gecnkrdnts tmggfgvgks fgnrgfsnsr fedgdssgfw rgyrdgnnse
121 asgpyrrggr gsfrgcrggf glgspnndld pdecmqrtgg lfgsrrpvls gtgngdtsqs
181 rsgsgsergg ykglneevit gsgknswkse aeggessdtq gpkvtyippp ppededsifa
241 hyqtginfdk ydtilvevsg hdappailtf eeanlcqtln nniakagytk ltpvqkysip
301 iilagrdlma caqtgsgkta afllpilahm mhdgitasrf kelqepecii vaptrelvnq
361 iylearkfsf gtcvravviy ggtqlghsir qivqgcnilc atpgrlmdii gkekiglkqi
421 kylvldeadr mldmgfgpem kkliscpgmp skeqrqtlmf satfpeeiqr laaeflksny
481 lfvavgqvgg acrdvqqtvl qvgqfskrek lveilrnigd ertmvfvetk kkadfiatfl
541 cqekisttsi hgdreqrere qalgdfrfgk cpvlvatsva argldienvq hvinfdlpst
601 ideyvhrigr tgrcgntgra isffdlesdn hlaqplvkvl tdaqqdvpaw leeiafstyi
661 pgfsgstrgn vfasvdtrkg kstlntagfs ssqapnpvdd eswd
```

Isoform 4 (NCBI ref. NP_001160006.1)

```
  1 mgsrnlfltn spessndced nptrnrgfsk rgdndldpde cmqrtgglfg srrpvlsgtg
 61 ngdtsqsrsg sgserdswks eaeggessdt qgpkvtyipp pppededsif ahyqtginfd
121 kydtilvevs ghdappailt feeanlcqtl nnniakagyt kltpvqkysi piilagrdlm
181 acaqtgsgkt aafllpilah mmhdgitasr fkelqepeci ivaptrelvn qiylearkfs
241 fgtcvravvi yggtqlghsi rqivqgcnil catpgrlmdi igkekiglkq ikylvldead
301 rmldmgfgpe mkkliscpgm pskeqrqtlm fsatfpeeiq rlaaeflksn ylfvavgqvg
361 gacrdvqqtv lqvgqfskre klveilrnig dertmvfvet kkkadfiatf lcqekistts
421 ihgdreqrer eqalgdfrfg kcpvlvatsv aargldienv qhvinfdlps tideyvhrig
481 rtgrcgntgr aisffdlesd nhlaqplvkv ltdaqqdvpa wleeiafsty ipgfsgstrg
541 nvfasvdtrk gkstlntagf sssqapnpvd deswd
```

C.1.2 DDX4 isoforms in *Mus musculus*

Isoform 1 (mature protein sequence) (NCBI ref. NP_001139357.1)

```
  1 mgdedweaei lkphvssyvp vfekdkyssg angdtfnrts assemedgps grddfmrsgf
 61 psgrslgsrd igesskkent sttggfgrgk gfgnrgflnn kfeegdssgf wkesnndced
121 nqtrsrgfsk rggcqdgnds easgpfrrgg rgsfrgcrgg fglgrpnses dqdqgtqrgg
181 glfgsrkpaa sdsgngdtyq srsgsgrggy kglneevvtg sgknswkset eggessdsqg
241 pkvtyipppp pededsifah yqtginfdky dtilvevsgh dappailtfe eanlcqtlnn
301 niakagytkl tpvqkysipi vlagrdlmac aqtgsgktaa fllpilahmm rdgitasrfk
```

```
361 elqepeciiv aptrelinqi ylearkfsfg tcvravviyg gtqfghsvrq ivqgcnilca
421 tpgrlmdiig kekiglkqvk ylvldeadrm ldmgfgpemk kliscpgmps keqrqtllfs
481 atfpeeiqrl agdflkssyl fvavgqvgga crdvqqtilq vgqyskrekl veilrnigde
541 rtmvfvetkk kadfiatflc qekisttsih gdreqrereq algdfrcgkc pvlvatsvaa
601 rgldienvqh vinfdlpsti deyvhrigrt grcgntgrai sffdtdsdnh laqplvkvls
661 daqqdvpawl eeiafstyvp psfssstrgg avfasvdtrk nyqgkhtlnt agisssqapn
721 pvddeswd
```

Isoform 2 (NCBI ref. NP_034159.1)

```
  1 mgdedweaei lkphvssyvp vfekdkyssg angdtfnrts assdigessk kentsttggf
 61 grgkgfgnrg flnnkfeegd ssgfwkesnn dcednqtrsr gfskrggcqd gndseasgpf
121 rrggrgsfrg crggfglgrp nsesdqdqgt qrggglfgsr kpaasdsgng dtyqsrsgsg
181 rggykglnee vvtgsgknsw kseteggess dsqgpkvtyi pppppededs ifahyqtgin
241 fdkydtilve vsghdappai ltfeeanlcq tlnnniakag ytkltpvqky sipivlagrd
301 lmacaqtgsg ktaafllpil ahmmrdgita srfkelqepe ciivaptrel inqiyleark
361 fsfgtcvrav viyggtqfgh svrqivqgcn ilcatpgrlm diigkekigl kqvkylvlde
421 adrmldmgfg pemkkliscp gmpskeqrqt llfsatfpee iqrlagdflk ssylfvavgq
481 vggacrdvqq tilqvgqysk reklveilrn igdertmvfv etkkkadfia tflcqekist
541 tsihgdreqr ereqalgdfr cgkcpvlvat svaargldie nvqhvinfdl pstideyvhr
601 igrtgrcgnt graisffdtd sdnhlaqplv kvlsdaqqdv pawleeiafs tyvppsfsss
661 trggavfasv dtrknyqgkh tlntagisss qapnpvddes wd
```

C.2 Human-to-mouse sequence comparison

C.2.1 Human-to-mouse alignment for the DDX4^{C25} epitope

PROTEIN	HUMAN-TO-MOUSE MATCH	MATCHING SEQUENCE	E-VALUE	LOCALIZATION	FUNCTION
ATP-binding cassette subfamily C member 12	7/7 (100%)	42 to 48 (1366)	1.3	Cell surface All tissues	Transmembrane transport
Histone acetyltransferase KAT2A	7/7 (100%)	13 to 19 (830)	2.5	Nucleus All tissues	Acetylation of histones for epigenetic transcription activation
NAD-dependent protein deacetylase sirtuin 2	7/8 (88%)	356 to 363 (389)	6.9	Cytoplasm, nucleus All tissues	Histone deacetilation, control of cell cycle, chromosome rearrangement in the oocyte
Trimethylguanosine synthase 1	10/13 (76%)	292 to 302 (615)	5	Cytoplasm, nucleus Heart, skeletal muscle, kidney, liver, placenta.	Pre-rRNA processing, snRNA trimethylation
AT-hook-containing transcription factor	10/13 (76%)	323 to 333 (1404)	5	Nucleus All tissues	Transcription, replication, chromosome rearrangement, formation of multiprotein complexes
Sentrin-specific protease 5	8/11 (72%)	481 to 491 (749)	0.45	Cytoplasm, nucleus All tissues	Maturation of SUMO for SUMOylation
Dynamin-3	9/13 (69%)	741 to 752 (859)	2.5	Cytoplasm Testes, lung, neurons	Membrane modelling
SAM and SH3 domain-containing protein 1	10/15 (66%)	726 to 740 (777)	1.8	Nucleus All tissues	Receptor for insulin stimulation, actin stress fibres
Armadillo repeat-containing X-linked protein 2	9/14 (64%)	68 to 78 (784)	9.7	Membrane Endocrine gland, male genital tract, renal tubule, breast	Unknown
Receptor type protein tyrosine phosphatase H	10/16 (63%)	149 to 159 (1153)	5.5	Cell surface Brain, liver, testis	Cell growth, differentiation, mitotic cycle, and oncogenic transformation
Fatty acid synthase	11/18 (61%)	1423 to 1434 (2504)	9.8	Cytoplasm All tissues	Synthesis of palmitate from acetyl- and malonyl-CoA
Serine protease 42	12/20 (60%)	29 to 48 (335)	2.5	Cell surface Testis, muscle	Spermatogenesis
Neurogenic locus notch homolog protein 3	9/16 (56%)	992 to 1004 (2318)	3.6	Nucleus, cell surface Muscle, nervous and immune system	Differentiation, proliferation and apoptotic
Coiled-coil domain-containing protein 85A	11/22 (50%)	445 to 466 (500)	14	Nucleus All tissues	Unknown
von Willebrand factor C	11/24 (46%)	892 to 913 (929)	9.8	Extracellular plasma All tissues	Adhesion of platelets, chaperone

C.2.2 Human-to-mouse alignment for the DDX4^{351} epitope

PROTEIN	HUMAN-TO-MOUSE MATCH	MATCHING SEQUENCE	E-VALUE	LOCALIZATION	FUNCTION
DDX3X	227/307 (73%)	275 to 579 (662)	3e-111	Cytoplasm All tissues	dsRNA interaction, S phase entry
DDX3/Pl10	230/317 (72%)	274 to 585 (660)	3e-111	Cytoplasm Testis	Spermatogenesis
DDX3Y	242/344 (70%)	274 to 611 (658)	1e-111	Cytoplasm, nucleus Testis	Early spermatogonial proliferation
DDX5/p68	190/300 (63%)	176 to 467 (614)	6e-67	Nucleus All tissues	Co-activators for oestrogen receptor alpha, pre-mRNA splicing
DDX17	188/298 (63%)	174 to 465 (652)	1e-65	Cytoplasm, nucleus All tissues	Endogenous miRNA biogenesis, surveillance against virus

C.3 Transmembrane Modelling

C.3.1 Transmembrane domain prediction analysis of the human DDX4 isoform 1

COMPUTATIONAL SIMULATION PROGRAMME	TRANSMEMBRANE RESIDUES IN HOMO SAPIENS	EXTRACYTOPLASMIC DOMAIN	CELL SURFACE TARGET OF ANTI-C-T ANTIBODY
HMMTOP	None found	None	NO
MEMSAT3	Outside to inside helices: 662 – 680	NH_2-terminus	NO
MEMSAT-SVM	Outside to inside helices: 337 – 352	NH_2-terminus	NO
MPEx	None found	None	NO
OCTOPUS	None found	None	NO
Phobius	None found	None	NO
PredictProtein	None found	None	NO
TMHMM	None found	None	NO
TMpred	Insignificant results	None	NO
TopPred 1.10	Outside to inside helices: 332 – 352	NH_2-terminus	NO
PRED-CLASS	None (fibrous protein)	None	NO

C.3.2 Transmembrane domain prediction analysis of the human DDX4 isoform 2

COMPUTATIONAL SIMULATION PROGRAMME	TRANSMEMBRANE RESIDUES IN HOMO SAPIENS	EXTRACYTOPLASMIC DOMAIN	CELL SURFACE TARGET OF ANTI-C-T ANTIBODY
HMMTOP	None found	None	NO
MEMSAT3	Outside to inside helices: 628 – 646	NH_2-terminus	NO
MEMSAT-SVM	Outside to inside helices: 463 – 478	NH_2-terminus	NO
MPEx	None found	None	NO
OCTOPUS	None found	None	NO
Phobius	None found	None	NO
PredictProtein	None found	None	NO
TMHMM	None found	None	NO
TMpred	Insignificant results	None	NO
TopPred 1.10	Outside to inside helices: 298 – 318	NH_2-terminus	NO
PRED-CLASS	None (fibrous protein)	None	NO

C.3.3 Transmembrane domain prediction analysis of the human DDX4 isoform 3

COMPUTATIONAL SIMULATION PROGRAMME	TRANSMEMBRANE RESIDUES IN HOMO SAPIENS	EXTRACYTOPLASMIC DOMAIN	CELL SURFACE TARGET OF ANTI-C-T ANTIBODY
HMMTOP	None found	None	NO
MEMSAT3	Outside to inside helices: 642 – 660	NH_2-terminus	NO
MEMSAT-SVM	Outside to inside helices: 317 – 332	NH_2-terminus	NO
MPEx (Snider et al., 2009)	None found	None	NO
OCTOPUS	None found	None	NO
Phobius	None found	None	NO
PredictProtein	None found	None	NO
TMHMM	None found	None	NO
TMpred	Insignificant results	None	NO
TopPred 1.10	Outside to inside helices: 312 – 332	NH_2-terminus	NO
PRED-CLASS	None (fibrous protein)	None	NO

C.3.4 Transmembrane domain prediction analysis of the human DDX4 isoform 4

COMPUTATIONAL SIMULATION PROGRAMME	TRANSMEMBRANE RESIDUES IN HOMO SAPIENS	EXTRACYTOPLASMIC DOMAIN	CELL SURFACE TARGET OF ANTI-C-T ANTIBODY
HMMTOP	None found	None	NO
MEMSAT3	Outside to inside helices: 512 – 530	NH_2-terminus	NO
MEMSAT-SVM	Outside to inside helices: 348 – 363	NH_2-terminus	NO
MPEx	None found	None	NO
OCTOPUS	None found	None	NO
Phobius	None found	None	NO
PredictProtein	None found	None	NO
TMHMM	None found	None	NO
TMpred	Insignificant results	None	NO
TopPred 1.10	Outside to inside helices: 183 – 203	NH_2-terminus	NO
PRED-CLASS	None (fibrous protein)	None	NO

C.3.5 Transmembrane domain prediction analysis of the mouse DDX4 isoform 1

COMPUTATIONAL SIMULATION PROGRAMME	TRANSMEMBRANE RESIDUES IN MUS MUSCULUS	EXTRACYTOPLASMIC DOMAIN	CELL SURFACE TARGET OF ANTI-C-T ANTIBODY
HMMTOP	None found	None	NO
MEMSAT3	Outside to inside helices: 660 – 679	NH_2-terminus	NO
MEMSAT-SVM	Outside to inside helices: 336 – 351	NH_2-terminus	NO
MPEx	None found	None	NO
OCTOPUS	None found	None	NO
Phobius	None found	None	NO
PredictProtein	None found	None	NO
TMHMM	None found	None	NO
TMpred	Outside to inside helices: 327 – 347 Inside to outside helices: 494 – 512	NH_2-terminus COOH-terminus	YES

TopPred 1.10	Outside to inside helices: 330 – 350	NH_2-terminus	NO
PRED-CLASS	None (fibrous protein)	None	NO

C.3.6 Transmembrane domain prediction analysis of the mouse DDX4 isoform 2

COMPUTATIONAL SIMULATION PROGRAMME	TRANSMEMBRANE RESIDUES IN MUS MUSCULUS	EXTRACYTOPLASMIC DOMAIN	CELL SURFACE TARGET OF ANTI-C-T ANTIBODY
HMMTOP	None found	None	NO
MEMSAT3	Outside to inside helices: 634 – 653	NH_2-terminus	NO
MEMSAT-SVM	Outside to inside helices: 310 – 325	NH_2-terminus	NO
MPEx	None found	None	NO
OCTOPUS	None found	None	NO
Phobius	None found	None	NO
PredictProtein	None found	None	NO
TMHMM	None found	None	NO
TMpred	Outside to inside helices: **301 – 324** Inside to outside helices: **468 – 488**	NH_2-terminus COOH-terminus	YES
TopPred 1.10	Outside to inside helices: 304 – 324	NH_2-terminus	NO
PRED-CLASS	None (fibrous protein)	None	NO

References

Abban, G. and Johnson, J. (2009). Stem cell support of oogenesis in the human. *Hum. Reprod.* **24**, 2974–2978.

Abby, E., Tourpin, S., Ribeiro, J., Daniel, K., Messiaen, S., Moison, D., Guerquin, J., Gaillard, J.-C., Armengaud, J., Langa, F., et al. (2016). Implementation of meiosis prophase I programme requires a conserved retinoid-independent stabilizer of meiotic transcripts. *Nat. Commun.* **7**, 10324.

Abir, R., Orvieto, R., Dicker, D., Zukerman, Z., Barnett, M. and Fisch, B. (2002). Preliminary studies on apoptosis in human fetal ovaries. *Fertil. Steril.* **78**, 259–264.

Adhikari, D. and Liu, K. (2009). Molecular mechanisms underlying the activation of mammalian primordial follicles. *Endocr. Rev.* **30**, 438–464.

Ahram, M., Litou, Z. I., Fang, R. and Al-Tawallbeh, G. (2006). Estimation of membrane proteins in the human proteome. *In Silico Biol.* **6**, 379–386.

Albertini, D. F. (2004). Micromanagement of the ovarian follicle reserve - Do stem cells play into the ledger? *Reproduction* **127**, 513–514.

Albertini, D. F. and Gleicher, N. (2015). A detour in the quest for oogonial stem cells: methods matter. *Nat. Med.* **21**, 1126–1127.

Allen, E. (1923). Ovogenesis during sexual maturity. *Am. J. Anat.* **31**, 439–470.

Ancelin, K., Lange, U. C., Hajkova, P., Schneider, R., Bannister, A. J., Kouzarides, T. and Surani, M. A. (2006). Blimp1 associates with Prmt5 and directs histone arginine methylation in mouse germ cells. *Nat Cell Biol* **8**, 623–630.

Anderson, E. and Albertini, D. F. (1976). Gap junctions between the oocyte and companion follicle cells in the mammalian ovary. *J. Cell Biol.* **71**, 680–686.

Anderson, E. L., Baltus, A. E., Roepers-Gajadien, H. L., Hassold, T. J., de Rooij, D. G., van Pelt, A. M. M. and Page, D. C. (2008). Stra8 and its inducer, retinoic acid, regulate meiotic initiation in both spermatogenesis and oogenesis in mice. *Proc. Natl. Acad. Sci.* **105**, 14976–14980.

Andrews, P. W., Przyborski, S. A. and Thomson, J. A. (2001). Embryonal carcinoma cells as embryonic stem cells. In *Stem Cell Biology* (ed. Marshak, D. R., Gardner, R. L., and Gottlieb, D.), Cold Spring Harbor Monograph Series.

Aoi, T., Yae, K., Nakagawa, M., Ichisaka, T., Okita, K., Takahashi, K., Chiba, T. and Yamanaka, S. (2008). Generation of pluripotent stem cells from adult mouse liver and stomach cells. *Science (80-.).* **321**, 699–702.

Arai, H. (1920). On the postnatal development of the ovary (albino rat), with especial reference to the number of ova. *Am. J. Anat.* **27**, 405–462.

Auersperg, N., Wong, A. S. T., Choi, K., Kang, S. K. and Leung, P. C. K. (2001). Ovarian surface epithelium: biology, endocrinology, and pathology. *Endocr. Rev.* **22**, 255–288.

Bach, F. H., Albertini, R. J., Joo, P., Anderson, J. L. and Bortin, M. M. (1968). Bone-marrow transplantation in a patient with the Wiskott-Aldrich syndrome. *Lancet* **292**, 1364–1366.

Bahmanpour, S., Zarei Fard, N., Talaei-Khozani, T., Hosseini, A. and Esmaeilpour, T. (2015). Effect of BMP4 preceded by retinoic acid and co-culturing ovarian somatic cells on differentiation of mouse embryonic stem cells into oocyte-like cells. *Dev. Growth Differ.* **57**, 378–388.

Baker, T. G. and Franchi, L. L. (1967). The fine structure of oogonia and oocytes in human ovaries. *J. Cell Sci.* **224**, 213–224.

Baker, S. M., Plug, A. W., Prolla, T. A., Bronner, C. E., Harris, A. C., Yao, X., Christie, D.-M., Monell, C., Arnheim, N., Bradley, A., et al. (1996). Involvement of mouse Mlh1 in DNA mismatch repair and meiotic crossing over. *Nat. Genet.* **13**, 336–342.

Baltus, A. E., Menke, D. B., Hu, Y. C., Goodheart, M. L., Carpenter, A. E., de Rooij, D. G. and Page, D. C. (2006). In germ cells of mouse embryonic ovaries, the decision to enter meiosis precedes premeiotic DNA replication. *Nat. Genet.* **38**, 1430–1434.

Bandyopadhyay, S., Banerjee, S., Pal, A. K., Goswami, S. K., Chakravarty, B. and Kabir, S. N. (2004). Primordial germ cell migration in the rat: preliminary evidence for a role of galactosyltransferase. *Biol. Reprod.* **71**, 1822–1827.

Barritt, J. a., Willadsen, S., Brenner, C. and Cohen, J. (2001). Cytoplasmic transfer in assisted reproduction. *Hum. Reprod. Update* **7**, 428–435.

Bastien, J. and Rochette-Egly, C. (2004). Nuclear retinoid receptors and the transcription of retinoid-target genes. *Gene* **328**, 1–16.

Bayne, R. A. L., da Silva, S. J. M. and Anderson, R. A. (2004). Increased expression of the FIGLA transcription factor is associated with primordial follicle formation in the human fetal ovary. *Mol. Hum. Reprod.* **10**, 373–381.

Bechard, M. and Dalton, S. (2009). Subcellular localization of glycogen synthase kinase 3 controls embryonic stem cell self-renewal. *Mol. Cell. Biol.* **29**, 2092–2104.

Becker, A. J., McCulloch, E. A. and Till, J. E. (1963). Cytological demonstration of the clonal nature of spleen colonies derived from transplanted mouse marrow cells. *Nature* **197**, 452–454.

Beddington, R. S. P. and Robertson, E. J. (1999). Axis development and early asymmetry in mammals. *Cell* **96**, 195–209.

Begum, S., Papaioannou, V. E. and Gosden, R. G. (2008). The oocyte population is not renewed in transplanted or irradiated adult ovaries. *Hum. Reprod.* **23**, 2326–2330.

Bellavia, D., Checquolo, S., Campese, A. F., Felli, M. P., Gulino, A. and Screpanti, I. (2008). Notch3: from subtle structural differences to functional diversity. *Oncogene* **27**, 5092–5098.

Bendall, S. C., Stewart, M. H., Menendez, P., George, D., Vijayaragavan, K., Werbowetski-Ogilvie, T., Ramos-Mejia, V., Rouleau, A., Yang, J., Bossé, M., et al. (2007). IGF and FGF cooperatively establish the regulatory stem cell niche of pluripotent human cells in vitro. *Nature* **448**, 1015–1021.

Bendel-Stenzel, M. R., Gomperts, M., Anderson, R., Heasman, J. and Wylie, C. (2000). The role of cadherins during primordial germ cell migration and early gonad formation in the mouse. *Mech. Dev.* **91**, 143–152.

Berlier, J. E., Rothe, A., Buller, G., Bradford, J., Gray, D. R., Filanoski, B. J., Telford, W. G., Yue, S., Liu, J., Cheung, C.-Y., et al. (2003). Quantitative comparison of long-wavelength Alexa Fluor dyes to Cy dyes: fluorescence of the dyes and their bioconjugates. *J Histochem Cytochem* **51**, 1699–1712.

Berman, H. M., Westbrook, J., Feng, Z., Gilliland, G., Bhat, T. N., Weissig, H., Shindyalov, I. N. and Bourne, P. E. (2000). The Protein Data Bank. *Nucleic Acids Res.* **28**, 235–242.

Bernstein, E., Caudy, A. A., Hammond, S. M. and Hannon, G. J. (2001). Role for a bidentate ribonuclease in the initiation step of RNA interference. *Nature* **409**, 363–366.

Bernstein, H., Bernstein, C. and Michod, R. (2011). Meiosis as an evolutionary adaptation for DNA repair. In *DNA Repair* (ed. Kruman, I.), pp. 357–382. InTech.

Besingi, R. N. and Clark, P. L. (2015). Extracellular protease digestion to evaluate membrane protein cell surface localization. *Nat. Protoc.* **10**, 2074–2080.

Bianchi, E., Doe, B., Goulding, D. and Wright, G. J. (2014). Juno is the egg Izumo receptor and is essential for mammalian fertilization. *Nature* **508**, 483–487.

Bier, E. and Robertis, E. M. De (2015). BMP gradients: A paradigm for morphogen-mediated developmental patterning. *Science (80-.).* **348**, aaa5838–10.

Bikoff, E. K., Morgan, M. A. and Robertson, E. J. (2009). An expanding job description for Blimp-1/PRDM1. *Curr. Opin. Genet. Dev.* **19**, 379–385.

Blum, B., Bar-Nur, O., Golan-Lev, T. and Benvenisty, N. (2009). The anti-apoptotic gene survivin contributes to teratoma formation by human embryonic stem cells. *Nat. Biotechnol.* **27**, 281–287.

Borgese, N. and Fasana, E. (2011). Targeting pathways of C-tail-anchored proteins. *Biochim. Biophys. Acta* **1808**, 937–946.

Bornslaeger, E. A. and Schultz, R. M. (1986). Involvement of cAMP-dependent protein kinase and protein phosphorylation in regulation of mouse oocyte maturation. *Dev. Biol.* **114**, 453–462.

Bortvin, A., Goodheart, M., Liao, M. and Page, D. C. (2004). Dppa3 / Pgc7 / stella is a maternal factor and is not required for germ cell specification in mice. *BMC Dev. Biol.* **4**,.

Bouniol-Baly, C., Hamraoui, L., Guibert, J., Beaujean, N., Szöllösi, M. S. and Debey, P. (1999). Differential transcriptional activity associated with chromatin configuration in fully grown mouse germinal vesicle oocytes. *Biol. Reprod.* **60**, 580–587.

Bourne, G. and Zuckerman, S. (1940a). The influence of the adrenals on cyclical changes in the accessory reproductive organs of female rats. *J. Endocrinol.* **2**, 268–282.

Bourne, G. and Zuckerman, S. (1940b). Changes in the adrenals in relation to the normal and artificial threshold oestrous cycle in the rat. *J. Endocrinol.* **2**, 283–310.

Bowles, J. and Koopman, P. (2007). Retinoic acid, meiosis and germ cell fate in mammals. *Development* **134**, 3401–3411.

Bowles, J., Knight, D., Smith, C., Wilhelm, D., Richman, J., Mamiya, S., Yashiro, K., Chawengsaksophak, K., Wilson, M. J., Rossant, J., et al. (2006). Retinoid signaling determines germ cell fate in mice. *Science (80-.).* **312**, 596–600.

Bradley, A., Evans, M., Kaufman, M. H. and Robertson, E. (1984). Formation of germ-line chimaeras from embryo-derived teratocarcinoma cell lines. *Nature* **309**, 255–256.

Brass, A. L., Huang, I. C., Benita, Y., John, S. P., Krishnan, M. N., Feeley, E. M., Ryan, B. J., Weyer, J. L., van der Weyden, L., Fikrig, E., et al. (2009). The IFITM proteins mediate cellular resistance to influenza A H1N1 virus, West Nile virus and dengue virus. *Cell* **139**, 1243–1254.

Breward, M. M. and Zuckerman, S. (1949). The reaction of the body to multiple ovarian grafts. *J. Endocrinol.* **6**, 226–234.

Bristol-Gould, S. K., Kreeger, P. K., Selkirk, C. G., Kilen, S. M., Mayo, K. E., Shea, L. D. and Woodruff, T. K. (2006). Fate of the initial follicle pool: Empirical and mathematical evidence supporting its sufficiency for adult fertility. *Dev. Biol.* **298**, 149–154.

Brons, I. G. M., Smithers, L. E., Trotter, M. W. B., Rugg-Gunn, P., Sun, B., Lopes, S. M. C. de S., Howlett, S. K., Clarkson, A., Ahrlund-Richter, L., Pedersen, R. A., et al. (2007). Derivation of pluripotent epiblast stem cells from mammalian embryos. *Nature* **448**, 191–195.

Buratti, E., Romano, M. and Baralle, F. E. (2012). Splicing in the RNA World. In *Alternative pre-mRNA Splicing: Theory and Protocols* (ed. Stamm, S., Smith, C. W. J., and Lührmann, R.), Weinheim, Germany: Wiley-VCH Verlag GmbH & Co. KGaA.

Butcher, E. O. (1927). The origin of definitive ova in the white rat (Mus norvegicus albinus). *Anat. Res.* **37**, 13–29.

Campbell, K. H. S., McWhir, J., Ritchie, W. A. and Wilmut, I. (1996). Sheep cloned by nuclear transfer from a cultured cell line. *Nature* **380**, 64–66.

Capel, B. (2014). Ovarian epithelium regeneration by Lgr5+ cells. *Nat. Cell Biol.* **16**, 743–744.

Carney, D. and Cunningham, D. (1977). Initiation of check cell division by trypsin action at the cell surface. *Nature* **268**, 602–606.

Castrillon, D. H., Quade, B. J., Wang, T. Y., Quigley, C. and Crum, C. P. (2000). The human VASA gene is specifically expressed in the germ cell lineage. *Proc. Natl. Acad. Sci.* **97**, 9585–9590.

Chakraborty, P. and Roy, S. K. (2015). Bone morphogenetic protein 2 promotes primordial follicle formation in the ovary. *Sci. Rep.* **5**, 12664.

Chang, H. and Matzuk, M. M. (2001). Smad5 is required for mouse primordial germ cell development. *Mech. Dev.* **104**, 61–67.

Chang, D. H., Angelin-Duclos, C. and Calame, K. (2000). BLIMP-1: trigger for differentiation of myeloid lineage. *Nat. iImunology* **1**, 169–176.

Chang, D. H., Cattoretti, G. and Calame, K. L. (2002). The dynamic expression pattern of B lymphocyte induced maturation protein-1 (Blimp-1) during mouse embryonic development. *Mech. Dev.* **117**, 305–309.

Chang, H. Y., Minahan, K., Merriman, J. A. and Jones, K. T. (2009). Calmodulin-dependent protein kinase gamma 3 (CamKIIgamma3) mediates the cell cycle resumption of metaphase II eggs in mouse. *Development* **136**, 4077–4081.

Chazaud, C. and Yamanaka, Y. (2016). Lineage specification in the mouse preimplantation embryo. *Development* **143**, 1063–1074.

Check, E. (2007). The hard copy. *Nature* **446**, 29–30.

Chen, C. P., Kernytsky, A. and Rost, B. (2002). Transmembrane helix predictions revisited. *Protein Sci.* **11**, 2774–2791.

Childs, A. J. and Anderson, R. A. (2009). Activin A selectively represses expression of the membrane-bound isoform of Kit ligand in human fetal ovary. *Fertil. Steril.* **92**, 1416–1419.

Childs, A. J., Bayne, R. A. L., Murray, A. A., Martins Da Silva, S. J., Collins, C. S., Spears, N. and Anderson, R. A. (2010a). Differential expression and regulation by activin of the neurotrophins BDNF and NT4 during human and mouse ovarian development. *Dev. Dyn.* **239**, 1211–1219.

Childs, A. J., Kinnell, H. L., Collins, C. S., Hogg, K., Bayne, R. A. L., Green, S. J., McNeilly, A. S. and Anderson, R. A. (2010b). BMP signaling in the human fetal ovary is developmentally regulated and promotes primordial germ cell apoptosis. *Stem Cells* **28**, 1368–1378.

Childs, A. J., Kinnell, H. L., He, J. and Anderson, R. A. (2012). LIN28 is selectively expressed by primordial and pre-meiotic germ cells in the human fetal ovary. *Stem Cells Dev.* **21**, 2343–2349.

Christensen, A., Bentley, G. ., Cabrera, R., Ortega, H. H., Perfito, N., Wu, T. J. and Micevych, P. (2012). Hormonal regulation of female reproduction. *Horm. Metab. Res.* **44**, 587–591.

Christian, J. L. (2012). Morphogen gradients in development: From form to function. *Wiley Interdiscip. Rev. Dev. Biol.* **1**, 3–15.

Chu, L.-F., Surani, M. A., Jaenisch, R. and Zwaka, T. P. (2011). Blimp1 expression predicts embryonic stem cell development in vitro. *Curr. Biol.* **21**, 1759–1765.

Chung, S. S. W., Sung, W., Wang, X. and Wolgemuth, D. J. (2004). Retinoic acid receptor alpha is required for synchronization of spermatogenic cycles and its absence results in progressive breakdown of the spermatogenic process. *Dev. Dyn.* **230**, 754–766.

Chuva de Sousa Lopes, S. M. and Roelen, B. A. J. (2008). Primordial germ cell specification: the importance of being “blimped”. *Histol. Histopathol.* **23**, 1553–1561.

Chuva de Sousa Lopes, S. M., Roelen, B. A. J., Monteiro, R. M., Emmens, R., Lin, H. Y., Li, E., Lawson, K. A. and Mummery, C. L. (2004a). BMP signaling mediated by ALK2 in the visceral endoderm is necessary for the generation of primordial germ cells in the mouse embryo. *Genes Dev.* **18**, 1838–1849.

Chuva de Sousa Lopes, S. M., Roelen, B. A. J., Monteiro, R. M., Emmens, R., Lin, H. Y., Li, E., Lawson, K. A. and Mummery, C. L. (2004b). BMP signaling mediated by ALK2 in the visceral endoderm is necessary for the generation of primordial germ cells in the mouse embryo. *Genes Dev.* **18**, 1838–1849.

Chuva de Sousa Lopes, S. M., van den Driesche, S., Carvalho, R. L. C., Larsson, J., Eggen, B., Surani, M. A. and Mummery, C. L. (2005). Altered primordial germ cell migration in the absence of transforming growth factor beta signaling via ALK5. *Dev. Biol.* **284**, 194–203.

Clark, A. T., Bodnar, M. S., Fox, M., Rodriquez, R. T., Abeyta, M. J., Firpo, M. T. and Pera, R. A. R. (2004). Spontaneous differentiation of germ cells from human embryonic stem cells in vitro. *Hum. Mol. Genet.* **13**, 727–739.

Claros, M. G. and von Heijne, G. (1994). TopPred II: An improved software for membrane protein structure predictions. *CABIOS* **10**, 685–686.

Comim, F. V, Hardy, K. and Franks, S. (2013). Adiponectin and its receptors in the ovary: further evidence for a link between obesity and hyperandrogenism in polycystic ovary syndrome. *Pl* **8**, e80416.

Connerty, P., Bajan, S., Remenyi, J., Fuller-Pace, F. V. and Hutvagner, G. (2016). The miRNA biogenesis factors, p72/DDX17 and KHSRP regulate the protein level of Ago2 in human cells. *Biochim. Biophys. Acta* **1859**, 1299–1305.

Conti, M., Hsieh, M., Zamah, A. M. and Oh, J. S. (2012). Novel signaling mechanisms in the ovary during oocyte maturation and ovulation. *Mol. Cell Endocrinol.* **356**, 65–73.

Cook, M. S., Coveney, D., Batchvarov, I., Nadeau, J. H. and Capel, B. (2009). BAX-mediated cell death affects early germ cell loss and incidence of testicular teratomas in Dnd1Ter/Ter mice. *Dev. Biol.* **328**, 377–383.

Cordin, O., Banroques, J., Tanner, N. K. and Linder, P. (2006). The DEAD-box protein family of RNA helicases. *Gene* **367**, 17–37.

Coutts, S. M., Childs, A. J., Fulton, N., Collins, C., Bayne, R. A. L., McNeilly, A. S. and Anderson, R. A. (2008). Activin signals via SMAD2/3 between germ and somatic cells in the human fetal ovary and regulates kit ligand expression. *Dev. Biol.* **314**, 189–199.

Cowan, C. A., Atienza, J., Melton, D. A. and Eggan, K. (2005). Nuclear reprogramming of somatic cells after fusion with human embryonic stem cells. *Science (80-.).* **309**, 1369–1373.

Da Silva-Buttkus, P., Marcelli, G., Franks, S., Stark, J. and Hardy, K. (2009). Inferring biological mechanisms from spatial analysis: prediction of a local inhibitor in the ovary. *Proc. Natl. Acad. Sci. U. S. A.* **106**, 456–461.

Dahéron, L., Opitz, S. L., Zaehres, H., Lensch, M. W., Andrews, P. W., Itskovitz-Eldor, J. and Daley, G. Q. (2004). LIF/STAT3 signaling fails to maintain self-renewal of human embryonic stem cells. *Stem Cells* **22**, 770–778.

Danner, S., Kajahn, J., Geismann, C., Klink, E. and Kruse, C. (2007). Derivation of oocyte-like cells from a clonal pancreatic stem cell line. *Mol. Hum. Reprod.* **13**, 11–20.

Dardenne, E., PolayEspinoza, M., Fattet, L., Germann, S., Lambert, M. P., Neil, H., Zonta, E., Mortada, H., Gratadou, L., Deygas, M., et al. (2014). RNA Helicases DDX5 and DDX17 Dynamically Orchestrate Transcription, miRNA, and Splicing Programs in Cell Differentiation. *Cell Rep.* **7**, 1900–1913.

Davenport, C. B. (1925). Regeneration of ovaries in mice. *J. Exp. Zool.* **42**, 1–12.

Davies, D. (2007). Cell sorting by flow cytometry. In *Flow Cytometry: Principles and Applications* (ed. Macey, M. G.), pp. 257–277. Totowa, New Jersey: Humana Press.

Davies, D. (2015). Design it, Run it, Analyse it, Publish it!

De Felici, M., Dolci, S. and Pesce, M. (1992). Cellular and molecular aspects of mouse primordial germ cell migration and proliferation in culture. *Int. J. Dev. Biol.* **36**, 205–213.

De Jonge, H. J. M., Fehrmann, R. S. N., de Bont, E. S. J. M., Hofstra, R. M. W., Gerbens, F., Kamps, W. A., de Vries, E. G. E., van der Zee, A. G. J., te Meerman, G. J. and ter Elst, A. (2007). Evidence based selection of housekeeping genes. *PLoS One* **2**, e898.

De La Fuente, R. (2006). Chromatin modifications in the germinal vesicle (GV) of mammalian oocytes. *Dev. Biol.* **292**, 1–12.

De Smedt, V., Szöllösi, D. and Kloc, M. (2000). The Balbiani body: Asymmetry in the mammalian oocyte. *Genesis* **26**, 208–212.

Deady, L. D. and Sun, J. (2015). A follicle rupture assay reveals an essential role for follicular adrenergic signaling in Drosophila ovulation. *PLoS Genet.* **11**, 1–21.

Dean, J. (2002). Oocyte-specific genes regulate follicle formation, fertility and early mouse development. *J. Reprod. Immunol.* **53**, 171–180.

Dear, T. N. (2000). Cloning, structure, expression analysis, and assignment to mouse Chromosome 7 of the gene Zfp296 encoding a zinc finger protein. *Mamm. Genome* **11**, 1037–1039.

Dekel, N. and Phillips, D. M. (1980). Cyclic AMP, prostaglandin E2 and steroids: possible mediators in the rat cumulus oophorus mucification. *Biol. Reprod.* **22**, 289–296.

Deshpande, G., Godishala, A. and Schedl, P. (2009). Ggamma1, a downstream target for the hmgcr-isoprenoid biosynthetic pathway, is required for releasing the Hedgehog ligand and directing germ cell migration. *PLoS Genet.* **5**, e1000333.

Desimio, M. G., Campolo, F., Dolci, S., Felici, M. De, Farini, D., Desimio, M. G., Campolo, F., Dolci, S., Felici, M. De and Farini, D. (2015). SOHLH1 and SOHLH2 directly down-regulate stimulated by retinoic acid 8 (STRA8) expression. *Cell Cycle* **14**, 1036–1045.

Di Carlo, A. and De Felici, M. (2000). A role for E-cadherin in mouse primordial germ cell development. *Dev. Biol.* **226**, 209–219.

Ding, X., Liu, G., Xu, B., Wu, C., Hui, N., Ni, X., Wang, J., Du, M., Teng, X. and Wu, J. (2016). Human GV oocytes generated by mitotically active germ cells obtained from follicular aspirates. *Sci. Rep.* **6**, 1–17.

Ditton, H. J., Zimmer, J., Kamp, C., Rajpert-De Meyts, E. and Vogt, P. H. (2004). The AZFa gene DBY (DDX3Y) is widely transcribed but the protein is limited to the male germ cells by translation control. *Hum. Mol. Genet.* **13**, 2333–2341.

Dobreva, M. P., Pereira, P. N. G., Deprest, J. and Zwijsen, A. (2010). On the origin of amniotic stem cells: of mice and men. *Int. J. Dev. Biol.* **54**, 761–777.

Doitsidou, M., Reichman-Fried, M., Stebler, J., Köprunner, M., Dörries, J., Meyer, D., Esguerra, C. V., Leung, T. and Raz, E. (2002). Guidance of primordial germ cell migration by the chemokine SDF-1. *Cell* **111**, 647–659.

Dokshin, G. a, Baltus, A. E., Eppig, J. J. and Page, D. C. (2013). Oocyte differentiation is genetically dissociable from meiosis in mice. *Nat. Genet.* **45**, 877–883.

Dong, J., Albertini, D. F., Nishimori, K., Kumar, T. R., Lu, N. and Matzuk, M. M. (1996). Growth differentiation factor-9 is required during early ovarian folliculogenesis. *Nature* **383**, 531–535.

Dovere, L., Fera, S., Grasso, M., Lamberti, D., Gargioli, C., Muciaccia, B., Lustri, A. M., Stefanini, M. and Vicini, E. (2013). The niche-derived glial cell line-derived neurotrophic factor (GDNF) induces migration of mouse spermatogonial stem/progenitor cells. *PLoS One* **8**, 1–9.

Doyle, T. J., Braun, K. W., McLean, D. J., Wright, R. W., Griswold, M. D. and Kim, K. H. (2007). Potential functions of retinoic acid receptor A in sertoli cells and germ cells during spermatogenesis. *Ann. N. Y. Acad. Sci.* **1120**, 114–130.

Dudley, B. M., Runyan, C., Takeuchi, Y., Schaible, K. and Molyneaux, K. (2007). BMP signaling regulates PGC numbers and motility in organ culture. *Mech. Dev.* **124**, 68–77.

Dunlop, C. E., McLaughlin, M., Bayne, R. A. L., Anderson, R. and Telfer, E. E. (2014). Isolation, propagation and characterisation of oogonial stem cells from human and bovine ovarian cortex. In *Society for Reproduction and Fertility 2014 Conference*, p. P007. Society for Reproduction and Fertility Conference 2014.

Durlinger, A. L. L., Gruijters, M. J. G., Kramer, P., Karels, B., Ingraham, H. A., Nachtigal, M. W., Uilenbroek, J. T. J., Grootegoed, J. A. and Themmen, A. P. N. (2002). Anti-Müllerian hormone inhibits initiation of primordial follicle growth in the mouse ovary. *Endocrinology* **143**, 1076–1084.

Duro, E. and Marston, A. L. (2015a). From equator to pole: splitting chromosomes in mitosis and meiosis. *Genes Dev.* **29**, 109–122.

Duro, E. and Marston, A. L. (2015b). From equator to pole: splitting chromosomes in mitosis and meiosis. *Genes Dev.* **29**, 109–122.

Edson, M. A., Nagaraja, A. K. and Matzuk, M. M. (2009). The mammalian ovary from genesis to revelation. *Endocr. Rev.* **30**, 624–712.

Eggan, K., Jurga, S., Gosden, R., Min, I. M. and Wagers, A. J. (2006). Ovulated oocytes in adult mice derive from non-circulating germ cells. *Nature* **441**, 1109–1114.

Eguizabal, C., Montserrat, N., Vassena, R., Barragan, M., Garreta, E., Garcia-Quevedo, L., Vidal, F., Giorgetti, A., Veiga, A. and Izpisua Belmonte, J. C. (2011). Complete meiosis from human induced pluripotent stem cells. *Stem Cells* **29**, 1186–1195.

Endo, T., Romer, K. a, Anderson, E. L., Baltus, A. E., de Rooij, D. G. and Page, D. C. (2015). Periodic retinoic acid–STRA8 signaling intersects with periodic germ-cell competencies to regulate spermatogenesis. *Proc. Natl. Acad. Sci.* **112**, E2347–E2356.

Eppig, J. J. (1991). Intercommunication between mammalian oocytes and companion somatic cells. *BioEssays* **13**, 569–574.

Eppig, J. J., Wigglesworth, K. and Pendola, F. L. (2002). The mammalian oocyte orchestrates the rate of ovarian follicular development. *Proc. Natl. Acad. Sci.* **99**, 2890–2894.

Evans, M. J. and Kaufman, M. H. (1981). Establishment in culture of pluripotential cells from mouse embryos. *Nature* **292**, 154–156.

Faddy, M. J., Telfer, E. and Gosden, R. G. (1987). The kinetics of pre-antral follicle development in ovaries of CBA/Ca mice during the first 14 weeks of life. *Cell Tissue Kinet.* **20**, 551–560.

Fakih, M. H., El Shmoury, M., Szeptycki, J., dela Cruz, D. B., Lux, C., Verjee, S., Burgess, C. M., Cohn, G. M. and Casper, R. F. (2015). The AUGMENT (SM) Treatment: Physician Reported Outcomes of the Initial Global Patient Experience. *JFIV Reprod. Med. Genet.* **3**, 1000154.

Faustino, L. R., Woods, D. C., White, Y. A. and Tilly, J. L. (2012). Oogonial stem cells increase in numbers in aged mouse ovaries. In *Reproductive Sciences 19 (S 3)*, p. 224A–224A.

Feeley, E. M., Sims, J. S., John, S. P., Chin, C. R., Pertel, T., Chen, L.-M., Gaiha, G. D., Ryan, B. J., Donis, R. O., Elledge, S. J., et al. (2011). IFITM3 inhibits influenza A virus infection by preventing cytosolic entry. *PLoS Pathog.* **7**, e1002337.

Feller, J., Schneider, A., Schuster-Gossler, K. and Gossler, A. (2008). Noncyclic Notch activity in the presomitic mesoderm demonstrates uncoupling of somite compartmentalization and boundary formation. *Genes Dev.* **22**, 2166–2171.

Feng, Y. M., Liang, G. J., Pan, B., Qin, X. S., Zhang, X. F., Chen, C. L., Li, L., Cheng, S. F., De Felici, M. and Shen, W. (2014). Notch pathway regulates female germ cell meiosis progression and early oogenesis events in fetal mouse. *Cell Cycle* **13**, 782–791.

Fenwick, M. A., Mora, J. M., Mansour, Y. T., Baithun, C., Franks, S. and Hardy, K. (2013). Investigations of TGF-β signaling in preantral follicles of female mice reveal differential roles for bone morphogenetic protein 15. *Endocrinology* **154**, 3423–3436.

Filmus, J., Capurro, M. and Rast, J. (2008). Glypicans. *Genome Biol.* **9**, 224.

Finak, G., Langweiler, M., Jaimes, M., Malek, M., Taghiyar, J., Korin, Y., Raddassi, K., Devine, L., Obermoser, G., Pekalski, M. L., et al. (2016). Standardizing flow cytometry immunophenotyping analysis from the Human ImmunoPhenotyping Consortium. *Sci. Rep.* **6**, 20686.

Fischedick, G., Klein, D. C., Wu, G., Esch, D., Höing, S., Han, D. W., Reinhardt, P., Hergarten, K., Tapia, N., Schöler, H. R., et al. (2012). Zfp296 is a novel, pluripotent-specific reprogramming factor. *PLoS One* **7**, e34645.

Fitzpatrick, K. A., Gorski, S. M., Ursuliak, Z. and Price, J. V. (1995). Expression of protein tyrosine phosphatase genes during oogenesis in Drosophila melanogaster. *Mechanisms* **53**, 171–183.

Flemr, M., Malik, R., Franke, V., Nejepinska, J., Sedlacek, R., Vlahovicek, K. and Svoboda, P. (2013). XA retrotransposon-driven dicer isoform directs endogenous small interfering rna production in mouse oocytes. *Cell* **155**, 807–816.

Foresta, C., Ferlin, a and Moro, E. (2000). Deletion and expression analysis of AZFa genes on the human Y chromosome revealed a major role for DBY in male infertility. *Hum. Mol. Genet.* **9**, 1161–1169.

Forman-Kay, J. D. and Mittag, T. (2013). From sequence and forces to structure, function, and evolution of intrinsically disordered proteins. *Structure* **21**, 1492–1499.

Fortune, J. E. (2003). The early stages of follicular development: activation of primordial follicles and growth of preantral follicles. *Anim. Reprod. Sci.* **78**, 135–163.

Fortune, J. E., Cushman, R. A., Wahl, C. M. and Kito, S. (2000). The primordial to primary follicle transition. *Mol. Cell. Endocrinol.* **163**, 53–60.

Franks, S., Stark, J. and Hardy, K. (2008). Follicle dynamics and anovulation in polycystic ovary syndrome. *Hum. Reprod. Update* **14**, 367–378.

Frumkin, D., Wasserstrom, A., Kaplan, S., Feige, U. and Shapiro, E. (2005). Genomic variability within an organism exposes its cell lineage tree. *PLoS Comput. Biol.* **1**, e50.

Frumkin, D., Wasserstrom, A., Itzkovitz, S., Stern, T., Harmelin, A., Eilam, R., Rechavi, G. and Shapiro, E. (2008). Cell lineage analysis of a mouse tumor. *Cancer Res.* **68**, 5924–5931.

Fuchs, E., Tumbar, T. and Guasch, G. (2004). Socializing with the neighbors: Stem cells and their niche. *Cell* **116**, 769–778.

Fujihara, Y., Okabe, M. and Ikawa, M. (2014). GPI-anchored protein complex, LY6K/TEX101, is required for sperm migration into the oviduct and male fertility in mice. *Biol. Reprod.* **90**, 1–6.

Fujii, Y., Kakegawa, M., Koide, H., Akagi, T. and Yokota, T. (2013). Zfp296 is a novel Klf4-interacting protein and functions as a negative regulator. *Biochem. Biophys. Res. Commun.* **441**, 411–417.

Fujimori, T., Kurotaki, Y., Miyazaki, J. and Nabeshima, Y. (2003). Analysis of cell lineage in two- and four-cell mouse embryos. *Development* **130**, 5113–5122.

Fujiwara, Y., Komiya, T., Kawabata, H., Sato, M., Fujimoto, H., Furusawa, M. and Noce, T. (1994). Isolation of a DEAD-family protein gene that encodes a murine homolog of Drosophila vasa and its specific expression in germ cell lineage. *Proc. Natl. Acad. Sci.* **91**, 12258–12262.

Fulka, H., Langerova, A., Barnetova, I., Novakova, Z., Mosko, T. and Fulka, J. (2009). How to repair the oocyte and zygote? *J. Reprod. Dev.* **55**, 583–587.

Fülöp, C., Salustri, A. and Hascall, V. C. (1997). Coding sequence of a hyaluronan synthase homologue expressed during expansion of the mouse cumulus–oocyte complex. *Arch. Biochem. Biophys.* **337**, 261–266.

Fülöp, C., Szántó, S., Mukhopadhyay, D., Bárdos, T., Kamath, R. V, Rugg, M. S., Day, A. J., Salustri, A., Hascall, V. C., Glant, T. T., et al. (2003). Impaired cumulus mucification and female sterility in tumor necrosis factor-induced protein-6 deficient mice. *Development* **130**, 2253–2261.

García-Castro, M. I., Anderson, R., Heasman, J. and Wylie, C. (1997). Interactions between germ cells and extracellular matrix glycoproteins during migration and gonad assembly in the mouse embryo. *J. Cell Biol.* **138**, 471–480.

Garcia-Cruz, R., Brieño, M. a., Roig, I., Grossmann, M., Velilla, E., Pujol, A., Cabero, L., Pessarrodona, A., Barbero, J. L. and Garcia Caldés, M. (2010). Dynamics of cohesin proteins REC8, STAG3, SMC1β and SMC3 are consistent with a role in sister chromatid cohesion during meiosis in human oocytes. *Hum. Reprod.* **25**, 2316–2327.

Gatti, R. A., Meuwissen, H. J., Allen, H. D., Hong, R. and Good, R. A. (1968). Immunological reconstitution of sex-linked lymphopenic immunological defficiency. *Lancet* **292**, 1366–1369.

Gehring, W. J. and Hiromi, Y. (1986). Homeotic genes and the homeobox. *Annu. Rev. Genet.* **20**, 147–173.

Gely-Pernot, A., Raverdeau, M., Célébi, C., Dennefeld, C., Feret, B., Klopfenstein, M., Yoshida, S., Ghyselinck, N. B. and Mark, M. (2012). Spermatogonia differentiation requires retinoic acid receptor γ. *Endocrinology* **153**, 438–449.

Gerard, P. (1920). Contribution a l'étude de l'ovaire des mammiferes. L'ovaire de Galago mosambicus. *Arch. de Biol.* **XXX**, 357–390.

Germain, P., Chambon, P., Eichele, G., Evans, R. M., Lazar, M. A., Leid, M., De Lera, A. R., Lotan, R., Mangelsdorf, D. J. and Gronemeyer, H. (2006). International Union of Pharmacology. LX. Retinoic acid receptors. *Pharmacol. Rev.* **58**, 712–725.

Ghadami, M., El-Demerdash, E., Zhang, D., Salama, S. A., Binhazim, A. A., Archibong, A. E., Chen, X., Ballard, B. R., Sairam, M. R. and Al-Hendy, A.

(2012). Bone marrow transplantation restores follicular maturation and steroid hormones production in a mouse model for primary ovarian failure. *PLoS One* **7**, 1–7.

Giacomo, M. Di, Barchi, M., Baudat, F., Edelmann, W., Keeney, S. and Jasin, M. (2005). Distinct DNA-damage-dependent and -independent responses drive the loss of oocytes in recombination-defective mouse mutants. *Proc. Natl. Acad. Sci.* **102**, 737–742.

Gilbert, S. F. (2000). Fertilization: Beginning a new organism. In *Developmental Biology* (ed. Gilbert, S. F.), p. 810. Sunderland, Maryland: Sinauer Associates.

Ginsburg, M., Snow, M. H. and McLaren, A. (1990). Primordial germ cells in the mouse embryo during gastrulation. *Development* **110**, 521–528.

Gomperts, M., Garcia-Castro, M., Wylie, C. and Heasman, J. (1994). Interactions between primordial germ cells play a role in their migration in mouse embryos. *Development* **120**, 135–141.

Gong, S. P., Lee, S. T., Lee, E. J., Kim, D. Y., Lee, G., Chi, S. G., Ryu, B. K., Lee, C. H., Yum, K. E., Lee, H. J., et al. (2010). Embryonic stem cell-like cells established by culture of adult ovarian cells in mice. *Fertil. Steril.* **93**, 2594–2601.e9.

Granseth, E., von Heijne, G. and Elofsson, A. (2005). A study of the membrane-water interface region of membrane proteins. *J. Mol. Biol.* **346**, 377–385.

Green, S. H. and Zuckerman, S. (1946). A comparison of the growth of the ovum and follicle in normal rhesus monkeys, and monkeys treated with oestrogens and androgens. *J. Endocrinol.* **5**, 207–219.

Green, S. H. and Zuckerman, S. (1951). The number of oocytes in the mature Rhesus monkey (Macaca mulatta). *J. Endocrinol.* **7**, 194–202.

Green, S. H., Mandl, A. M. and Zuckerman, S. (1951). The proportion of ovarian follicles in different stages of development in rats and monkeys. *J. Anat.* **85**, 325–329.

Greenfeld, C. and Flaws, J. A. (2004). Renewed debate over postnatal oogenesis in the mammalian ovary. *BioEssays* **26**, 829–832.

Grieve, K., Deleva, A. I., Dunlop, C. E., Anderson, R., Williams, S. A. and Telfer, E. E. (2014). Aggregation of bovine oogonial stem cells with mouse somatic cells results in follicle formation. In *Society for Reproduction and Fertility 2014 Conference*, .

Grieve, K. M., McLaughlin, M., Dunlop, C. E., Telfer, E. E. and Anderson, R. A. (2015). The controversial existence and functional potential of oogonial stem cells. *Maturitas* **82**, 278–281.

Griffin, N. M. and Schnitzer, J. E. (2011). Overcoming key technological challenges in using mass spectrometry for mapping cell surfaces in tissues. *Mol. Cell. Proteomics* **10**, R110.000935.

Grive, K. J., Seymour, K. A., Mehta, R. and Freiman, R. N. (2014). TAF4b promotes mouse primordial follicle assembly and oocyte survival. *Dev. Biol.* **392**, 42–51.

Grive, K. J., Gustafson, E. A., Seymour, K. A., Baddoo, M., Schorl, C., Golnoski, K., Rajkovic, A., Brodsky, A. S. and Freiman, R. N. (2016). TAF4b regulates oocyte-specific genes essential for meiosis. *PLoS Genet.* **12**, 1–18.

Grove, J. E., Bruscia, E. and Krause, D. S. (2004). Plasticity of bone marrow-derived stem cells. *Stem Cells* **22**, 487–500.

Gstraunthaler, G. (2003). Alternatives to the use of fetal bovine serum: serum-free cell culture. *ALTEX* **20**, 275–281.

Gu, Y., Runyan, C., Shoemaker, A., Surani, A. and Wylie, C. (2009). Steel factor controls primordial germ cell survival and motility from the time of their specification in the allantois, and provides a continuous niche throughout their migration. *Development* **136**, 1295–1303.

Gu, Y., Runyan, C., Shoemaker, A., Surani, M. A. and Wylie, C. (2011). Membrane-bound steel factor maintains a high local concentration for mouse primordial germ cell motility, and defines the region of their migration. *PLoS One* **6**, e25984.

Gupta, S. (2000). Hepatic polyploidy and liver growth control. *Semin. Cancer Biol.* **10**, 161–171.

Gura, B. Y. T. (2012). Fertile Mind. *Nature* **491**, 318–320.

Haele, M. Van and Roskams, T. (2017). Hepatic progenitor cells : an update. *Gastroenterol. Clin. North Am.* **46**, 409–420.

Hamazaki, T., Kehoe, S. M., Nakano, T. and Terada, N. (2006). The Grb2/Mek pathway represses Nanog in murine embryonic stem cells. *Mol. Cell. Biol.* **26**, 7539–7549.

Hamdan, M., Jones, K. T., Cheong, Y. and Lane, S. I. R. (2016). The sensitivity of the DNA damage checkpoint prevents oocyte maturation in endometriosis. *Sci. Rep.* **6**, 36994.

Hanna, C. B. and Hennebold, J. D. (2014). Ovarian germline stem cells: An unlimited source of oocytes? *Fertil. Steril.* **101**, 20–30.

Hanna, J., Markoulaki, S., Mitalipova, M., Cheng, A. W., Cassady, J. P., Staerk, J., Carey, B. W., Lengner, C. J., Foreman, R., Love, J., et al. (2009). Metastable pluripotent states in NOD-mouse-derived ESCs. *Cell Stem Cell* **4**, 513–524.

Hashimoto, H., Sudo, T., Mikami, Y., Otani, M., Takano, M., Tsuda, H., Itamochi, H., Katabuchi, H., Ito, M. and Nishimura, R. (2008). Germ cell specific protein VASA is over-expressed in epithelial ovarian cancer and disrupts DNA damage-induced G2 checkpoint. *Gynecol. Oncol.* **111**, 312–319.

Haston, K. M., Tung, J. Y. and Reijo Pera, R. A. (2009). Dazl functions in maintenance of pluripotency and genetic and epigenetic programs of differentiation in mouse primordial germ cells in vivo and in vitro. *PLoS One* **4**, e5654.

Hayakawa, K., Ohgane, J., Tanaka, S., Yagi, S. and Shiota, K. (2012). Oocyte-specific linker histone H1foo is an epigenomic modulator that decondenses chromatin and impairs pluripotency. *Epigenetics* **7**, 1029–1036.

Hayashi, K. and Saitou, M. (2013). Generation of eggs from mouse embryonic stem cells and induced pluripotent stem cells. *Nat. Protoc.* **8**, 1513–1524.

Hayashi, K., Kobayashi, T., Umino, T. and Goitsuka, R. (2002). SMAD1 signaling is critical for initial commitment of germ cell lineage from mouse epiblast. **118**, 99–109.

Hayashi, K., Chuva de Sousa Lopes, S. M. and Surani, M. A. (2007). Germ cell specification in mice. *Science (80-.).* **316**, 394–396.

Hayashi, K., Ogushi, S., Kurimoto, K., Shimamoto, S., Ohta, H. and Saitou, M. (2012a). Offspring from oocytes derived from in vitro primordial germ cell-like cells in mice. *Science (80-.).* **971**, 10–15.

Hayashi, K., Ogushi, S., Kurimoto, K., Shimamoto, S., Ohta, H. and Saitou, M. (2012b). Offspring from oocytes derived from in vitro primordial germ cell-like cells in mice. *Science (80-.).* **338**, 971–975.

Henderson, S. A. and Edwards, R. G. (1968). Chiasma frequency and maternal age in mammals. *Nature* **218**, 22–28.

Hernandez, S. F., Vahidi, N. A., Park, S., Weitzel, R. P., Tisdale, J., Rueda, B. R. and Wolff, E. F. (2015). Characterization of extracellular DDX4- or Ddx4-positive ovarian cells. *Nat. Med.* **21**, 1114–1116.

Hickford, D. E., Frankenberg, S., Pask, A. J., Shaw, G. and Renfree, M. B. (2011). DDX4 (VASA) is conserved in germ cell development in marsupials and monotremes. *Biol. Reprod.* **85**, 733–743.

Hikabe, O., Hamazaki, N., Nagamatsu, G., Obata, Y., Hirao, Y., Hamada, N., Shimamoto, S., Imamura, T., Nakashima, K., Saitou, M., et al. (2016). Reconstitution in vitro of the entire cycle of the mouse female germ line. *Nature* **539**, 299–303.

Hill, M. and Parkes, A. S. (1931). Attempts to promote the re-formation of germ cells. *J. Anat.* **65**, 212–214.

Hirai, H., Karian, P. and Kikyo, N. (2011). Regulation of embryonic stem cell self-renewal and pluripotency by leukaemia inhibitory factor. *Biochem. J.* **438**, 11–23.

Hofmann, K. and Stoffel, W. (1993). TMbase: A Database of Membrane Spanning Protein Segments. *Biol. Chem.* **374**, 166.

Hogan, B. L. M. (1976). Changes in the behaviour of teratocarcinoma cells cultivated in vitro. *Nature* **263**, 136–137.

Holt, J. E., Lane, S. I. R. and Jones, K. T. (2013). The control of meiotic maturation in mammalian oocytes. In *Current Topics in Developmental Biology: Gametogenesis* (ed. Wassarman, P. M.), pp. 207–226. Amsterdam: Elsevier Inc.

Horsley, V., O'Carroll, D., Tooze, R., Ohinata, Y., Saitou, M., Obukhanych, T., Nussenzweig, M., Tarakhovsky, A. and Fuchs, E. (2006). Blimp1 defines a progenitor population that governs cellular input to the sebaceous gland. *Cell* **126**, 597–609.

Hubner, K., Fuhrmann, G., Christenson, L. K., Kehler, J., Reinbold, R., Fuente, R. D. La, Wood, J., Iii, J. F. S., Boiani, M. and Scho, H. R. (2003). Derivation of oocytes from mouse embryonic stem cells. *Science (80-.).* **300**, 1251–1257.

Humphrey, R. K., Beattie, G. M., Lopez, A. D., Bucay, N., King, C. C., Firpo, M. T., Rose-John, S. and Hayek, A. (2004). Maintenance of pluripotency in human embryonic stem cells is STAT3 independent. *Stem Cells* **22**, 522–530.

Ichida, J. K., Blanchard, J., Lam, K., Son, E. Y., Chung, J. E., Egli, D., Loh, K. M., Carter, A. C., Di Giorgio, F. P., Koszka, K., et al. (2009). A small-molecule inhibitor of TGF-β signaling replaces Sox2 in reprogramming by inducing Nanog. *Cell Stem Cell* **5**, 491–503.

Ikami, K., Tokue, M., Sugimoto, R., Noda, C., Kobayashi, S., Hara, K. and Yoshida, S. (2015). Hierarchical differentiation competence in response to retinoic acid ensures stem cell maintenance during mouse spermatogenesis. *Development* **142**, 1582–1592.

Ikeda, M., Arai, M., Lao, D. M. and Shimizu, T. (2002). Transmembrane topology prediction methods: A re-assessment and improvement by a consensus method using a dataset of experimentally characterized transmembrane topologies. *In Silico Biol.* **2**, 19–33.

Imamura, M., Aoi, T., Tokumasu, A., Mise, N., Abe, K., Yamanaka, S. and Noce, T. (2010). Induction of primordial germ cells from mouse induced pluripotent stem cells derived from adult hepatocytes. *Mol. Reprod. Dev.* **77**, 802–811.

Imudia, A. N., Wang, N., Tanaka, Y., White, Y. A. R., Woods, D. C. and Tilly, J. L. (2013). Comparative gene expression profiling of adult mouse ovary-derived oogonial stem cells supports a distinct cellular identity. *Fertil. Steril.* **100**, 1451–1458.

Inoue, A., Nakajima, R., Nagata, M. and Aoki, F. (2008). Contribution of the oocyte nucleus and cytoplasm to the determination of meiotic and developmental competence in mice. *Hum. Reprod.* **23**, 1377–1384.

Jaenisch, R. and Young, R. (2008). Stem cells, the molecular circuitry of pluripotency and nuclear reprogramming. *Cell* **132**, 567–582.

Jalal, C., Uhlmann-Schiffler, H. and Stahl, H. (2007). Redundant role of DEAD box proteins p68 (Ddx5) and p72/p82 (Ddx17) in ribosome biogenesis and cell proliferation. *Nucleic Acids Res.* **35**, 3590–3601.

James, D., Levine, A. J., Besser, D. and Hemmati-Brinvalou, A. (2005). TGF /activin/nodal signaling is necessary for the maintenance of pluripotency in human embryonic stem cells. *Development* **132**, 1273–1282.

Jaroszeski, M. J. (1998). *Flow Cytometry Protocols. Methods in Molecular Biology, Vol. 91*. First. (ed. Jaroszeski, M. J. and Heller, R.) Totowa, New Jersey: Humana Press.

Johnson, J., Canning, J., Kaneko, T., Pru, J. K. and Tilly, J. L. (2004). Germline stem cells and follicular renewal in the postnatal mammalian ovary. *Nature* **428**, 145–150.

Johnson, J., Bagley, J., Skaznik-Wikiel, M., Lee, H.-J., Adams, G. B., Niikura, Y., Tschudy, K. S., Tilly, J. C., Cortes, M. L., Forkert, R., et al. (2005). Oocyte generation in adult mammalian ovaries by putative germ cells in bone marrow and peripheral blood. *Cell* **122**, 303–315.

Jones, K. T. (2004). Turning it on and off: M-phase promoting factor during meiotic maturation and fertilization. *Mol. Hum. Reprod.* **10**, 1–5.

Jones, K. T. (2005). Mammalian egg activation: From Ca2+ spiking to cell cycle progression. *Reproduction* **130**, 813–823.

Jones, D. T. (2007). Improving the accuracy of transmembrane protein topology prediction using evolutionary information. *Bioinformatics* **23**, 538–544.

Jones, K. T. (2008). Meiosis in oocytes: predisposition to aneuploidy and its increased incidence with age. *Hum. Reprod. Update* **14**, 143–158.

Jones, R. E. and Lopez, K. H. (2013). *Human Reproductive Biology, Fourth Edition*. Fourth. (ed. Press, A.) San Diego: Elsevier.

Kageyama, S. I., Liu, H., Kaneko, N., Ooga, M., Nagata, M. and Aoki, F. (2007). Alterations in epigenetic modifications during oocyte growth in mice. *Reproduction* **133**, 85–94.

Kakiuchi, K., Tsuda, A., Goto, Y., Shimada, T., Taniguchi, K., Takagishi, K. and Kubota, H. (2014). Cell-surface DEAD-box polypeptide 4-immunoreactive cells and gonocytes are two distinct populations in postnatal porcine testes. *Biol. Reprod.* **90**, 82.

Kamran, P., Sereti, K.-I., Zhao, P., Ali, S. R., Weissman, I. L. and Ardehali, R. (2013). Parabiosis in mice: a detailed protocol. *J. Vis. Exp.* 1–5.

Kanatsu-Shinohara, M., Ogonuki, N., Inoue, K., Miki, H., Ogura, A., Toyokuni, S. and Shinohara, T. (2003). Long-term proliferation in culture and germline transmission of mouse male germline stem cells. *Biol. Reprod.* **69**, 612–616.

Kanatsu-Shinohara, M., Inoue, K., Lee, J., Yoshimoto, M., Ogonuki, N., Miki, H., Baba, S., Kato, T., Kazuki, Y., Toyokuni, S., et al. (2004). Generation of pluripotent stem cells from neonatal mouse testis. *Cell* **119**, 1001–1012.

Kapuscinski, J. (1995). DAPI: a DNA-specific fluorescent probe. *Biotech. Histochem.* **70**, 220–233.

Kashyap, V., Laursen, K. B., Brenet, F., Viale, A. J., Scandura, J. M. and Gudas, L. J. (2013). RARγ is essential for retinoic acid induced chromatin remodeling and transcriptional activation in embryonic stem cells. *J. Cell Sci.* **126**, 999–1008.

Kastner, P., Krust, A., Mendelsohn, C., Garnier, J. M., Zelent, A., Leroy, P., Staub, A. and Chambon, P. (1990). Murine isoforms of retinoic acid receptor gamma with specific patterns of expression. *Proc. Natl. Acad. Sci. U. S. A.* **87**, 2700–2704.

Kastner, P., Mark, M., Leid, M., Gansmuller, a, Chin, W., Grondona, J. M., Decimo, D., Krezel, W., Dierich, a and Chambon, P. (1996). Abnormal spermatogenesis in RXR beta mutant mice. *Genes Dev* **10**, 80–92.

Kaufman, M. H., Robertson, E. J., Handyside, a H. and Evans, M. J. (1983). Establishment of pluripotential cell-lines from haploid mouse embryos. *J. Embryol. Exp. Morphol.* **73**, 249–261.

Keeney, S. and Neale, M. J. (2006). Initiation of meiotic recombination by formation of DNA double-strand breaks : mechanism and regulation. *Biochem. Soc. Trans.* **34**, 523–525.

Kelly, S. J. (1977). Studies of the developmental potential of 4- and 8-cell stage mouse blastomeres. *J. Exp. Zool.* **200**, 365–376.

Kerr, J. B., Duckett, R., Myers, M., Britt, K. L., Mladenovska, T. and Findlay, J. K. (2006). Quantification of healthy follicles in the neonatal and adult mouse ovary: Evidence for maintenance of primordial follicle supply. *Reproduction* **132**, 95–109.

Kerr, J. B., Hutt, K. J., Michalak, E. M., Cook, M., Vandenberg, C. J., Liew, S. H., Bouillet, P., Mills, A., Scott, C. L., Findlay, J. K., et al. (2012). DNA damage-induced primordial follicle oocyte apoptosis and loss of fertility require TAp63-mediated induction of Puma and Noxa. *Cell* **48**, 343–352.

Kerr, J. B., Myers, M. and Anderson, R. A. (2013). The dynamics of the primordial follicle reserve. *Reproduction* **146**, R205–15.

Khokha, M., Yeh, J., Grammer, T. and Harland, R. (2005). Depletion of three BMP antagonists from Spemann's organizer leads to a catastrophic loss of dorsal structures. *Dev. Cell* **8**, 401–411.

Khosravi-Farsani, S., Amidi, F., Habibi Roudkenar, M. and Alighori, S. (2015). Isolation and enrichment of mouse female germ line stem cells. *Cell J.* **16**, 406–415.

Kim, S. J. (2015). Immunological function of Blimp-1 in dendritic cells and relevance to autoimmune diseases. *Immunol. Res.* **63**, 113–120.

Kingery, H. M. (1917). Oogenesis in the white mouse. *J. Morphol.* **30**, 261–315.

Kingsley, D. M. (1994). The TGF-beta superfamily: new members, new receptors, and new genetic tests of function in different organisms. *Genes Dev.* **8**, 133–146.

Kipp, J. L., Kilen, S. M., Woodruff, T. K. and Mayo, K. E. (2007). Activin regulates estrogen receptor gene expression in the mouse ovary. *J. Biol. Chem.* **282**, 36755–36765.

Kirino, Y., Vourekas, A., Kim, N., De Lima Alves, F., Rappsilber, J., Klein, P. S., Jongens, T. A. and Mourelatos, Z. (2010). Arginine methylation of Vasa protein is conserved across phyla. *J. Biol. Chem.* **285**, 8148–8154.

Knight, P. G. and Glister, C. (2006). TGF-beta superfamily members and ovarian follicle development. *Reproduction* **132**, 191–206.

Ko, K., Tapia, N., Wu, G., Kim, J. B., Bravo, M. J. A., Sasse, P., Glaser, T., Ruau, D., Han, D. W., Greber, B., et al. (2009). Induction of pluripotency in adult unipotent germline stem cells. *Cell Stem Cell* **5**, 87–96.

Ko, K., Araúzo-Bravo, M. J., Tapia, N., Kim, J., Lin, Q., Bernemann, C., Han, D. W., Gentile, L., Reinhardt, P., Greber, B., et al. (2010). Human adult germline stem cells in question. *Nature* **465**, E1.

Koller, B. H., Hagemann, L. J., Doetschman, T., Hagaman, J. R., Huang, S., Williams, P. J., First, N. L., Maeda, N. and Smithies, O. (1989). Germ-line transmission of a planned alteration made in a hypoxanthine phosphoribosyltransferase gene by

homologous recombination in embryonic stem cells. *Proc. Natl. Acad. Sci.* **86**, 8927–8931.

Koshimizu, U., Taga, T., Watanabe, M., Saito, M. and Shirayoshi, Y. (1996). Functional requirement of gp130-mediated signaling for growth and survival of mouse primordial germ cells in vitro and derivation of embryonic germ (EG) cells. *Development* **1242**, 1235–1242.

Kotaja, N. and Sassone-Corsi, P. (2007). The chromatoid body: a germ-cell-specific RNA-processing centre. *Nat. Rev. Mol. Cell Biol.* **8**, 85–90.

Kotaja, N., Bhattacharyya, S. N., Jaskiewicz, L., Kimmins, S., Parvinen, M., Filipowicz, W. and Sassone-Corsi, P. (2006). The chromatoid body of male germ cells: similarity with processing bodies and presence of Dicer and microRNA pathway components. *Proc. Natl. Acad. Sci. U. S. A.* **103**, 2647–2652.

Koubova, J., Hu, Y.-C., Bhattacharyya, T., Soh, Y. Q. S., Gill, M. E., Goodheart, M. L., Hogarth, C. A., Griswold, M. D. and Page, D. C. (2014). Retinoic acid activates two pathways required for meiosis in mice. *PLoS Genet.* **10**, e1004541.

Krebs, L. T., Xue, Y., Norton, C. R., Sundberg, J. P., Beatus, P., Lendahl, U., Joutel, A. and Gridley, T. (2003). Characterization of Notch3-deficient mice: normal embryonic development and absence of genetic interactions with a Notch1 mutation. *Genesis* **37**, 139–143.

Krezel, W., Dupé, V., Mark, M., Dierich, A., Kastner, P. and Chambon, P. (1996). RXR gamma null mice are apparently normal and compound RXR alpha +/-/RXR beta -/-/RXR gamma -/- mutant mice are viable. *Proc. Natl. Acad. Sci. U. S. A.* **93**, 9010–9014.

Kristensen, D. M., Nielsen, J. E., Skakkebaek, N. E., Graem, N., Jacobsen, G. K., Rajpert-De Meyts, E. and Leffers, H. (2008). Presumed pluripotency markers UTF-1 and REX-1 are expressed in human adult testes and germ cell neoplasms. *Hum. Reprod.* **23**, 775–782.

Krogh, A., Larsson, B., von Heijne, G. and Sonnhammer, E. L. (2001). Predicting transmembrane protein topology with a Hidden Markov model: application to complete genomes. *J. Mol. Biol.* **305**, 567–580.

Kruh, G. D., Guo, Y., Hopper-Borge, E., Belinsky, M. G. and Chen, Z. S. (2007). ABCC10, ABCC11, and ABCC12. *Pflugers Arch. Eur. J. Physiol.* **453**, 675–684.

Kumar, D. and Boehm, U. (2013). Genetic dissection of puberty in mice. *Exp. Physiol.* **98**, 1528–1534.

Kunath, T., Saba-El-Leil, M. K., Almousailleakh, M., Wray, J., Meloche, S. and Smith, a. (2007). FGF stimulation of the Erk1/2 signalling cascade triggers transition of pluripotent embryonic stem cells from self-renewal to lineage commitment. *Development* **134**, 2895–2902.

Lai, M.-C., Chang, W.-C., Shieh, S.-Y. and Tarn, W.-Y. (2010). DDX3 regulates cell growth through translational control of cyclin E1. *Mol. Cell. Biol.* **30**, 5444–5453.

Lamm, G. M., Nicol, S. M., Fuller-Pace, F. V. and Lamond, A. L. (1996). P72: A human nuclear DEAD box protein highly related to p68. *Nucleic Acids Res.* **24**, 3739–3747.

Lange, U. C., Saitou, M., Western, P. S., Barton, S. C. and Surani, M. A. (2003). The fragilis interferon-inducible gene family of transmembrane proteins is associated with germ cell specification in mice. *BMC Dev. Biol.* **3**, 1.

Laprise, P., Chailler, P., Houde, M., Beaulieu, J.-F., Boucher, M.-J. and Rivard, N. (2002). Phosphatidylinositol 3-kinase controls human intestinal epithelial cell differentiation by promoting adherens junction assembly and p38 MAPK activation. *J. Biol. Chem.* **277**, 8226–8234.

Law, S. M. (2013). Retinoic acid receptor alpha in germ cells is important for mitosis of spermatogonia, spermatogonial differentiation and meiosis. 322.

Lawson, K. A. and Hage, W. J. (1994). Clonal analysis of the origin of primordial germ cells in the mouse. *Ciba Found Symp.* **182**, 68–84.

Lawson, K. A., Dunn, N. R., Roelen, B. A., Zeinstra, L. M., Davis, A. M., Wright, C. V, Korving, J. P. and Hogan, B. L. (1999). Bmp4 is required for the generation of primordial germ cells in the mouse embryo. *Genes Dev.* **13**, 424–436.

Le Bouffant, R., Souquet, B., Duval, N., Duquenne, C., Hervé, R., Frydman, N., Robert, B., Habert, R. and Livera, G. (2011). Msx1 and Msx2 promote meiosis initiation. *Development* **138**, 5393–5402.

Lee, J., Kotliarova, S., Kotliarov, Y., Li, A., Su, Q., Donin, N. M., Pastorino, S., Purow, B. W., Christopher, N., Zhang, W., et al. (2006). Tumor stem cells derived from glioblastomas cultured in bFGF and EGF more closely mirror the phenotype and genotype of primary tumors than do serum-cultured cell lines. *Cancer Cell* **9**, 391–403.

Lee, H. J., Selesniemi, K., Niikura, Y., Niikura, T., Klein, R., Dombkowski, D. M. and Tilly, J. L. (2007). Bone marrow transplantation generates immature oocytes and rescues long-term fertility in a preclinical mouse model of chemotherapy-induced premature ovarian failure. *J. Clin. Oncol.* **25**, 3198–3204.

Legro, R. S. (2016). Ovulation induction in polycystic ovary syndrome: Current options. *Best Pract. Res. Clin. Obstet. Gynaecol.* **37**, 152–159.

Lei, L. and Spradling, A. C. (2013). Female mice lack adult germ-line stem cells but sustain oogenesis using stable primordial follicles. *Proc. Natl. Acad. Sci.* **110**, 8585–8590.

Lei, L. and Spradling, A. C. (2016). Mouse oocytes differentiate through organelle enrichment from sister cyst germ cells. *Science (80-.).* **352**, 95–99.

Lewis, R. (2000). A stem cell legacy: Leroy Stevens. *Sci.* 14(5): 1–4.

Li, E., Sucov, H. M., Lee, K. F., Evans, R. M. and Jaenisch, R. (1993). Normal development and growth of mice carrying a targeted disruption of the alpha 1 retinoic acid receptor gene. *Proc. Natl. Acad. Sci. U. S. A.* **90**, 1590–1594.

Li, J., Shen, H., Himmel, K. L., Dupuy, A. J., Largaespada, D. A., Nakamura, T., Shaughnessy, J. D., Jenkins, N. A. and Copeland, N. G. (1999). Leukaemia disease genes: large-scale cloning and pathway predictions. *Nat. Genet.* **23**, 348–353.

Liang, L., Soyal, S. M. and Dean, J. (1997). FIGalpha, a germ cell specific transcription factor involved in the coordinate expression of the zona pellucida genes. *Development* **124**, 4939–4947.

Lin, S. and Talbot, P. (2011). Methods for culturing mouse and human embryonic stem cells. In *Embryonic Stem Cell Therapy for Osteo-Degenerative Diseases, Methods in Molecular Biology* (ed. Nieden, N. I.), pp. 31–56. Totowa, NJ: Humana Press.

Lin, C., Yang, L., Yang, J. J., Huang, Y. and Liu, Z. (2005). ATPase / Helicase Activities of p68 RNA Helicase Are Required for Pre-mRNA Splicing but Not for Assembly of the Spliceosome ATPase / Helicase Activities of p68 RNA Helicase Are Required for Pre-mRNA Splicing but Not for Assembly of the Spliceosome. *Mol. Cell. Biol.* **25**, 7484–7493.

Linder, P. and Lasko, P. (2006). Bent out of shape: RNA unwinding by the DEAD-box helicase Vasa. *Cell* **125**, 219–221.

Liu, H. and Aoki, F. (2002). Transcriptional activity associated with meiotic competence in fully grown mouse GV oocytes. *Zygote* **10**, 327–332.

Liu, Y., Wu, C., Lyu, Q., Yang, D., Albertini, D. F., Keefe, D. L. and Liu, L. (2007). Germline stem cells and neo-oogenesis in the adult human ovary. *Dev. Biol.* **306**, 112–120.

Liu, C. F., Parker, K. and Humphrey, Y. (2010). WNT4/b-catenin pathway maintains female germ cell survival by inhibiting activin bB in the mouse fetal ovary. *PLoS One* **5**, e10382.

Llames, S., García-Pérez, E., Meana, Á., Larcher, F. and del Río, M. (2015). Feeder layer cell actions and applications. *Tissue Eng. Part B Rev.* **21**, 345–353.

Lodde, V., Modina, S., Galbusera, C., Franciosi, F. and Luciano, A. M. (2007). Large-scale chromatin remodeling in germinal vesicle bovine oocytes: Interplay with gap junction functionality and developmental competence. *Mol. Reprod. Dev.* **74**, 740–749.

Lohnes, D., Kastner, P., Dierich, A., Mark, M., LeMeur, M. and Chambon, P. (1993). Function of retinoic acid receptor gamma in the mouse. *Cell* **73**, 643–658.

Lorgeoux, R.-P., Pan, Q., Duff, Y. Le and Liang, C. (2013). DDX17 promotes the production of infectious HIV-1 particles through modulating viral RNA packaging and translation frameshift. *Virology* **443**, 384–392.

Lu, C.-W., Yabuuchi, A., Chen, L., Viswanathan, S., Kim, K. and Daley, G. Q. (2008). Ras-MAPK signaling promotes trophectoderm formation from embryonic stem cells and mouse embryos. *Nat. Genet.* **40**, 921–926.

Lu, Z., Wu, M., Zhang, J., Xiong, J., Cheng, J., Shen, W., Luo, A., Fang, L. and Wang, S. (2016). Improvement in isolation and identification of mouse oogonial stem cells. *Stem Cells Int.* **2016**, 2749461.

Lufkin, T., Lohnes, D., Mark, M., Dierich, A., Gorry, P., Gaub, M. P., LeMeur, M. and Chambon, P. (1993). High postnatal lethality and testis degeneration in retinoic acid receptor alpha mutant mice. *Proc. Natl. Acad. Sci. U. S. A.* **90**, 7225–7229.

Luo, M., Yang, F., Leu, N. A., Landaiche, J., Handel, M. A., Benavente, R., La Salle, S. and Wang, P. J. (2013). MEIOB exhibits single-stranded DNA-binding and exonuclease activities and is essential for meiotic recombination. *Nat. Commun.* **4**, 2788.

Ma, J.-Y., Li, M., Luo, Y.-B., Song, S., Tian, D., Yang, J., Zhang, B., Hou, Y., Schatten, H., Liu, Z., et al. (2013). Maternal factors required for oocyte developmental competence in mice: transcriptome analysis of non-surrounded nucleolus (NSN) and surrounded nucleolus (SN) oocytes. *Cell Cycle* **12**, 1928–1938.

Macara, I. G. (2004). Par proteins: Partners in polarization. *Curr. Biol.* **14**, R160–R162.

MacColl, R. (2004). Allophycocyanin and energy transfer. *Biochim. Biophys. Acta - Bioenerg.* **1657**, 73–81.

MacGregor, G. R., Zambrowicz, B. P. and Soriano, P. (1995). Tissue non-specific alkaline phosphatase is expressed in both embryonic and extraembryonic lineages during mouse embryogenesis but is not required for migration of primordial germ cells. *Development* **121**, 1487–1496.

Madgwick, S. and Jones, K. T. (2007). How eggs arrest at metaphase II: MPF stabilisation plus APC/C inhibition equals Cytostatic Factor. *Cell Div.* **2**, 4.

Madgwick, S., Levasseur, M. and Jones, K. T. (2005). Calmodulin-dependent protein kinase II, and not protein kinase C, is sufficient for triggering cell-cycle resumption in mammalian eggs. *J. Cell Sci.* **118**, 3849–3859.

Mahi-Brown, C. A. and Yanagimachi, R. (1983). Parameters influencing ovum pickup by oviductal fimbria in the golden hamster. *Mol. Reprod. Dev.* **8**, 1–10.

Maillard, I., Koch, U., Dumortier, A., Shestova, O., Xu, L., Sai, H., Pross, S. E., Aster, J. C., Bhandoola, A., Radtke, F., et al. (2008). Canonical Notch signaling is

dispensable for the maintenance of adult hematopoietic stem cells. *Cell Stem Cell* **2**, 356–366.

Maldonado-Saldivia, J., van den Bergen, J., Krouskos, M., Gilchrist, M., Lee, C., Li, R., Sinclair, a H., Surani, M. A. and Western, P. S. (2007). Dppa2 and Dppa4 are closely linked SAP motif genes restricted to pluripotent cells and the germ line. *Stem Cells* **25**, 19–28.

Mandl, A. M. and Zuckerman, S. (1950). The numbers of normal and atretic ova in the mature rat. *J. Endocrinol.* **6**, 426–435.

Mandl, A. M. and Zuckerman, S. (1951a). Changes in ovarian structure following the injection of carbolic acid into the ovarian bursa. *J. Endocrinol.* **7**, 227–NP.

Mandl, A. M. and Zuckerman, S. (1951b). The effect of destruction of the germinal epithelium on the numbers of oocytes. *J. Endocrinol.* **7**, 103–111.

Mandl, A. M. and Zuckerman, S. (1951c). Numbers of normal and atretic oocytes in unilaterally spayed rats. *J. Endocrinol.* **7**, 112–119.

Mandl, A. M. and Zuckerman, S. (1951d). The relation of age to numbers of oocytes. *J. Endocrinol.* **7**, 190–193.

Mandl, A. M. and Zuckerman, S. (1952). The growth of the oocyte and follicle in the adult rat. *J. Endocrinol.* **8**, 126–132.

Mandl, A. M. and Zuckerman, S. (1956a). The reactivity of the X-irradiated ovary of the rat. *J. Endocrinol.* **13**, 243–261.

Mandl, A. M. and Zuckerman, S. (1956b). Changes in the mouse after X-ray sterilization. *J. Endocrinol.* **13**, 262–268.

Marjoram, L. and Wright, C. (2011). Rapid differential transport of Nodal and Lefty on sulfated proteoglycan-rich extracellular matrix regulates left-right asymmetry in Xenopus. *Development* **138**, 475–485.

Marshak, D. R., Gardner, R. L. and Gottlieb, D. eds. (2001). Primordial germ cells as stem cells. In *Stem Cell Biology*, Cold Spring Harbor Monograph Series.

Martin, G. R. (1981). Isolation of a pluripotent cell line from early mouse embryos cultured in medium conditioned by teratocarcinoma stem cells. *Proc. Natl. Acad. Sci.* **78**, 7634–7638.

Martin, G. R. and Evans, M. J. (1975). Differentiation of clonal lines of teratocarcinoma cells: formation of embryoid bodies in vitro. *Proc. Natl. Acad. Sci. U. S. A.* **72**, 1441–5.

Martins, G. A., Cimmino, L., Shapiro-Shelef, M., Szabolcs, M., Herron, A., Magnusdottir, E. and Calame, K. (2006). Transcriptional repressor Blimp-1 regulates T cell homeostasis and function. *Nat. Immunol.* **7**, 457–465.

Masui, S., Nakatake, Y., Toyooka, Y., Shimosato, D., Yagi, R., Takahashi, K., Okochi, H., Okuda, A., Matoba, R., Sharov, A. A., et al. (2007). Pluripotency governed by Sox2 via regulation of Oct3/4 expression in mouse embryonic stem cells. *Nat. Cell Biol.* **9**, 625–635.

Matozaki, T., Suzuki, T., Uchida, T., Inazawa, J., Ariyama, T., Matsuda, K., Horita, K., Noguchi, H., Mizuno, H. and Sakamoto, C. (1994). Molecular cloning of a human transmembrane-type protein tyrosine phosphatase and its expression in gastrointestinal cancers. *J. Biol. Chem.* **269**, 2075–2081.

Matsui, Y. and Okamura, D. (2005). Mechanisms of germ-cell specification in mouse embryos. *BioEssays* **27**, 136–143.

Matsui, Y., Zsebo, K. and Hogan, B. L. M. (1992). Derivation of pluripotential embryonic stem cells from murine primordial germ cells in culture. *Cell* **70**, 841–847.

Matsui, Y., Takehara, A., Tokitake, Y., Ikeda, M., Obara, Y., Morita-Fujimura, Y., Kimura, T. and Nakano, T. (2014). The majority of early primordial germ cells acquire pluripotency by AKT activation. *Development* **141**, 4457–4467.

Mattioli, M. and Barboni, B. (2000). Signal transduction mechanism for LH in the cumulus-oocyte complex. *Mol. Cell. Endocrinol.* **161**, 19–23.

McGee, E. A. and Hsueh, A. J. (2000). Initial and cyclic recruitment of ovarian follicles. *Endocr. Rev.* **21**, 200–214.

Medrano, J. V, Ramathal, C., Nguyen, H. N., Simon, C. and Reijo Pera, R. A. (2012). Divergent RNA-binding proteins, DAZL and VASA, induce meiotic progression in human germ cells derived in vitro. *Stem Cells* **30**, 441–451.

Meduri, G., Bachelot, A., Cocca, M. P., Vasseur, C., Rodien, P., Kuttenn, F., Touraine, P. and M. Misrahi (2008). Molecular pathology of the FSH receptor: New insights into FSH physiology. *Mol. Cell. Endocrinol.* **282**, 130–142.

Meissner, A., Mikkelsen, T. S., Gu, H., Wernig, M., Sivachenko, A., Zhang, X., Bernstein, B. E., Nusbaum, C., Jaffe, D. B., Gnirke, A., et al. (2008). Genome-scale DNA methylation maps of pluripotent and differentiated cells. *Nature* **454**, 766–770.

Meldrum, D. R., Casper, R. F., Diez-Juan, A., Simon, C., Domar, A. D. and Frydman, R. (2016). Aging and the environment affect gamete and embryo potential: Can we intervene? *Fertil. Steril.* **105**, 548–559.

Meng, X., Lindahl, M., Hyvönen, M. E., Parvinen, M., Rooij, D. G. de, Hess, M. W., Raatikainen-Ahoka, A., Sainio, K., Rauvala, H., Lakso, M., et al. (2000). Regulation of cell fate decision of undifferentiated spermatogonia by GDNF. *Science (80-.).* **287**, 1489–1493.

Miazek, A., Brockhaus, M., Langen, H., Braun, A. and Kisielow, P. (1997). Identification of a T cell lineage-specific RNA/DNA helicase and its cell surface expression during intrathymic education of alpha beta and gamma delta T cells. *Eur J Immunol* **27**, 3269–3282.

Mintz, B. and Illmensee, K. (1975). Normal genetically mosaic mice produced from malignant teratocarcinoma cells. *Proc. Natl. Acad. Sci. U. S. A.* **72**, 3585–3589.

Miyauchi, Y., Miyamoto, H., Yoshida, S., Mori, T., Kanagawa, H., Katsuyama, E., Fujie, A., Hao, W., Hoshi, H., Miyamoto, K., et al. (2012). Conditional inactivation of Blimp1 in adult mice promotes increased bone mass. *J. Biol. Chem.* **287**, 28508–28517.

Mizusaki, H., Kawabe, K., Mukai, T., Ariyoshi, E., Kasahara, M., Yoshioka, H., Swain, A. and Morohashi, K.-I. (2003). Dax-1 (dosage-sensitive sex reversal-adrenal hypoplasia congenita critical region on the X chromosome, gene 1) gene

transcription is regulated by wnt4 in the female developing gonad. *Mol. Endocrinol.* **17**, 507–519.

Mizusawa, Y., Kuji, N., Tanaka, Y., Tanaka, M., Ikeda, E., Komatsu, S., Kato, S. and Yoshimura, Y. (2010). Expression of human oocyte-specific linker histone protein and its incorporation into sperm chromatin during fertilization. *Fertil. Steril.* **93**, 1134–1141.

Molyneaux, K. A., Zinszner, H., Kunwar, P. S., Schaible, K., Stebler, J., Sunshine, M. J., O'Brien, W., Raz, E., Littman, D., Wylie, C., et al. (2003). The chemokine SDF1/CXCL12 and its receptor CXCR4 regulate mouse germ cell migration and survival. *Development* **130**, 4279–4286.

Mora, J. M., Fenwick, M. A., Castle, L., Baithun, M., Ryder, T. A., Mobberley, M., Carzaniga, R., Franks, S. and Hardy, K. (2012). Characterization and significance of adhesion and junction-related proteins in mouse ovarian follicles. *Biol. Reprod.* **86**, 153–153.

Morgan, S., Anderson, R. A., Gourley, C., Wallace, W. H. and Spears, N. (2012). How do chemotherapeutic agents damage the ovary? *Hum. Reprod. Update* **18**, 525–535.

Mork, L., Tang, H., Batchvarov, I. and Capel, B. (2012a). Mouse germ cell clusters form by aggregation as well as clonal divisions. *Mech. Dev.* **128**, 591–596.

Mork, L., Maatouk, D. M., McMahon, J. A., Guo, J. J., Zhang, P., McMahon, A. P. and Capel, B. (2012b). Temporal differences in granulosa cell specification in the ovary reflect distinct follicle fates in mice. *Biol. Reprod.* **86**, 37: 1–9.

Morstyn, G., Nicola, N. A. and Metcalf, D. (1980). Purification of hemopoietic progenitor cells from human marrow using a fucose-binding lectin and cell sorting. *Blood* **56**, 798–805.

Moy, R. H., Cole, B. S., Yasunaga, A., Gold, B., Shankarling, G., Varble, A., Molleston, J. M., TenOever, B. R., Lynch, K. W. and Cherry, S. (2014). Stem loop recognition by DDX17 facilitates miRNA processing and antiviral defense. *Cell* **158**, 764–777.

Muncan, V., Heijmans, J., Krasinski, S. D., Büller, N. V, Wildenberg, M. E., Meisner, S., Radonjic, M., Stapleton, K. A., Lamers, W. H., Biemond, I., et al. (2011).

Blimp1 regulates the transition of neonatal to adult intestinal epithelium. *Nat. Commun.* **2**, 452.

Nagata, M., Yamaguchi, Y., Komatsu, Y. and Ito, K. (1995). Mitosis and the presence of binucleate cells among glomerular podocytes in diseased human kidneys. *Nephron* **70**, 68–71.

Nagy, A., Gertsenstein, M., Vintersten, K. and Behringer, R. (2003). *Isolation and culture of blastocyst-derived stem cell lines*. Third. (ed. Nagy, A., Gertsenstein, M., Vintersten, K., and Behringer, R.) New York: Cold Spring Harbor Laboratory Press.

Namba, M., Fukushima, F. and Kimoto, T. (1982). Effects of feeder layers made of human, mouse, hamster, and rat cells on the cloning efficiency of transformed human cells. *In Vitro* **18**, 469–475.

Navaroli, D. M., Tilly, J. L. and Woods, D. C. (2016). Isolation of mammalian Oogonial Stem Cells by antibody-based fluorescence-activated cell sorting. In *Oogenesis: Methods and Protocols. Methods in Molecular Biology* (ed. Nezis, I. P.), pp. 253–268. New York: Springer Science+Business Media.

Ng, A., Tan, S., Singh, G., Rizk, P., Swathi, Y., Tan, T. Z., Huang, R. Y., Leushacke, M. and Barker, N. (2014). Lgr5 marks stem/progenitor cells in ovary and tubal epithelia. *Nat. Cell Biol.* **16**, 745–757.

Nicholas, C. R., Haston, K. M., Grewall, A. K., Longacre, T. A. and Reijo Pera, R. A. (2009). Transplantation directs oocyte maturation from embryonic stem cells and provides a therapeutic strategy for female infertility. *Hum. Mol. Genet.* **18**, 4376–4389.

Nicholls, P. K., Harrison, C. A., Gilchrist, R. B., Farnworth, P. G. and Stanton, P. G. (2009). Growth differentiation factor 9 is a germ cell regulator of Sertoli cell function. *Endocrinology* **150**, 2481–2490.

Nichols, J. and Smith, A. (2009). Naive and primed pluripotent states. *Cell Stem Cell* **4**, 487–492.

Nichols, J., Jones, K., Phillips, J. M., Newland, S. A., Roode, M., Mansfield, W., Smith, A. and Cooke, A. (2009). Validated germline-competent embryonic stem cell lines from nonobese diabetic mice. *Nat. Med.* **15**, 814–818.

Nicol, S. M., Causevic, M., Prescott, A. R. and Fuller-Pace, F. V. (2000). The nuclear DEAD box RNA helicase p68 interacts with the nucleolar protein fibrillarin and colocalizes specifically in nascent nucleoli during telophase. *Exp. Cell Res.* **257**, 272–280.

Niu, W., Wang, Y., Wang, Z., Xin, Q., Wang, Y., Feng, L., Zhao, L., Wen, J., Zhang, H., Wang, C., et al. (2016). JNK signaling regulates E-cadherin junctions in germline cysts and determines primordial follicle formation in mice. *Development* 1778–1787.

Niwa, H., Burdon, T., Chambers, I. and Smith, a (1998). Self-renewal of pluripotent embryonic stem cells is mediated via activation of STAT3. *Genes Dev.* **12**, 2048–60.

Niwa, H., Miyazaki, J. and Smith, A. G. (2000). Quantitative expression of Oct-3/4 defines differentiation, dedifferentiation or self-renewal of ES cells. *Nat. Genet.* **24**, 372–376.

Noce, T., Okamoto-Ito, S. and Tsunekawa, N. (2001). Vasa homolog genes in mammalian germ cell development. *Cell Struct. Funct.* **26**, 131–136.

Norris, R. P., Freudzon, M., Mehlmann, L. M., Cowan, A. E., Simon, A. M., Paul, D. L., Lampe, P. D. and Jaffe, L. A. (2008). Luteinizing hormone causes MAP kinase-dependent phosphorylation and closure of connexin 43 gap junctions in mouse ovarian follicles: one of two paths to meiotic resumption. *Development* **135**, 3229–3238.

Nott, T. J., Petsalaki, E., Farber, P., Jervis, D., Fussner, E., Plochowietz, A., Craggs, T. D., Bazett-Jones, D. P., Pawson, T., Forman-Kay, J. D., et al. (2015). Phase transition of a disordered nuage protein generates environmentally responsive membraneless organelles. *Mol. Cell* **57**, 936–947.

Nusse, R. (2008). Wnt signaling and stem cell control. *Cell Res.* **18**, 523–527.

Ogura, A., Inoue, K., Takano, K., Wakayama, T. and Yanagimachi, R. (2000). Birth of mice after nuclear transfer by electrofusion using tail tip cells. *Mol. Reprod. Dev.* **57**, 55–59.

Ohinata, Y., Payer, B., O'Carroll, D., Ancelin, K., Ono, Y., Sano, M., Barton, S. C., Obukhanych, T., Nussenzweig, M., Tarakhovsky, A., et al. (2005). Blimp1 is a critical determinant of the germ cell lineage in mice. *Nature* **436**, 207–213.

Ohinata, Y., Ohta, H., Shigeta, M., Yamanaka, K., Wakayama, T. and Saitou, M. (2009). A signaling principle for the specification of the germ cell lineage in mice. *Cell* **137**, 571–584.

Okamura, D., Kimura, T., Nakano, T. and Matsui, Y. (2003). Cadherin-mediated cell interaction regulates germ cell determination in mice. *Development* **130**, 6423–6430.

Okamura, D., Hayashi, K. and Matsui, Y. (2005). Mouse epiblasts change responsiveness to BMP4 signal required for PGC formation through functions of extraembryonic ectoderm. *Mol. Reprod. Dev.* **70**, 20–29.

Okita, K., Ichisaka, T. and Yamanaka, S. (2007). Generation of germline-competent induced pluripotent stem cells. *Nature* **448**, 313–317.

Oktay, K. and Oktem, O. (2007). Regeneration of oocytes after chemotherapy: Connecting the evidence from mouse to human. *J. Clin. Oncol.* **25**, 3185–3187.

Oktay, K., Briggs, D. and Gosden, R. G. (1997). Ontogeny of follicle-stimulating hormone receptor gene expression in isolated human ovarian follicles. *J. Clin. Endocrinol. Metab.* **82**, 3748–3751.

Oktem, O. and Urman, B. (2010). Understanding follicle growth in vivo. *Hum. Reprod.* **25**, 2944–2954.

Okuda, A., Fukushima, A., Nishimoto, M., Orimo, A., Yamagishi, T., Nabeshima, Y., Kuro-o, M., Nabeshima, Y. I., Boon, K., Keaveney, M., et al. (1998). UTF1, a novel transcriptional coactivator expressed in pluripotent embryonic stem cells and extra-embryonic cells. *EMBO J.* **17**, 2019–2032.

Olsen, L. C., Aasland, R. and Fjose, A. (1997). A vasa-like gene in zebrafish identifies putative primordial germ cells. *Mech. Dev.* **66**, 95–105.

Oshiumi, H., Sakai, K., Matsumoto, M. and Seya, T. (2010). DEAD/H BOX 3 (DDX3) helicase binds the RIG-I adaptor IPS-1 to up-regulate IFN-??-inducing potential. *Eur. J. Immunol.* **40**, 940–948.

Pacchiarotti, J., Maki, C., Ramos, T., Marh, J., Howerton, K., Wong, J., Pham, J., Anorve, S., Chow, Y.-C. and Izadyar, F. (2010). Differentiation potential of germ line stem cells derived from the postnatal mouse ovary. *Differentiation* **79**, 159–170.

Page, S. L. and Hawley, R. S. (2004a). The genetics and molecular biology of the synaptonemal complex. *Annu. Rev. Cell Dev. Biol.* **20**, 525–558.

Page, S. L. and Hawley, R. S. (2004b). The genetics and molecular biology of the synaptonemal complex. *Annu. Rev. Cell Dev. Biol.* **20**, 525–558.

Pangas, S. A., Choi, Y., Ballow, D. J., Zhao, Y., Westphal, H., Matzuk, M. M. and Rajkovic, A. (2006). Oogenesis requires germ cell-specific transcriptional regulators Sohlh1 and Lhx8. *Proc. Natl. Acad. Sci. U. S. A.* **103**, 8090–8095.

Parfitt, G. J., Kavianpour, B., Wu, K. L., Xie, Y., Brown, D. J. and Jester, J. V. (2015). Immunofluorescence tomography of mouse ocular surface epithelial stem cells and their niche microenvironment. *Investig. Opthalmology Vis. Sci.* **56**, 7338–7344.

Park, E. and Tilly, J. L. (2014). Use of DEAD-box polypeptide-4 (Ddx4) gene promoter-driven fluorescent reporter mice to identify mitotically active germ cells in postnatal mouse ovaries. *Mol. Hum. Reprod.* **21**, 58–65.

Park, T. S., Galic, Z., Conway, A. E., Lindgren, A., van Handel, B. J., Magnusson, M., Richter, L., Teitell, M. A., Mikkola, H. K. A., Lowry, W. E., et al. (2009). Derivation of primordial germ cells from human embryonic and induced pluripotent stem cells is significantly improved by coculture with human fetal gonadal cells. *Stem Cells* **27**, 783–795.

Park, E., Woods, D. C. and Tilly, J. L. (2013). Bone morphogenetic protein 4 promotes mammalian oogonial stem cell differentiation via Smad1/5/ 8 signaling. *Fertil. Steril.* **100**, 1468 – 1475.

Park, Y.-G., Lee, S.-E., Kim, E.-Y., Hyun, H., Shin, M.-Y., Son, Y.-J., Kim, S.-Y. and Park, S.-P. (2015). Effects of feeder cell types on culture of mouse embryonic stem cell in vitro. *Dev. Reprod.* **19**, 119–126.

Parkers, A. S., U Fielding and Brambell, W. R. (1927). Ovarian regeneration in the mouse after complete double ovariectomy. *Proc. R. Soc. London Biol. Sci.* **101**, 328–354.

Pece, S., Chiariello, M., Murga, C. and Gutkind, J. S. (1999). Activation of the protein kinase Akt / PKB by the formation of E-cadherin-mediated cell-cell- junctions. *J. Biol. Chem.* **274**, 19347–19351.

Pellegrini, M., Grimaldi, P., Rossi, P., Geremia, R. and Dolci, S. (2003). Developmental expression of BMP4/ALK3/SMAD5 signaling pathway in the mouse testis: a potential role of BMP4 in spermatogonia differentiation. *J. Cell Sci.* **116**, 3363–3372.

Pepling, M. E. and Spradling, A. C. (1998). Female mouse germ cells form synchronously dividing cysts. *Development* **125**, 3323–3328.

Pepling, M. E. and Spradling, A. C. (2001). Mouse ovarian germ cell cysts undergo programmed breakdown to form primordial follicles. *Dev. Biol.* **234**, 339–351.

Pepling, M. E., Wilhelm, J. E., O'Hara, A. L., Gephardt, G. W. and Spradling, A. C. (2007). Mouse oocytes within germ cell cysts and primordial follicles contain a Balbiani body. *Proc. Natl. Acad. Sci. U. S. A.* **104**, 187–192.

Perfetto, S. P., Chattopadhyay, P. K. and Roederer, M. (2004). Seventeen-colour flow cytometry: unravelling the immune system. *Nat. Rev. Immunol.* **4**, 648–655.

Perfetto, S. P., Ambrozak, D., Nguyen, R., Chattopadhyay, P. and Roederer, M. (2006). Quality assurance for polychromatic flow cytometry. *Nat. Protoc.* **1**, 1522–1530.

Pesce, M., Klinger, F. G. and De Felici, M. (2002). Derivation in culture of primordial germ cells from cells of the mouse epiblast: phenotypic induction and growth control by Bmp4 signalling. *Mech. Dev.* **112**, 15–24.

Peters, H. (1969). The development of the mouse ovary from birth to maturity. *Acta Endocrinol. (Copenh).* **62**, 98–116.

Pincus, B. Y. G. and Enzmann, E. V. (1935). The comparative behavior of mammalian eggs in vivo and in vitro. I. The activation of ovarian eggs. *J. Exp. Med.* **62**, 665–675.

Pöpperl, H. and Featherstone, M. S. (1993). Identification of a retinoic acid response element upstream of the murine Hox-4.2 gene. *Mol. Cell. Biol.* **13**, 257–265.

Potten, C. S. (1998). Stem cells in gastrointestinal epithelium: numbers, characteristics and death. *Philos. Trans. R. Soc. Lond. B. Biol. Sci.* **353**, 821–830.

Poulton, J., Chiaratti, M. R., Meirelles, F. V., Kennedy, S., Wells, D. and Holt, I. J. (2010). Transmission of mitochondrial DNA diseases and ways to prevent them. *PLoS Genet.* **6**, e1001066.

Powell, K. (2007). Going against the grain. *PLoS Biol.* **5**, e338.

Qing, T., Shi, Y., Qin, H., Ye, X., Wei, W., Liu, H., Ding, M. and Deng, H. (2007). Induction of oocyte-like cells from mouse embryonic stem cells by co-culture with ovarian granulosa cells. *Differentiation* **75**, 902–911.

Rajkovic, A., Pangas, S. A., Ballow, D., Suzumori, N. and Matzuk, M. M. (2004). NOBOX deficiency disrupts early folliculogenesis and oocyte-specific gene expression. *Science (80-.).* **305**, 1157–1159.

Rastan, S. and Robertson, E. J. (1985). X-chromosome deletions in embryo-derived (EK) cell lines associated with lack of X-chromosome inactivation. *J. Embryol. Exp. Morphol.* **90**, 379–388.

Reddy, P., Zheng, W. and Liu, K. (2010). Mechanisms maintaining the dormancy and survival of mammalian primordial follicles. *Trends Endocrinol. Metab.* **21**, 96–103.

Red-Horse, K., Ueno, H., Weissman, I. L. and Krasnow, M. (2010). Coronary arteries form by developmental reprogramming of venous cells. *Nature* **464**, 549–553.

Reizel, Y., Chapal-ilani, N., Adar, R., Itzkovitz, S., Elbaz, J. and Maruvka, Y. E. (2011). Colon stem cell and crypt dynamics exposed by cell lineage reconstruction. *PLoS Genet.* **7**, e1002192.

Reizel, Y., Itzkovitz, S., Adar, R., Elbaz, J., Jinich, A., Chapal-Ilani, N., Maruvka, Y. E., Nevo, N., Marx, Z., Horovitz, I., et al. (2012). Cell lineage analysis of the mammalian female germline. *PLoS Genet.* **8**, e1002477.

Resnick, J. L., Bixler, L. S., Cheng, L. and Donovan, P. J. (1992). Long-term proliferation of mouse primordial germ cells in culture. *Nature* **359**, 550–551.

Reynolds, N., Collier, B., Maratou, K., Bingham, V., Speed, R. M., Taggart, M., Semple, C. A., Gray, N. K. and Cooke, H. J. (2005). Dazl binds in vivo to specific transcripts and can regulate the pre-meiotic translation of Mvh in germ cells. *Hum. Mol. Genet.* **14**, 3899–3909.

Rinkevich, Y., Lindau, P., Ueno, H., Longaker, M. T. and Weissman, I. L. (2011). Germ and lineage restricted stem/progenitors regenerate the mouse digit tip. *Nature* **476**, 409–413.

Roberts, R. M. and Fisher, S. J. (2011). Trophoblast stem cells. *Biol. Reprod.* **84**, 412–421.

Robertson, E. J., Evans, M. J. and Kaufman, M. H. (1983). X-chromosome instability in pluripotent stem cell lines derived from parthenogenetic embryos. *J. Embryol. Exp. Morphol.* **74**, 297–309.

Robertson, E., Bradley, A., Kuehn, M. and Evans, M. (1986). Germ-line transmission of genes introduced into cultured pluripotential cells by retroviral vector. *Nature* **323**, 445–448.

Robertson, E. J., Charatsi, I., Joyner, C. J., Koonce, C. H., Morgan, M., Islam, A., Paterson, C., Lejsek, E., Arnold, S. J., Kallies, A., et al. (2007). Blimp1 regulates development of the posterior forelimb, caudal pharyngeal arches, heart and sensory vibrissae in mice. *Development* **134**, 4335–4345.

Rochat, A., Kobayashi, K. and Barrandon, Y. (1994). Location of stem cells of human hair follicles by clonal analysis. *Cell* **76**, 1063–1073.

Romero-Lanman, E. E., Pavlovic, S., Amlani, B., Chin, Y. and Benezra, R. (2011). Id1 maintains embryonic stem cell self-renewal by up-regulation of Nanog and repression of Brachyury expression. *Stem Cells Dev.* **21**, 384–393.

Romito, A. and Cobellis, G. (2016). Pluripotent stem cells: Current understanding and future directions. *Stem Cells Int.* **2016**,.

Roos, S., Lindgren, S. and Jonsson, H. (1999). Autoaggregation of Lactobacillus reuteri is mediated by a putative DEAD-box helicase. *Mol. Microbiol.* **32**, 427–436.

Ross, A., Munger, S. and Capel, B. (2007). Bmp7 regulates germ cell proliferation in mouse fetal gonads. *Sex. Dev.* **1**, 127–137.

Ross, A. J., Tilman, C., Yao, H., MacLaughin, D. and Capel, B. (2014). AMH induces mesonephric cell migration in XX gonads. *Mol. Cell. Endocrinol.* **211**, 1–7.

Rössler, O. G., Hloch, P., Schütz, N., Weitzenegger, T. and Stahl, H. (2000). Structure and expression of the human p68 RNA helicase gene. *Nucleic Acids Res.* **28**, 932–939.

Ruggiu, M., Speed, R., Taggart, M., McKay, S. J., Kilanowski, F., Saunders, P., Dorin, J. and Cooke, H. J. (1997). The mouse Dazla gene encodes a cytoplasmic protein essential for gametogenesis. *Nature* **389**, 73–77.

Runyan, C., Schaible, K., Molyneaux, K., Wang, Z., Levin, L. and Wylie, C. (2006). Steel factor controls midline cell death of primordial germ cells and is essential for their normal proliferation and migration. *Development* **133**, 4861–4869.

Saitou, M. (2009). Germ cell specification in mice. *Curr. Opin. Genet. Dev.* **19**, 386–395.

Saitou, M., Barton, S. C. and Surani, M. A. (2002). A molecular programme for the specification of germ cell fate in mice. *Nature* **418**, 293–300.

Salustri, A., Yanagishita, M. and Hascall, V. C. (1989). Synthesis and accumulation of hyaluronic acid and proteoglycans in the mouse cumulus cell-oocyte complex during follicle-stimulating hormone-induced mucification. *J. Biol. Chem.* **264**, 13840–13847.

Salustri, A., Camaioni, A., Di Giacomo, M., Fulop, C. and Hascall, V. C. (1999). Hyaluronan and proteoglycans in ovarian follicles. *Hum. Reprod. Update* **5**, 293–301.

Salustri, A., Garlanda, C., Hirsch, E., De Acetis, M., Maccagno, A., Bottazzi, B., Doni, A., Bastone, A., Mantovani, G., Beck Peccoz, P., et al. (2004). PTX3 plays a key role in the organization of the cumulus oophorus extracellular matrix and in in vivo fertilization. *Development* **131**, 1577–1586.

Salvador, L. M., Silva, C. P., Kostetskii, I., Radice, G. L. and Strauss, J. F. (2008). The promoter of the oocyte-specific gene, Gdf9, is active in population of cultured mouse embryonic stem cells with an oocyte-like phenotype. *Methods* **45**, 172–181.

Samaan, S., Tranchevent, L. C., Dardenne, E., Polay Espinoza, M., Zonta, E., Germann, S., Gratadou, L., Dutertre, M. and Auboeuf, D. (2014). The Ddx5 and Ddx17 RNA helicases are cornerstones in the complex regulatory array of steroid hormone-signaling pathways. *Nucleic Acids Res.* **42**, 2197–2207.

Sang, X., Curran, M. S. and Wood, A. W. (2008). Paracrine insulin-like growth factor signaling influences primordial germ cell migration: in vivo evidence from the zebrafish model. *Endocrinology* **149**, 5035–5042.

Santiquet, N., Vallières, L., Pothier, F., Sirard, M.-A., Robert, C. and Richard, F. (2012). Transplanted bone marrow cells do not provide new oocytes but rescue

fertility in female mice following treatment with chemotherapeutic agents. *Cell Reprogr.* **14**, 123–129.

Santos, F., Hendrich, B., Reik, W. and Dean, W. (2002). Dynamic reprogramming of DNA methylation in the early mouse embryo. *Dev. Biol.* **241**, 172–182.

Santucci-Darmanin, S., Walpita, D., Lespinasse, F., Desnuelle, C., Ashley, T. and Paquis-Flucklinger, V. (2000). MSH4 acts in conjunction with MLH1 during mammalian meiosis. *FASEB* **14**, 1539–1547.

Sato, M., Kimura, T., Kurokawa, K., Fujita, Y., Abe, K., Masuhara, M., Yasunaga, T., Ryo, A., Yamamoto, M. and Nakano, T. (2002). Identification of PGC7, a new gene expressed specifically in preimplantation embryos and germ cells. *Mech. Dev.* **113**, 91–94.

Scadden, D. T. (2006). The stem-cell niche as an entity of action. *Nature* **441**, 1075–1079.

Schiemann, W. P., Bartoe, J. L. and Nathanson, N. M. (1997). Box 3-independent signaling mechanisms are involved in leukemia inhibitory factor receptor - and gp130-mediated stimulation of mitogen-activated protein kinase. *J. Biol. Chem.* **272**, 16631–16636.

Schofield, R. (1983). The stem cell system. *Biomed. Pharmacother.* **37**, 375–380.

Scholer, H. R., Hatzopoulos, A. K., Balling, R., Suzuki, N. and Gruss, P. (1989). Mouse embryogenesis: evidence for germline-specific expression of an Oct factor. *EMBO J.* **8**, 2543–2550.

Schramm, S., Fraune, J., Naumann, R., Hernandez-Hernandez, A., Höög, C., Cooke, H. J., Alsheimer, M. and Benavente, R. (2011). A novel mouse synaptonemal complex protein is essential for loading of central element proteins, recombination, and fertility. *PLoS Genet.* **7**, e1002088.

Schröeder, M. (2010). Human DEAD-box protein 3 has multiple functions in gene regulation and cell cycle control and is a prime target for viral manipulation. *Biochem. Pharmacol.* **79**, 297–306.

Seale, P., Asakura, A. and Rudnicki, M. a (2001). The potential of muscle stem cells. *Dev. Cell* **1**, 333–342.

Sefton, B. and Rubin, H. (1970). Release from density dependent growth inhibition by proteolytic enzymes. *Nature* **227**, 843–845.

Selesniemi, K., Lee, H. J., Niikura, T. and Tilly, J. L. (2009). Young adult donor bone marrow infusions into female mice postpone age-related reproductive failure and improve offspring survival. *Aging (Albany. NY).* **1**, 49–57.

Sen, A., Prizant, H., Light, A., Biswas, A., Hayes, E., Lee, H.-J., Barad, D., Gleicher, N. and Hammes, S. R. (2014). Androgens regulate ovarian follicular development by increasing follicle stimulating hormone receptor and microRNA-125b expression. *Proc. Natl. Acad. Sci. U. S. A.* **111**, 3008–3013.

Sengoku, T., Nureki, O., Nakamura, A., Kobayashi, S. and Yokoyama, S. (2006). Structural basis for RNA unwinding by the DEAD-box protein Drosophila Vasa. *Cell* **125**, 287–300.

Shamblott, M. J., Axelman, J., Wang, S., Bugg, E. M., Littlefield, J. W., Donovan, P. J., Blumenthal, P. D., Huggins, G. R. and Gearhart, J. D. (1998). Derivation of pluripotent stem cells from cultured human primordial germ cells. *Proc. Natl. Acad. Sci.* **95**, 13726–13731.

Shen, L., Hillebrand, A., Wang, D. Q.-H. and Liu, M. (2012). Isolation and primary culture of rat hepatic cells. *J. Vis. Exp.* 1–4.

Shi, Y. and Massagué, J. (2003). Mechanisms of TGF-beta signaling from cell membrane to the nucleus. *Cell* **113**, 685–700.

Shibata, N., Tsunekawa, N., Okamoto-Ito, S., Akasu, R., Tokumasu, A. and Noce, T. (2004). Mouse RanBPM is a partner gene to a germline specific RNA helicase, mouse vasa homolog protein. *Mol. Reprod. Dev.* **67**, 1–7.

Shoji, S., Yoshida, N., Amanai, M., Ohgishi, M., Fukui, T., Fujimoto, S., Nakano, Y., Kajikawa, E. and Perry, a C. (2006). Mammalian Emi2 mediates cytostatic arrest and transduces the signal for meiotic exit via Cdc20. *Embo J.* **25**, 834–845.

Shuhaibar, L. C., Egbert, J. R., Norris, R. P., Lampe, P. D., Nikolaev, V. O., Thunemann, M., Wen, L., Feil, R. and Jaffe, L. a (2015). Intercellular signaling via cyclic GMP diffusion through gap junctions restarts meiosis in mouse ovarian follicles. *Proc. Natl. Acad. Sci. U. S. A.* **112**, 5527–5532.

Snider, C., Jayasinghe, S., Hristova, K. and White, S. H. (2009). MPEx: a tool for exploring membrane proteins. *Protein Sci.* **18**, 2624–2628.

Soh, Y. Q. S., Junker, J. P., Gill, M. E., Mueller, J. L., van Oudenaarden, A. and Page, D. C. (2015). A gene regulatory program for meiotic prophase in the fetal ovary. *PLoS Genet.* **11**, e1005531.

Solis, N., Larsen, M. R. and Cordwell, S. J. (2010). Improved accuracy of cell surface shaving proteomics in Staphylococcus aureus using a false-positive control. *Proteomics* **10**, 2037–2049.

Song, X., Zhu, C.-H., Doan, C. and Xie, T. (2002). Germline stem cells anchored by adherens junctions in the Drosophila ovary niches. *Science (80-.).* **296**, 1855–1857.

Souquet, B., Abby, E., Hervé, R., Finsterbusch, F., Tourpin, S., Le Bouffant, R., Duquenne, C., Messiaen, S., Martini, E., Bernardino-Sgherri, J., et al. (2013). MEIOB targets single-strand DNA and is necessary for meiotic recombination. *PLoS Genet.* **9**, e1003784.

Soyal, S. M., Amleh, A. and Dean, J. (2000). FIGalpha, a germ cell-specific transcription factor required for ovarian follicle formation. *Development* **127**, 4645–4654.

Srivastava, J. (2015). Introduction to panel design and sample preparation.

Stein, P., Rozhkov, N. V, Li, F., Cárdenas, F. L., Davydenk, O., Vandivier, L. E., Gregory, B. D., Hannon, G. J. and Schultz, R. M. (2015). Essential role for endogenous siRNAs during meiosis in mouse oocytes. *PLoS Genet.* **11**, e1005013.

Steinhauer, J. and Treisman, J. E. (2009). Lipid-modified morphogens: functions of fats. *Curr. Opin. Genet. Dev.* **19**, 308–314.

Stevens, L. C. (1970). The development of transplantable teratocarcinomas from intratesticular grafts of pre- and postimplantation mouse embryos. *Dev. Biol.* **21**, 364–382.

Stith, B. J., Goalstone, M., Silva, S. and Jaynes, C. (1993). Inositol 1,4,5-trisphosphate mass changes from fertilization through first cleavage in Xenopus laevis. *Mol. Biol. Cell* **4**, 435–443.

Story, R. M., Li, H. and Abelson, J. N. (2001). Crystal structure of a DEAD box protein from the hyperthermophile Methanococcus jannaschii. *Proc. Natl. Acad. Sci. U. S. A.* **98**, 1465–1470.

Stricker, S. A. (1999). Comparative biology of calcium signaling during fertilization and egg activation in animals. *Dev. Biol.* **211**, 157–176.

Strome, S. and Lehmann, R. (2007). Germ versus soma decisions: lessons from flies and worms. *Science (80-.).* **316**, 392–393.

Su, Y.-Q., Wu, X., O'Brien, M. J., Pendola, F. L., Denegre, J. N., Matzuk, M. M. and Eppig, J. J. (2004). Synergistic roles of BMP15 and GDF9 in the development and function of the oocyte-cumulus cell complex in mice: genetic evidence for an oocyte-granulosa cell regulatory loop. *Dev. Biol.* **276**, 64–73.

Sucov, H. M., Dyson, E., Gumeringer, C. L., Price, J., Chien, K. R. and Evans, R. M. (1994). RXRa mutant mice establish a genetic basis for vitamin A signalling in heart morphogenesis. *Genes Dev.* **8**, 1007–1018.

Sugimoto, K., Koh, E., Sin, H.-S., Maeda, Y., Narimoto, K., Izumi, K., Kobori, Y., Kitamura, E., Nagase, H., Yoshida, A., et al. (2009). Tissue-specific differentially methylated regions of the human VASA gene are potentially associated with maturation arrest phenotype in the testis. *J. Hum. Genet.* **54**, 450–456.

Suh, E.-K., Yang, A., Kettenbach, A., Bamberger, C., Michaelis, A. H., Zhu, Z., Elvin, J. A., Bronson, R. T., Crum, C. P. and McKeon, F. (2006). p63 protects the female germ line during meiotic arrest. *Nature* **444**, 624–628.

Sun, Q. Y., Miao, Y. L. and Schatten, H. (2009). Towards a new understanding on the regulation of mammalian oocyte meiosis resumption. *Cell Cycle* **8**, 2741–2747.

Sutherland, H. J., Lansdorp, P. M., Henkelman, D. H., Eaves, a C. and Eaves, C. J. (1990). Functional characterization of individual human hematopoietic stem cells cultured at limiting dilution on supportive marrow stromal layers. *Proc. Natl. Acad. Sci. U. S. A.* **87**, 3584–3588.

Suzuki, H., Tsuda, M., Kiso, M. and Saga, Y. (2008). Nanos3 maintains the germ cell lineage in the mouse by suppressing both Bax-dependent and -independent apoptotic pathways. *Dev. Biol.* **318**, 133–142.

Suzuki, A., Hirasaki, M., Hishida, T., Wu, J., Okamura, D., Ueda, A., Nishimoto, M., Nakachi, Y., Mizuno, Y., Okazaki, Y., et al. (2016). Loss of MAX results in meiotic entry in mouse embryonic and germline stem cells. *Nat. Commun.* **7**, 11056.

Swann, K. and Parrington, J. (1999). Mechanism of Ca2+ release at fertilization in mammals. *J. Exp. Zool.* **285**, 267–275.

Swann, K. and Yu, Y. (2008). The dynamics of calcium oscillations that activate mammalian eggs. *Int. J. Dev. Biol.* **52**, 585–594.

Swezy, O. (1933). The changing concept of ovarian rhythms. *Q. Rev. Biol.* **8**, 423–433.

Tabansky, I., Lenarcic, A., Draft, R. W., Loulier, K., Keskin, D. B., Rosains, J., Rivera-Feliciano, J., Lichtman, J. W., Livet, J., Stern, J. N. H., et al. (2013). Developmental bias in cleavage-stage mouse blastomeres. *Curr. Biol.* **23**, 21–31.

Tada, M., Takahama, Y., Abe, K., Nakatsuji, N. and Tada, T. (2001). Nuclear reprogramming of somatic cells by in vitro hybridization with ES cells. *Curr. Biol.* **11**, 1553–1558.

Takahashi, K. and Yamanaka, S. (2006). Induction of pluripotent stem cells from mouse embryonic and adult fibroblast cultures by defined factors. *Cell* **126**, 663–676.

Tam, P. P. and Snow, M. H. (1981). Proliferation and migration of primordial germ cells during compensatory growth in mouse embryos. *J. Embryol. Exp. Morphol.* **64**, 133–147.

Tam, P. P. and Zhou, S. X. (1996). The allocation of epiblast cells to ectodermal and germ-line lineages is influenced by the position of the cells in the gastrulating mouse embryo. *Dev. Biol.* **178**, 124–132.

Tanaka, S. S. and Matsui, Y. (2002). Developmentally regulated expression of mil-1 and mil-2, mouse interferon-induced transmembrane protein like genes, during formation and differentiation of primordial germ cells. *Mech. Dev.* **119 Suppl**, S261–S267.

Tanaka, S., Kunath, T., Hadjantonakis, A.-K., Nagy, A. and Rossant, J. (1998). Promotion of trophoblast stem cell proliferation by FGF4. *Science (80-.).* **282**, 2072–2075.

Tanaka, S. S., Toyooka, Y., Akasu, R., Katoh-Fukui, Y., Nakahara, Y., Suzuki, R., Yokoyama, M. and Noce, T. (2000). The mouse homolog of Drosophila Vasa is required for the development of male germ cells. *Genes Dev.* **14**, 841–853.

Tanaka, S. S., Yamaguchi, Y. L., Tsoi, B., Lickert, H. and Tam, P. P. L. (2005). IFITM/Mil/fragilis family proteins IFITM1 and IFITM3 play distinct roles in mouse primordial germ cell homing and repulsion. *Dev. Cell* **9**, 745–756.

Taylor, G., Lehrer, M. S., Jensen, P. J., Sun, T.-T. and Lavker, R. M. (2000). Involvement of follicular stem cells in forming not only the follicle but also the epidermis. *Cell* **102**, 451–461.

Telfer, E. E. and Albertini, D. F. (2012). The quest for human ovarian stem cells. *Nat. Med.* **18**, 353–354.

Telfer, E. E., Gosden, R. G., Byskov, A. G., Spears, N., Albertini, D., Andersen, C. Y., Anderson, R., Braw-Tal, R., Clarke, H., Gougeon, A., et al. (2005). On regenerating the ovary and generating controversy. *Cell* **122**, 821–822.

Tesar, P. J., Chenoweth, J. G., Brook, F. A., Davies, T. J., Evans, E. P., Mack, D. L., Gardner, R. L. and McKay, R. D. G. (2007). New cell lines from mouse epiblast share defining features with human embryonic stem cells. *Nature* **448**, 196–199.

Thomas, K. R. and Capecchi, M. R. (1987). Site-directed mutagenesis by gene targeting in mouse embryo-derived stem cells. *Cell* **51**, 503–512.

Thomas, K. R., Deng, C. and Capecchi, M. R. (1992). High-fidelity gene targeting in embryonic stem cells by using sequence replacement vectors. *Mol Cell Biol* **12**, 2919–2923.

Thomson, J. A., Kalishman, J., Golos, T. G., Durning, M., Harris, C. P., Becker, R. A. and Hearn, J. P. (1995). Isolation of a primate embryonic stem cell line. *Proc. Natl. Acad. Sci. U. S. A.* **92**, 7844–7848.

Thomson, J. A., Itskovitz-Eldor, J., Shapiro, S. S., Waknitz, M. A., Swiergiel, J. J., Marshall, V. S. and Jones, J. M. (1998). Embryonic stem cell lines derived from human blastocysts. *Science (80-.).* **282**, 1145–1147.

Tilgner, K., Atkinson, S. P., Golebiewska, A., Stojkovic, M., Lako, M. and Armstrong, L. (2008). Isolation of primordial germ cells from differentiating human embryonic stem cells. *Stem Cells* **26**, 3075–3085.

Tilly, J. L., Niikura, Y. and Rueda, B. R. (2009). The current status of evidence for and against postnatal oogenesis in mammals: a case of ovarian optimism versus pessimism? *Biol. Reprod.* **80**, 2–12.

Toyooka, Y., Tsunekawa, N., Takahashi, Y., Matsui, Y., Satoh, M. and Noce, T. (2000). Expression and intracellular localization of mouse Vasa-homologue protein during germ cell development. *Mech. Dev.* **93**, 139–149.

Tremblay, K. D., Dunn, N. R. and Robertson, E. J. (2001). Mouse embryos lacking Smad1 signals display defects in extra-embryonic tissues and germ cell formation. *Development* **128**, 3609–3621.

Trombly, D. J., Woodruff, T. K. and Mayo, K. E. (2009). Suppression of notch signaling in the neonatal mouse ovary decreases primordial follicle formation. *Endocrinology* **150**, 1014–1024.

Tu, S., Narendra, V., Yamaji, M., Vidal, S. E., Rojas, L. A., Wang, X., Kim, S. Y., Garcia, B. a, Tuschl, T., Stadtfeld, M., et al. (2016). Co-repressor CBFA2T2 regulates pluripotency and germline development. *Nature* **534**, 1–11.

Turing, A. M. (1952). The chemical basis of morphogenesis. *Philos. Trans. R. Soc. Lond. B. Biol. Sci.* **237**, 37–72.

Turner, C. A., Mack, D. H. and Davis, M. M. (1994). Pillars article: Blimp-1, a novel zinc finger-containing protein that can drive the maturation of B lymphocytes into immunoglobulin-secreting cells. *Cell* **77**, 297–306.

Tusnady, G. E. and Simon, I. (1998). Principles governing amino acid composition of integral membrane proteins: application to topology prediction. *J. Mol. Biol.* **283**, 489–506.

Tusnády, G. E. and Simon, I. (2010). Topology prediction of helical transmembrane proteins: how far have we reached? *Curr. Protein Pept. Sci.* **11**, 550–561.

Vaccari, S., Weeks, J. L., Hsieh, M., Menniti, F. S. and Conti, M. (2009). Cyclic GMP signaling is involved in the luteinizing hormone-dependent meiotic maturation of mouse oocytes. *Biol. Reprod.* **81**, 595–604.

Valente, M. J., Henrique, R., Costa, V. L., Jerónimo, C., Carvalho, F., Bastos, M. L., de Pinho, P. G. and Carvalho, M. (2011). A rapid and simple procedure for the establishment of human normal and cancer renal primary cell cultures from surgical specimens. *PLoS One* **6**, 21–23.

Van Bragt, M. P. A., Roepers-Gajadien, H. L., Korver, C. M., Bogerd, J., Okuda, A., Eggen, B. J. L., de Rooij, D. G. and van Pelt, A. M. M. (2008). Expression of the pluripotency marker UTF1 is restricted to a subpopulation of early A spermatogonia in rat testis. *Reproduction* **136**, 33–40.

Van den Boom, V., Kooistra, S. M., Boesjes, M., Geverts, B., Houtsmuller, A. B., Monzen, K., Komuro, I., Essers, J., Drenth-Diephuis, L. J. and Eggen, B. J. L. (2007). UTF1 is a chromatin-associated protein involved in ES cell differentiation. *J. Cell Biol.* **178**, 913–924.

Vermande-Van Eck, G. J. (1956). Neo-ovogenesis in the adult monkey; consequences of atresia of ovocytes. *Anat. Rec.* **125**, 207–224.

Viklund, H. and Elofsson, A. (2004). Best alpha-helical transmembrane protein topology predictions are achieved using hidden Markov models and evolutionary information. *Protein Sci.* **13**, 1908–1917.

Vit, O. and Petrak, J. (2016). Integral membrane proteins in proteomics. How to break open the black box? *J. Proteomics* S1874–3919(16)30361–X.

Voet, D. and Voet, J. G. (2011). Mechanisms of enzyme action - Enzymatic Catalysis. In *Biochemistry* (ed. Voet, D. and Voet, J. G.), pp. 506–557. Hoboken, NJ: Wiley.

Vogel, G. (2012). Potential egg stem cells reignite debate. *Science (80-.).* **335**, 1029–1030.

Von Heijne, G. (1986). The distribution of positively charged residues in bacterial inner membrane proteins correlates with the trans-membrane topology. *EMBO J.* **5**, 3021–3027.

Wakayama, T., Perry, A. C. F., Zuccotti, M., Johnson, K. R. and Yanagimachi, R. (1998). Full-term development of mice from enucleated oocytes injected with cumulus cell nuclei. *Nature* **394**, 369–374.

Wallin, E. and von Heijne, G. (1998). Genome-wide analysis of integral membrane proteins from eubacterial, archaean, and eukaryotic organisms. *Protein Sci.* **7**, 1029–1038.

Walsh, D. W., Godson, C., Brazil, D. P. and Martin, F. (2010). Extracellular BMP-antagonist regulation in development and disease: Tied up in knots. *Trends Cell Biol.* **20**, 244–256.

Wang, N., Satirapod, C. and Tilly, J. L. (2012). Progressive decline of oogonial stem cell activity contributes to ovarian aging. In *Reproductive Sciences 19 (S 3)*, p. 110A–110A.

Wang, C., Zhou, B. and Xia, G. (2017). Mechanisms controlling germline cyst breakdown and primordial follicle formation. *Cell. Mol. Life Sci.* 10.1007/s00018–017–2480–6.

Wassarman, P. M. and Josefowicz, W. J. (1978). Oocyte development in the mouse: An ultrastructural comparison of oocytes isolated at various stages of growth and meiotic competence. *J. Morphol.* **156**, 209–235.

Wasserstrom, A., Frumkin, D., Adar, R., Itzkovitz, S., Stern, T., Kaplan, S., Shur, I., Zangi, L., Reizel, Y., Harmelin, A., et al. (2008). Estimating cell depth from somatic mutations. *PLoS Comput. Biol.* **4**, e1000058.

Watt, F. M. (1998). Epidermal stem cells: markers, patterning and the control of stem cell fate. *Philos. Trans. R. Soc. Lond. B. Biol. Sci.* **353**, 831–837.

Watt, F. M. and Hogan, B. L. M. (2000). Out of Eden: Stem cells and their niches. *Science (80-.).* **287**, 1427–1430.

Weiss, M. L. and Troyer, D. L. (2006). Stem cells in the umbilical cord. *Stem Cell Rev* **2**, 155–162.

Wen, J., Zhang, H., Li, G., Mao, G., Chen, X., Wang, J., Guo, M., Mu, X., Ouyang, H., Zhang, M., et al. (2009). PAR6, a potential marker for the germ cells selected to form primordial follicles in mouse ovary. *PLoS One* **4**, e7372.

Wessel, G. M. (2012). Clouded by terminology. *Mol. Reprod. Dev.* **79**, 1.

West, F. D., Machacek, D. W., Boyd, N. L., Pandiyan, K., Robbins, K. R. and Stice, S. L. (2008). Enrichment and differentiation of human germ-like cells mediated by feeder cells and basic fibroblast growth factor signaling. *Stem Cells* **26**, 2768–2776.

West, J. a, Viswanathan, S. R., Yabuuchi, A., Cunniff, K., Takeuchi, A., Park, I.-H., Sero, J. E., Zhu, H., Perez-Atayde, A., Frazier, a L., et al. (2009). A role for Lin28 in primordial germ cell development and germ cell malignancy. *Nature* **460**, 909–913.

Wharton, K. and Derynck, R. (2009). TGFbeta family signaling: novel insights in development and disease. *Development* **136**, 3691–3697.

Whetton, A. D. and Graham, G. J. (1999). Homing and mobilization in the stem cell niche. *Trends Cell Biol.* **9**, 233–238.

Whitaker, M. (2006). Calcium at fertilization and in early development. *Physiol. Rev.* **86**, 25–88.

White, Y. A. R., Woods, D. C., Takai, Y., Ishihara, O., Seki, H. and Tilly, J. L. (2012). Oocyte formation by mitotically active germ cells purified from ovaries of reproductive-age women. *Nat. Med.* **18**, 413–421.

Wickramasinghe, D., Ebert, K. M. and Albertini, D. F. (1991). Meiotic competence acquisition is associated with the appearance of M-phase characteristics in growing mouse oocytes. *Dev. Biol.* **143**, 162–172.

Wilmut, I., Schnieke, A. E., McWhir, J., Kind, A. J. and Campbell, K. H. (1997). Viable offspring derived from fetal and adult mammalian cells. *Nature* **385**, 810–813.

Woods, D. C. and Tilly, J. L. (2012). The next (re)generation of ovarian biology and fertility in women: is current science tomorrow's practice? *Fertil. Steril.* **98**, 3–10.

Woods, D. C. and Tilly, J. L. (2013a). An evolutionary perspective on adult female germline stem cell function from flies to humans. *Semin. Reprod. Med.* **31**, 24–32.

Woods, D. C. and Tilly, J. L. (2013b). Isolation, characterization and propagation of mitotically active germ cells from adult mouse and human ovaries. *Nat. Protoc.* **8**, 966–988.

Woods, D. C. and Tilly, J. L. (2015). Reply to Adult human and mouse ovaries lack DDX4-expressing functional oogonial stem cells. *Nat. Med.* **21**, 1118–1121.

Woods, D. C., White, Y. A. R. and Tilly, J. (2012a). DDX4-positive cells isolated from oogonial stem cell (OSC)-derived tumors initiate tumorigenesis. In *Annual meeting of the Society for Reproduction and Fertility*, p. 1. Edinburgh: Society for Reproduction and Fertility Conference 2012.

Woods, D. C., White, Y. A. R., Rueda, B. R. and Tilly, J. L. (2012b). Tumorigenic potential of oogonial stem cells is actively suppressed by the intraovarian microenvironment. In *Reproductive Sciences 19 (S 3)*, p. 93A–93A.

Woods, D. C., White, Y. A. R. and Tilly, J. L. (2012c). Purification of oogonial stem cells from adult mouse and human ovaries: an assessment of the literature and a view toward the future. *Reprod. Sci.* **20**, 7–15.

Wu, J. Q., Hansen, D. V, Guo, Y., Wang, M. Z., Tang, W., Freel, C. D., Tung, J. J., Jackson, P. K. and Kornbluth, S. (2007). Control of Emi2 activity and stability through Mos-mediated recruitment of PP2A. *Proc. Natl. Acad. Sci. U. S. A.* **104**, 16564–16569.

Xiao, Y., Pollack, D., Andrusier, M., Levy, A., Callaway, M., Nieves, E., Reddi, P. and Vigodner, M. (2016). Identification of cell-specific targets of sumoylation during mouse spermatogenesis. *Reproduction* **151**, 149–166.

Xu, J. and Gridley, T. (2013). Notch2 is required in somatic cells for breakdown of ovarian germ-cell nests and formation of primordial follicles. *BMC Biol* **11**, 13.

Xu, R.-H., Chen, X., Li, D. S., Li, R., Addicks, G. C., Glennon, C., Zwaka, T. P. and Thomson, J. A. (2002). BMP4 initiates human embryonic stem cell differentiation to trophoblast. *Nat. Biotechnol.* **20**, 1261–1264.

Xu, R.-H., Peck, R. M., Li, D. S., Feng2, X., Ludwig, T. and Thomson, J. A. (2005a). Basic FGF and suppression of BMP signaling sustain undifferentiated proliferation of human ES cells. *Nat. Methods* **2**, 185–190.

Xu, H., Beasley, M. D., Warren, W. D., van der Horst, G. T. J. and McKay, M. J. (2005b). Absence of mouse REC8 cohesin promotes synapsis of sister chromatids in meiosis. *Dev. Cell* **8**, 949–961.

Xu, R. H., Sampsell-Barron, T. L., Gu, F., Root, S., Peck, R. M., Pan, G., Yu, J., Antosiewicz-Bourget, J., Tian, S., Stewart, R., et al. (2008). NANOG is a direct target of TGFβ/Activin-mediated SMAD signaling in human ESCs. *Cell Stem Cell* **3**, 196–206.

Xu, B., Hua, J., Zhang, Y., Jiang, X., Zhang, H., Ma, T., Zheng, W., Sun, R., Shen, W., Sha, J., et al. (2011a). Proliferating cell nuclear antigen (PCNA) regulates primordial follicle assembly by promoting apoptosis of oocytes in fetal and neonatal mouse ovaries. *PLoS One* **6**, e16046.

Xu, X., Pantakani, D. V. K., Lührig, S., Tan, X., Khromov, T., Nolte, J., Dressel, R., Zechner, U. and Engel, W. (2011b). Stage-specific germ-cell marker genes are expressed in all mouse pluripotent cell types and emerge early during induced pluripotency. *PLoS One* **6**, e22413.

Yamada, K. M., Yamada, S. S. and Pastan, I. (1975). The major cell surface glycoprotein of chick embryo fibroblasts is an agglutinin. *Proc. Natl. Acad. Sci.* **72**, 3158–3162.

Yamada, K. M., Yamada, S. S. and Pastan, I. (1976). Cell surface protein partially restores morphology, adhesiveness, and contact inhibition of movement to transformed fibroblasts. *Proc. Natl. Acad. Sci. U. S. A.* **73**, 1217–1221.

Yamaguchi, S., Kimura, H., Tada, M., Nakatsuji, N. and Tada, T. (2005). Nanog expression in mouse germ cell development. *Gene Expr. Patterns* **5**, 639–646.

Yamaguchi, S., Kurimoto, K., Yabuta, Y., Sasaki, H., Nakatsuji, N., Saitou, M. and Tada, T. (2009). Conditional knockdown of Nanog induces apoptotic cell death in mouse migrating primordial germ cells. *Development* **136**, 4011–4020.

Yamaji, M., Seki, Y., Kurimoto, K., Yabuta, Y., Yuasa, M., Shigeta, M., Yamanaka, K., Ohinata, Y. and Saitou, M. (2008). Critical function of Prdm14 for the establishment of the germ cell lineage in mice. *Nat. Genet.* **40**, 1016–1022.

Yang, J., Medvedev, S., Yu, J., Tang, L. C., Agno, J. E., Matzuk, M. M., Schultz, R. M. and Hecht, N. B. (2005). Absence of the DNA-/RNA-binding protein MSY2 results in male and female infertility. *Proc. Natl. Acad. Sci.* **102**, 5755–5760.

Yeo, J. C., Jiang, J., Tan, Z. Y., Yim, G. R., Ng, J. H., Göke, J., Kraus, P., Liang, H., Gonzales, K. A. U., Chong, H. C., et al. (2014). Klf2 is an essential factor that sustains ground state pluripotency. *Cell Stem Cell* **14**, 864–872.

Yeom, Y. I., Fuhrmann, G., Ovitt, C. E., Brehm, A., Ohbo, K., Gross, M., Hübner, K. and Schöler, H. R. (1996). Germline regulatory element of Oct-4 specific for the totipotent cycle of embryonal cells. *Development* **122**, 881–894.

Ying, Y. and Zhao, G. Q. (2001). Cooperation of endoderm-derived BMP2 and extraembryonic ectoderm-derived BMP4 in primordial germ cell generation in the mouse. *Dev. Biol.* **232**, 484–492.

Ying, Y., Liu, X. M., Marble, A., Lawson, K. a and Zhao, G. Q. (2000). Requirement of Bmp8b for the generation of primordial germ cells in the mouse. *Mol. Endocrinol.* **14**, 1053–1063.

Ying, Y., Qi, X. and Zhao, G. Q. (2001). Induction of primordial germ cells from murine epiblasts by synergistic action of BMP4 and BMP8B signaling pathways. *Proc. Natl. Acad. Sci.* **98**, 7858–7862.

Ying, Q. L., Nichols, J., Chambers, I. and Smith, A. (2003). BMP induction of Id proteins suppresses differentiation and sustains embryonic stem cell self-renewal in collaboration with STAT3. *Cell* **115**, 281–292.

Yoshimizu, T., Obinata, M. and Matsui, Y. (2001). Stage-specific tissue and cell interactions play key roles in mouse germ cell specification. *Development* **128**, 481–490.

Yoshinaga, K., Mununatsu, H. and Muramabu, T. (1991). Immunohistochemical localization of the carbohydrate antigen 4C9 in the mouse embryo: a reliable marker of mouse primordial germ cells. *Differentiation* **48**, 75–82.

Young, J. M. and McNeilly, A. S. (2010). Theca: the forgotten cell of the ovarian follicle. *Reproduction* **140**, 489–504.

Yount, J. S., Moltedo, B., Yang, Y., Charron, G., Moran, T. M., López, C. B. and Hang, H. C. (2011). Palmitoylome profiling reveals S-palmitoylation–dependent antiviral activity of IFITM3. *Nat. Chem. Biol.* **6**, 610–614.

Yu, J., Vodyanik, M. A., Smuga-Otto, K., Antosiewicz-Bourget, J., Frane, J. L., Tian, S., Nie, J., Jonsdottir, G. A., Ruotti, V., Stewart, R., et al. (2007). Induced pluripotent stem cell lines derived from human somatic cells. *Science (80-.).* **318**, 1917–1920.

Yu, P., Pan, G., Yu, J. and Thomson, J. a. (2011). FGF2 sustains NANOG and switches the outcome of BMP4-induced human embryonic stem cell differentiation. *Cell Stem Cell* **8**, 326–334.

Yuan, L., Liu, J. G., Zhao, J., Brundell, E., Daneholt, B. and Höög, C. (2000). The murine SCP3 gene is required for synaptonemal complex assembly, chromosome synapsis, and male fertility. *Mol. Cell* **5**, 73–83.

Yuan, L., Liu, J.-G., Hoja, M.-R., Wilbertz, J., Nordqvist, K. and Höög, C. (2002). Female germ cell aneuploidy and embryo death in mice lacking the meiosis-specific protein SCP3. *Science (80-.).* **296**, 1115–1118.

Yuan, J., Zhang, D., Wang, L., Liu, M., Mao, J., Yin, Y., Ye, X., Liu, N., Han, J., Gao, Y., et al. (2013). No evidence for neo-oogenesis may link to ovarian senescence in adult monkey. *Stem Cells* **31**, 2538–2550.

Zarate-Garcia, L., Lane, S. I. R., Merriman, J. A. and Jones, K. T. (2016). FACS-sorted putative oogonial stem cells from the ovary are neither DDX4-positive nor germ cells. *Sci. Rep.* **6**, 27991.

Zelent, A., Krust, A., Petkovich, M., Kastner, P. and Chambon, P. (1989). Cloning of murine alpha and beta retinoic acid receptors and a novel receptor gamma predominantly expressed in skin. *Nature* **342**, 189–192.

Zetter, B., Chen, L. and Buchanan, J. (1976). Effects of protease treatment on growth, morphology, adhesion, and cell surface proteins of secondary chick embryo fibroblasts. *Cell* **7**, 407–412.

Zhang, C. and Wu, J. (2016). Production of offspring from a germline stem cell line derived from prepubertal ovaries of germline reporter mice. *Mol. Hum. Reprod.* **22**, 457–464.

Zhang, F.-P., Mikkonen, L., Toppari, J., Palvimo, J. J., Thesleff, I. and Jänne, O. a (2008). Sumo-1 function is dispensable in normal mouse development. *Mol. Cell. Biol.* **28**, 5381–5390.

Zhang, Y., Yang, Z., Yang, Y., Wang, S., Shi, L., Xie, W., Sun, K., Zou, K., Wang, L., Xiong, J., et al. (2011). Production of transgenic mice by random recombination of targeted genes in female germline stem cells. *J. Mol. Cell Biol.* **3**, 132–141.

Zhang, B., Shan, H., Li, D., Li, Z., Zhu, K., Jiang, Z. and Huang, M. (2012a). Different methods of detaching adherent cells significantly affect the detection of TRAIL receptors. *Tumori* **98**, 800–803.

Zhang, H., Zheng, W., Shen, Y., Adhikari, D., Ueno, H. and Liu, K. (2012b). Experimental evidence showing that no mitotically active female germline progenitors exist in postnatal mouse ovaries. *Proc. Natl. Acad. Sci.* **109**, 12580–12585.

Zhang, H., Panula, S., Petropoulos, S., Edsgärd, D., Busayavalasa, K., Liu, L., Li, X., Risal, S., Shen, Y., Shao, J., et al. (2015). Adult human and mouse ovaries lack DDX4-expressing functional oogonial stem cells. *Nat. Med.* **21**, 1116–1118.

Zhao, X., Li, W., Lv, Z., Liu, L., Tong, M., Hai, T., Hao, J., Guo, C., Ma, Q., Wang, L., et al. (2009). iPS cells produce viable mice through tetraploid complementation. *Nature* **461**, 86–90.

Zheng, W., Zhang, H., Gorre, N., Risal, S., Shen, Y. and Liu, K. (2014). Two classes of ovarian primordial follicles exhibit distinct developmental dynamics and physiological functions. *Hum. Mol. Genet.* **23**, 920–928.

Zhou, L., Wang, L., Kang, J. X., Xie, W., Li, X., Wu, C., Xu, B. and Wu, J. (2014). Production of fat-1 transgenic rats using a post-natal female germline stem cell line. *Mol. Hum. Reprod.* **20**, 271–281.

Zickler, D. and Kleckner, N. (2015a). Recombination, pairing and synapsis of homologs during meiosis. *Cold Spring Harb. Lab. Press* **7**, a016626.

Zickler, D. and Kleckner, N. (2015b). Recombination, pairing and synapsis of homologs during meiosis. *Cold Spring Harb. Lab. Press* **7**, a016626.

Zou, K., Yuan, Z., Yang, Z., Luo, H., Sun, K., Zhou, L., Xiang, J., Shi, L., Yu, Q., Zhang, Y., et al. (2009). Production of offspring from a germline stem cell line derived from neonatal ovaries. *Nat. Cell Biol.* **11**, 631–636.

Zou, K., Hou, L., Sun, K., Xie, W. and Wu, J. (2011). Improved efficiency of female germline stem cell purification using fragilis-based magnetic bead sorting. *Stem Cells Dev.* **20**, 2197–2204.

Zuccotti, M., Ponce, R. H., Boiani, M., Guizzardi, S., Govoni, P., Scandroglio, R., Garagna, S. and Redi, C. A. (2002). The analysis of chromatin organisation allows selection of mouse antral oocytes competent for development to blastocyst. *Zygote* **10**, 73–78.

Zuccotti, M., Merico, V., Sacchi, L., Bellone, M., Brink, T. C., Stefanelli, M., Redi, C. A., Bellazzi, R., Adjaye, J. and Garagna, S. (2009a). Oct-4 regulates the expression of Stella and Foxj2 at the Nanog locus: implications for the developmental competence of mouse oocytes. *Hum. Reprod.* **24**, 2225–2237.

Zuccotti, M., Merico, V., Redi, C. A., Bellazzi, R., Adjaye, J. and Garagna, S. (2009b). Role of Oct-4 during acquisition of developmental competence in mouse oocyte. *Reprod. Biomed. Online* **19**, 57–62.

Zuccotti, M., Merico, V., Belli, M., Mulas, F., Sacchi, L., Zupan, B., Redi, C. A., Prigione, A., Adjaye, J., Bellazzi, R., et al. (2012). OCT4 and the acquisition of oocyte developmental competence during folliculogenesis. *Int. J. Dev. Biol.* **56**, 853–858.

Zuckerman, S. (1940). Periodic uterine bleeding in spayed Rhesus monkeys injected daily with a constant threshold dose of oestrone. *J. Endocrinol.* **2**, 263–267.

Zuckerman, S. (1951). The number of oocytes in the mature ovary. *Recent Prog. Horm. Res.* **6**, 63–108.